

UNIVERSITE LOUIS PASTEUR DE STRASBOURG

# THESE

pour obtenir le grade de

DOCTEUR DE L'UNIVERSITE LOUIS PASTEUR

Présentée par

Carole Foltz-César

TRISOXAZOLINES: SYNTHESIS AND APPLICATION IN  
ENANTIOSELECTIVE PALLADIUM- AND COPPER-CATALYSED  
REACTIONS

Présentée le 30 novembre 2007 devant la commission d'examen:

Prof. A. Dedieu	Université Louis Pasteur, Strasbourg
Prof. K. Muñoz	Université Louis Pasteur, Strasbourg
PD Dr. M. Enders	Ruprecht-Karls-Universität Heidelberg, Allemagne
Prof. G. Helmchen	Ruprecht-Karls-Universität Heidelberg, Allemagne
Dr. S. Bellemin-Laponnaz	Université Louis Pasteur, Strasbourg
Prof. L. H. Gade	Ruprecht-Karls-Universität Heidelberg, Allemagne

Institut de Chimie, Université Louis Pasteur, Strasbourg  
Anorganisch-Chemisches Institut, Ruprecht-Karls-Universität, Heidelberg



## *Acknowledgements*

*Am ertser Stelle möchte ich Herrn Prof. L. H. Gade für die wertvolle Unterstützung und Diskussionsbereitschaft danken.*

*Je remercie également Stéphane Bellemin-Laponnaz pour la confiance qu'il m'a accordée tout au long de ce travail de thèse. Malgré la distance, il a toujours su rester disponible pour partager son expérience et ses conseils.*

*Herrn Prof. H. Wadepohl danke ich für die Durchführung und Auswertung der Röntgenstrukturanalysen und seine Diskussionsbereitschaft. Ich danke auch Herrn Dr. M. Enders für seine stete Hilfsbereitschaft.*

*I am grateful to the Université Franco-Allemande and the European Doctoral College for funding.*

*Irene Meyer und Stefan Schweizer möchte ich für ihre Mitarbeit im Rahmen eines Forschungspraktikums danken.*

*Ein besonderer Dank geht an Beate, Dana und Lorenz für die grosse Hilfsbereitschaft und gute Zusammenarbeit.*

*I would like to thank the members of Lab 2.11, to whom I am indebted for a friendly environment within which to work: Adeline, Felix and Nathanaëlle. I would also like to express my thanks to Ben for his endless help. Für die schnelle Dursicht des Manuskriptes danke ich Susanne.*

*Ein grosser Dank gilt den ehemaligen und gegenwärtigen Kollegen des Arbeitskreises für die gute Zusammenarbeit und die angenehme Arbeitsatmosphäre. Ein spezieller Dank geht an das FFF-Team: Heike, Katharina, Michaela und Susanne für die vielen Dinge, die über den normalen Arbeitsalltag hinausgingen.*

*Je ne saurais également oublier celles et ceux qui sont sur l'autre rive du Rhin et qui ont accompagné dans la bonne humeur et l'amitié mes études ou ma thèse, notamment Aline, Clémence, Hélène, Sophie et Véronique.*

*Un grand merci à Felix pour son amitié et son aide précieuse tout au long de ces trois années passées côte à côte.*

*Merci à Nadia et Natha pour leurs bons petits plats concoctés pendant notre WG ! Mais surtout merci pour leur soutien et leur amitié. Leur présence durant ces trois années m'aura beaucoup aidée.*

*Mention particulière à Vincent : merci pour tout ...*

*Enfin, cette thèse n'aurait peut être pas vu le jour sans le soutien inconditionnel de mes parents, de Claire et Clémence et de ma famille. Par ces quelques mots, je tiens à les remercier chaleureusement.*



# TABLE OF CONTENTS

<b>CHAPTER 1</b>	General introduction	1
<b>CHAPTER 2</b>	Ligand synthesis and rearrangement of 2-bromooxazolines	31
<b>CHAPTER 3</b>	Dynamic coordination of chiral trisoxazolines to palladium	63
<b>CHAPTER 4</b>	Dynamic coordination of chiral trisoxazolines to copper	109
<b>GENERAL CONCLUSION</b>		141
<b>CHAPTER 5</b>	Experimental part	145



# - Chapter 1 -

<b>I. Introduction.....</b>	<b>3</b>
1. The oxazoline ring .....	3
2. Development of oxazoline-based ligands for asymmetric catalysis .....	4
<b>II. Development of chiral trisoxazolines and applications in asymmetric catalysis.....</b>	<b>7</b>
1. Introduction.....	7
2. Synthesis .....	8
a. Direct synthesis .....	9
b. A modular strategy in the synthesis of trisoxazolines .....	12
c. Conclusion .....	14
3. Applications in asymmetric catalysis and molecular recognition.....	14
a. Chiral trisoxazolines of type <b>A</b> and <b>B</b> .....	14
b. Chiral trisoxazolines of type <b>C</b> .....	17
c. Chiral trisoxazolines of type <b>D</b> and <b>E</b> .....	17
d. Chiral trisoxazolines of type <b>F</b> .....	19
e. Conclusion .....	20
4. 1,1,1-tris(oxazoliny)ethane: precedent in the group .....	21
<b>III. 1,1,1-tris(oxazoliny)ethane and the influence of <math>C_3</math> symmetry in catalysis.....</b>	<b>25</b>
1. $C_3$ symmetry in asymmetric catalysis .....	25
a. Introduction.....	25
b. Symmetry in metal complexes.....	26
2. Definition of the research project .....	29





## I. Introduction

### 1. The oxazoline ring

Heterocycles represent important structural motifs in organic chemistry, serving as latent functionalities for the construction, elaboration and functionalisation of organic molecules. They are also used as protecting groups for sensitive moieties in synthetic sequences and for directing chemical reactions when acting as organocatalysts<sup>1</sup> or as chiral ligands in metal-catalysed reactions.<sup>2</sup> A very well established class of heterocyclic units are the 4,5-dihydro-1,3-oxazole rings which are present in many biologically active natural products.<sup>3</sup> The rigid and quasi-planar 4,5-dihydro-1,3-oxazoles, commonly known as 2-oxazolines or simply oxazolines (Figure 1.1.1), first appeared in the literature in 1884.<sup>4</sup>

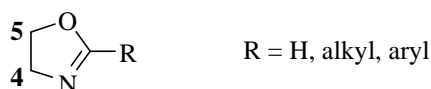


**Figure 1.1.1:** 4,5-dihydro-1,3-oxazole

When the oxazoline ring contains a substituent (other than hydrogen) at the 4- and/or the 5-carbon positions, the molecule is chiral. Early attempts to obtain enantiomerically pure compounds go back to E. Fischer, in 1894. A number of reliable preparative methods developed for this heterocycle at that time are still valuable and in use today. Oxazolines are usually prepared from  $\alpha$ -amino alcohols (easily obtained by reduction of the corresponding  $\alpha$ -amino acids) and nitriles or carboxylic acid derivatives (chiral pool-based synthesis, see Scheme 1.1.1).<sup>5</sup>

One major advantage that oxazolines offer to the synthetic chemist is the fact that they can readily be prepared in enantiomerically pure form from optically pure  $\alpha$ -amino alcohols. This attractive characteristic along with their stability towards hydrolysis and oxidation renders the oxazoline unit suitable for the design of chiral ligands for enantioselective catalysis. Indeed, upon *N*-coordination, the stereodirecting substituents are located in close proximity to the metal centre and high selectivities may be expected in catalytic reactions.

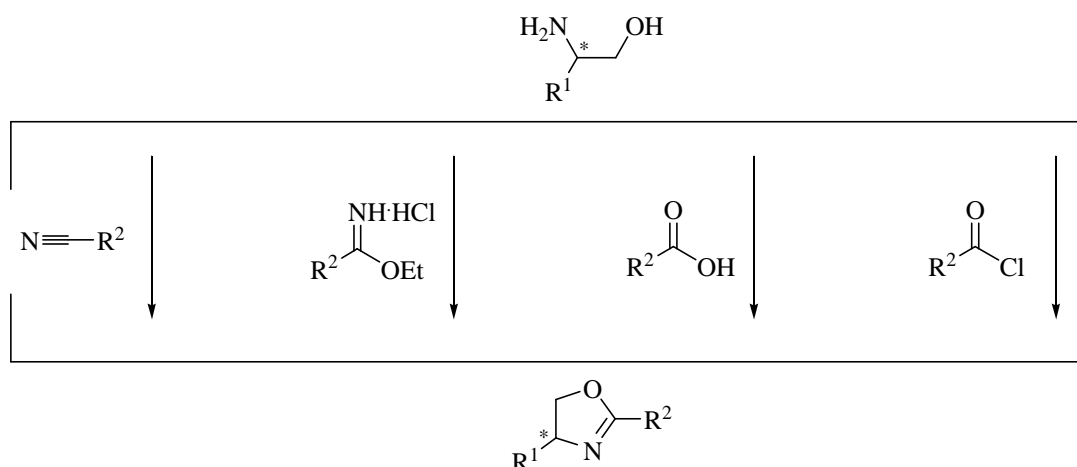
<sup>1</sup> For examples, see: a) G. C. Fu, *Acc. Chem. Res.* **2004**, *37*, 542; b) K. N. Houk, B. List, *Acc. Chem. Res.* **2004**, *37*, 487; c) N. Marion, S. Díez-González, S. P. Nolan, *Angew. Chem. Int. Ed.* **2007**, *46*, 2988; *Angew. Chem.* **2007**, *119*, 3046.

<sup>2</sup> I. Ojima, *Catalytic Asymmetric Catalysis*, Second Edition, Wiley-VCH **2000**.

<sup>3</sup> a) B. S. Davidson, *Chem. Rev.* **1993**, *93*, 1771; b) J. P. Michael, G. Pattenden, *Angew. Chem. Int. Ed. Engl.* **1993**, *32*, 1; *Angew. Chem.* **1993**, *105*, 1 and references therein.

<sup>4</sup> R. Andreasch, *Monatsh. Chem.* **1884**, *5*, 33.

<sup>5</sup> T. G. Gant, A. I. Meyers, *Tetrahedron* **1994**, *50*, 2297.



**Scheme 1.1.1:** General procedures for the preparation of enantiopure oxazolines

## 2. Development of oxazoline-based ligands for asymmetric catalysis

Metal-catalysed asymmetric synthesis is a powerful tool since large amounts of optically active products can be synthesised using a small amount of active catalyst.<sup>6</sup> Most of these catalysts are metal complexes containing a chiral organic ligand which sterically and/or electronically controls a metal-mediated process in such a way that one stereoisomer is preferentially formed.<sup>7</sup>

It is only since 1986 that oxazoline-based ligands have been used in asymmetric catalysis, originally for the monophenylation of diols<sup>8,9</sup> and later the hydrosilylation of ketones.<sup>10,11,12</sup> This initiated considerable research activity in the field and triggered the synthesis of numerous chiral ligands containing at least one oxazoline structural unit.<sup>13</sup> Oxazoline units are expected to readily coordinate a metal centre and they have been shown to bind to a wide range of transition metals.<sup>14</sup> The diverse range of ligands with one, two or more oxazoline rings incorporating

<sup>6</sup> a) H. Brunner, W. Zettlmeier, *Handbook of Enantioselective Catalysis with Transition Metal Compounds, Vol. 1 and Vol. 2*, VCH, New-York, **1993**; b) I. Ojima, *Asymmetric Catalysis in Organic Synthesis*, VCH, New-York, **1993**; c) R. Noyori, *Asymmetric Catalysis in Organic Synthesis*, VCH, New-York, **1994**; d) D. J. Berrisford, C. Bolm, K. B. Sharpless, *Angew. Chem. Int. Ed. Engl.* **1995**, *34*, 1059; *Angew. Chem.* **1995**, *107*, 1159; e) C. Girard, H. B. Kagan, *Angew. Chem. Int. Ed.* **1998**, *37*, 2922; *Angew. Chem.* **1998**, *110*, 3088; f) E. N. Jacobsen, A. Pfaltz, H. Yamamoto, *Comprehensive Asymmetric Catalysis, Vol. 1*, Springer, Berlin, **1999**; g) J. S. Johnson, D. A. Evans, *Acc. Chem. Res.* **2000**, *33*, 325.

<sup>7</sup> A. Togni, L. M. Venanzi, *Angew. Chem. Int. Ed. Engl.* **1994**, *33*, 497; *Angew. Chem.* **1994**, *106*, 517.

<sup>8</sup> H. Brunner, U. Obermann, P. Wimmer, *J. Organomet. Chem.* **1986**, *316*, C1.

<sup>9</sup> H. Brunner, U. Obermann, P. Wimmer, *Organometallics* **1989**, *8*, 821.

<sup>10</sup> H. Brunner, U. Obermann, P. Wimmer, *Chem. Ber.* **1989**, *122*, 499.

<sup>11</sup> H. Nishiyama, H. Sakaguchi, T. Nakamura, M. Horihata, M. Kondo, K. Itoh, *Organometallics* **1989**, *8*, 846.

<sup>12</sup> G. Balavoine, J.-C. Clinet, I. Lellouche, *Tetrahedron Lett.* **1989**, *30*, 5141.

<sup>13</sup> a) C. Bolm, *Angew. Chem. Int. Ed. Engl.* **1991**, *30*, 542; *Angew. Chem.* **1991**, *103*, 556; b) C. Bolm, K. Weickhardt, M. Zehnder, D. Glasmacher, *Helv. Chim. Acta* **1991**, *74*, 717; c) A. Pfaltz, *Acta Chem. Scand.* **1996**, *50*, 189; d) A. K. Ghosh, P. Mathivanan, J. Cappiello, *Tetrahedron: Asymmetry* **1998**, *9*, 1.

<sup>14</sup> a) M. Gómez, G. Muller, M. Rocamora, *Coord. Chem. Rev.* **1999**, *193*, 769; b) P. Braunstein, F. Naud, *Angew. Chem. Int. Ed.* **2001**, *40*, 680; *Angew. Chem.* **2001**, *113*, 702.

various heteroatoms, additional chiral elements, and specific structural features have been used in a wide range of asymmetric reactions.<sup>15</sup>

A selection of chiral *P,N*-, *C,N*-, *N,N*-, *O,N*-, *S,N*-oxazoline-based ligands which are widely applied as powerful tools in asymmetric catalysis is depicted in Figure 1.1.2.<sup>13,16</sup>

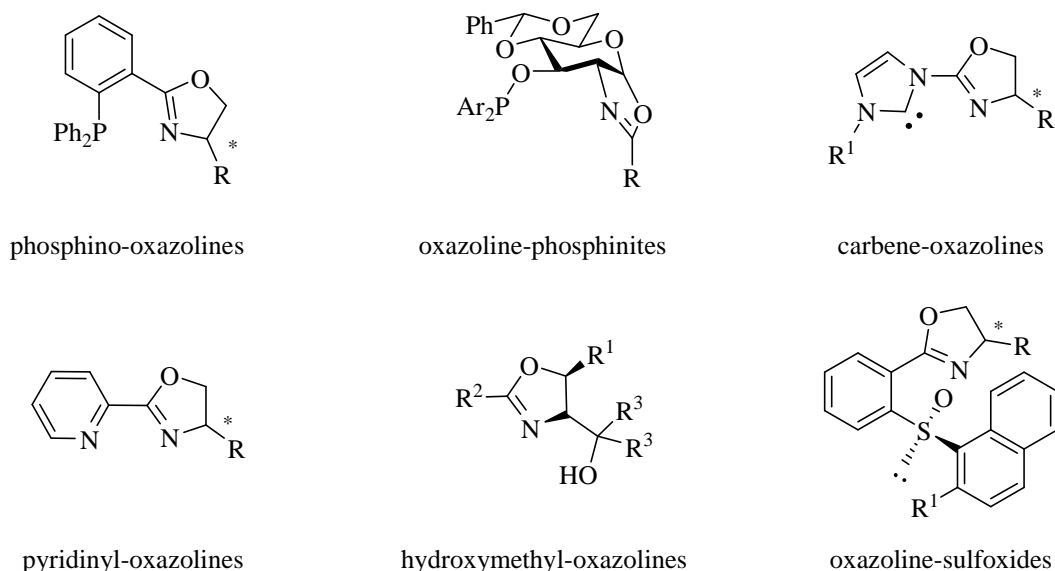


**Figure 1.1.2:** Selected chiral oxazoline-based ligands for asymmetric catalysis

The successful use of oxazoline-based ligands was paralleled by that of  $C_2$ -symmetric semicorrin ligands (Figure 1.1.3), of which the first examples were also published in 1986.<sup>17</sup>

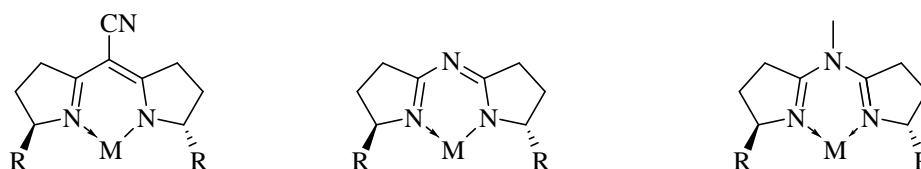


**Figure 1.1.3:** Semicorrin derivatives for asymmetric catalysis

The advantage of these ligands lies in the fact that the two stereogenic centres are held in close proximity to the metal and thus have a strong and direct influence on the stereochemical course of a metal-catalysed process. Semicorrin ligands were successfully applied in asymmetric

<sup>15</sup> H. A. McManus, P. J. Guiry, *Chem. Rev.* **2004**, *104*, 4151.

<sup>16</sup> a) F. Fache, E. Schulz, M. L. Tommasino, M. Lemaire, *Chem. Rev.* **2000**, *100*, 2159; b) G. Helmchen, A. Pfaltz, *Acc. Chem. Res.* **2000**, *33*, 336; c) O. B. Sutcliffe, M. R. Bryce, *Tetrahedron: Asymmetry* **2003**, *14*, 2297; d) A. I. Meyers, *J. Org. Chem.* **2005**, *70*, 6137; e) L. H. Gade, S. Bellemin-Laponnaz, *Coord. Chem. Rev.* **2007**, *251*, 718.

<sup>17</sup> H. Fritschi, U. Leutenegger, A. Pfaltz, *Angew. Chem. Int. Ed. Engl.* **1986**, *25*, 1005; *Angew. Chem.* **1986**, *98*, 1028.

catalysis.<sup>18</sup> The related structure of bisoxazolines and semicorrins prompted several groups to investigate the synthesis and the potential of bisoxazoline ligands (BOX) in enantioselective catalysis. Chiral  $C_2$ -symmetric bisoxazoline ligands with a wide structural diversity have been introduced since 1989, going from bidentate to tetradentate bisoxazoline ligands. Representative structures of these ligands are shown in Figure 1.1.4.

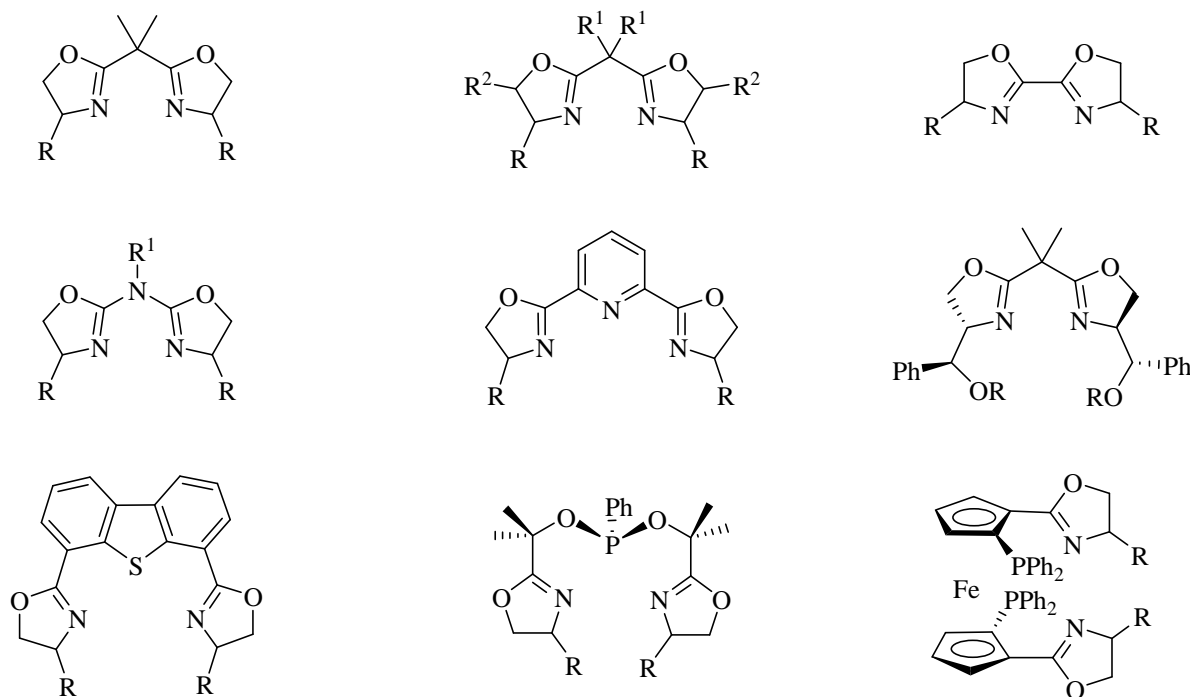


**Figure 1.1.4:** Some examples of chiral bisoxazoline ligands

The development of bisoxazolines added a new dimension in ligand design in terms of flexibility, convenient synthesis and availability of ligands in both enantiomeric forms. During the past two decades there has been a rapid growth in the applications of these ligands in asymmetric catalysis and they have proven their potential to give both high activity and selectivity in metal-catalysed enantioselective reactions.<sup>4g,11d,13,19</sup>

Given the extensive body of synthetic work carried out for the design of bisoxazoline ligands leading to efficient catalysts, the related trisoxazolines have begun to receive increasing attention. The next part of this chapter focusses on the development of trisoxazoline ligands for asymmetric catalysis.

<sup>18</sup> A. Pfaltz, *Acc. Chem. Res.* **1993**, 26, 339.

<sup>19</sup> G. Desimoni, G. Faita, K. A. Jørgensen, *Chem. Rev.* **2006**, 106, 3561.

## II. Development of chiral trisoxazolines and applications in asymmetric catalysis

### 1. Introduction

Bisoxazolines possess a number of attractive advantages: versatility of ligand design, straightforward synthesis of the ligands from readily available precursors and variability of the chiral centres, which are located near the donor atoms. Based on the straightforward accessibility and applicability of bisoxazolines, the development of their tridentate analogues, trisoxazolines (trisox), has gained increasing interest. The third oxazoline unit is anticipated to increase the stability of a metal complex to give rise to more air- and (possibly) water-stable catalysts. Moreover, trisoxazolines are expected to create a more sterically hindered chiral space, compared to bisoxazolines allowing the use of less sterically hindered and cheaper chiral sources to reach high enantioselectivity.

Concerning symmetry, it is known that bidentate  $C_2$  symmetry may reduce the number of possible diastereomers for tetrahedral or square planar catalytic intermediates while  $C_3$  symmetry may create a favorable situation in an octahedral environment.<sup>20</sup> Thus,  $C_3$ -symmetric trisoxazolines can be viewed as versatile ligands in metal-catalysed enantioselective reactions involving higher deltahedral intermediates, an aspect which will be developed in the next part of the chapter.

In the early 90s the group of Sorrell initiated a study aimed to extend the family of oxazoline ligands to include those possessing threefold symmetry. This led to the first report of the synthesis of an achiral trisoxazoline in 1993 (Figure 1.2.1).<sup>21</sup>

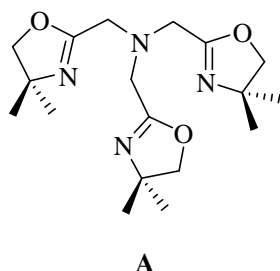


Figure 1.2.1: The first trisoxazoline reported in the literature

<sup>20</sup> C. Moberg, *Angew. Chem. Int. Ed.* **1998**, 37, 248; *Angew. Chem.* **1998**, 110, 260.

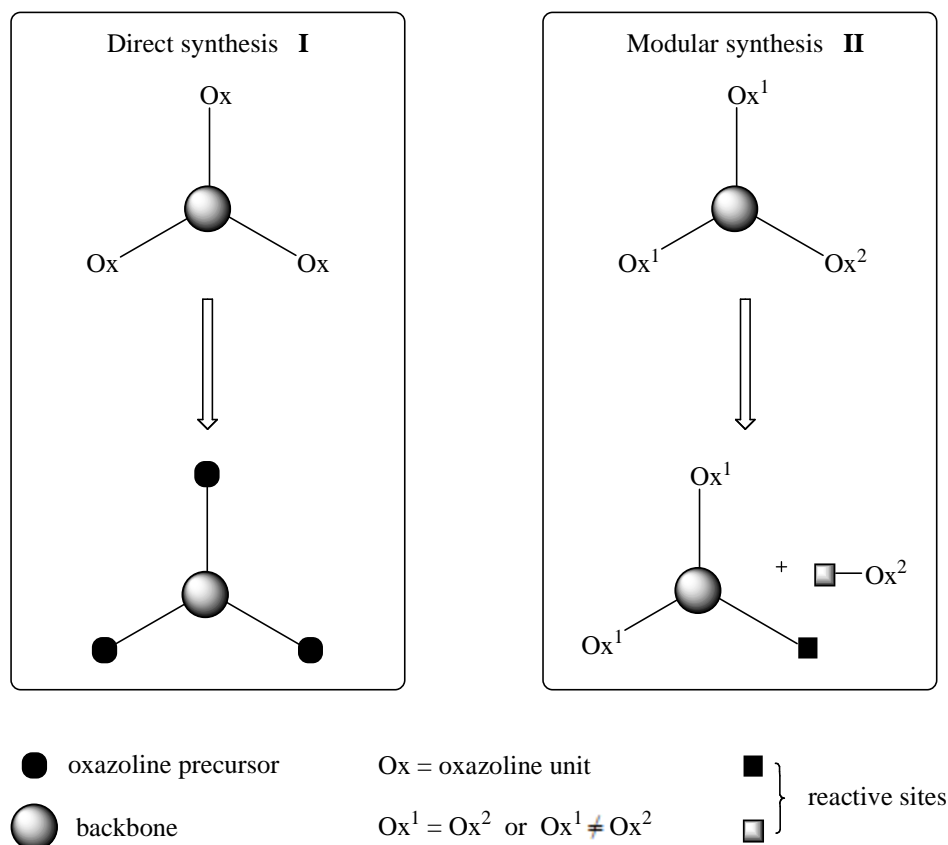
<sup>21</sup> T. N. Sorrell, F. C. Pigge, P. S. White, *Inorg. Chim. Acta* **1993**, 210, 87.

Since Sorrell *et al.* reported a simple and inexpensive route to obtain trisoxazoline ligands new trisoxazolines, including chiral derivatives, have emerged in the literature. The synthetic strategies and methods developed for the preparation of trisoxazolines are summarised and some interesting applications of these ligands are described in the next part. For further information the readers can refer to the recent review from Tang *et al.*<sup>22</sup>

## 2. Synthesis

According to the literature on the design of new trisoxazoline ligands, one can clearly identify two different synthetic strategies (Scheme 1.2.1). The first one consists in the formation of the three oxazoline units in one step by sequential cyclisation (**I**) and the second one is a modular strategy (**II**) based on the reaction between pre-formed oxazoline-based intermediates.

First, method **I** is presented and the advantages as well as the limitations of this strategy are discussed. This will lead to the investigation of the other synthetic method (**II**). In a second part, the modular strategy and its implications in ligand design is delineated.

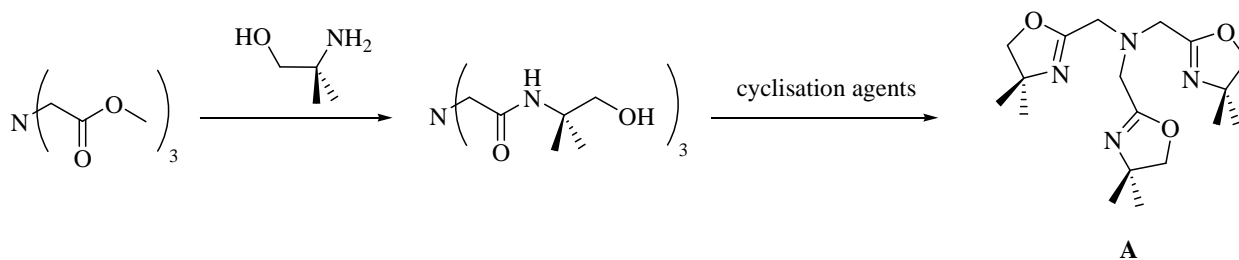


**Scheme 1.2.1:** The two strategies designed for the synthesis of trisoxazolines

<sup>22</sup> J. Zhou, Y. Yang, *Chem. Soc. Rev.* **2005**, 34, 664.

a. Direct synthesis

The first reported trisoxazoline, the achiral  $C_3$ -symmetric trisoxazoline **A** (Scheme 1.2.2), was prepared using classical procedures for the formation of oxazoline units. This implies that the trisox was obtained either by a reaction of a carboxylic acid, or its derivatives, with  $\alpha$ -amino alcohols followed by cyclisation or by direct condensation of nitriles with  $\alpha$ -amino alcohols in the presence of a Lewis acid. The synthetic procedure reported by Sorrell for the preparation of the tetradentate trisoxazoline **A** starting from a triester is depicted in Scheme 1.2.2.<sup>21</sup>



**Scheme 1.2.2:** Synthetic procedure to obtain trisoxazoline **A**

They suggested at the time that a variation of the  $\alpha$ -amino alcohol could allow facile synthesis of chiral analogues using this simple synthetic route. Various optically pure  $\alpha$ -amino alcohols are commercially available (with *i*Pr, *s*Bu, *t*Bu, Me or Ph as substituents) or can be readily prepared by reduction of the corresponding  $\alpha$ -amino acids.<sup>23</sup> Synthetic methods to obtain new chiral  $\alpha$ -amino acids have also been developed by organic chemist,<sup>24</sup> a non negligible advantage for the further synthesis of chiral trisoxazolines, as well as for the synthesis of other chiral oxazoline-based ligands.

The synthesis of chiral analogues of **A** was achieved by Katsuki *et al.* in 1995.<sup>25</sup> They reported the preparation of two chiral  $C_3$ -symmetric trisoxazolines using the synthetic procedure depicted in Scheme 1.2.2 with (*S*)-valinol and (*S*)-phenylglycinol as amino alcohols (Figure 1.2.2).

<sup>23</sup> a) A. Abiko, S. Masamune, *Tetrahedron Lett.* **1992**, *33*, 5617; b) M. McKennon, A. I. Meyers, *J. Org. Chem.* **1993**, *58*, 3568.

<sup>24</sup> J.-A. Ma, *Angew. Chem. Int. Ed.* **2003**, *42*, 4290; *Angew. Chem.* **2003**, *115*, 4426.

<sup>25</sup> K. Kawasaki, S. Tsumura, T. Katsuki, *Synlett* **1995**, 1245.

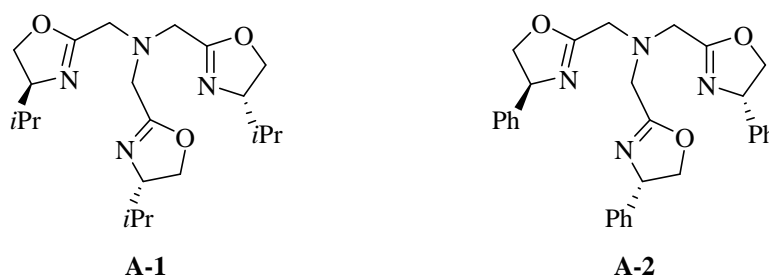
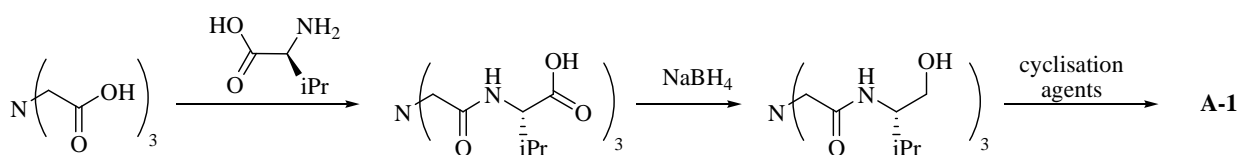


**Figure 1.2.2:** The first two chiral  $C_3$ -symmetric trisoxazolines

Two years later they described the synthesis of another series of  $C_3$ -symmetric chiral trisoxazolines of the same type using, among others, chiral synthetic amino alcohols.<sup>26</sup> Yields from 24 to 75% were obtained for the last step (cyclisation) which was generally the step with the lowest yield observed during the synthesis.

An alternative synthetic route for the preparation of **A**-type trisox was developed by Chan *et al.*<sup>27</sup> They reported the synthesis of **A-1** in three steps starting from a triacid and (*S*)-valine (Scheme 1.2.3).



**Scheme 1.2.3:** Alternative route for the synthesis of type **A** trisoxazolines

The success of the direct synthesis of trisoxazolines based on the method developed by Sorrell led to the design of several new chiral  $C_3$ -symmetric trisoxazolines with various cores *via* the same synthetic strategy. All the trisoxazolines incorporating a new backbone obtained *via* method **I** are represented in Figure 1.2.3.

<sup>26</sup> K. Kawasaki, T. Katsuki, *Tetrahedron* **1997**, 53, 6337.

<sup>27</sup> T. H. Chan, G. Z. Zheng, *Can. J. Chem.* **1997**, 75, 629.



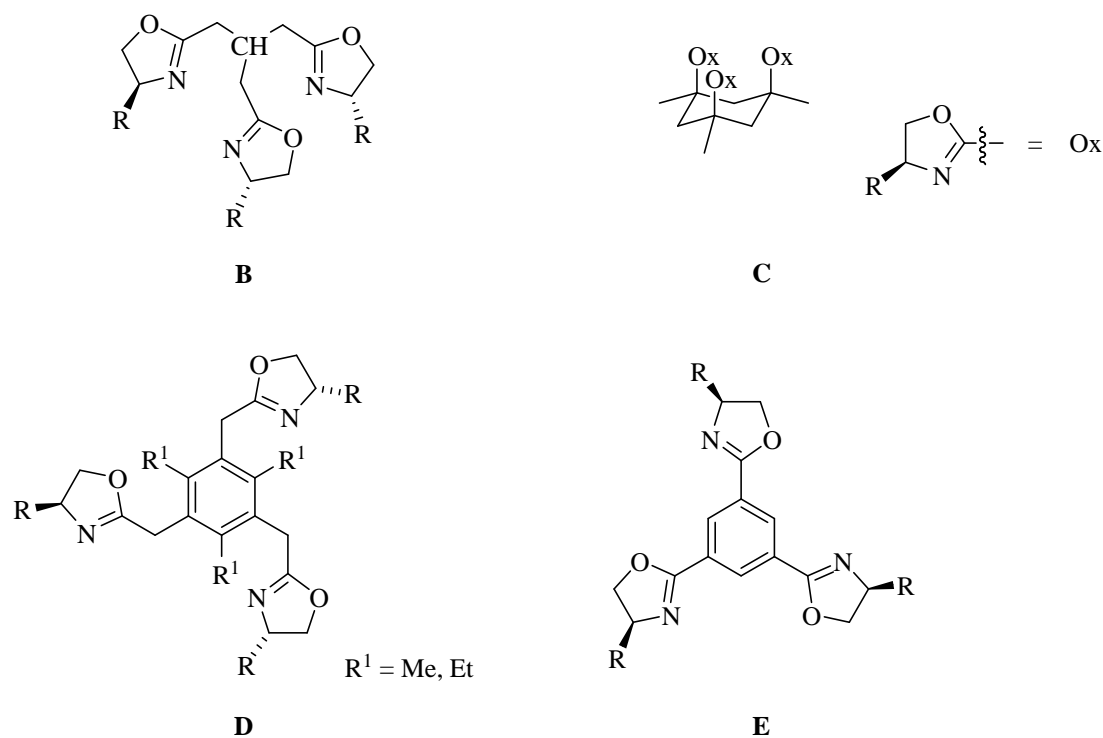


**Figure 1.2.3:** Chiral  $C_3$ -symmetric trisoxazolines incorporating various backbones

Synthesis of **B**-type trisox (Figure 1.2.3) with a central carbon atom was accomplished in the group of Katsuki in 2000.<sup>28</sup> This ligand was designed to investigate the influence of the central nitrogen atom on the catalytic species and on the enantioselectivity by comparing both **A**- and **B**-type trisox. That same year, Bolm *et al.* reported the preparation of **C**-type trisoxazolines.<sup>29</sup> These tripods, incorporating a rigid cyclohexane backbone, were prepared starting from Kemp's triacid. For applications in host-guest complexes, two benzene-based  $C_3$ -symmetric trisoxazolines were independently synthesised by Ahn *et al.* in 2000<sup>30</sup> (**D**, Figure 1.2.3) and the following year in the group of Hong (**E**, Figure 1.2.3).<sup>31</sup> The synthetic methods employed to obtain the two benzene containing trisoxazolines are similar.

Pseudo  $C_3$ -symmetric trisoxazolines were also prepared using the direct route starting from a triester. Tang *et al.* accomplished the synthesis of a new type of tripods, **F**, where **F-1**<sup>32</sup> and **F-2**<sup>33</sup> differs in the length of the alkyl-chain bridging the apical methyl group and the third oxazoline unit (Figure 1.2.4).

<sup>28</sup> Y. Kohmura, T. Katsuki, *Tetrahedron Lett.* **2000**, 41, 3941.

<sup>29</sup> T.-H. Chuang, J.-M. Fang, C. Bolm, *Synth. Commun.* **2000**, 30, 1627.

<sup>30</sup> S.-G. Kim, K. H. Ahn, *Chem. Eur. J.* **2000**, 6, 3399.

<sup>31</sup> H.-J. Kim, Y.-H. Kim, J.-I. Hong, *Tetrahedron Lett.* **2001**, 42, 5049.

<sup>32</sup> J. Zhou, Y. Tang, *J. Am. Chem. Soc.* **2002**, 124, 9030.

<sup>33</sup> J. Zhou, M.-C. Ye, Y. Tang, *J. Comb. Chem.* **2004**, 6, 301.

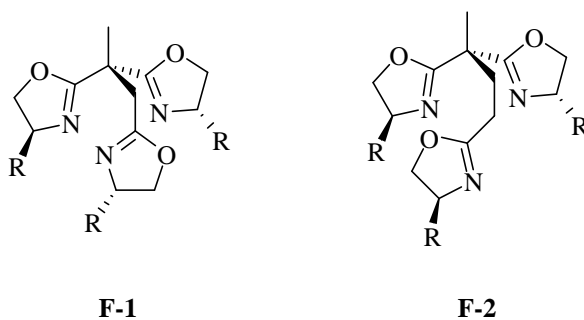


Figure 1.2.4: Pseudo  $C_3$ -symmetric trisoxazolines

In summary, method **I** has proved to be an inexpensive and simple procedure to obtain  $C_3$ - and pseudo  $C_3$ -symmetric trisoxazolines. The desired tripods are obtained in two or three steps and the diversity of  $\alpha$ -amino alcohols provides access to a large variety of ligands. However, the direct synthesis usually gives poor yields in the key step (the ring closure). Additionally, this method suffers from an important drawback: the possibility to generate only  $C_3$ -symmetric (or pseudo  $C_3$ -symmetric) trisoxazolines. Even if it is a convenient method to afford the desired highly symmetrical ligands, it fails to provide non-symmetric trisoxazolines. This significant limitation of the direct synthesis strategy can be overcome by using an alternative synthetic procedure for the preparation of trisoxazolines in the form of a modular strategy.

b. A modular strategy in the synthesis of trisoxazolines

The use of a modular strategy for the synthesis of achiral and chiral trisoxazolines was first introduced by our group in 2002.<sup>34,35</sup> A new synthetic procedure was developed to give access to 1,1,1-tris(oxazoliny)ethane ligands (Figure 1.2.5), the trisoxazolines which derive directly from 1,1-bis(oxazoliny)ethane species. Indeed the synthesis of these trisoxazolines, which provides a geometry of the metal binding site which is in principle most adapted to a tripodal coordination mode, proved to be elusive for a long time.<sup>20</sup>

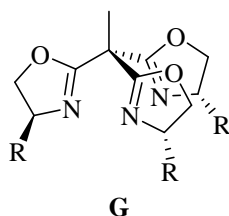
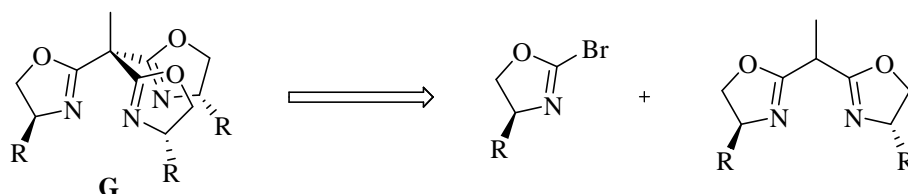


Figure 1.2.5: Structure of 1,1,1-tris(oxazoliny)ethane ligands

<sup>34</sup> S. Bellemin-Lapponnaz, L. H. Gade, *Chem. Commun.* **2002**, 1286.

<sup>35</sup> S. Bellemin-Lapponnaz, L. H. Gade, *Angew. Chem. Int. Ed.* **2002**, *41*, 3473, *Angew. Chem.* **2002**, *114*, 3623.

Attempts to synthesise these tripodal ligands by sequential formation of the three oxazoline units failed due to decarboxylation and related decomposition of the precursors during the formation of the third oxazoline ring. Direct synthesis is not suited for the preparation of **G**-type ligands (Figure 1.2.5). Coupling of a readily accessible bisoxazoline derivative with a preformed activated monooxazoline ring affords the desired 1,1,1-tris(oxazoliny)ethane ligands (Scheme 1.2.4). This condensation reaction constitutes the basis of the modular strategy.

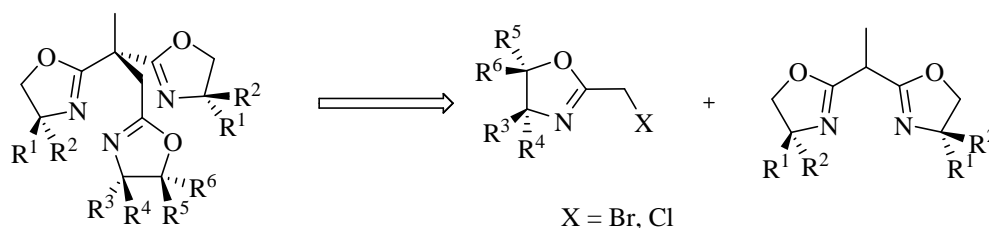


**Scheme 1.2.4:** Modular assembly of the trisoxazolines **G** by reaction of metalated bisoxazolines with 2-bromooxazoline derivatives

The strategy, which is formally based on a {1+2} condensation scheme of a lithiated bisoxazoline with a 2-bromooxazoline, has proven to be efficient for the synthesis of highly symmetric chiral 1,1,1-tris(oxazoliny)ethane ligands (chiral  $C_3$ -symmetric trisox with  $R = iPr$  and  $R = tBu$ ).

Our synthetic method allows the high-yield access to symmetric trisoxazolines and tripods with mixed substitution patterns. The modular synthesis turned out to be a versatile method to combine three oxazoline units to form ligands possessing  $C_3$  as well as  $C_1$  symmetry.<sup>35</sup>

With the aim to expand the library of pseudo  $C_3$ -symmetric trisoxazoline based ligands **F**, Tang *et al.* applied the modular synthesis in 2004. Coupling between deprotonated bisoxazolines and 2-halogenomethyl oxazolines gives access to the expected trisoxazolines (Scheme 1.2.5). This strategy allows the incorporation of a broad variety of substituents at the stereogenic centre, such as benzyl, *t*-butyl and indanyl groups, to form pseudo  $C_3$ -symmetric trisoxazolines and trisoxazolines with mixed oxazoline units.<sup>32,36</sup>



**Scheme 1.2.5:** Modular assembly of the trisoxazolines **F-1** by reaction of metalated bisoxazolines with 2-halogenomethyl oxazolines

<sup>36</sup> M.-C. Ye, B. Li, J. Zhou, X.-L. Sun, Y. Tang, *J. Org. Chem.* **2005**, *70*, 6108.

Notably, some pseudo  $C_3$ -symmetric trisoxazolines could not be obtained by the previously described direct synthesis, demonstrating the superiority of the modular synthesis.

c. Conclusion

Both methods **I** and **II** for the synthesis of chiral trisoxazolines have proven to be efficient. They allow the formation of a broad range of ligands with various backbones and with facile variation of the substituents present on the stereogenic centre.

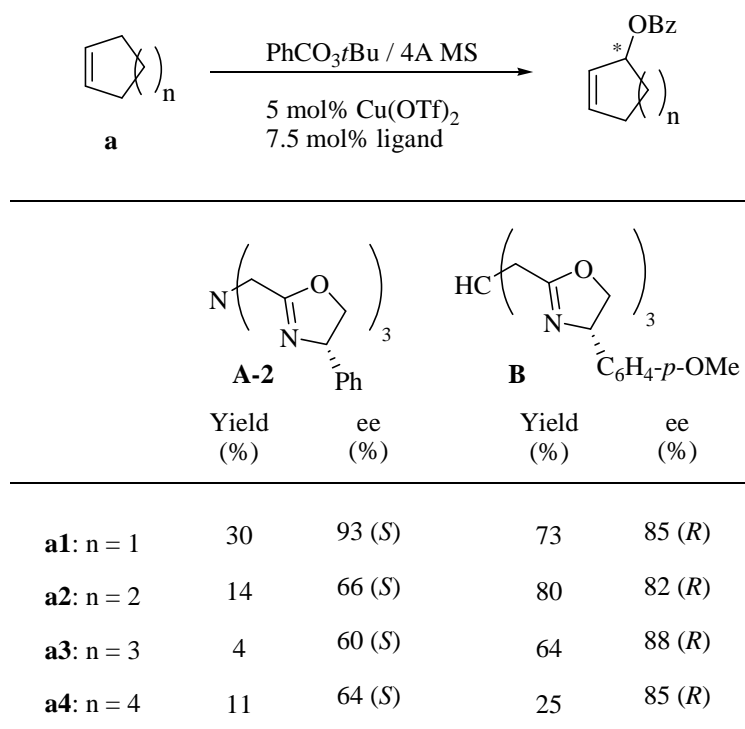
Inspired by the versatility of bisoxazoline ligands, trisoxazoline ligands have been applied in asymmetric catalysis to test their catalytic efficiency and selectivity. Examples of application in asymmetric catalysis or in molecular recognition of the different types of trisoxazolines **A-F** described above are presented in the next part.

**3. Applications in asymmetric catalysis and molecular recognition**

Katsuki *et al.* were the first to report the use of trisoxazoline ligands in asymmetric catalysis.<sup>25</sup> Optically active trisoxazoline **A** was synthesised to mimic the active site of non-heme oxygenases and its copper(II) complex was found to be an efficient catalyst for enantioselective allylic oxidation of cycloalkenes. Since this first description of the successful application of a trisoxazoline in asymmetric catalysis, trisox ligands with different backbones have already found use in several enantioselective reactions such as Friedel-Crafts, Michael addition, 1,3-dipolar cycloaddition, Diels-Alder reaction, addition of diethylzinc to aldehydes and cyclopropanation.<sup>22</sup> Excellent results have been achieved in some of these reactions. Molecular recognition has also been the focus of research interest with some chiral trisoxazolines.

a. Chiral trisoxazolines of type **A** and **B**

As previously said, the use of **A** in the Kharash-Sosnovsky reaction was the first reported application of chiral trisoxazolines in asymmetric catalysis. After carefully examining the effect of metal salt, solvent, oxidant, ligand structure and additive, it was found that phenyl-substituted ligand **A-2** in combination with  $\text{Cu}(\text{OTf})_2$  could promote the oxidation of cyclopentene with ee value up to 93% in acetone. However, other cycloalkenes only afforded low yield and moderate enantioselectivity (Scheme 1.2.6).<sup>25,26</sup>

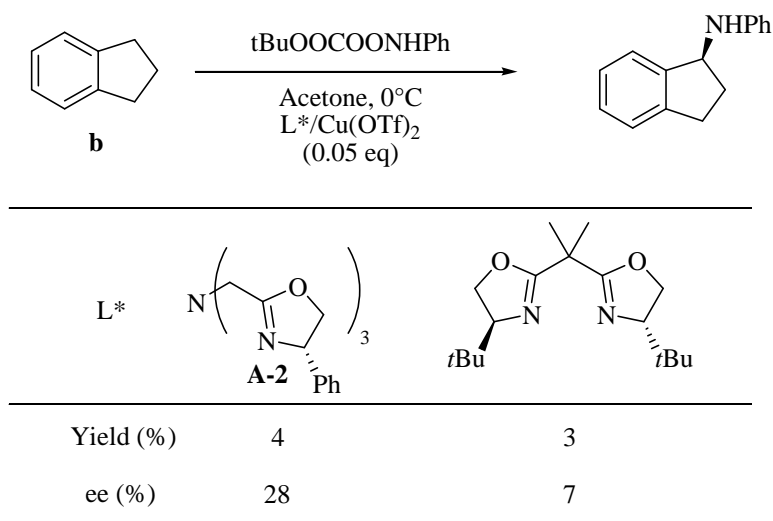


**Scheme 1.2.6:** Kharash-Sosnovsky reaction catalysed by **A**- and **B**-type chiral trisoxazolines

**A**-type ligands are potentially tetradentate and one can consider that the nitrogen atom at the core of the trisox might coordinate to the copper centre. It was anticipated that the structure of the catalytic intermediate would be different when the backbone do not possess a potentially coordinating atom. Thus, **B**-type trisoxazolines were synthesised by Katsuki *et al.* and applied to the same reaction.<sup>28</sup> The results are summarised in Scheme 1.2.6 for a direct comparison with the corresponding tetradentate ligand. Notably, one ligand led to the formation of the *S* enantiomer and the other to the formation of the *R* enantiomer, under the same reaction conditions even if both ligands had stereogenic centres with the same chirality. This suggests that the geometry of the copper ion coordinated by **B** is different from the geometry of the copper ion ligated by **A-2**. Generally, the use of **B**-type trisoxazoline led to higher enantiomeric excesses and yields in the oxidation of cycloalkenes **a1-a4**.

Regarding the mechanism of allylic oxidation, allylic amination was expected to proceed in the same way. Thus, Katsuki *et al.* also tried ligand **A** in the asymmetric allylic reaction.<sup>37</sup> After optimisation of the reaction conditions with the achiral version of the trisox, they applied ligand **A-2** in the asymmetric amination of compound **b** (Scheme 1.2.7).

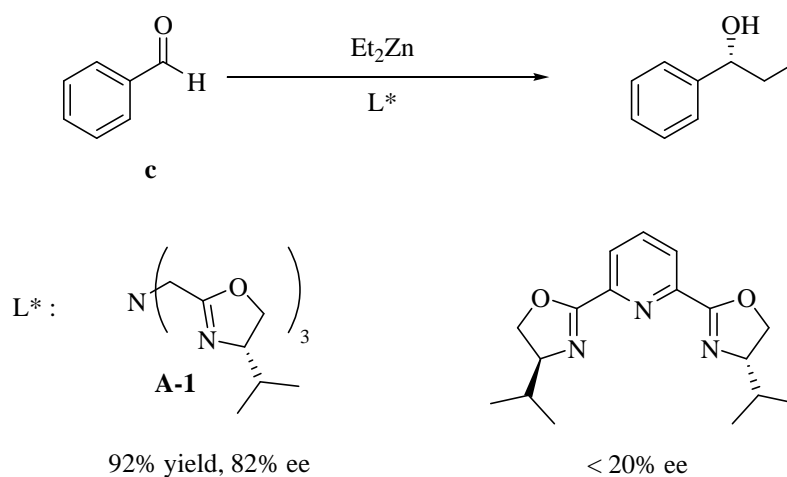
<sup>37</sup> Y. Kohmura, K. Kawasaki, T. Katsuki, *Synlett* **1997**, 1456.



**Scheme 1.2.7:** Allylic amination catalysed by **A-2** trisox and *t*Bu-BOX

Even if this application of the  $C_3$ -symmetric trisoxazoline **A-2** was not successful one can notice that the trisoxazoline gave higher selectivity than the bisoxazoline under the same reaction conditions.

The same observation was made by Chan *et al.* when they applied trisoxazoline **A-1** in the enantioselective addition of diethylzinc to benzaldehyde. They found that their ligand was able to catalyse the addition of diethylzinc to benzaldehyde with ee up to 82% (Scheme 1.2.8).<sup>27</sup>



**Scheme 1.2.8:** Addition of  $Et_2Zn$  to benzaldehyde catalysed by **A-1** and *i*Pr-Pybox

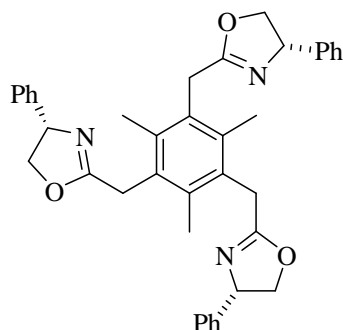
Noticeably, the tridentate bisoxazoline (*i*Pr-Pybox) achieved only less than 20% ee under the same reaction conditions. This suggests that the chiral environment created by the trisoxazoline was more effective for this reaction than the one from the Pybox.

b. Chiral trisoxazolines of type C

Kemp's acid derived **C**-type trisoxazolines were also applied in asymmetric catalysis.<sup>29</sup> In the allylic oxidation of cyclopentene **a1** (Scheme 1.2.6) the phenyl-substituted ligand proved to be better than its analogues (methyl- and isopropyl-substituted trisox) but only a moderate ee value was obtained: 94% yield, 45% ee (*S*). In the asymmetric addition of diethylzinc to aldehyde the isopropyl-substituted trisox was the most efficient. However, the cyclohexane-based ligands again only afforded moderate ee values (43% ee, 46% yield).

c. Chiral trisoxazolines of type D and E

Benzene-based trisoxazolines were initially applied in molecular recognition and the group of Ahn mainly contributed to the use of trisox in host-guest complexes. The first successful result reported in the literature was the promising application of **D**-type trisoxazolines as artificial receptors for alkylammonium ions.<sup>30</sup> The chiral recognition of  $\alpha$ -chiral primary ammonium ions was mostly achieved in a  $C_1$ - or  $C_2$ -symmetric environment. Ahn *et al.* accomplished for the first time the enantiomeric recognition of  $\alpha$ -chiral primary ammonium ions using  $C_3$ -symmetric trisoxazolines **D** as the acceptor (Figure 1.2.6).<sup>38</sup>



Racemic ammonium guest	Enantioselectivity <sup>a</sup>	Extraction
<i>α</i> -phenylethylamine	71 ( <i>R</i> ) : 29 ( <i>S</i> )	82
<i>α</i> -(1-naphtyl)ethylamine	70 : 30	99
phenylglycine methyl ester	78 ( <i>S</i> ) : 22 ( <i>R</i> )	60
alanine methyl ester	53 ( <i>S</i> ) : 47 ( <i>R</i> )	41

<sup>a</sup>ee of the ammonium ion extracted from excess racemic  $\text{RNH}_3^+\text{Cl}^-$

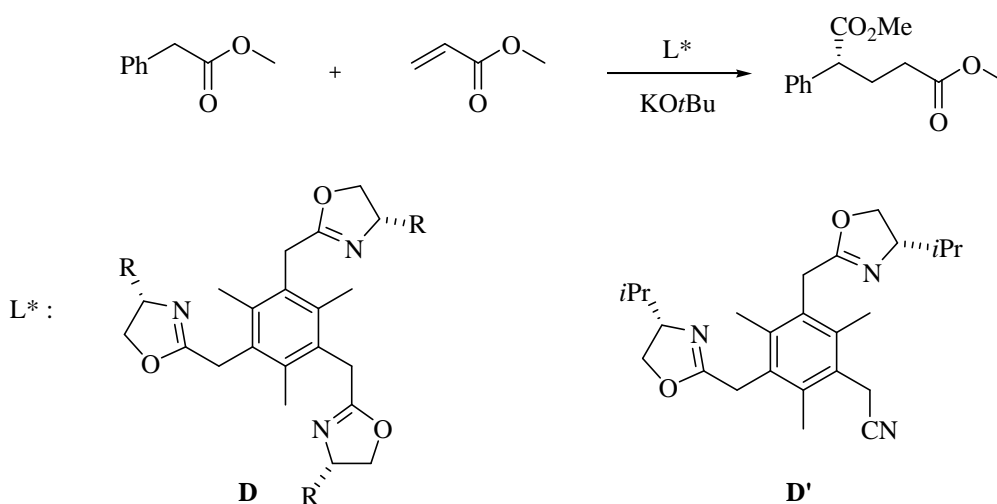
**Figure 1.2.6:** Enantioselective binding of trisoxazoline **D** toward racemic ammonium salts and % extraction

With the knowledge that the three nitrogen atoms from the trisoxazolines can act as H-bonding acceptors and that a central aromatic groups can act as  $\pi$ -donor for CH- $\pi$  interactions,

<sup>38</sup> S.-G. Kim, K.-H. Kim, J. Jung, S. K. Shin, K. H. Ahn, *J. Am. Chem. Soc.* **2002**, 124, 591.

Hong *et al.* focused on the application of their benzene-based trisox **E** as artificial receptors for sugar and alcohols.<sup>31</sup>

In the course of their study on the selective molecular recognition of ammonium over potassium ions using benzene-based trisoxazolines **D** as artificial receptors, Ahn *et al.* found that these ligands have significant affinities towards potassium ions.<sup>39</sup> This finding led to the evaluation of the trisoxazolines as chiral ligands in catalytic enantioselective reactions that involve complexes of potassium ions such as potassium enolates. They applied **D**-type trisoxazolines in the Michael addition of methyl phenylacetate to methyl acrylate (Scheme 1.2.9).



**Scheme 1.2.9:** Enantioselective Michael addition catalysed by L\*-KOtBu complexes

It was found that the **D**-type trisoxazolines in combination with potassium *t*-butoxide afforded the desired product in moderate to high yields with ee values up to 82% using the *t*-butyl-substituted trisoxazoline. Ahn *et al.* proposed that the ligand coordinates to the potassium enolate in a tripodal fashion. Two control experiments confirmed this suggestion: i) **D** in combination with sodium *t*-butoxide proved to be unsuccessful in this reaction; ii) bisoxazoline **D'** failed to promote this reaction.

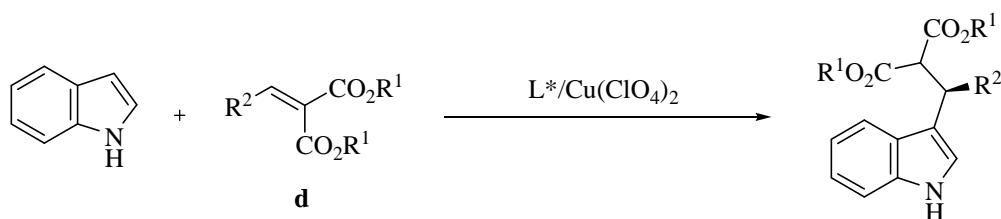
<sup>39</sup> K. H. Ahn, S.-G. Kim, J. Jung, K.-H. Kim, J. Kim, J. Chin, K. Kim, *Chem. Lett.* **2000**, 170.



#### d. Chiral trisoxazolines of type **F**

Pseudo  $C_3$ -symmetric trisoxazolines have been employed in various enantioselective catalytic reactions.<sup>40</sup> Tang *et al.*, who were interested in the potential “sidearm effect” chose the modular synthesis to prepare pseudo  $C_3$ -symmetric trisoxazolines, trisoxazolines with mixed oxazoline units and bisoxazolines functionalised with a large variety of sidearms.

With the aim of probing the effect of the structural differences between bisoxazolines and pseudo  $C_3$ -symmetric trisoxazolines, **F-1** was first applied in the Friedel-Crafts reaction of indole with alkylidene malonates **d** (Scheme 1.2.10).



**Scheme 1.2.10:** Enantioselective Friedel-Crafts reaction of indole with alkylidene malonates

The first enantioselective version of this reaction was reported by Jørgensen *et al.* with bisoxazolines as chiral ligands and the catalyst  $tBu$ -BOX/ $Cu(OTf)_2$  afforded ee values up to 69%.<sup>41</sup> Tang and coworkers found that the chiral catalyst **F-1**/ $Cu(ClO_4)_2$  could catalyse this reaction with yields and ee values up to 99 and 93% respectively.<sup>30</sup> A screening of the reaction conditions and the ligands was carried out to improve the enantiomeric excess and to understand the differences observed between the ligands.<sup>33,36,42,43</sup> All their results support the idea that coordination of the side-armed oxazoline in trisox **F-1** tuned the electronic and steric properties of the catalyst to influence the enantioselectivity and reactivity and to lead to improved catalytic properties compared to the bisoxazoline analogues.

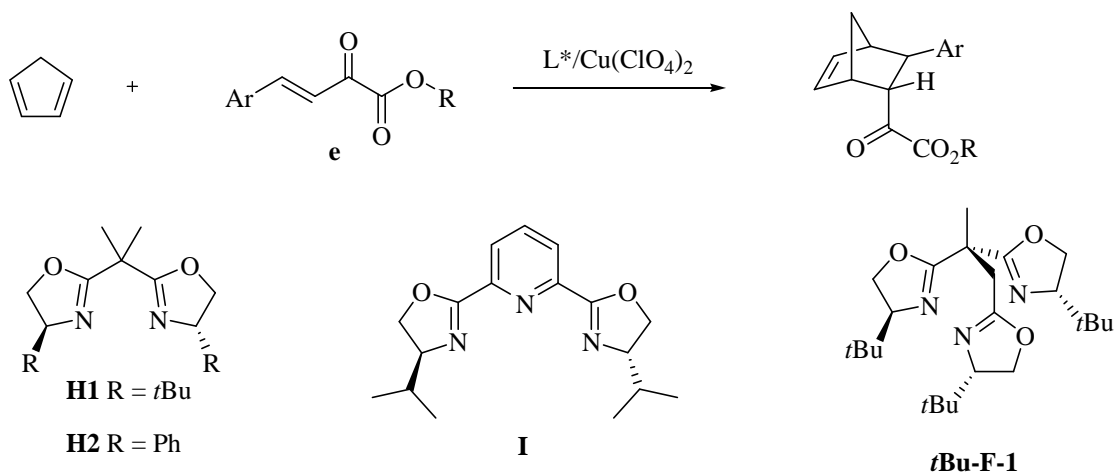
Pseudo  $C_3$ -symmetric **F**-type trisoxazolines also proved to be efficient in the copper catalysed Diels-Alder reaction of cyclopentadiene with ketoester **e** (Scheme 1.2.11).

<sup>40</sup> See for example: a) M.-C. Ye, J. Zhou, Z.-Z. Huang, Y. Tang, *Chem. Commun.* **2003**, 2554; b) Z.-Z. Huang, Y.-B. Kang, J. Zhou, M.-C. Ye, Y. Tang, *Org. Lett.* **2004**, 6, 1677; c) M.-C. Ye, J. Zhou, Y. Tang, *J. Org. Chem.* **2006**, 71, 3576.

<sup>41</sup> W. Zhuang, T. Hansen, K. A. Jørgensen, *Chem. Commun.* **2001**, 347.

<sup>42</sup> J. Zhou, M.-C. Ye, Z.-Z. Huang, Y. Tang, *J. Org. Chem.* **2004**, 69, 1309.

<sup>43</sup> J. Zhou, Y. Tang, *Chem. Commun.* **2004**, 432.



L*	Temp (°C)	Yield (%)	exo/endo	ee% (endo)
<b>H1</b>	-35	52	8/92	53
<b>H2</b>	-35	58	8/92	0
<b>I</b>	0	63	12/88	4
<b><i>t</i>Bu-F-1</b>	-35	64	3/97	71

**Scheme 1.2.11:** Enantioselective Diels-Alder reaction of cyclopentadiene with ketoester

Here again, the bisoxazolines (**H1** and **H2**) failed to achieve better activity as well as selectivity than the trisoxazolines. It should be noted that the tridentate bisoxazoline **I** showed almost no selectivity as well as much lower catalytic activity and thus higher temperatures were required to complete the reaction.

#### e. Conclusion

Despite the development of new synthetic strategies, there are only few trisoxazoline ligands known compared to the large number of bisoxazolines reported in the literature. Nevertheless, inspired by the versatility of the latter, trisoxazolines have been applied in asymmetric catalysis and have proven to afford, in numerous cases, superior catalysts than the bisoxazolines-based systems.

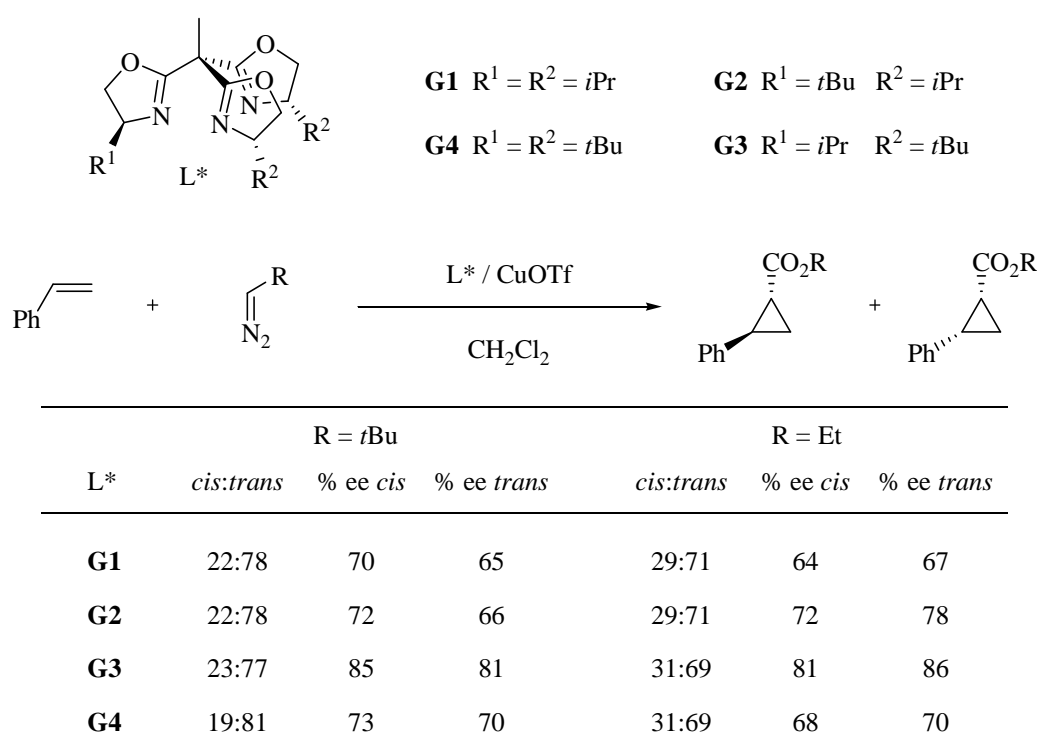
However, one should notice that the trisoxazolines successfully applied in asymmetric catalysis are conformationally very flexible and the way they coordinate to the metal centres in the active catalysts remains an open, unsolved question. Indeed the facial coordination to transition metals has not been firmly established for all these trisoxazolines.

The development of the class of 1,1,1-tris(oxazolinyl)ethane ligands gives us access to highly symmetrical ligands which provide a geometry of the metal binding site that is most

adapted to tripodal coordination of the metal centre and would lead to relatively rigid and well-defined coordination geometry.

#### 4. 1,1,1-tris(oxazolinyl)ethane: precedent in the group

The new class of chiral trisoxazolines developed in our group was first applied in the copper(I) catalysed cyclopropanation of styrene with *t*-butyl or ethyl diazoacetate (Scheme 1.2.12).<sup>35</sup>

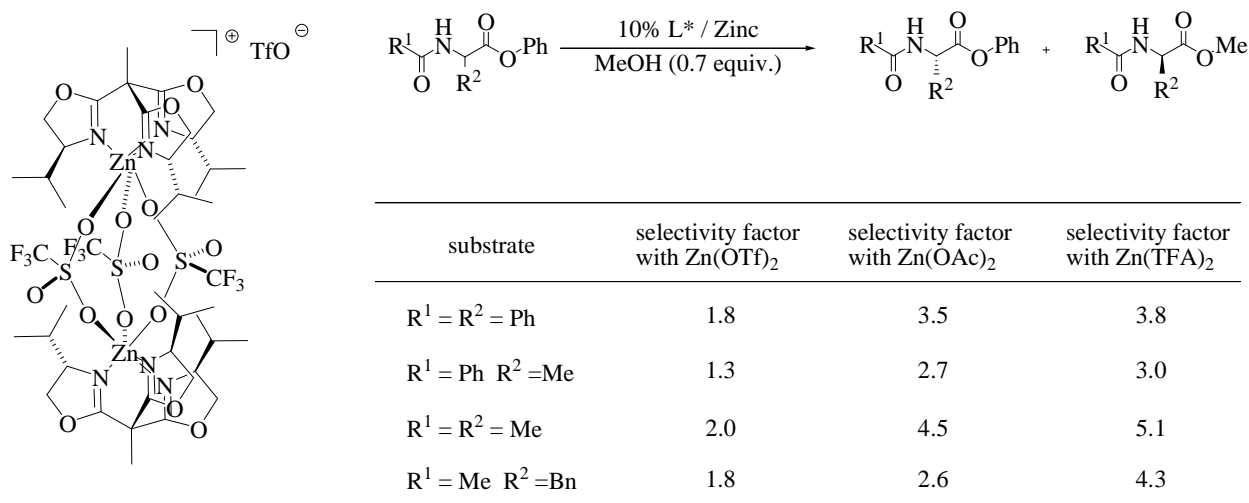


**Scheme 1.2.12:** Copper-catalysed asymmetric cyclopropanation of styrene with *t*-butyl diazoacetate

The strong preference for the *trans* diastereomer is similar to results which were previously obtained with bisoxazoline derivatives. Variation of the stereoselectivity was observed depending on the substituents present on the oxazoline units and was maximised for the non-symmetrical ligand **G3**. Although these results did not surpass those obtained with bisoxazolines, they revealed that mixed trisoxazolines might be sometimes more efficient than highly symmetric trisox derivatives due to a better compatibility with catalytic intermediates thus achieving higher enantiofacial control.

Knowing that in many of the zinc-based peptidases a tris(histidine) binding site acts as a tripodal ligand for the metal ion, a trisoxazoline/zinc complex was applied as a functional enzyme model in the kinetic resolution of racemic chiral esters by transesterification (Scheme

1.2.13). In this system the trisox ligand acts as a mimic of both the tris(histidine) binding site and the chiral environment of a protein skeletal structure.<sup>44</sup>



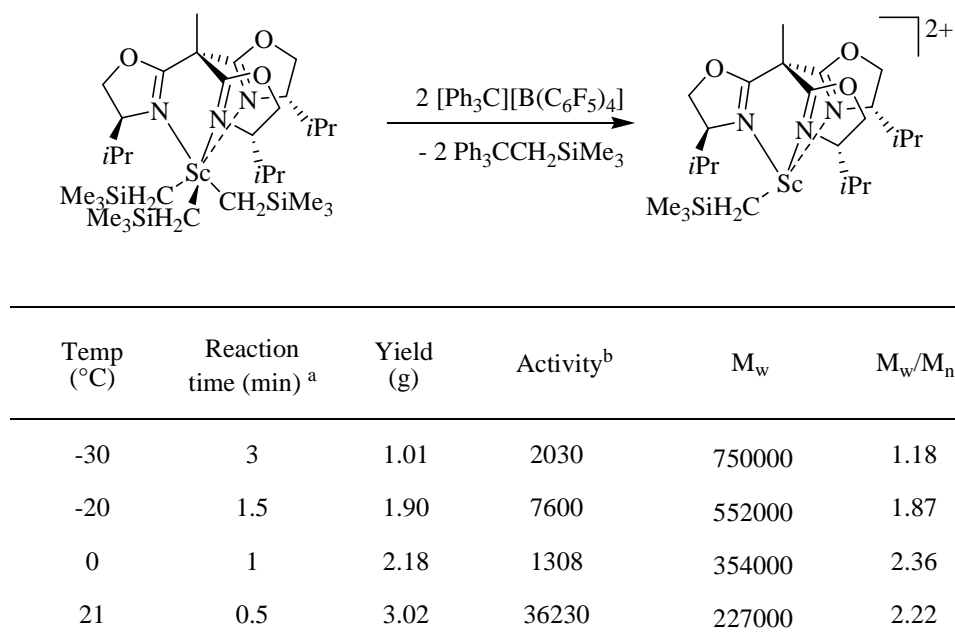
**Scheme 1.2.13:** Partial kinetic resolution of activated amino acid esters by streoselective [trisox-Zn]-catalysed transesterification

This was the first example of non-enzymatic zinc(II) catalyst for asymmetric transesterification of activated esters. The anions of the zinc(II) complex obviously influenced the selectivity factors. Upon going from the zinc triflate to the zinc acetate complex and further to the trifluoroacetate complex, an increase of the selectivity factor for all the substrates was observed (up to  $s = 5.1$ ). The importance of the chiral tripod-zinc environment for the observed stereoselectivity was inferred from the observation that the coordination of a range of bisoxazolines to a zinc salt did not induce kinetic resolution.

More recently it has been shown that the  $C_3$ -chiral trisox ligands are suitable supporting ligands for scandium(III) catalysed olefin polymerisation. The trialkyl complex [Sc(*i*Pr-trisox)(CH<sub>2</sub>SiMe<sub>3</sub>)<sub>3</sub>] was activated with two equivalents of the trityl salt [Ph<sub>3</sub>C][B(C<sub>6</sub>F<sub>5</sub>)<sub>4</sub>], thus affording a double charged species which was assigned as [Sc(*i*Pr-trisox)(CH<sub>2</sub>SiMe<sub>3</sub>)<sub>3</sub>]<sup>2+</sup>. This dicationic species was found to be highly active for the polymerisation of 1-hexene at low temperatures, producing highly isotactic poly(1-hexene) (Scheme 1.2.14).<sup>45</sup>

<sup>44</sup> C. Dro, S. Bellemin-Lapponnaz, R. Welter, L. H. Gade, *Angew. Chem. Int. Ed.* **2004**, *43*, 4479; *Angew. Chem.* **2004**, *116*, 4579.

<sup>45</sup> B. D. Ward, S. Bellemin-Lapponnaz, L. H. Gade, *Angew. Chem. Int. Ed.* **2005**, *44*, 1668; *Angew. Chem.* **2005**, *117*, 1696.



<sup>a</sup> reaction judged complete when reaction stopped stirring. <sup>b</sup> kg·mol[Sc]<sup>-1</sup>·h<sup>-1</sup>

**Scheme 1.2.14:** Polymerisation of 1-hexene catalysed by the dicationic [Sc(*i*Pr-trisox)(CH<sub>2</sub>SiMe<sub>3</sub>)]<sup>2+</sup> species

In light of these results for a group 3 metal, the polymerisation of  $\alpha$ -olefins with lanthanide catalysts has also been investigated, revealing the first example of isospecific polymerisation of  $\alpha$ -olefins with a C<sub>3</sub>-chiral thulium(III) complex.<sup>46</sup> It has also been shown that the trisox ligand is a suitable supporting environment for a range of lanthanide metals, going from lutetium to dysprosium.<sup>47</sup> To summarise, the C<sub>3</sub>-symmetric environment is efficient at transmitting the chiral information to the catalytic site in the stereoselective olefin polymerisation, with a remarkable degree of tacticity being observed for a range of  $\alpha$ -olefins.

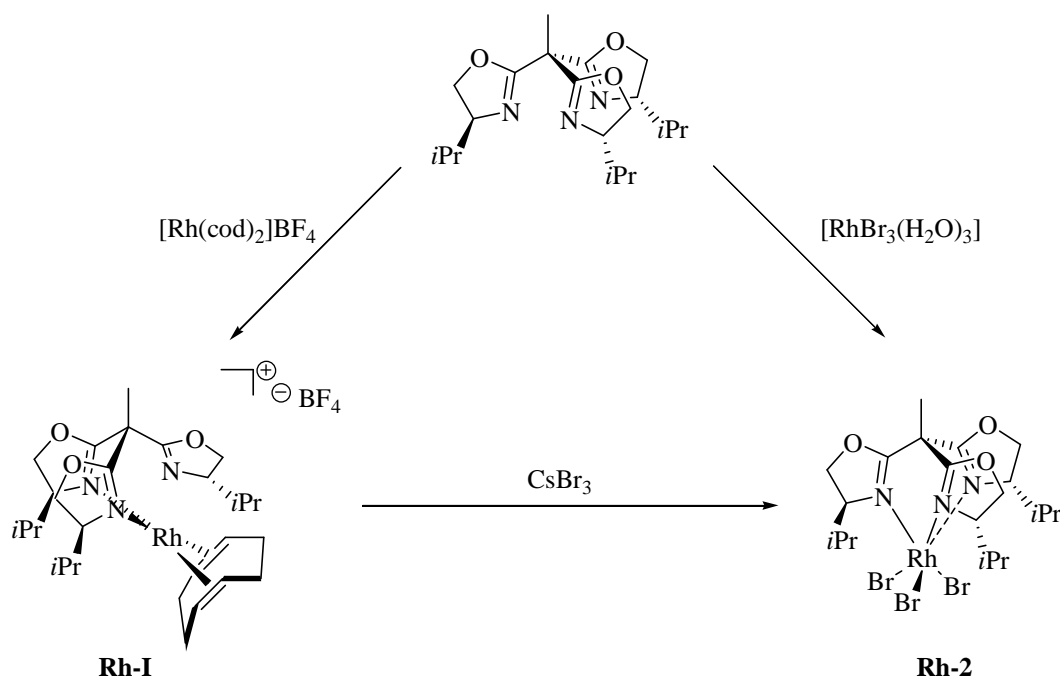
We have seen that 1,1,1-tris(oxazolinyl)ethane ligands are versatile supporting ligands for a variety of early and late transition metals as well as lanthanides and that the chiral centre on the ligand framework is such that the chiral information is efficiently transferred to the catalytically active site. In addition, the facial coordination to transition metals in octahedral complexes has been firmly established.

Nevertheless the formation of this structural motif may be impeded if the transition metal centre stereoelectronically strongly favours a non-delta-hedral coordination sphere. This is generally the case for the heavier *d*<sup>8</sup>-transition metal atoms/ions and their preference for square planar coordination geometries. In order to assess the coordinating behaviour of the trisox ligands towards metal centres which favour or disfavour facial coordination, depending on their

<sup>46</sup> L. Lukešová, B. D. Ward, S. Bellemin-Laponnaz, H. Wadepl, L. H. Gade, *Dalton Trans.* **2007**, 920.

<sup>47</sup> L. Lukešová, B. D. Ward, S. Bellemin-Laponnaz, H. Wadepl, L. H. Gade, *Organometallics*, **2007**, DOI: 10.1021/om700504f.

oxidation state (and thus *d* electron count), the coordination chemistry of *i*Pr-trisox with rhodium(I) and (III) has been investigated (Scheme 1.2.15).<sup>48</sup>



**Scheme 1.2.15:** Synthesis of  $[\text{Rh}(\textit{i}\text{Pr-trisox})(\text{cod})]\text{BF}_4$  **g** and its reaction by way of oxidative addition with  $\text{CsBr}_3$  giving the octahedral complex  $[\text{RhBr}_3(\textit{i}\text{Pr-trisox})]$  **h**

A possible way to get all the three oxazolines of *i*Pr-trisox coordinated to rhodium is the oxidation of the rhodium(I) complex to rhodium(III). A clean oxidation of **Rh-1** was achieved by stoichiometric reaction with  $\text{CsBr}_3$  which acts both as an oxidant and ligand transfer reagent. The resulting  $\text{Rh}^{\text{III}}$ -complex  $[\text{RhBr}_3(\textit{i}\text{Pr-trisox})]$  (**Rh-2**) could also be directly obtained by heating  $[\text{RhBr}_3(\text{H}_2\text{O})_3]$  in the presence of *i*Pr-trisox.

The crystal structure of **Rh-1** indicates that the overall arrangement of the coordinated bisoxazoline unit is such that the uncoordinated oxazoline ring points towards the rhodium atom. Thus, the unbound oxazoline appears to be ready to exchange with a coordinated heterocycle suggesting a potentially fluxional structure with a very low energy barrier for chemical exchange. This was demonstrated by variable temperature  $^1\text{H}$  NMR studies.

The transformation described has shown that the coordination mode of the trisox ligand adapts to the stereoelectronic requirements of the metal centre and may change in the process of an elementary transformation such as the oxidative addition of bromine. This may be viewed as a model reaction for such reaction steps in a catalytic cycle. If the stereoselectivity determining

<sup>48</sup> L. H. Gade, G. Marconi, C. Dro, B. D. Ward, M. Poyatos, S. Bellemin-Lapponnaz, H. Wadepohl, L. Sorace, G. Poneti, *Chem. Eur. J.* **2007**, *13*, 3058.

step involves an octahedral species, the facial coordination of the trisox ligand and consequent threefold symmetry of the trisox-metal fragment will simplify the “stereoselection” whilst the symmetry of the ligand will act “dynamically” in species in which it is bidentate.

### III. 1,1,1-tris(oxazoliny)ethane and the influence of $C_3$ symmetry in catalysis

#### I. $C_3$ symmetry in asymmetric catalysis

##### a. Introduction

Symmetry is a fascinating phenomenon which provides endless stimulation and challenges. It gives an impression of harmonious or aesthetically-pleasing proportionality and balance and reflects beauty or perfection. An additional appeal of symmetry is that of simplicity, implying of safety, security, and familiarity. Symmetry is to be found in many creations of nature and in some of the greatest achievements of mankind. In chemistry, higher order symmetry has always attracted interest. Given that rotational axes are the only elements of symmetry compatible with chirality,  $C_2$ - and  $C_3$ -symmetrical molecules have attracted considerable attention. In recent years, the aesthetic appeal of  $C_2$ -symmetrical molecules has been translated into many widely used applications in asymmetric synthesis and catalysis, in particular those involving phosphines and bisoxazolines.<sup>13d,49</sup> In contrast, exploitation of  $C_3$  symmetry (Figure 1.3.1) is still in its infancy, as reflected in the paucity of trisoxazolines in comparison to bisoxazolines.

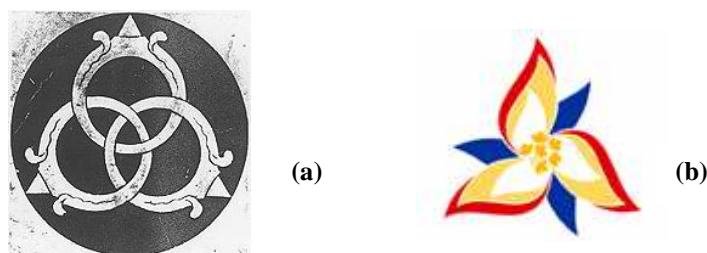


**Figure 1.3.1:** (a) The Borromean rings, (b) Trillium flower, floral emblem of the Province of Ontario (Canada)

Nevertheless the usefulness and potential advantages of  $C_3$  symmetry in the design of chiral stereodirecting ligands for asymmetric catalysis has already been demonstrated.<sup>50,51,52</sup> In

<sup>49</sup> a) A. Pfaltz, W. J. Drury, *Proc. Natl. Acad. Sci. USA* **2004**, *101*, 5723; b) S. Castillon, C. Claver, Y. Diaz, *Chem. Soc. Rev.* **2005**, *34*, 702; c) G. Desimoni, G. Faita, K. A. Jørgensen, *Chem. Rev.* **2006**, *106*, 3561.

<sup>50</sup> a) S. E. Gibson, M. P. Castaldi, *Chem. Commun.* **2006**, 3045; b) S. E. Gibson, M. P. Castaldi, *Angew. Chem. Int. Ed.* **2006**, *45*, 4718; *Angew. Chem.* **2006**, *118*, 4834; c) C. Moberg, *Angew. Chem. Int. Ed.* **2006**, *45*, 4721; *Angew. Chem.* **2006**, *118*, 4838.

most of the cases,  $C_3$  symmetry is related to facially coordinating tripodal ligands because threefold rotational symmetry represents the only possibility adapted to this topology of ligation, in the same way that  $C_2$  symmetry is related to simple chelation.<sup>53</sup>

Transition metal complexes of threefold symmetric ligands are of interest because three equivalent open coordination sites can be obtained. Potentially such systems could provide highly stereocontrolled catalysis for reactions which proceed via octahedral intermediates. This concept is discussed in the following paragraph.

#### b. Symmetry in metal complexes

In the most favourable case symmetry of the ancillary ligand fits symmetry of the complex. In that case, a symmetrical stereodirecting ligand may lead to a reduced number of transition states and diastereomeric reaction intermediates in transformations occurring in the coordination sphere of its complexes. In such favourable cases, this degeneration of alternative reaction pathways may lead to high stereoselectivity in catalytic reactions and greatly simplifies the analysis of such transformations.

Let us consider the case of  $C_2$ - and  $C_3$ -symmetric ligands to explain the molecular equivalence caused by rotational axes in metal complexes.<sup>20</sup>  $C_2$  symmetry is characterised by the fact that upon rotation of the  $C_2$ -symmetric species by  $180^\circ$  about the rotational axis an identical species is obtained. This implies that two complexes which are identical in the case of  $C_2$  symmetry would be diastereomeric in the case of  $C_1$  symmetry. Concerning threefold rotational symmetry, each rotation of  $120^\circ$  about the rotation axis affords an identical species.

We can illustrate this by considering a square planar metal complex containing a bidentate  $C_2$ -symmetric ligand. This situation is the most favourable since it renders the two remaining coordination sites identical, *i.e.* homotopic (Scheme 1.3.1. a, A = B). In the case of static  $\kappa^3$ -facial coordination of a tridentate  $C_3$ -symmetric ligand the same type of favourable

---

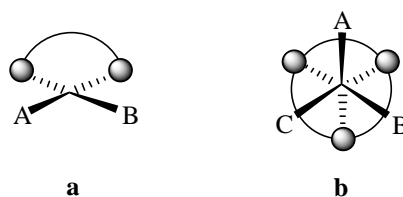
<sup>51</sup> Examples of the use of chiral  $C_3$ -symmetrical ligands in asymmetric catalysis: a) H. Brunner, A. F. M. M. Rahman, *Chem. Ber.* **1984**, *117*, 710; b) M. J. Burk, R. L. Harlow, *Angew. Chem. Int. Ed. Engl.* **1990**, *29*, 1467; *Angew. Chem.* **1990**, *102*, 1511; c) M. J. Burk, J. E. Feaster, R. L. Harlow, *Tetrahedron: Asymmetry* **1991**, *2*, 569; d) H. Adolfsson, K. Wärnmark, C. Moberg, *J. Chem. Soc., Chem. Commun.* **1992**, 1054; e) D. D. LeCloux, W. B. Tolman, *J. Am. Chem. Soc.* **1993**, *115*, 1153; f) D. D. LeCloux, C. J. Tokar, M. Osawa, R. P. Houser, M. C. Keyes, W. B. Tolman, *Organometallics* **1994**, *13*, 2855; g) K. Kawasaki, S. Tsumura, T. Katsuki, *Synlett* **1995**, 1245; h) M. C. Keyes, V. G. Young Jr., W. B. Tolman, *Organometallics* **1996**, *15*, 4133; i) W. A. Nugent, *J. Am. Chem. Soc.* **1998**, *120*, 7139; j) T. Fang, D.-M. Du, S.-F. Lu, J. Xu, *Org. Lett.* **2005**, *7*, 2081.

<sup>52</sup> Recent advances in the design of  $C_3$ -chiral podands: a) G. Bringmann, M. Breuning, R.-M. Pfeifer, P. Schreiber, *Tetrahedron: Asymmetry* **2003**, *14*, 2225; b) G. Bringmann, R.-M. Pfeifer, C. Rummey, K. Hartner, M. Breuning, *J. Org. Chem.* **2003**, *68*, 6859; c) T. Fang, D.-M. Du, S.-F. Lu, J. Xu, *Org. Lett.* **2005**, *7*, 2081; d) M. P. Castaldi, S. E. Gibson, M. Rudd, A. J. P. White, *Angew. Chem. Int. Ed.* **2005**, *44*, 3432; *Angew. Chem.* **2005**, *117*, 3498; e) M. P. Castaldi, S. E. Gibson, M. Rudd, A. J. P. White, *Chem. Eur. J.* **2005**, *12*, 138.

<sup>53</sup> H. B. Kagan, T.-P. Dang, *J. Am. Chem. Soc.* **1972**, *94*, 6429.

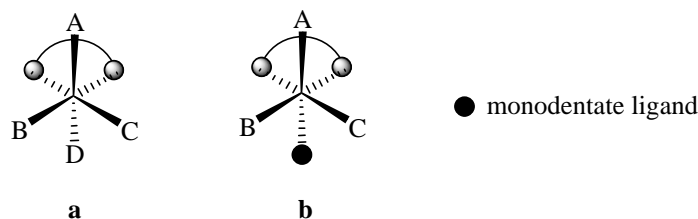


situation is created in octahedral complexes where the three remaining coordination sites are homotopic (Scheme 1.3.1 **b**,  $A = B = C$ ).



**Scheme 1.3.1:** Favourable situations in square planar (**a**) and octahedral (**b**) complexes with  $C_2$ - and  $C_3$ -symmetric ligands respectively

An unfavourable situation is obtained by combination of octahedral complexes and  $C_2$ -symmetric ligands. Introduction of a bidentate  $C_2$ -symmetric ligand in an octahedral environment results in a complex with two sets of coordination sites which are pairwise homotopic (A/D and B/C) but mutually diastereotopic (Scheme 1.3.2 **a**). Coordination of an additional monodentate ligand affords a complex with three diastereotopic coordination sites (Scheme 1.3.2 **b**,  $A \neq B \neq C$ ).

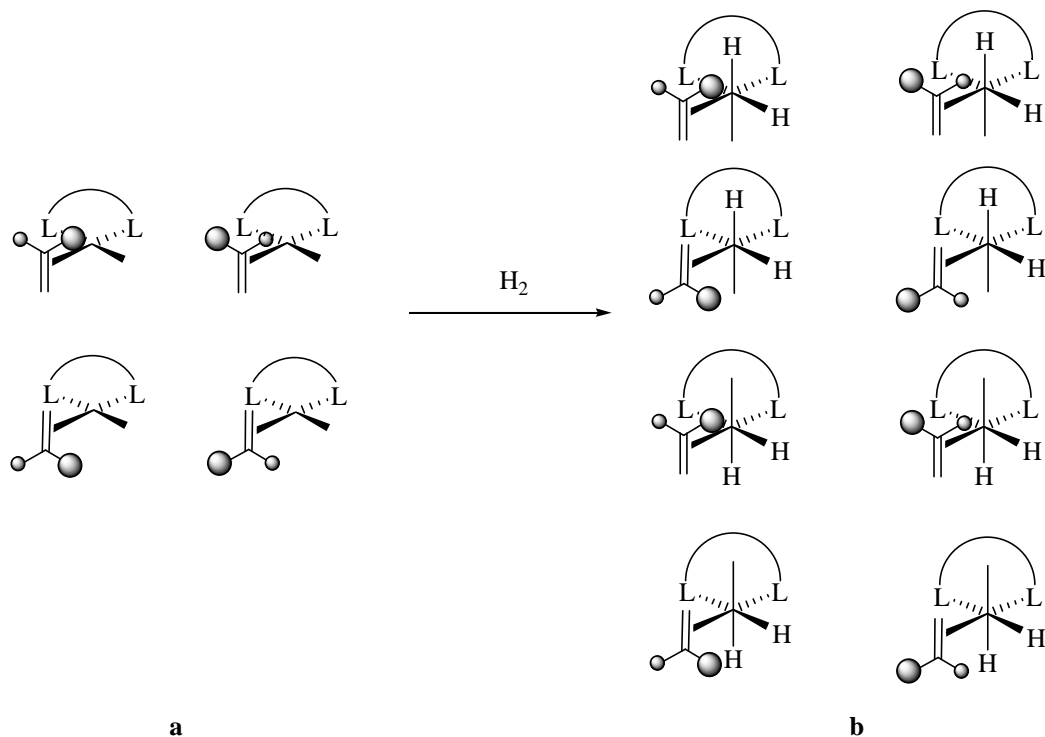


**Scheme 1.3.2:** Unfavourable situation with  $C_2$ -symmetric ligands in octahedral environment

Thus, we can conclude that  $C_2$ -symmetric ligands are adapted to square planar geometries whereas  $C_3$ -symmetric ligands act similarly for octahedral environments. To illustrate this, we can analyse the case of a prochiral olefin which is coordinated to a complex containing either a bidentate ligand with a twofold rotational axis or a tridentate ligand with a threefold rotational axis. These situations take place in common catalytic reactions such as hydroformylations or hydrogenations. For our illustration, we consider the specific example of a catalytic hydrogenation where the coordination of the olefin is assumed to occur before the oxidative addition of hydrogen.

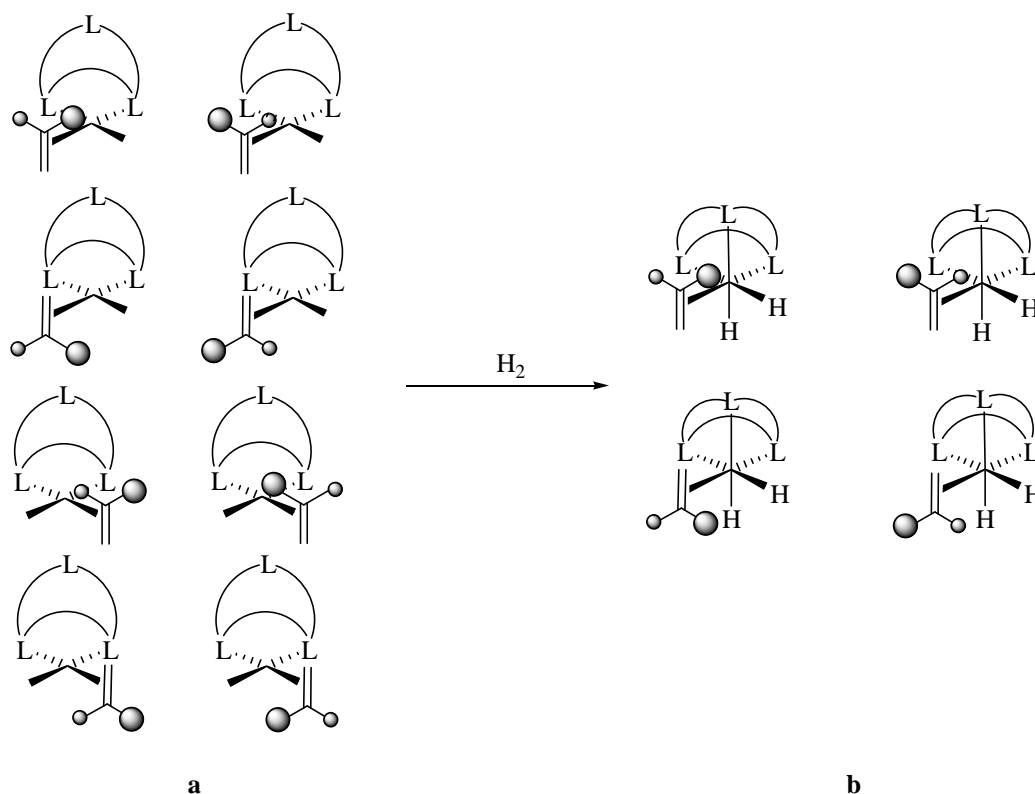
In a square planar complex containing a bidentate  $C_2$ -symmetric ligand, there are two homotopic free coordination sites. In that case, four possibilities exist for the coordination of the prochiral olefin (Scheme 1.3.3 **a**) since coordination to the second site would lead to a set of

identical complexes due to the  $C_2$  symmetry of the ligand. The oxidative addition of dihydrogen affords an octahedral complex and renders the two coordination sites left diastereotopic. In consequence, eight diastereomeric complexes are possible (Scheme 1.3.3 **b**).



**Scheme 1.3.3:** Square planar metal-olefin complexes containing a bidentate  $C_2$ -symmetric ligand (**a**); eight diastereomeric octahedral species after oxidative addition of H<sub>2</sub> (**b**)

In contrast, in a square planar complex containing a tridentate  $C_3$ -symmetric ligand there are two diastereotopic free coordination sites. In that case, eight possibilities exist for the coordination of the prochiral olefin (Scheme 1.3.4 **a**). But here the oxidative addition of dihydrogen affords an octahedral complex where the three coordination sites are homotopic in presence of a tridentate  $C_3$ -symmetric ligand. In consequence, only four diastereomeric complexes are possible (Scheme 1.3.4 **b**).

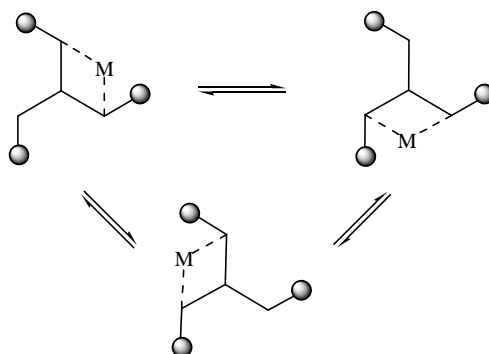


**Scheme 1.3.4:** Square planar metal-olefin complexes containing a tridentate C<sub>3</sub>-symmetric ligand (**a**); four diastereomeric octahedral species after oxidative addition of H<sub>2</sub> (**b**)

To summarise C<sub>2</sub>-symmetric ligands should reduce the number of possible diastereomers in catalytic cycles involving square planar intermediates whereas C<sub>3</sub>-symmetric ligands do so for octahedral catalytic intermediates.<sup>20</sup>

## 2. Definition of the research project

The stereochemical points made above have been illustrated for static coordination of a symmetrical chiral tripod. However, threefold symmetrical chiral ligand may generate a simplification in the stereochemistry of the key catalytic intermediates when it acts as a bidentate ligand in the stereoselectivity determining step, that is to say for metal complexes with stereoelectronic preference for non-octahedral coordination geometries. This will be the case for systems in which chemical exchange between the different  $\kappa^2$ -coordinated species takes place. Such an exchange which induces an equilibrium between identical species for a symmetrical tripod is depicted in Scheme 1.3.5.



**Scheme 1.3.5:** Dynamic exchange of  $\kappa^2$ -coordinated tridentate ligand coordinated to a complex fragment (M)

We have seen that for the reduction of the number of transition states and diastereomeric reaction intermediates, octahedral complexes are associated to threefold rotational symmetry in the same way as square planar complexes are associated to  $C_2$  symmetry. However, one question arises: What is the effect of tridentate  $C_3$ -symmetric ligands on catalytic reactions with intermediates preferring a bidentate coordination mode?

To answer this question, trisoxazolines will be used in several model reactions. The modularity of the ligand design will help us to quantify this influence by applying  $C_3$ - as well as  $C_1$ -symmetric ligands in the different catalytic reactions studied. In addition a direct comparison with the corresponding 2,2-bis(oxazoliny)propane, from which the structure of our trisoxazolines directly stems, will lighten the role of threefold rotational symmetry as well as the role of the third oxazoline arm.

In chapter 2 the synthesis of new  $C_3$ - and  $C_1$ -symmetrical trisoxazolines is described along with the study of the thermal rearrangement of 2-bromooxazolines. The following chapter is devoted to the study of palladium-catalysed asymmetric allylic substitution reactions. Finally, chapter 4 focuses on the use of trisoxazolines in copper-catalysed aminations and Mannich reactions.

## -Chapter 2 -

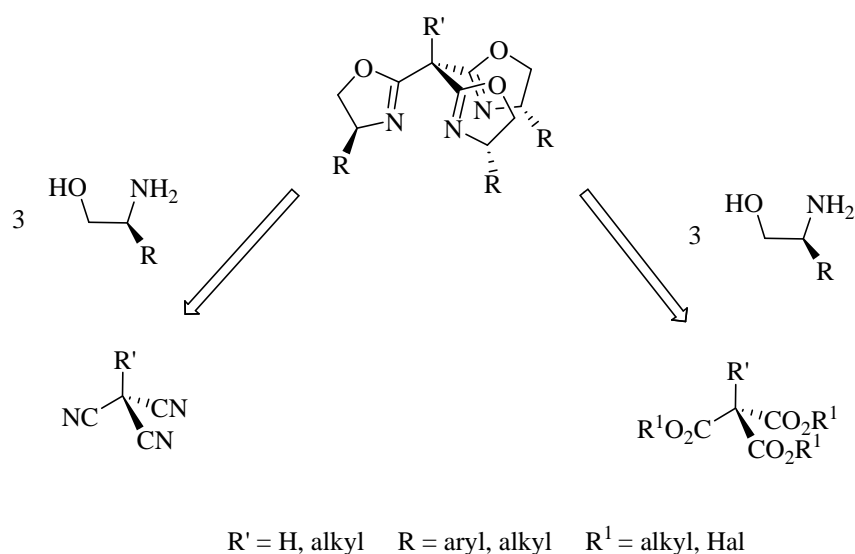
<b>I. Synthesis of highly symmetric trisoxazolines .....</b>	<b>33</b>
1. Principles of the synthetic strategy .....	33
2. Bisoxazolines: Synthesis of synthons containing identical oxazoline rings .....	35
a. Bisoxazolines with phenyl and benzyl substituents .....	35
b. Bisoxazoline with indanyl substituents .....	36
3. Bromooxazolines: From the 2H-oxazolines to the key intermediates .....	37
a. Synthesis of 2H-oxazolines .....	37
b. Synthesis of 2-bromooxazolines .....	38
4. The coupling step: New C <sub>3</sub> -symmetric trisoxazolines .....	39
<b>II. Synthesis of mixed tris- and bisoxazolines.....</b>	<b>42</b>
1. C <sub>1</sub> -symmetric trisoxazolines via the modular approach .....	42
2. Synthesis of mixed 2,2-bis(oxazolinyl)propane ligands .....	43
<b>III. Instability of the 2-bromooxazolines .....</b>	<b>45</b>
1. Ring-opening of the oxazoline unit: General aspects .....	45
2. Thermally induced rearrangement of the 2-bromooxazolines .....	46
3. Conclusion .....	54
<b>IV. Reaction with the <math>\alpha</math>-bromo-isocyanate derivatives.....</b>	<b>54</b>
1. Precedent in the literature .....	54
2. Reaction with phenylethylamine.....	55
a. <b>Pathway I:</b> characterisation of <b>Prod. A</b> .....	56
b. <b>Pathway II:</b> characterisation of <b>Prod. B</b> and <b>Prod. C</b> .....	58
c. Determination of the enantiomeric excess of primary amine .....	61



## I. Synthesis of highly symmetric trisoxazolines

### 1. Principles of the synthetic strategy

Synthesis of 1,1,1-tris(oxazoliny)ethane ligands has been the focus of research interests but attempts to obtain these ligands by sequential cyclisation of the oxazoline rings were unsuccessful.<sup>1</sup> Starting from tris nitrile or tris acid derivatives, decomposition and decarboxylation were observed during the ring closure of the third oxazoline unit (Scheme 2.1.1).



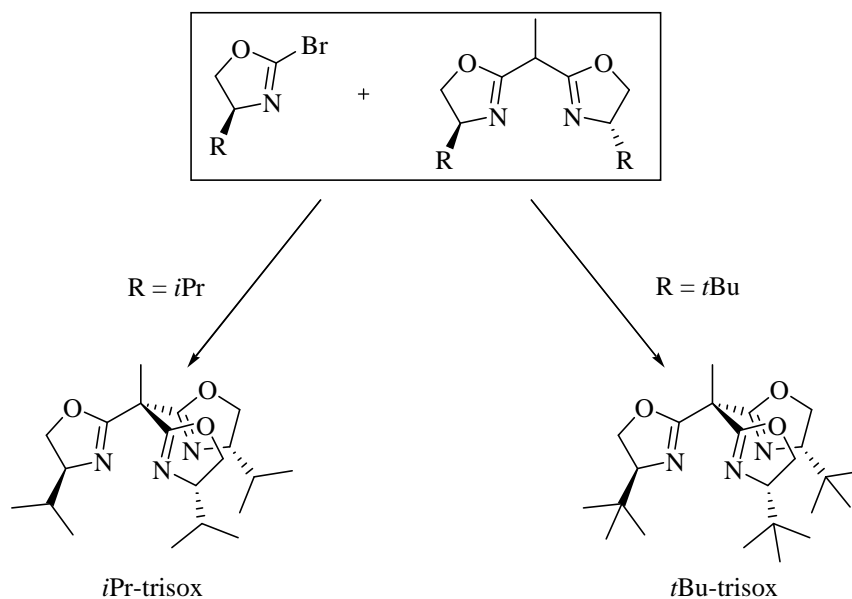
**Scheme 2.1.1:** Attempts to synthesise the trisoxazoline using the direct synthesis

The structure of these particular trisoxazolines with the three heterocycle units bound to the same quaternary carbon centre derives directly from the 1,1-bis(oxazoliny)ethane ligands. The modular strategy developed in our group based on the coupling of two synthons with preformed oxazoline rings, a 1,1-bis(oxazoliny)ethane derivative and an activated 2*H*-oxazoline, enables to overcome the difficulties described above and gives access to the 1,1,1-tris(oxazoliny)ethane ligands which will be abbreviated “substituent-trisox”.<sup>2</sup> Using this novel synthetic approach the preparation of two chiral highly symmetric ligands has first been successfully achieved (Scheme 2.1.2).<sup>3</sup> Reaction of readily accessible lithiated bisoxazolines with the corresponding 2-bromooxazolines affords the *i*Pr-trisox and *t*Bu-trisox in high yields.

<sup>1</sup> C. Moberg, *Angew. Chem. Int. Ed.* **1998**, 37, 248; *Angew. Chem.* **1998**, 110, 260.

<sup>2</sup> S. Bellemin-Laponnaz, L. H. Gade, *Chem. Commun.* **2002**, 1286.

<sup>3</sup> S. Bellemin-Laponnaz, L. H. Gade, *Angew. Chem. Int. Ed.* **2002**, 41, 3473, *Angew. Chem.* **2002**, 114, 3623.



**Scheme 2.1.2:** First chiral  $C_3$ -symmetric trisoxazolines synthesised in our group

In asymmetric catalysis small variations of the ligand structure can dramatically affect the the selectivity of the transformation. This effect is well known in enantioselective reactions with bisoxazoline ligands<sup>4</sup> and thus renders the development of trisoxazolines with new substituents of great importance. Starting from various  $\alpha$ -amino alcohols, coupling between bisoxazolines and 2-bromooxazolines with new substituents can afford novel highly symmetric trisoxazolines. (*R*)-phenylglycinol, (*S*)-phenylalaninol (obtained by reduction of the corresponding amino acid)<sup>5</sup> and (*1R,2S*)-*cis*-1-amino-2-indanol (commercially available) were employed to synthesise new chiral  $C_3$ -symmetric trisoxazolines (Figure 2.1.1).

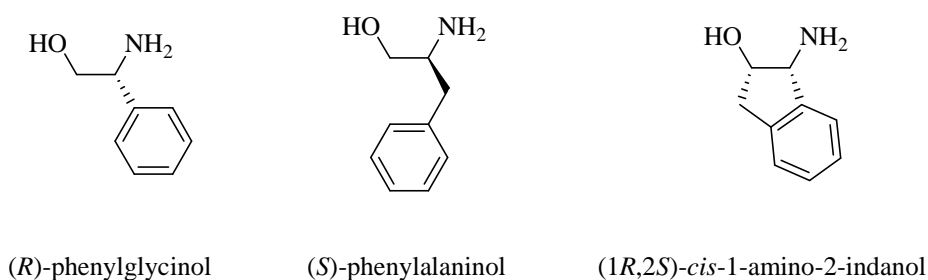


**Figure 2.1.1:** The three  $\alpha$ -amino alcohols used as starting material for the synthesis of new chiral trisoxazolines

In several different enantioselective catalytic reactions, bisoxazolines possessing phenyl substituents have proven to be more efficient than the corresponding ligands with isopropyl or

<sup>4</sup> G. Desimoni, G. Faita, K. A. Jørgensen, *Chem. Rev.* **2006**, *106*, 3561.

<sup>5</sup> a) A. Abiko, S. Masamune, *Tetrahedron Lett.* **1992**, *33*, 5617; b) M. McKennon, A. I. Meyers, *J. Org. Chem.* **1993**, *58*, 3568.



*t*butyl groups. In terms of chiral environment, the benzyl substituent increases the flexibility. In contrast, one major advantage of the indanyl rest is its rigidity. For the development of 1,1,1-(trioxazoliny)ethane ligands the synthesis of the two precursors had to be done first.

## 2. Bisoxazolines: Synthesis of synthons containing identical oxazoline rings

As introduced in the first chapter the design of oxazoline-based ligands for asymmetric catalysis has led to the development of a large variety of bisoxazolines including 2,2-bis(oxazoliny)propane ligands (see Figure 1.1.4). Synthetic strategies of the bisoxazoline intermediates, 1,1-bis(oxazoliny)ethanes, are based on those described for the latter.

### a. Bisoxazolines with phenyl and benzyl substituents

The two target molecules are shown in Figure 2.1.2. The synthesis of 1,1-bis[(4*R*)-4-phenyloxazolin-2-yl]ethane (**1**) has already been reported in the literature<sup>6</sup> and 1,1-bis[(4*S*)-4-benzyloxazolin-2-yl]ethane (**2**) was prepared using the same procedure.

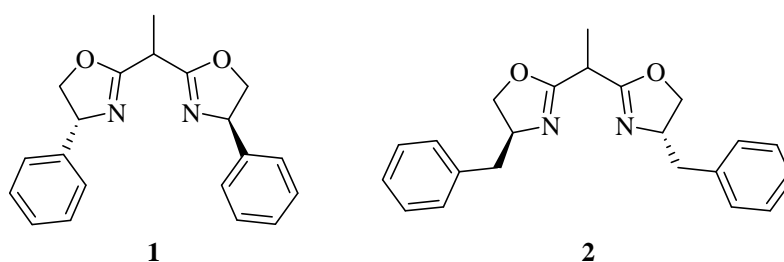
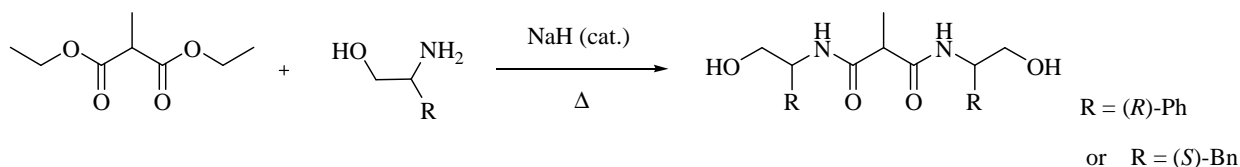


**Figure 2.1.2:** 1,1-bis[(4*R*)-4-phenyloxazolin-2-yl]ethane (**1**) and 1,1-bis[(4*S*)-4-benzyloxazolin-2-yl]ethane (**2**)

The classical first step of the synthesis of 1,1-bis(oxazoliny)ethane ligands is the formation of a diamide starting from a diester or a diacid derivative. Reaction between diethylmethyl malonate and the desired chiral amino alcohol is depicted in Scheme 2.1.3.

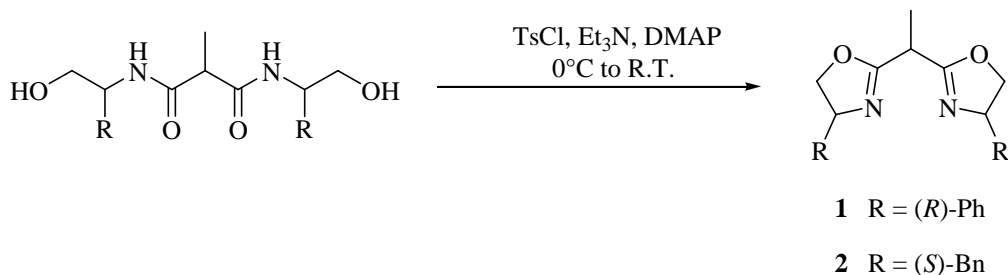


**Scheme 2.1.3:** Synthesis of the chiral diamide from diethylmethyl malonate

<sup>6</sup> J. Bourguignon, U. Bremberg, G. Dupas, K. Hallman, L. Hagberg, L. Hortala, V. Levacher, S. Lutsenko, E. Macedo, C. Moberg, G. Quéguiner, F. Rahm, *Tetrahedron* **2003**, 59, 9583.

In the presence of a catalytic amount of sodium hydride the expected dihydroxy diamides are obtained after transesterification followed by intramolecular amidation. It has to be noted that for the diamide bearing the phenyl substituent the reaction should not be carried out at more than 110°C due to racemisation of the chiral carbon at the benzylic position.

Ring closure is the next step of the synthesis of the bisoxazolines. Several mild approaches have been developed for the cyclisation of hydroxy amides including activation of the alcohol functions with mesylchloride followed by exposure to aqueous methanolic base,<sup>7</sup> use of molybdenum oxide catalysts<sup>8</sup> or of a tetranuclear zinc carboxylate catalyst.<sup>9</sup> To prepare bisoxazolines **1** and **2** the alcohol functions of the corresponding dihydroxy diamides are activated with tosylchloride in the presence of triethylamine and a catalytic amount of dimethylaminopyridine (DMAP). The ring closure is carried out at room temperature over several days without further addition of a base (Scheme 2.1.4).



**Scheme 2.1.4:** Cyclisation of the dihydroxy diamides to form bisoxazolines **1** and **2**

.Cyclisation gives bisoxazoline **1** in 60% yield, in agreement with the results reported by Moberg *et al.*<sup>6</sup> Bisoxazoline **2** is obtained with an overall yield of 45%.

#### b. Bisoxazoline with indanyl substituents

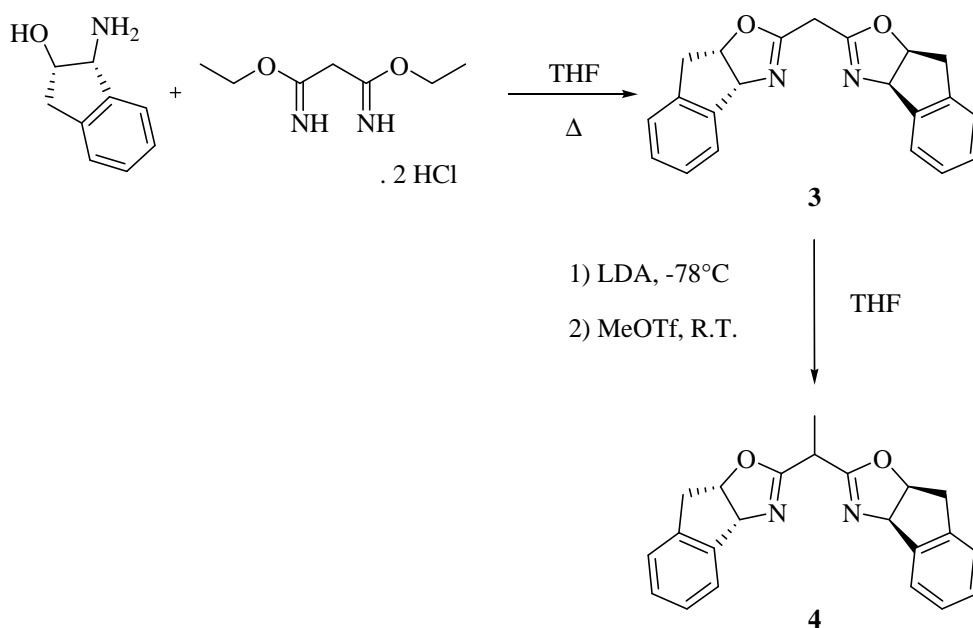
1,1-bis[(4*R*,5*S*)-4,5-indanediyloxazolin-2-yl]ethane must be prepared starting from the strained (1*R*-2*S*)-*cis*-1-amino-2-indanol. However formation of a dihydroxy diamide followed by ring closure is not mechanistically possible in this case. Attack of the amide-oxygen onto the carbon attached to the activated alcohol would involve an inversion of configuration of the latter to give a *trans* indanyl substituent on the oxazoline ring, and this is not possible. The synthesis

<sup>7</sup> a) E. J. Corey, K. Ishihara, *Tetrahedron Lett.* **1992**, 33, 6807; b) S. E. Denmark, N. Nakajima, O. J.-C. Nicaise, A.-M. Faucher, J. P. Edwards, *J. Org. Chem.* **1995**, 60, 4884; c) A. V. Bedekar, E. B. Koroleva, P. G. Andersson, *J. Org. Chem.* **1997**, 62, 2518; d) S. Dagorne, S. Bellemin-Laponnaz, R. Welter, *Organometallics* **2004**, 23, 3053.

<sup>8</sup> A. Sakakura, R. Kondo, K. Ishihara, *Org. Lett.* **2005**, 7, 1971.

<sup>9</sup> T. Ohshima, T. Iwasaki, K. Mashima, *Chem. Commun.* **2006**, 2711.

can be successfully achieved using a procedure which involves another mechanistical pathway and which proceeds *via* the bis[oxazoline-2-yl]methane intermediate **3** (Scheme 2.1.5).



**Scheme 2.1.5:** Reaction scheme of the synthesis of 1,1-bis[(4*R*,5*S*)-4,5-indanediyl]oxazolin-2-yl]ethane **4**

Following a reported procedure, condensation of the corresponding amino alcohol and diethyl malonimidate affords the bis[(4*R*,5*S*)-4,5-indanediyl]oxazolin-2-yl]methane **3** with 60% yield.<sup>10</sup> Treatment with lithium diisopropylamide (LDA) followed by addition of methyl trifluoromethanesulfonate gives the desired monoalkylated bisoxazoline **4** with 59% yield.

### 3. Bromooxazolines: From the 2*H*-oxazolines to the key intermediates

2-Bromooxazolines, the key intermediates in the ligand synthesis, are activated monooxazolines and their synthesis involves the initial formation of 2*H*-oxazolines.

#### a. Synthesis of 2*H*-oxazolines

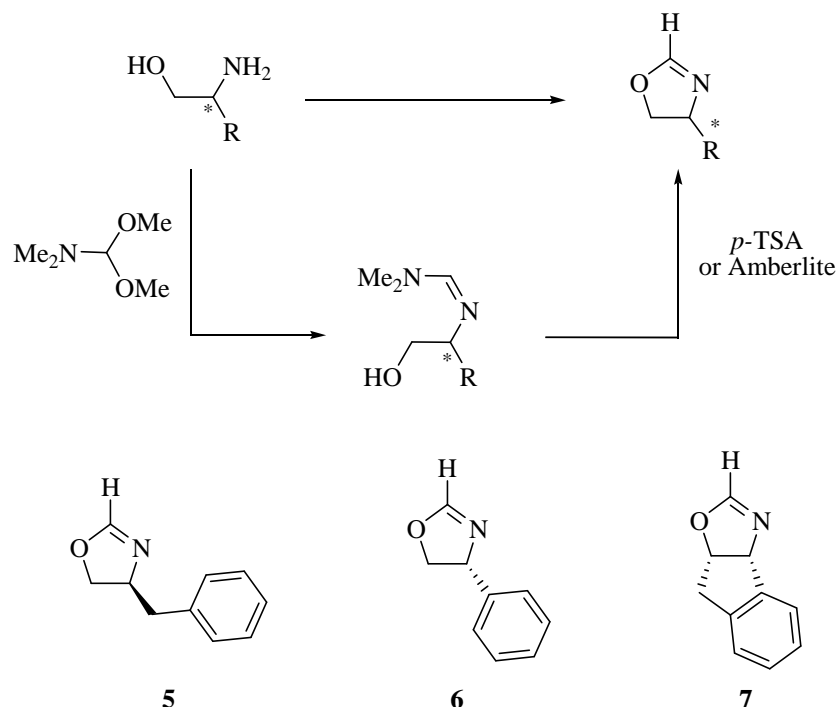
Chiral 2*H*-oxazolines are part of the interesting class of 2-oxazolines and are intermediates for the functionalisation of position 2 of oxazoline units.<sup>11</sup> They are prepared by condensation of an  $\alpha$ -amino alcohol and an activated ester.<sup>12</sup> Meyers *et al.* reported the treatment

<sup>10</sup> D. M. Barnes, J. Ji, M. G. Fickes, M. A. Fitzgerald, S. A. King, H. E. Morton, F. A. Plagge, M. Preskill, S. H. Wagaw, S. J. Wittenberger, J. Zhang, *J. Am. Chem. Soc.* **2002**, *124*, 13097.

<sup>11</sup> T. G. Gant, A. I. Meyers, *Tetrahedron* **1994**, *50*, 2297.

<sup>12</sup> a) W. R. Leonard, J. L. Romine, A. I. Meyers, *J. Org. Chem.* **1991**, *56*, 1961; b) K. Kamata, I. Agata, *J. Org. Chem.* **1998**, *63*, 3113.

of  $\alpha$ -amino alcohols with dimethylformamide dimethylacetal (DMF-DMA) which leads to the formation of a formamidine intermediate.<sup>12a</sup> Acid-catalysed cyclisation produces the 2*H*-oxazolines **5** and **6** by concurrent loss of dimethylamine (Scheme 2.1.6).



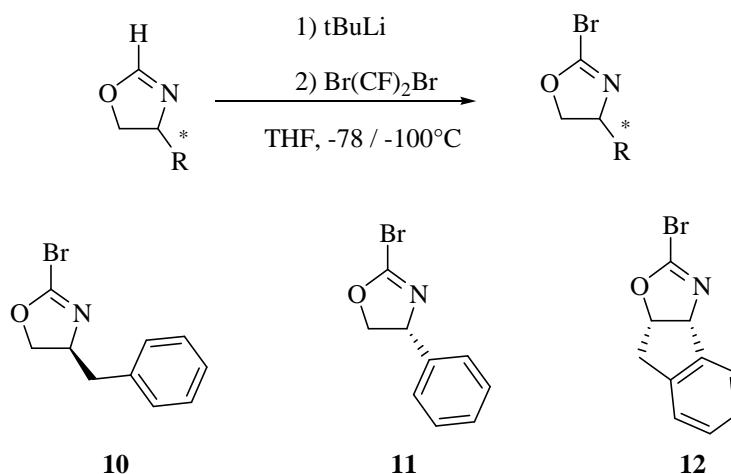
*Scheme 2.1.6:* Formation of the 2*H*-oxazolines **5-7**

Using the same synthetic strategy the 2*H*-oxazoline **7** could be obtained in 70-90% yield.

#### b. Synthesis of 2-bromooxazolines

Meyers and Novachek first reported the synthesis of a 2-bromooxazoline in 1996 starting from the (4*S*)-4-*t*butyloxazoline.<sup>13</sup> They showed that lithiation of the 2*H*-oxazoline followed by addition of 1,2-dibromo-1,1,2,2-tetrafluoroethane, a smooth and non-oxidising Br<sup>+</sup> provider, affords the activated monooxazoline. 2-Bromo-4,4-dimethyloxazoline (**8**) and (4*S*)-2-bromo-4-isopropyloxazoline (**9**) have first been synthesised using this method.<sup>2,3</sup> Based on the same synthetic procedure three novel 2-bromooxazolines (**10-12**) have been prepared (Scheme 2.1.7).

<sup>13</sup> A. I. Meyers, K. A. Novachek, *Tetrahedron Lett.* **1996**, 37, 1747.



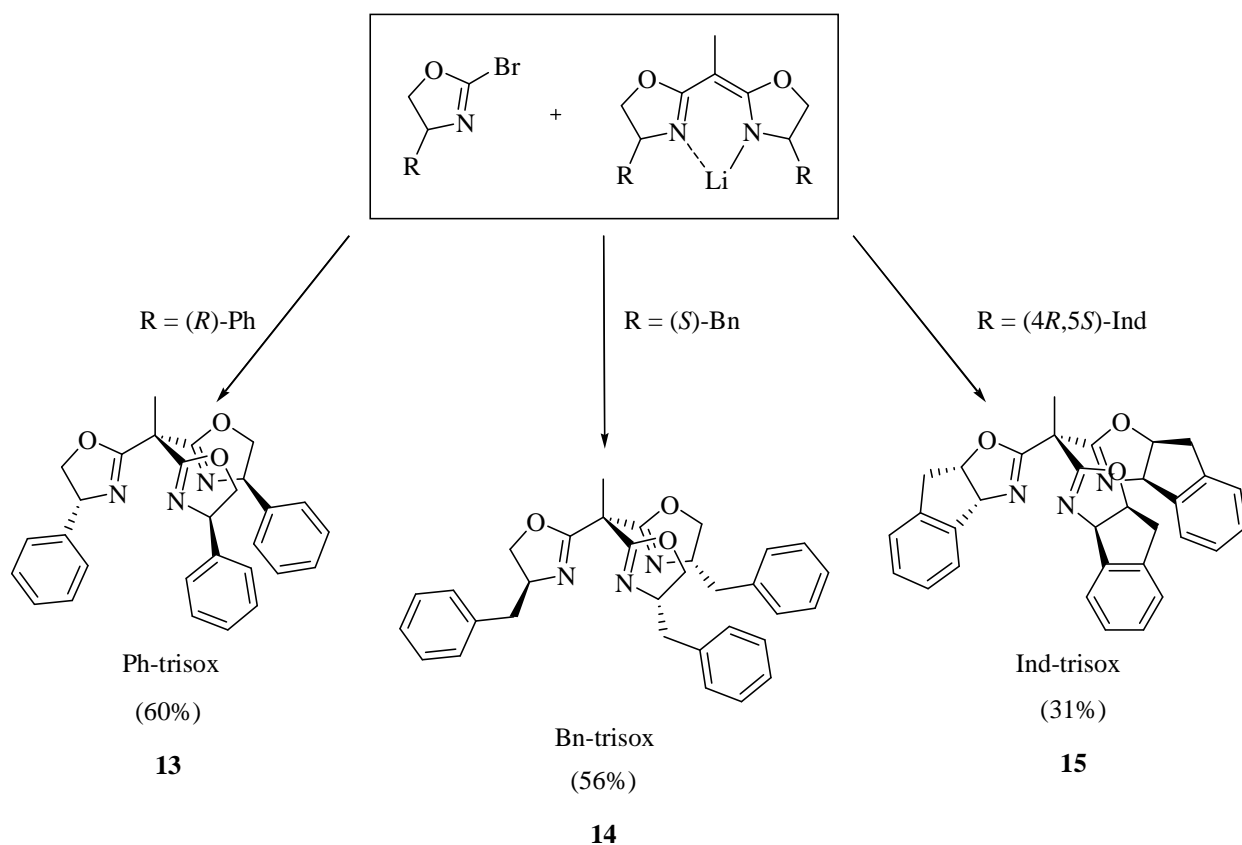
**Scheme 2.1.7:** Synthesis of the 2-bromooxazolines **10-12**

To achieve the synthesis of 2-bromooxazoline **11** the addition of *tert*-butyl lithium and the following reaction with the  $\text{Br}^+$  provider have to be done very slowly and at low temperature ( $-100^\circ\text{C}$ ) due to degradation under the standard conditions. Activated monooxazolines **10** and **11** are purified by bulb to bulb distillation and are kept in solution in tetrahydrofuran at  $-78^\circ\text{C}$  to avoid decomposition. The 2-bromooxazoline **12** is a white solid which is purified by sublimation (cooling at  $-78^\circ\text{C}$ ). It has been observed that yields may vary considerably.

#### 4. The coupling step: New $C_3$ -symmetric trisoxazolines

The two coupling partners for the synthesis of the trisoxazolines, the bisoxazoline derivatives and the 2-bromooxazolines, are accessible through straightforward synthesis; this contributes to the efficiency of the overall approach.

The three novel trisoxazolines were synthesised by coupling of the two precursors using the modular strategy (Scheme 2.1.8). Preparation of Ph-trisox and Bn-trisox can be achieved by standard reaction conditions used for the synthesis of *i*Pr-trisox and *t*Bu-trisox: after addition of the 2-bromooxazoline to the lithiated bisoxazoline at low temperature the reaction mixture is stirred at  $70^\circ\text{C}$  in tetrahydrofuran for several days. To obtain higher yields the coupling of 1,1-bis[(4*R*,5*S*)-4,5-indanediylloxazolin-2-yl]ethane **4** with (4*R*,5*S*)-2-bromo-4,5-indanediylloxazoline **12** has to be carried out in toluene and at lower temperature ( $50\text{--}60^\circ\text{C}$ ). After two days, the  $^1\text{H}$  NMR spectrum of the reaction mixture showed that there were no precursors left and the low yields observed were probably due to relative instability of Ind-trisox on the chromatography column.



**Scheme 2.1.8:** Synthesis of Ph-trisox, Bn-trisox and Ind-trisox

Both Ph-trisox and Bn-trisox are white solids. Suitable crystals for X-ray diffraction of Ph-trisox could be obtained by slow diffusion of pentane into a solution of the trisox in dichloromethane. The molecular structure of Ph-trisox in the solid state is shown in Figure 2.1.3 and selected bond lengths are given in Table 2.1.1.

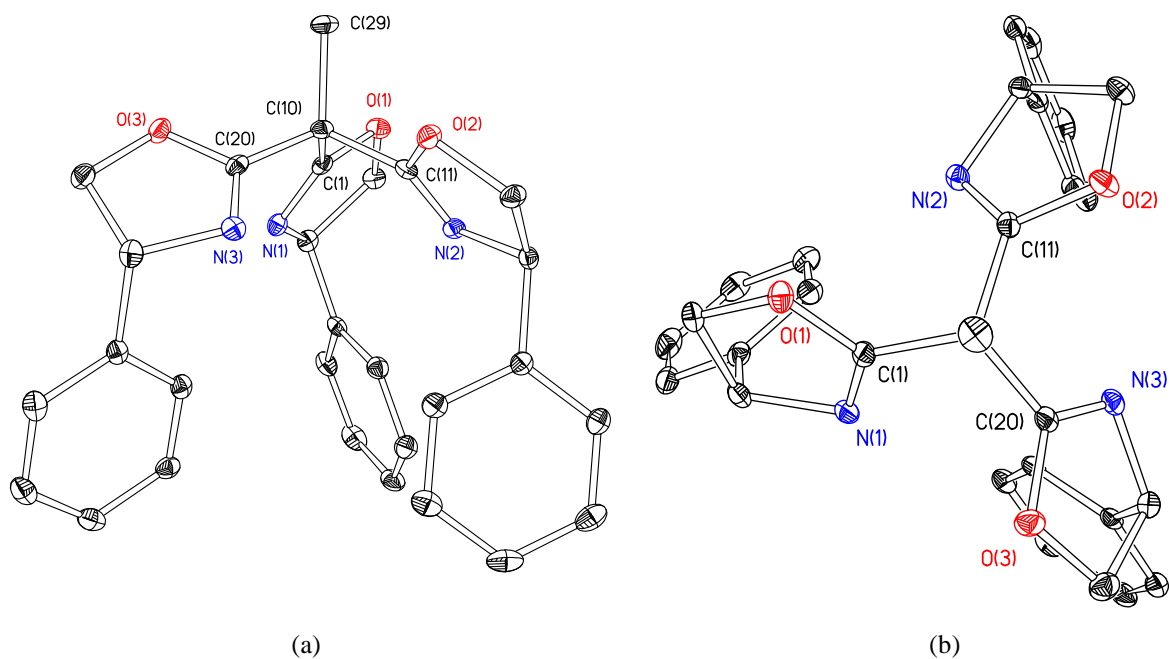


**Figure 2.1.3:** Thermal ellipsoid plot (25%) of Ph-trisox: (a) perspective view; (b) view along the C(29)-C(10) bond

Ph-trisox		Bn-trisox	
N(1)-C(1)	1.263	N(1)-C(1)	1.261
N(2)-C(11)	1.257	N(2)-C(11)	1.264
N(3)-C(20)	1.261	N(3)-C(21)	1.266

**Table 2.1.1:** Selected bond lengths (Å) for Ph-trisox and Bn-trisox ligands

Similarly, Bn-trisox crystallises by slow diffusion of pentane into a solution of the ligand in dichloromethane. The structure of Bn-trisox is depicted in Figure 2.1.4. and selected bond lengths are given in Table 2.1.1.

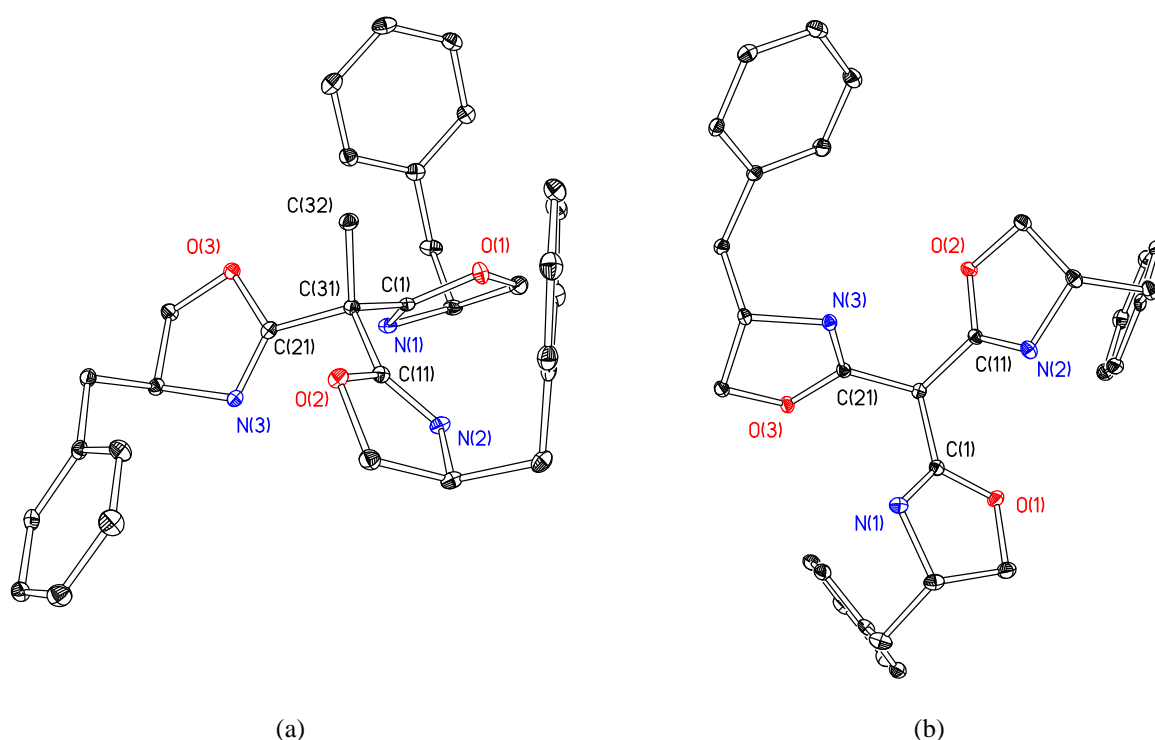


**Figure 2.1.4:** Thermal ellipsoid plot (25%) of Bn-trisox: (a) perspective view; (b) view along the C(31)-C(32) bond

The molecular structures of Ph-trisox and Bn-trisox indicate that the benzyl substituents are more flexible than the phenyl groups. The Ph-trisox ligand should therefore give more rigid structures upon complexation to a metal centre.

## II. Synthesis of mixed tris- and bisoxazolines

### 1. $C_1$ -symmetric trisoxazolines via the modular approach

The novel approach, which consists in a modular synthesis, allows the formation of highly symmetric trisox as well as trisoxazolines with destroyed rotational symmetry.<sup>14</sup> To synthesise chiral  $C_1$ -symmetric trisoxazolines, several approaches are possible. One is to introduce three oxazoline units possessing the same configuration but at least one different substituent (Figure 2.2.1 **I**). Another approach is to introduce an oxazoline ring which has the opposite stereochemistry relative to the others and with either the same (Figure 2.2.1 **II**) or a different substituent (Figure 2.2.1 **III**).

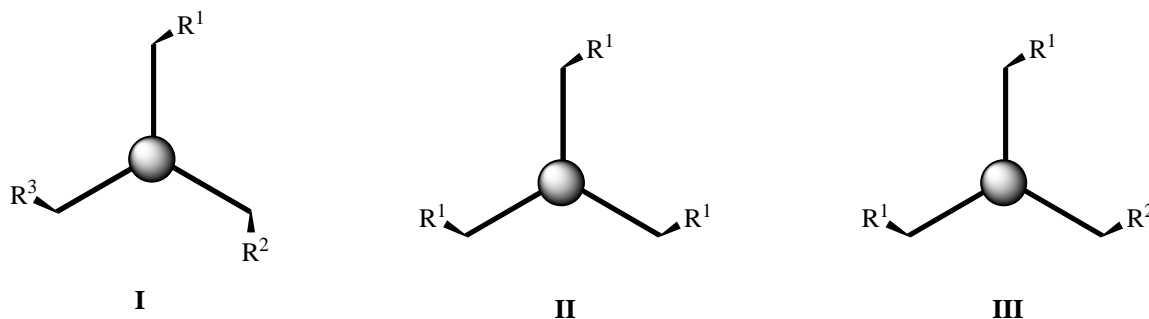
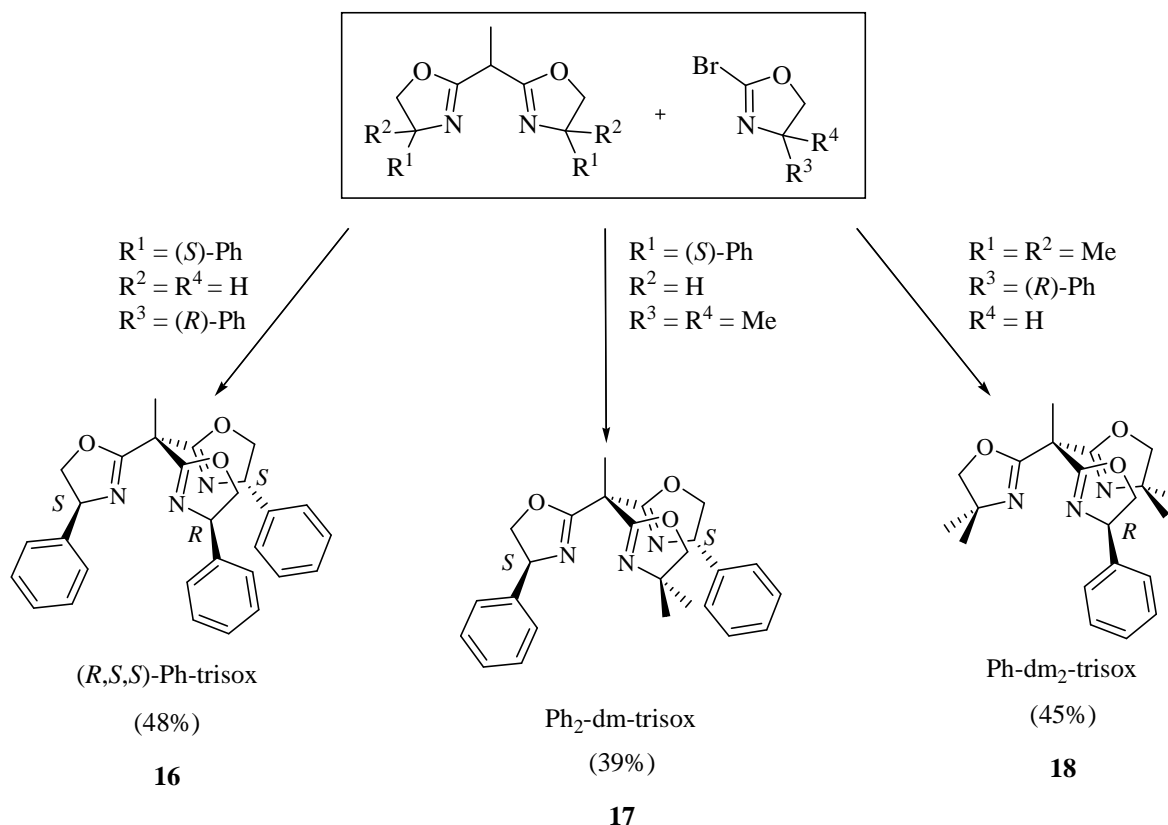


**Figure 2.2.1:** Different approaches to introduce  $C_1$  symmetry in trisoxazolines  
 R is the substituent at the 4 position of the oxazoline unit  
 For type **I**,  $R^1=R^2 \neq R^3$  or  $R^1 \neq R^2 \neq R^3$

The modular approach developed in our group allows the formation of trisox of type **I** as well as of type **II** and **III**. For further application in asymmetric catalysis we were interested in the preparation of trisox of type **I** and **II**. For that purpose bisoxazolines with identical oxazoline units were employed as coupling partners. The synthesis of three chiral  $C_1$ -symmetric tripods was achieved in moderate yields. The general reaction scheme along with the structure of the different ligands prepared is depicted in Scheme 2.2.1. (*R,S,S*)-Ph-trisox (type **II**) was obtained by coupling 1,1-bis[(4*S*)-4-phenyloxazolin-2-yl]ethane with the corresponding activated monooxazoline possessing the opposite stereochemistry.

<sup>14</sup> Recently, Ahn *et al.* reported the preparation of  $C_1$ -symmetric **D**-type trisox through an oxazoline exchange reaction with amino alcohols in the presence of zinc(II) chloride with yields between 12 and 34%: S.-G. Kim, H. R. Seong, J. Kim, K. H. Ahn, *Tetrahedron Lett.* **2004**, *45*, 6835.





**Scheme 2.2.1:** Application of the modular strategy for the synthesis of  $C_1$ -symmetric trisoxazolines (dm = dimethyl)

$\text{Ph}_2\text{-dm}$ -trisox and  $\text{Ph-dm}_2$ -trisox are chiral ligands of type **I** possessing one or two achiral oxazoline units respectively (dm = dimethyl).

## 2. Synthesis of mixed 2,2-bis(oxazoliny)propane ligands

There are two different possibilities to synthesise mixed bisoxazolines. The first one is to introduce two oxazoline units bearing different substituents and the second one consists of the introduction of one oxazoline ring possessing the same substituent as the other but with inverted stereochemistry (Figure 2.2.2).

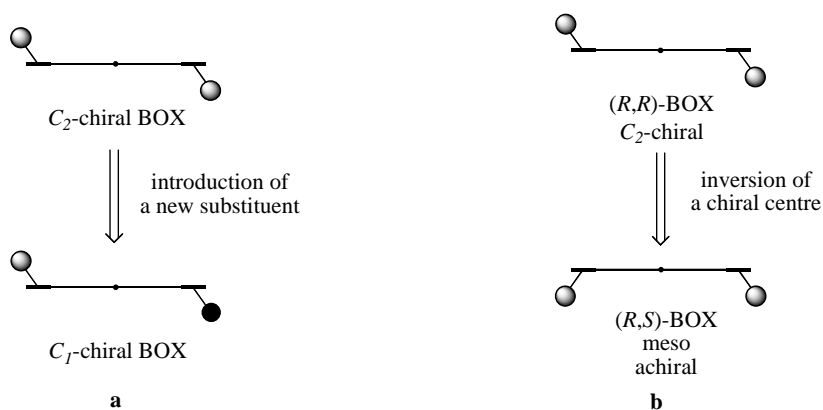
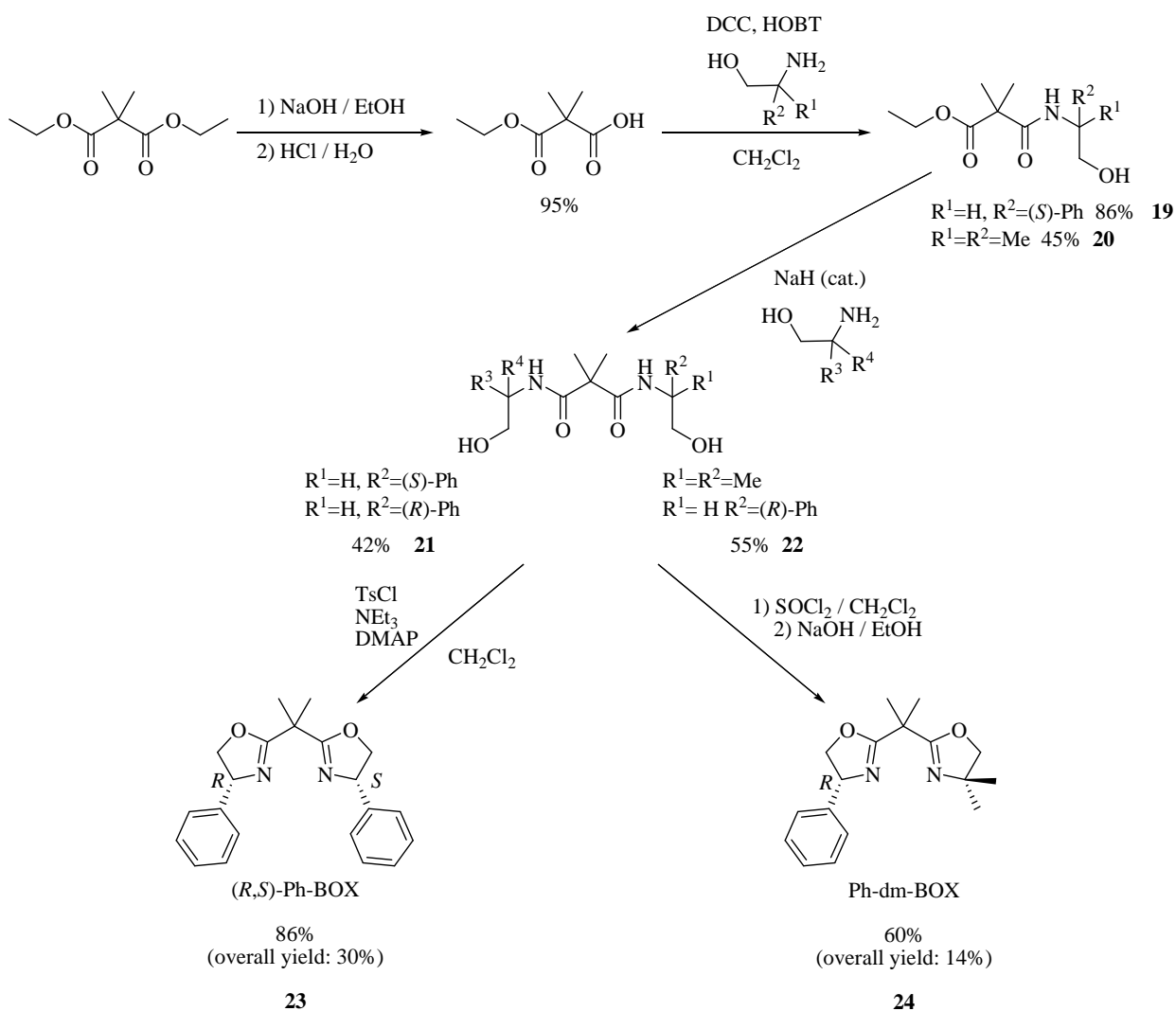


**Figure 2.2.2:** Transformation of a  $C_2$ -chiral bisoxazoline upon introduction of a new substituent (**a**) or inversion of the configuration of an oxazoline unit (**b**)

Introduction of non-identical rests on the oxazoline rings breaks the  $C_2$  symmetry of the ligand and gives rise to a  $C_1$ -symmetric molecule (Figure 2.2.2 a). Whereas the inversion of a chiral centre in a  $C_3$  chiral tripod renders the system chiral and  $C_1$ -symmetrical, the same process carried out for  $C_2$ -symmetrical chelate ligand generates a *meso*-structure, *i.e.* an achiral ligand possessing mirror symmetry (Figure 2.2.2 b). For further application in asymmetric catalysis two mixed bisoxazolines have been synthesised. The synthetic strategy employed to prepare mixed bisoxazolines is depicted in Scheme 2.2.2. It is also possible to use other synthetic pathways to get access to bisoxazolines bearing non-identical oxazoline units.<sup>15</sup>



Scheme 2.2.2: Synthesis of mixed bisoxazolines

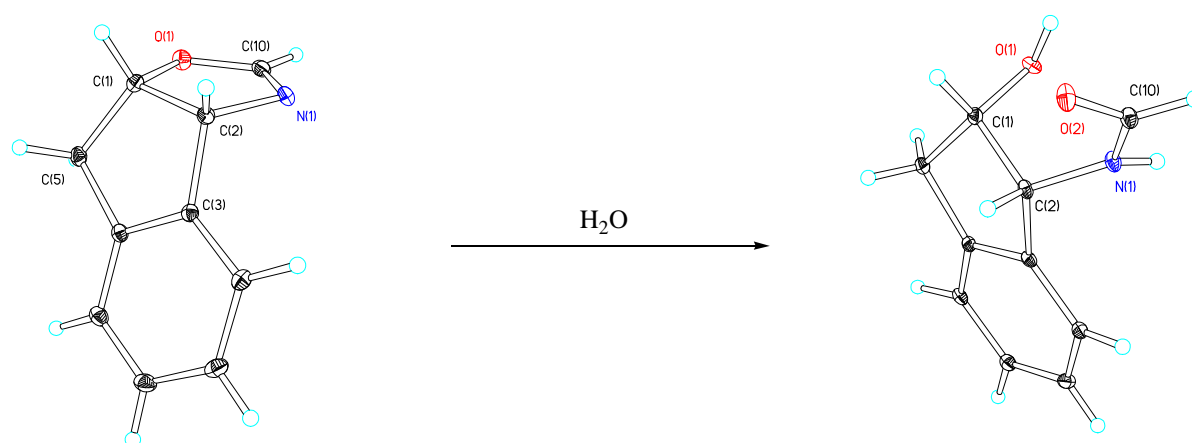
<sup>15</sup> See for example: J. I. García, J. A. Mayoral, E. Pires, I. Vallalba, *Tetrahedron: Asymmetry* **2006**, *17*, 2270.

The first step is the mono-saponification of diethyl dimethylmalonate which gives the corresponding mono-acid with 95% yield.<sup>16</sup> Peptide coupling between the mono-acid and the first  $\alpha$ -amino alcohol in the presence of *N,N'*-dicyclohexylcarbodiimide (DCC) and 1-hydroxybenzotriazole (HOBT) affords the mono-amide. Introduction of the second group is done by reacting the mono-amide with the desired  $\alpha$ -amino alcohol in the presence of a catalytic amount of sodium hydride as described for the diamide intermediate for the synthesis of 1,1-bis(oxazoliny)ethanes. Activation of the alcohol functions with tosylchloride and subsequent cyclisation afforded the *meso* bisoxazoline in high yield but this activation proved not to be efficient in the synthesis of the  $C_1$ -symmetric bisoxazoline. Bisoxazoline **24** has been obtained by activation with thionyl chloride followed by cyclisation under basic conditions.

### III. Instability of the 2-bromooxazolines

#### 1. Ring-opening of the oxazoline unit: General aspects

The oxazoline unit is widely applied in ligand design for asymmetric catalysis due to their numerous advantages: i) they are rigid, quasi-planar; ii) they are normally stable towards hydrolysis and oxidation; iii) they can readily be prepared in enantiomerically pure form from optically pure  $\alpha$ -amino alcohols; iv) the stereodirecting substituents are located in close proximity to the metal center upon coordination through the nitrogen atom. However, depending on the structure of the oxazolines, they are sometimes not stable towards hydrolysis. This is the case for very strained oxazoline rings such as (4*R*,5*S*)-4,5-indanediylloxazoline (**7**). Ring-opening through hydrolysis of this 2*H*-oxazoline has been confirmed by X-ray analysis (Scheme 2.3.1).



**Scheme 2.3.1:** Thermal ellipsoid plot (25%) of (4*R*,5*S*)-4,5-indanediylloxazoline and of the ring-opening product afforded through hydrolysis

<sup>16</sup> R. E. Strube, *Org. Synth.* **1963**, *4*, 417.

Oxazoline units can undergo ring-opening under certain conditions, by way of electrophilic attacks<sup>17</sup> their acidolysis<sup>18</sup> or glycolysis<sup>19</sup> and rearrangement in organometallic compounds.<sup>20</sup> Ring-opening polymerisation of 2-oxazolines is also the focus of current interest.<sup>21</sup> The main driving force of the polymerisations is not the relief of ring strain, as it is for many ring-opening polymerisations, but instead is the isomerisation of the oxazoline unit to the amide, which is thermodynamically more stable. The ring-opening of oxazolines has also been employed as practical entry to interesting organic molecules such as amino esters.<sup>22</sup>

## 2. Thermally induced rearrangement of the 2-bromooxazolines

A practical limitation has been observed during the synthesis of the trisoxazolines: the thermal degradation of the 2-bromooxazolines. This degradation can be easily noticed due to the change of colour of the compound from colorless to yellow/brown. It has first been observed for the (4*R*)-2-bromo-4-phenyloxazoline. The compound obtained has been characterised by spectroscopic and spectrometric methods. The analyses show the ring-opening of the oxazoline unit leading to a new compound, in particular the IR spectrum shows the characteristic stretching band of an isocyanate function ( $\nu_{\text{C}=\text{N}} = 2265 \text{ cm}^{-1}$ ). The <sup>1</sup>H NMR spectra of the two compounds are represented in Figure 2.3.1, showing the shifts of the signals of the protons from the oxazoline rings.

---

<sup>17</sup> J. A. Frump, *Chem. Rev.* **1971**, 71, 483.

<sup>18</sup> a) D. F. Elliott, *J. Chem. Soc.* **1950**, 62; b) E. M. Fry, *J. Org. Chem.* **1950**, 15, 802; c) M. Fritz, H. Köchling, *Chem. Ber.* **1958**, 673; d) B. Lindberg, H. Agback, *Acta Chem. Scand.* **1964**, 18, 185.

<sup>19</sup> M. Fritz, E. Drescher, *Chem. Ber.* **1958**, 670.

<sup>20</sup> a) A. B. Kazi, G. D. Jones, D. A. Vicic, *Organometallics* **2005**, 24, 6051; b) B. D. Ward, H. Risler, K. Weitershaus, S. Bellemin-Laponnaz, H. Wadepohl, L. H. Gade, *Inorg. Chem.* **2006**, 45, 7777; c) A. L. Gott, S. R. Coles, A. J. Clarke, G. J. Clarkson, P. Scott, *Organometallics*, **2007**, 26, 136.

<sup>21</sup> See for example: a) J. S. Hrkach, K. Matyjaszewski, *Macromolecules* **1992**, 25, 2070; b) R. Jordan, A. Ulman, *J. Am. Chem. Soc.* **1998**, 120, 243 c) F. Wiesbrock, R. Hoogenboom, M. A. M. Leenen, M. A. R. Meier, U. S. Schubert, *Macromolecules* **2005**, 38, 5025 d) R. Hoogenboom, F. Wiesbrock, H. Huang, M. A. M. Leenen, H. M. L. Thijs, S. F. G. M. van Nispen, M. van der Loop, C.-A. Fustin, A. M. Jonas, Alain M.J.-F. Gohy, U. S. Schubert, *Macromolecules* **2006**, 39, 4719; e) C. Guerrero-Sanchez, R. Hoogenboom, U. S. Schubert, *Chem. Commun.* **2006**, 3797.

<sup>22</sup> a) A. Laaziri, J. Uziel, S. Jugé, *Tetrahedron: Asymmetry* **1998**, 437; b) S.-H. Lee, J. Yoon, K. Nakamura, Y.-S. Lee, *Org. Lett.* **2000**, 2, 1243.

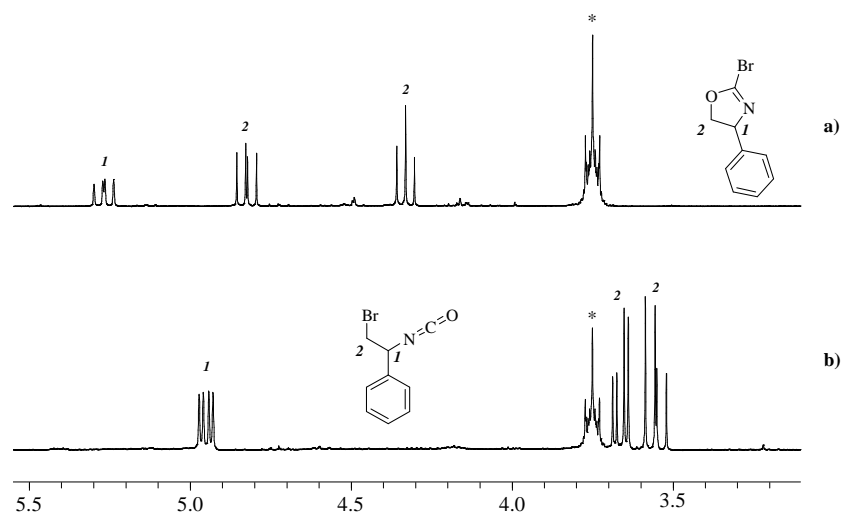


**Figure 2.3.1:**  $^1\text{H}$  NMR spectra in chloroform- $d_1$  (300 MHz) of the (4*R*)-2-bromo-4-phenyloxazoline (a) and its corresponding rearrangement product (b); \* = tetrahydrofuran

The ring-opening leading to the formation of an isocyanate-based product was confirmed by X-ray crystallography. Suitable crystals for an X-ray diffraction study of the rearranged product of the (4*R*, 5*S*)-2-bromo-4,5-indanediylloxazoline were obtained (Figure 2.3.2).

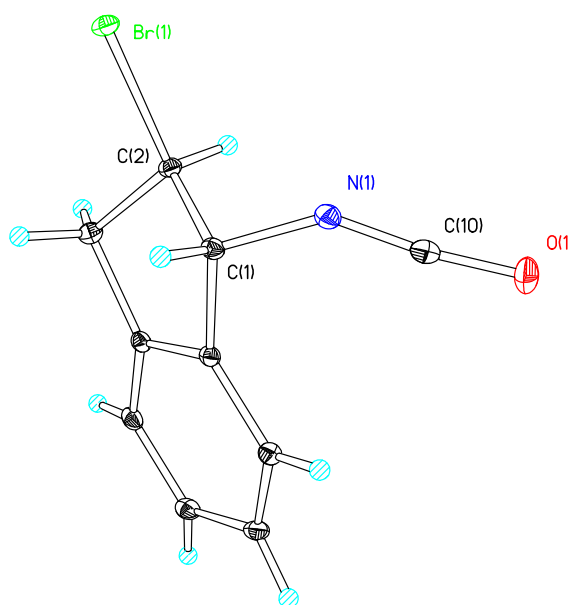


**Figure 2.3.2:** Thermal ellipsoid plot (25%) of (1*R*, 2*R*)-2-bromo-1-isocyanato-2,3-dihydro-1*H*-indene

Ring-opening of the oxazoline unit induces the inversion of the absolute configuration of the C(2) carbon atom. It is of interest to note that the crystals employed for the X-ray diffraction study of the rearrangement product consisted only of one diastereomeric form. Moreover  $^1\text{H}$  NMR spectrum of the compound indicates a diastereomeric ratio of 95/5. Inversion of

configuration was induced in the nucleophilic attack of the bromine atom ending up at the opposite side of the position of the leaving group.

It has been found that the same rearrangement occurs for all the bromooxazolines studied, independent of the substituent present on the heterocycle. The four rearrangement products that have been characterised are displayed in Figure 2.3.3.

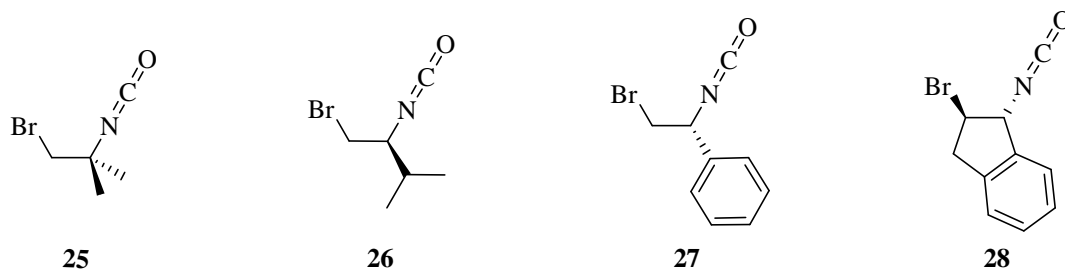
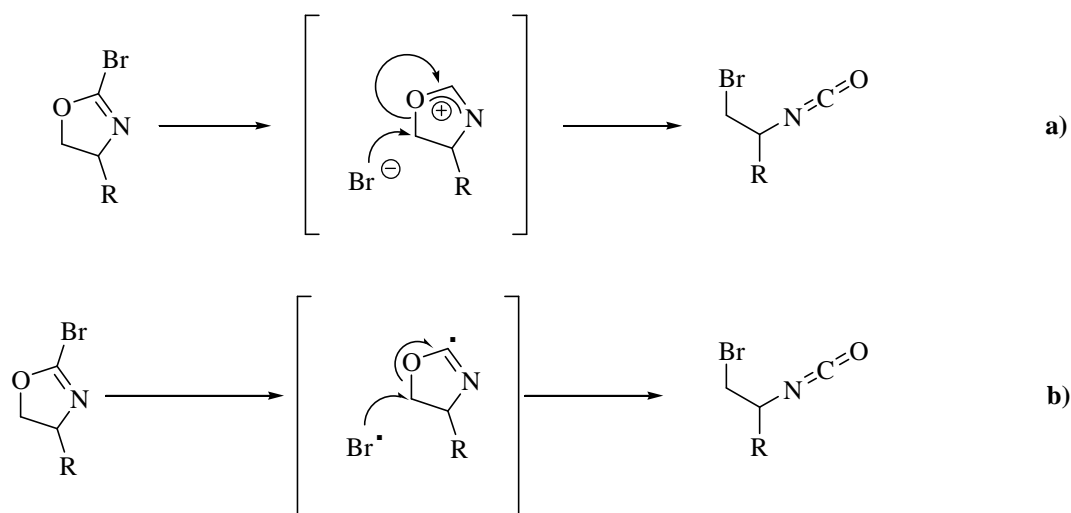


Figure 2.3.3: The four isocyanate derivatives characterised

At room temperature, the rate of rearrangement varies, depending on the substituent of the monooxazoline derivative. Based on experimental observations during the syntheses, we could classify the bromooxazolines from the more to the less stable: *i*Pr  $\gg$  Me<sub>2</sub>  $\gg$  Ph  $>$  Ind. The (4*R*, 5*S*)-2-bromo-4,5-indanediylthioisocyanate is the least stable derivative presumably due to the presence of three strained rings. It has been observed that higher dilution in tetrahydrofuran induce higher stability at room temperature. Notably, the derivative with phenyl substituent seems to be more stable than the 4,4'-dimethylated compound when the solution is diluted.

Knowing the structure of the rearrangement product, we initially proposed two different rearrangement pathways (Scheme 2.3.2): a) heterolytic cleavage of the C-Br bond followed by nucleophilic attack of the Br<sup>-</sup> anion on the oxazolinium moiety; b) radical mechanism with homolytic cleavage of the Br-C bond or, possibly a radical chain mechanism.



**Scheme 2.3.2:** Two possible reaction pathways for the rearrangement of the 2-bromooxazolines

In order to gain more insight into the reaction mechanism several test reactions have been carried out with the 2-bromo-4,4'-dimethyloxazoline. The conversion of the bromooxazoline into the corresponding isocyanate derivative can be easily followed by  $^1\text{H}$  NMR by monitoring the two characteristic singlets of the brominated compounds (Figure 2.3.4).

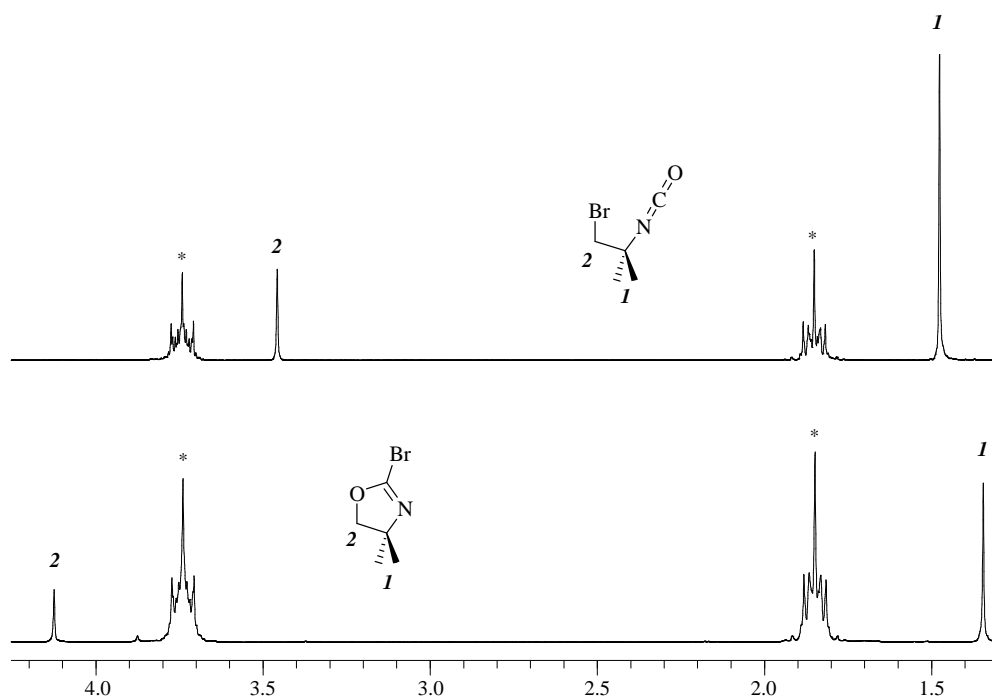


**Figure 2.3.4:**  $^1\text{H}$  NMR spectra in chloroform- $d_1$  (200 MHz) of the 2-bromo-4,4'-dimethyloxazoline (down) and the 1-bromo-2-isocyanato-2-methylpropane (up): \* = tetrahydrofuran

The different reactions carried out in tetrahydrofuran, tetrahydrofuran- $d_8$  or chloroform- $d_1$  and their corresponding results are summarised in Table 2.3.1.

Entry	Solvent	Temperature	Additive / Conditions	Reaction time	Rearrangement
1	THF	R.T.	H <sub>2</sub> O	3 d	-
2	CDCl <sub>3</sub>	R.T.	H <sub>2</sub> O	1 d	-
3	THF	R.T.	compressed air	5 h	-
4	CDCl <sub>3</sub>	15°C	UV	3 d	-
5	THF	25°C	UV	2 d	-
6	CDCl <sub>3</sub>	heat from the lamp	UV	2 d	complete
7	CDCl <sub>3</sub>	-78°C to R.T.	radical initiator	1 d	-
8	THF- <i>d</i> <sub>8</sub>	-78°C to R.T.	radical initiator	1 d	-
9	THF- <i>d</i> <sub>8</sub>	R.T.	Br <sub>2</sub>	1 d	rearrangement (~10%) + by-products
10	CDCl <sub>3</sub>	R.T.	Bu <sub>4</sub> NBr	2 d	rearrangement (10%)
11	CDCl <sub>3</sub>	R.T.	HBr	2 h	starting material + rearrangement (~30%) + by-product
12	CDCl <sub>3</sub>	R.T.	HBr	1 d	starting material (~20%) + by-product
13	THF	75°C	/	2 d	complete
14	CDCl <sub>3</sub>	75°C	/	2 d	complete

**Table 2.3.1:** Attempts to obtain the rearrangement product of 2-bromo-4,4-dimethyloxazoline

Addition of water (entries 1-2) to a solution containing the bromooxazoline did not lead to the rearrangement product even after three days of reaction. Air was bubbled through a solution of the monooxazoline derivative in tetrahydrofuran and no reaction was observed. This indicates that a radical reaction initiated by oxygen is not involved. Exposure of a tetrahydrofuran or chloroform solution of the compound to UV irradiation (entries 4-5) was unsuccessful. Notably, when the reaction mixture was not cooled with a cryostat to room temperature or lower, the conversion was complete (entry 6). Comparison of entries 4, 5 and 6, enables us to conclude that the heat coming from the lamp was the source of reaction and that photochemical reaction is not the cause of the isomerisation. Trying to obtain the isocyanate-based compound by addition of a radical initiator (2,2'-azobis(4-methoxy-2,4-dimethylvaleronitrile), AIBN) to the bromooxazoline is unsuccessful (entry 7-8). Addition of Br<sub>2</sub>



mostly led to degradation of the bromooxazoline giving unknown compounds. In view of the results of entries 4-9, we assume that the reaction pathway (b) from Scheme 2.3.2 is wrong and that the rearrangement is not induced by a radical cleavage of the Br-C bond. In the presence of Br<sup>-</sup> anions (from Bu<sub>4</sub>NBr) rearrangement is observed but the reaction is very slow (10% conversion after 2 days; entry 10). Addition of a concentrated aqueous solution of HBr led to the formation of the isocyanate derivative (30%) with some by-products after 2 hours. The next day, the degradation of the desired product was observed. Addition of an acid to the compound is not conclusive due to the total degradation of the isocyanate which has been partially obtained (the same was observed in case of HCl). The most interesting results have been obtained when a solution of the bromooxazoline has been heated (entries 13-14). In tetrahydrofuran, as well as in chloroform, complete conversion of the bromooxazoline into the isocyanate derivative has been observed after two days at 75°C. These results are in agreement with those observed for entry 6 where conversion is obtained when heat and UV are combined, knowing that irradiations do not have any influence alone. A thermal heterolytic Br-C bond cleavage could be proposed for the rearrangement (Scheme 2.3.2 (a)).

The thermal instability of the bromooxazolines has been confirmed by heating the different derivatives or simply by removing them from their cold bath. In fact, after sublimation, the (4*R*, 5*S*)-2-bromo-4,5-indanediylloxazoline must be kept at a -78°C otherwise complete rearrangement happens in less than two minutes. The rearrangements appeared to be quite selective (~95%) and yields of 85-90% could be obtained after distillation for the isopropyl, dimethyl and phenyl derivatives.

The degradation of the 2-bromo-4,4'-dimethyloxazoline has been followed by <sup>1</sup>H NMR at 60°C. The result showing the evolution of the concentrations of the bromooxazoline and isocyanate derivative in function of time is represented in Figure 2.3.5.

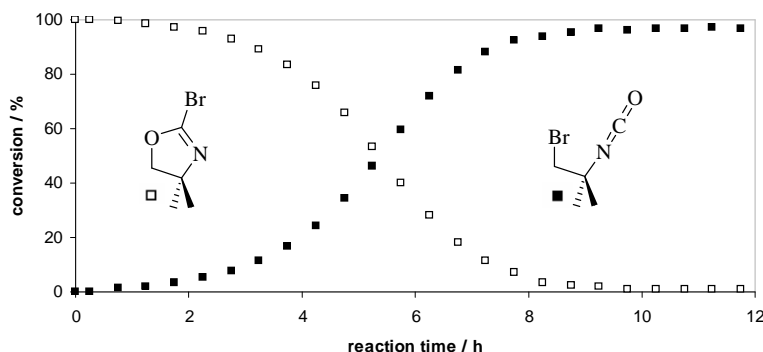


**Figure 2.3.5:** Proportions of 2-bromo-4,4'-dimethyloxazoline and 1-bromo-2-isocyanato-2-methylpropane in function of time at 60°C ( $C = 0.42 \text{ mol.L}^{-1}$ , followed by <sup>1</sup>H NMR in THF-*d*<sub>8</sub>, 200 MHz)

These results show that the conversion from the bromooxazoline into the isocyanate derivative is quite fast at 60°C. After twelve hours there is no bromooxazoline left. Trisoxazoline syntheses by coupling between monooxazoline derivatives and bisoxazolines are carried out in solution of concentrations around 0.08-0.12 mol. L<sup>-1</sup> and generally at higher temperature (70-75°C). A low yield is obtained after five days of reflux (17%)<sup>2</sup> for the 1,1,1-tris[4,4-dimethyloxazolin-2-yl]ethane. The rearrangement of the bromooxazoline could explain this result. For the other bromooxazolines, it has been observed that higher temperatures are needed to form the rearrangement product and this explains the higher yields obtained for the coupling reaction.

During the course of the tripod synthesis it has been observed that the rearrangement occurs more or less rapidly depending on the concentration of the tetrahydrofuran solution of the 2-bromooxazolines. To confirm this observation the evolution of the concentration of bromine- and isocyanate-based compound in function of time has been followed by <sup>1</sup>H NMR starting with different concentrations of 2-bromooxazoline. The two graphs summarising the results are depicted in Figure 2.3.6.

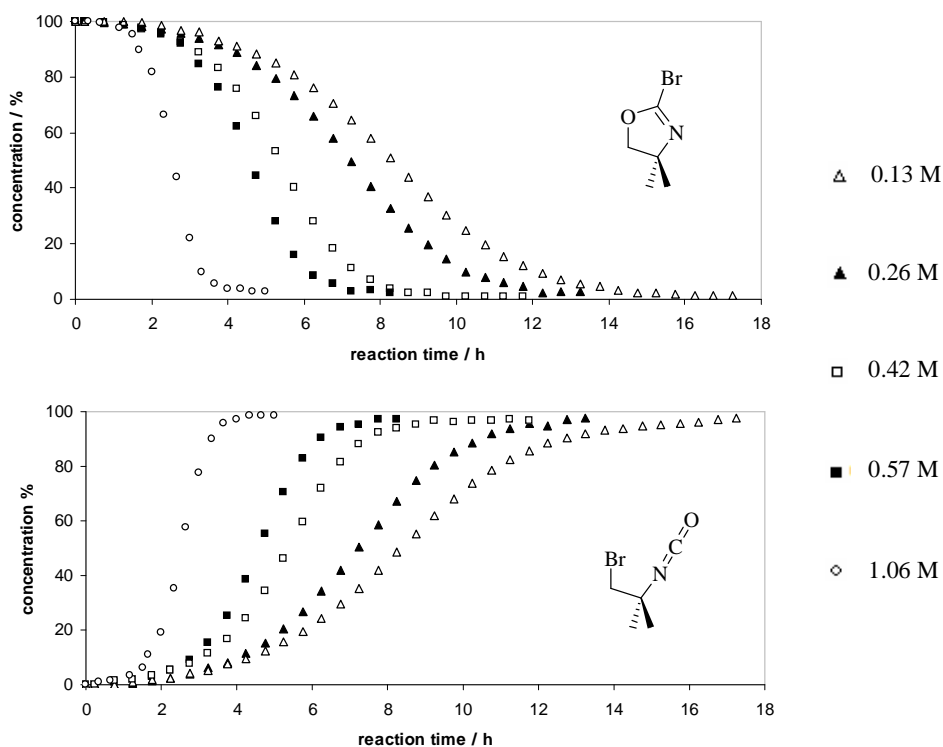
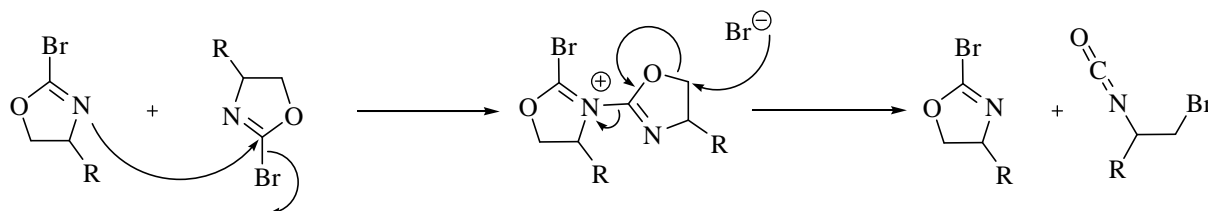


**Figure 2.3.6:** Proportions of 2-bromo-4,4'-dimethyloxazoline and 1-bromo-2-isocyanato-2-methylpropane as function of time at different concentrations (followed by <sup>1</sup>H NMR in THF-*d*<sub>8</sub>, 200 MHz, 60°C)

The rate determining step of the rearrangement is probably the heterolytic cleavage of the Br-C bond because high activation energy is needed to break heterolytic bonds. The shape of the

curves and the concentration dependence indicate that the bond cleavage step is not first order related to the concentration of bromooxazoline. The mechanism proposed in Scheme 2.3.2 a) is in that case not possible. A process involving dissociation of the bromine by attack of a second bromooxazoline and further nucleophilic substitution on the C5 carbon by the free bromine appears to be more likely (Scheme 2.3.3).



**Scheme 2.3.3:** Reaction pathway proposed for the rearrangement of the bromooxazolines

The first step of this mechanism is similar to the nucleophilic addition of an imidazole on a 2-bromooxazoline which affords an oxazoline-imidazolium.<sup>23</sup> The formation of this salt stabilises the oxazoline ring which undergoes the Br-C bond cleavage and activates its C5 carbon for further nucleophilic attack. To confirm that the rearrangement involves an ionic and not a radical process, one more experiment has been carried out. The evolution of the concentration of the two compounds in function of time with the addition of one equivalent tetrabutylammonium bromine has been followed by <sup>1</sup>H NMR. The corresponding graph is depicted in Figure 2.3.7.

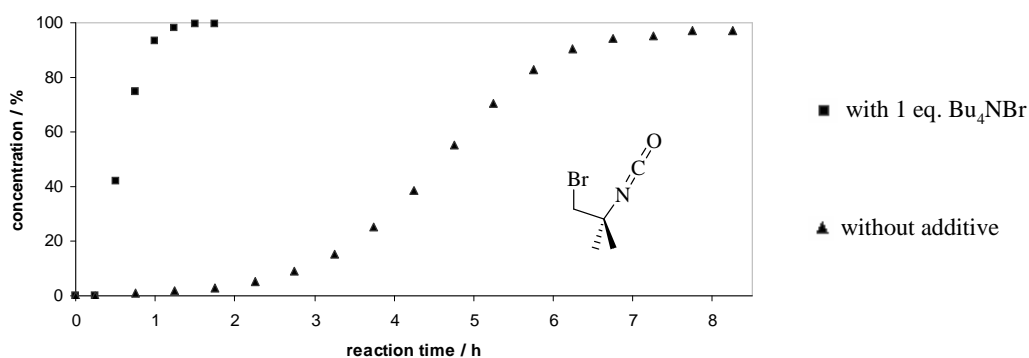


**Figure 2.3.7:** Evolution of the concentration of 1-bromo-2-isocyanato-2-methylpropane in function of time with additive (■) and without additive (▲) ( $C = 0.57 \text{ mol.L}^{-1}$ , followed by <sup>1</sup>H NMR in THF-*d*<sub>8</sub>, 200 MHz, 60°C)

Addition of an excess of Br<sup>-</sup> anions increases the reaction rate. In the presence of one equivalent tetrabutylammonium bromine the rearrangement is completed after two hours indicating the involvement of the anion.

<sup>23</sup> V. Cesar, S. Bellemin-Lapponnaz, L. H. Gade, *Organometallics* **2002**, *21*, 5204.

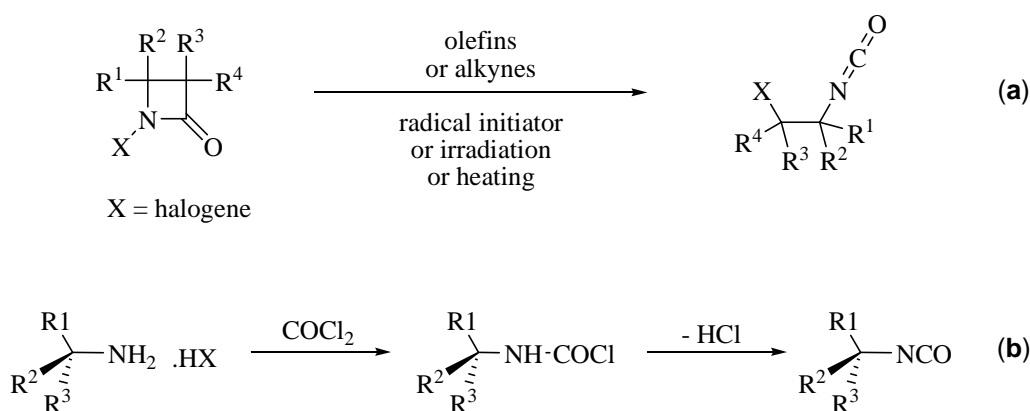
### 3. Conclusion

It has been found that 2-bromooxazolines rearrange into isocyanate derivatives. The isomerisation is thermally induced and is dependent on the concentration of the solution of bromooxazolines in tetrahydrofuran. Upon heating, 2-bromo-4-substituted oxazolines can be converted into 2-bromo isocyanates with high selectivity. Yields of 85-90% are obtained with 2-bromo-4-phenyloxazoline, 2-bromo-4-isopropyloxazoline or 2-bromo-4,4'-dimethyloxazoline. The mechanism of the rearrangement involves a heterolytic cleavage of the Br-C bond probably induced by a nucleophilic attack of a second bromooxazoline.

## IV. Reaction with the $\alpha$ -bromo-isocyanate derivatives

### 1. Precedent in the literature

Two of the isocyanates obtained by isomerisation of the bromooxazolines have been reported previously: the 1-bromo-2-isocyanato-2-methylpropane (**25**) and the 1-(2-bromo-1-isocyanatoethyl)benzene (**27**), as well as other derivatives such as the 1-bromo-2-isocyanatopropane. Rearrangement of *N*-halogenated  $\beta$ -lactames in the presence of olefins or alkynes leads to the isocyanates by adding catalytic amounts of radical generators or by irradiation or heating (Scheme 2.4.1 (a)).<sup>24</sup> A method based on the dehydrochlorination of compounds of type RNHCOCl in the presence of H<sub>2</sub>O and HCl enables to obtain, *inter alia*, 1-bromo-2-isocyanato-2-methylpropane (Scheme 2.4.1 (b)).<sup>25</sup>



**Scheme 2.4.1:** Procedures described in the literature for the synthesis of the isocyanate derivatives

<sup>24</sup> a) K. D. Kampe, *Tetrahedron Lett.* **1969**, 2, 117 ; b) Farbwerke Hoechst A.-G., **1969**, Patent FR 1565226; c) K. D. Kampe, **1970**, Patent DE 1930329; d) K. D. Kampe, *Justus Liebigs Ann. Chem.* **1971**, 752, 142.

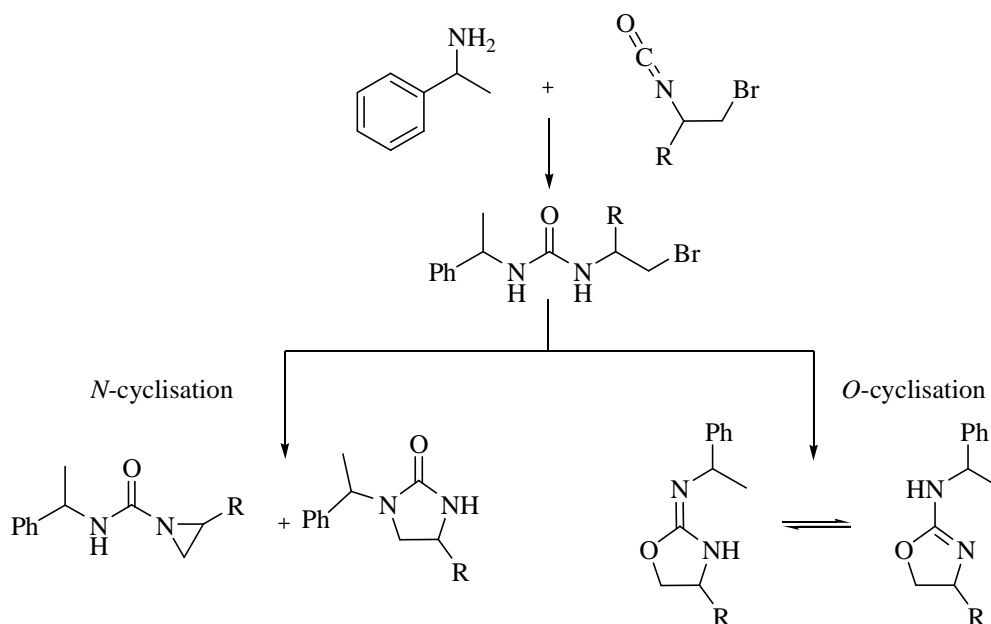
<sup>25</sup> a) K. H. Koenig, W. Rohr, A. Fischer, **1972**, Patent DE 2045907; b) K. H. Koenig, F. Zanker, D. Mangold, A. Fischer, **1972**, Patent DE 2045906; c) F. Zanker, **1973**, Patent DE 2156761.

The mechanism of the rearrangement of *N*-halogenated  $\beta$ -lactames is not fully understood but evidence for radical reactions have been found.<sup>27a,d</sup> Various applications of this type of isocyanates to generate new compounds, such as benzimidazoles derivatives,<sup>26</sup> oxazolinylpiperazines derivatives,<sup>27</sup> oxazoloquinazolines,<sup>28</sup> 2-amino-2-oxazolines,<sup>29</sup> fullerene derivatives<sup>30</sup> and 1-amidino-2-imidazolidinones,<sup>31</sup> are reported in the literature.

Rearrangement of the 2-bromooxazolines does not affect the position 4 of the oxazoline unit and enantiomerically pure isocyanates are obtained after isomerisation. Considering the reactivity of isocyanates, an interesting application may be their use for the determination of the enantiomeric excess of primary or secondary amines.

## 2. Reaction with phenylethylamine

The enantiomerically pure as well as achiral isocyanate derivatives have been reacted with (*S*)-1-phenylethylamine or *rac*-phenylethylamine. Depending on the conditions, reaction between the isocyanates and the primary amine is expected to lead to either two *N*-cyclised regioisomers: a 2-imidazolidinone and an aziridine or to an *O*-cyclised 2-aminooxazoline (Scheme 2.4.2).



**Scheme 2.4.2:** Possible isomers formed by reaction between the isocyanate derivatives and phenylethylamine

<sup>26</sup> G. Hoerlein, H. Mildenberger, A. Kroeniger, K. Haertel, **1972**, Patent DE 2125815.

<sup>27</sup> a) A. Gobel, K. Schmitt, I. Linde-Ranke, **1973**, Patent DE 2205814 ; b) A. Gobel, K. Schmitt, I. Linde-Ranke, **1973**, Patent DE 2205815.

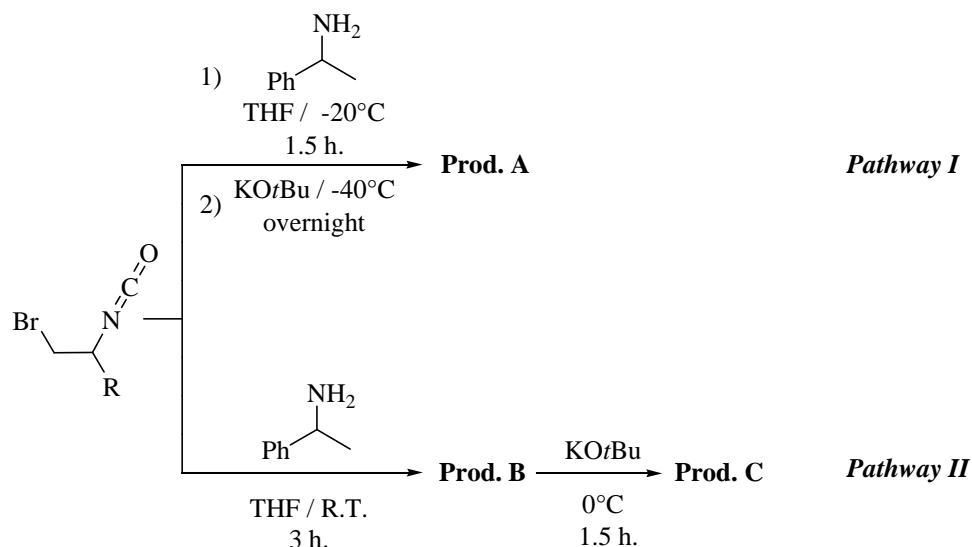
<sup>28</sup> K. D. Kampe, **1974**, Patent DE 2252122.

<sup>29</sup> a) K. D. Kampe, *Justus Liebigs Ann. Chem.* **1974**, *4*, 593; b) K. D. Kampe, M. Babej, J. Kaiser, **1974**, Patent DE 2253554

<sup>30</sup> K. D. Kampe, **1995**, Patent EP 653424.

<sup>31</sup> B. Kulitzscher, C. Sommer, B. Kammermeier, **1996**, Patent DE 19502790.

Before the cyclisation, reaction between the isocyanate and phenylethylamine leads to the formation of an urea. This urea is obtained by nucleophilic attack of the isocyanate function by the amine. The subsequent step is the intramolecular cyclisation of this intermediate. Two different reaction conditions have been employed to react the isocyanate derivatives with the amine. They are depicted in Scheme 2.4.3.

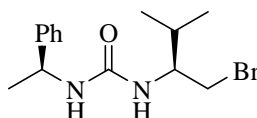


**Scheme 2.4.3:** The two reaction pathways studied and the three different products observed: **Prod. A**, **Prod. B** and **Prod. C**

The reactions have been carried out for both reaction protocols with the isocyanate derivatives with dimethyl, (*S*)-isopropyl and (*R*)-phenyl substituents. In the two following sections determination of the products formed through *Pathway I* and *Pathway II* is described.

a. **Pathway I: characterisation of Prod. A**

Following *Pathway I* the reaction between the isocyanate derivative and the primary amine at -20°C followed by the addition of potassium *tert*-butoxide at -40°C leads to the formation of **Prod. A**. It has been confirmed by variable temperature  $^1\text{H}$  NMR studies in THF- $d_8$  that the urea is formed at low temperature. The urea bearing the isopropyl substituent (**27**) has been characterised by  $^1\text{H}$ ,  $^{13}\text{C}$  { $^1\text{H}$ } and  $^{15}\text{N}$  NMR spectroscopy (Figure 2.4.1).



**29**

**Figure 2.4.1:** Urea formed by reaction between (*S*)-1-phenylethylamine and the isocyanate derivative bearing the (*S*)-isopropyl substituent

The NMR scale reactions conducted at low temperature ( $-20^{\circ}\text{C}$ ) have shown that the urea remains stable at least for five hours. Thus, when the base is added, the reaction that occurs is the intramolecular cyclisation of the urea. This cyclisation has proven to be selective and  $^1\text{H}$  NMR spectra of the reaction mixture show no by-products. Based on the spectroscopic and mass spectrometric data recorded it has been difficult to conclude whether the urea undergoes *N*- or *O*-cyclisation.

Suitable crystals for an X-ray diffraction study have been obtained by slow diffusion of pentane into a solution of **Prod. A** bearing the (*S*)-isopropyl substituent in dichloromethane. The molecular structure of the compound is depicted in Figure 2.4.2. The selected bond lengths and angles are summarised in Table 2.4.1.

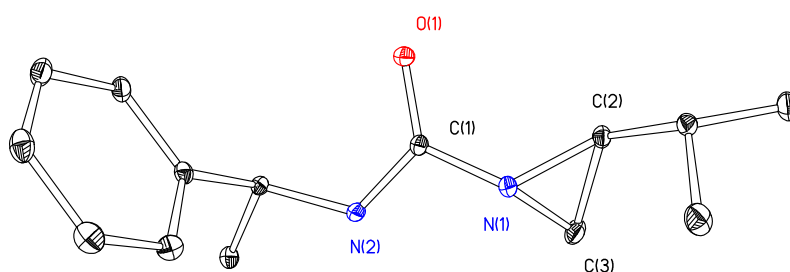


**Figure 2.4.2:** Thermal ellipsoid plot (25%) of (*S*)-2-isopropyl-*N*-((*S*)-1-phenylethyl)aziridine-1-carboxamide (**31a**)

C(1)-O(1)	1.228(3)	C(1)-N(2)	1.342(3)
C(1)-N(1)	1.408(3)	C(2)-N(1)	1.456(3)
C(2)-C(3)	1.485(3)	C(3)-N(1)	1.469(3)
N(2)-C(1)-N(1)	113.25(18)	N(1)-C(2)-C(3)	59.94(15)
N(1)-C(3)-C(2)	59.06(15)	C(2)-N(1)-C(3)	61.00(15)
C(1)-N(1)-C(2)	118.87(18)	C(1)-N(1)-C(3)	119.14(19)

**Table 2.4.1:** Selected bond lengths (Å) and angles ( $^{\circ}$ )

The formation of the 3-membered ring is confirmed by X-ray diffraction. Addition of the base to the pre-formed urea leads to the intramolecular *N*-cyclisation of the latter affording the aziridine. Following the procedure of **Pathway I** four aziridine derivatives have been isolated as the kinetically favoured product (Figure 2.4.3).

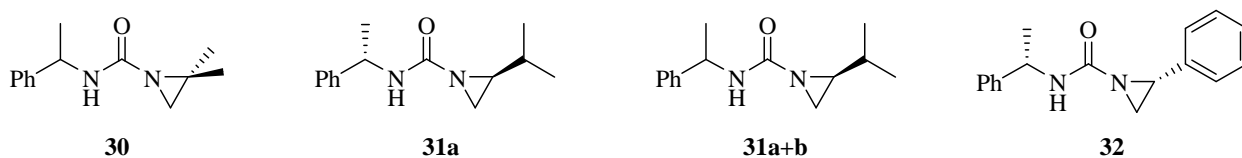


**Figure 2.4.3:** The compounds formed following the procedures of *Pathway I*

Derivatives of this type of aziridines with two methyl groups on the carbon C(2) (2,2-dimethyl-*N*-(1-phenylethyl)aziridine-1-carboxamide) (**30**) or two hydrogen atoms on the C(2) carbon (*N*-(1-phenylethyl)aziridine-1-carboxamide) have already been published and were obtained by reaction of the corresponding aziridine with 1-(1-isocyanatoethyl)benzene.<sup>32</sup>

b. ***Pathway II***: characterisation of **Prod. B** and **Prod. C**

Following *Pathway II* the reaction between the isocyanate derivative and the primary amine at room temperature for three hours leads to the formation of **Prod. B**. This intermediate, a white foam, upon attempted isolation has only been characterised by NMR spectroscopy after evaporation of the solvent *in vacuo*. After dissolution in tetrahydrofuran and addition of potassium *tert*-butoxide at 0°C **Prod. C** is formed. This type of compounds has been isolated and fully characterised.

The <sup>1</sup>H NMR of **Prod. B** does not correspond to that of the urea. Interestingly during the course of our <sup>1</sup>H NMR experiments it has been observed that, at room temperature, the urea is not stable and rearranges after less than two hours to give a product possessing the same <sup>1</sup>H NMR spectrum as **Prod. B**. Thus, it has been assumed that the latter is already a cyclisation product of the urea.

Identification of **Prod. B** and **Prod. C** proved to be not trivial. They present similar resonance patterns in the <sup>1</sup>H and <sup>13</sup>C {<sup>1</sup>H} NMR spectra with sometimes only slight variation in the chemical shifts. For the reaction between the amine and the isocyanate derivative with the 4,4'-dimethyl substitution the two <sup>1</sup>H NMR spectra are given in Figure 2.4.4.

<sup>32</sup> a) A. P. Terent'ev, R. A. Gracheva, V. T. Bezruchko, *Doklady Akademii Nauk SSSR* **1967**, 172, 622; b) R. G. Kostyanovskii, K. S. Zakharov, M. Zarinova, V. F. Rudchenko, *Izvestiya Akademii, Nauk SSSR, Seriya Khimicheskaya* **1975**, 4, 875.



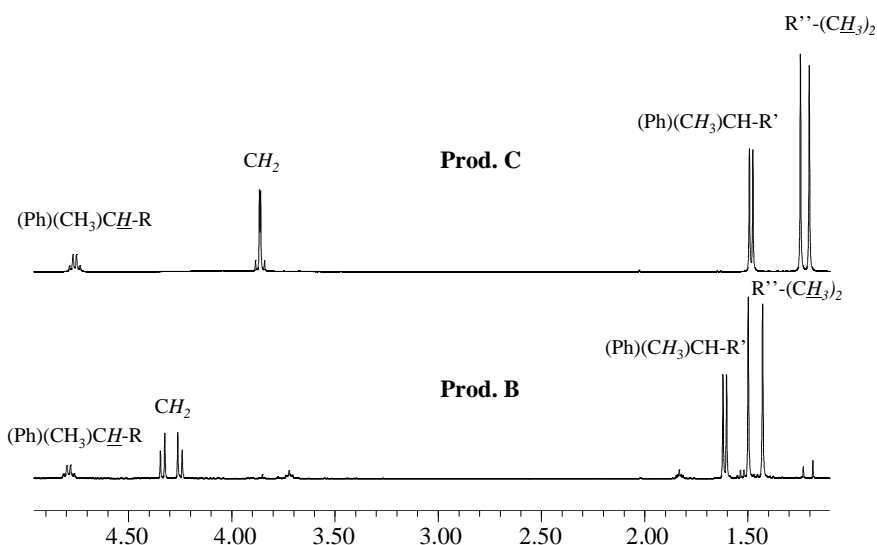


**Figure 2.4.4:**  $^1\text{H}$  NMR spectra in chloroform- $d_1$  (400 MHz) of **Prod. B** and **Prod. C** obtained by reaction between phenylethylamine and the achiral isocyanate derivative

For both compounds all the signals expected in case of cyclisation are present. Looking only at the  $^1\text{H}$  and  $^{13}\text{C}$   $\{^1\text{H}\}$  NMR spectra it is not possible to conclude whether the imidazolidinone or the aminooxazoline have been formed. Therefore  $^{15}\text{N}$  NMR and infrared data have been collected. The results are summarised in Table 2.4.2.

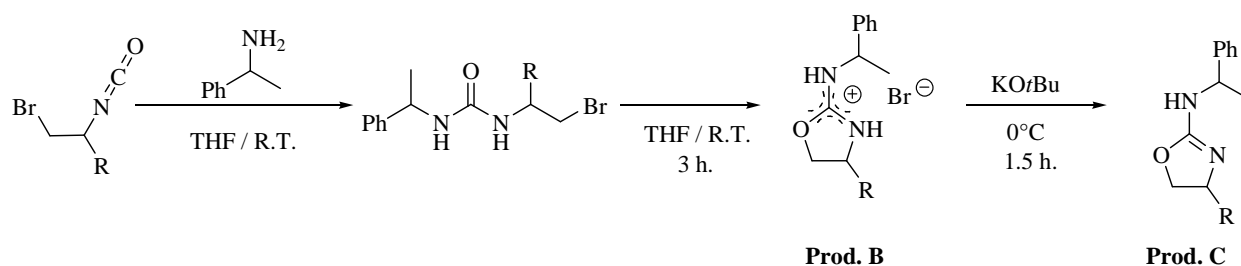
R	<b>Prod. B</b>			<b>Prod. C</b>		
	Me <sub>2</sub>	<i>i</i> Pr	Ph	Me <sub>2</sub>	<i>i</i> Pr	Ph
C1	160.5	161.5	161.6	158.3	159.2	160.7
C2	81.6	73.8	76.9	79.1	70.2	75.1
C3	60.0	61.7	61.3	65.1	70.0	67.9
N1	103	101	100	78	79	80
N2	112	97	/	177	160	/
IR	-	-	-	1687	1672	1686

**Table 2.4.2:**  $^{13}\text{C}$   $\{^1\text{H}\}$  and  $^{15}\text{N}$  NMR (in ppm) and infrared data ( $\nu_{\text{CN}}$  in  $\text{cm}^{-1}$ ) collected for **Prod. B.** and **Prod. C**

From the results presented in Table 2.4.2 it is possible to draw a first conclusion: **Prod. C** is an aminooxazoline, an assignment supported by different data. The chemical shifts of the  $^{15}\text{N}$

resonances of both nitrogens present in the compound are drastically different. This would not be expected for a cyclic urea and is in agreement with the formation of an aminooxazoline ring.<sup>33</sup> Moreover the chemical shifts of the  $^{13}\text{C}$  resonances (as well as the  $^1\text{H}$  resonances) are in agreement with those reported for the cyclohexyl-(4,4-dimethyloxazolin-2-yl)amine (C1: 158.3 ppm, C2: 78.8 ppm, C3: 65.0 ppm).<sup>34</sup> In addition the infrared data confirm the formation the aminooxazoline. The infrared spectra of the three derivatives of **Prod. C** show an absorption between 1672 and 1687  $\text{cm}^{-1}$  which is assigned to the  $\nu_{\text{C=N}}$  stretching mode of the oxazoline. In the literature, aminooxazolines display a vibrational band between 1655 and 1687  $\text{cm}^{-1}$  depending on the substituents<sup>34,35</sup> whereas those of imidazolidinones are observed between 1684 and 1716  $\text{cm}^{-1}$ .<sup>36</sup>

Addition of potassium *tert*-butoxide to **Prod. B** leads to the formation of **Prod. C**. In Table 2.4.2, the  $^{15}\text{N}$  resonances of **Prod. B** could correspond to those of imidazolidinones. However *N*-cyclisation of the urea to form **Prod. B** can not be envisaged. Indeed, knowing that **Prod. C** is an aminooxazoline is not possible that the intramolecular cyclisation of the urea afford an imidazolidinone. Based on the NMR data, on the fact that **Prod. C** stems from the *O*-cyclisation and that the **Prod. B** derivatives appear as foam, we suggest that the latter are the hydrobromide salts of the corresponding aminooxazolines. In summary, reaction between the isocyanate derivatives and the primary amine generates the urea. The intramolecular *O*-cyclisation of the latter then gives the hydrobromide salts which, after addition of potassium *tert*-butoxide affords the aminooxazoline (Scheme 2.4.4).



**Scheme 2.4.4:** Reaction pathway for the synthesis of the aminooxazolines

<sup>33</sup> It has been calculated that in an aminooxazoline the  $^{15}\text{N}$  nucleus of the C=N bond resonates at around 160 ppm and the  $^{15}\text{N}$  nucleus of the H-N bond resonates at around 95 ppm. In an imidazolidinone, it has been found that the  $^{15}\text{N}$  nucleus of the C-N bond resonates at around 118 ppm and the  $^{15}\text{N}$  nucleus of the H-N bond resonates at around 88 ppm.

<sup>34</sup> E. J. Crust, I. J. Munslow, P. Scott, *J. Organomet. Chem.* **2005**, 690, 3373.

<sup>35</sup> T. H. Kim, N. Lee, G.-J. Lee, J. N. Kim, *Tetrahedron* **2001**, 57, 7137.

<sup>36</sup> T. H. Kim, G.-J. Lee, *J. Org. Chem.* **1999**, 64, 2941.

Formation of the salt also accounts for the differences observed in the chemical shifts in the  $^1\text{H}$  NMR spectra (see Figure 2.4.4). Addition of HCl (from a 2M solution in diethylether) to **Prod. C** in chloroform- $d_1$  clearly confirms that **Prod. B** is the protonated aminooxazoline. Indeed the  $^1\text{H}$  NMR spectrum of **Prod. C** in the presence of HCl is similar to the one of **Prod. B**.

Using *Pathway II*, four different hydrobromide salts have been characterised by NMR spectroscopy and their four corresponding aminooxazolines have been isolated (Figure 2.4.5).

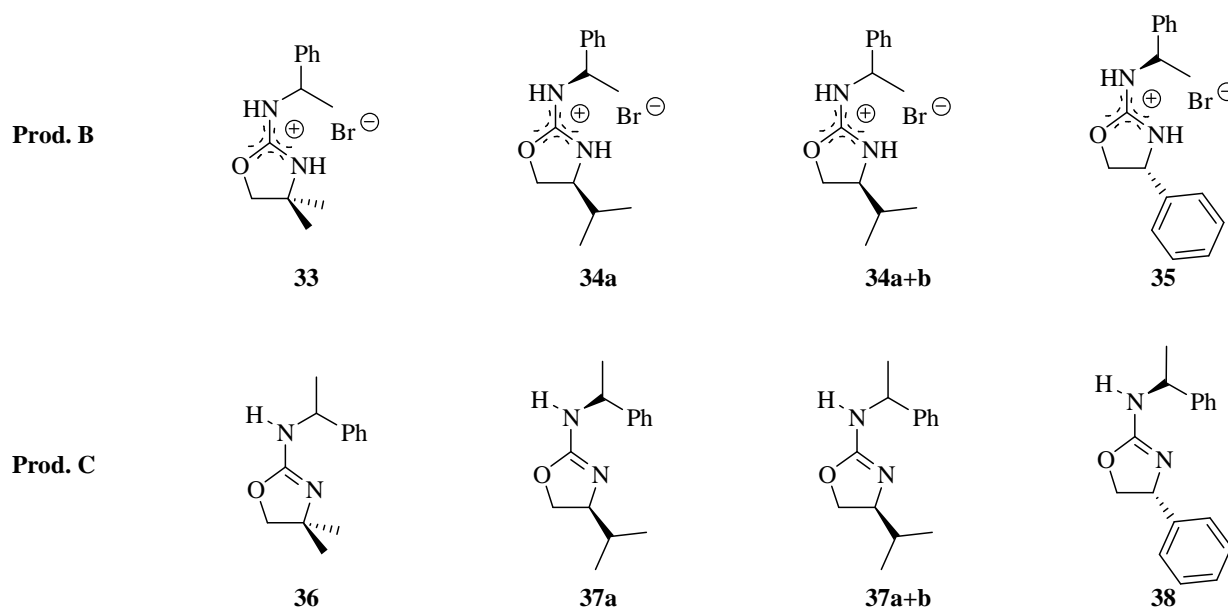


Figure 2.4.5: The compounds formed following the procedure of *Pathway II*

c. Determination of the enantiomeric excess of primary amine

Following *Pathway I* and *II* in the presence of *rac*-phenylethylamine and the isocyanate derivative bearing the (*S*)-isopropyl substituent the aziridine (**31a+b**), the salt of the aminooxazoline (**34a+b**) and the aminooxazoline (**37a+b**) have been prepared. It is possible to assign completely in the  $^1\text{H}$  NMR spectra the signals of the two diastereoisomers for all three of them. Formation of either the 2-aminoxazoline or the aziridine in principle enables the determination of the enantiomeric excess of the primary amine by NMR spectroscopy.



## - Chapter 3 -

<b>I. Synthesis and structural characterisation of trisox-based palladium complexes .....</b>	<b>65</b>
1. [Pd <sup>II</sup> Cl <sub>2</sub> (trisox)] complexes .....	65
2. A [Pd <sup>II</sup> (allyl)(trisox)] complex.....	68
3. [Pd <sup>0</sup> (trisox)(alkene)] complexes .....	70
4. Conclusion .....	75
<b>II. Dynamic behaviour of trisox-based palladium complexes in solution.....</b>	<b>75</b>
1. [Pd <sup>II</sup> Cl <sub>2</sub> (trisox)]complexes.....	75
a. Principle of the magnetisation transfer .....	77
b. Experimental determination of the activation parameters for the fluxional process in complex <b>39</b> .....	79
c. Experimental determination of the activation parameters for the fluxional process in complex <b>42</b> .....	82
d. Solution dynamics of complexes <b>39-42</b> .....	85
2. The [Pd <sup>II</sup> (allyl)(Ph-trisox)] complex.....	86
3. [Pd <sup>0</sup> (alkene)(trisox)] complexes .....	88
a. VT-NMR spectroscopic study of complexes <b>44-46</b> .....	88
b. VT-NMR spectroscopic study of complex <b>47</b> .....	90
c. VT-NMR spectroscopic study of complex <b>48</b> .....	91
4. Conclusion .....	92
<b>III. Palladium-catalysed asymmetric allylic substitution .....</b>	<b>93</b>
1. The test reaction.....	93

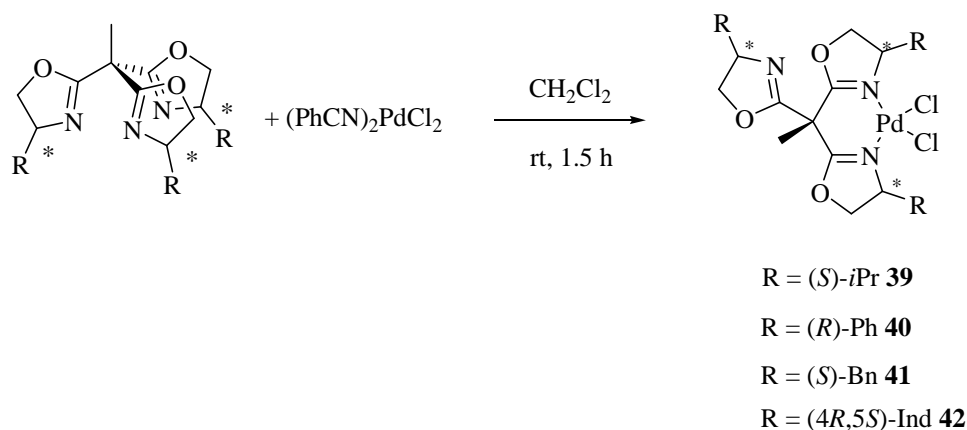
2.	Palladium-catalysed asymmetric allylic substitution: general aspects .....	94
a.	Introduction.....	94
b.	Mechanism.....	94
c.	Catalysts.....	97
3.	Trisox/palladium catalysts in allylic substitutions.....	98
a.	Experimental conditions .....	98
b.	Preliminary results .....	101
c.	Trisoxazoline vs bisoxazoline.....	102
d.	Extension of the study to functionalised bisoxazolines .....	105
4.	Conclusion .....	107

This chapter is devoted to the application of the trisoxazolines in palladium chemistry. The synthesis and structural characterisation of trisoxazoline-based palladium(II) and palladium(0) complexes are presented. The second part concentrates on the study of the dynamic fluxional behaviour of the Pd(II) and Pd(0) complexes. Finally, the application of the palladium complexes in asymmetric allylic substitution is discussed.

## I. Synthesis and structural characterisation of trisox-based palladium complexes

### 1. $[Pd^{II}Cl_2(trisox)]$ complexes

Palladium(II) chloride complexes can easily be obtained by reaction of the desired ligand with a precursor from type  $[PdCl_2L_2]$  where L is a labile ligand. A series of neutral dichloropalladium(II) complexes was synthesized by reaction of the trisox derivatives with  $[PdCl_2(PhCN)_2]$  in dichloromethane at room temperature (Scheme 3.1.1). All four complexes  $[PdCl_2(iPr-trisox)]$  (**39**),  $[PdCl_2(Ph-trisox)]$  (**40**),  $[PdCl_2(Bn-trisox)]$  (**41**) and  $[PdCl_2(Ind-trisox)]$  (**42**) were isolated as crystalline orange air-stable solids. The analytical data confirmed the formation of the target complexes and the resonance pattern of the  $^1H$ ,  $^{13}C\{^1H\}$  and  $^{15}N$  NMR spectra recorded at 296 K are consistent with a  $\kappa^2$ -coordination of the trisoxazoline ligands.



**Scheme 3.1.1:** Synthesis of palladium(II) complexes **39-42**

It was possible to obtain crystals suitable for X-ray diffraction of  $[PdCl_2(iPr-trisox)]$  by slow diffusion of diethylether into a solution of **39** in dichloromethane. The molecular structure of compound **39** in the solid state is shown in Figure 3.1.1 and selected bond lengths and angles are given in Table 3.1.1.

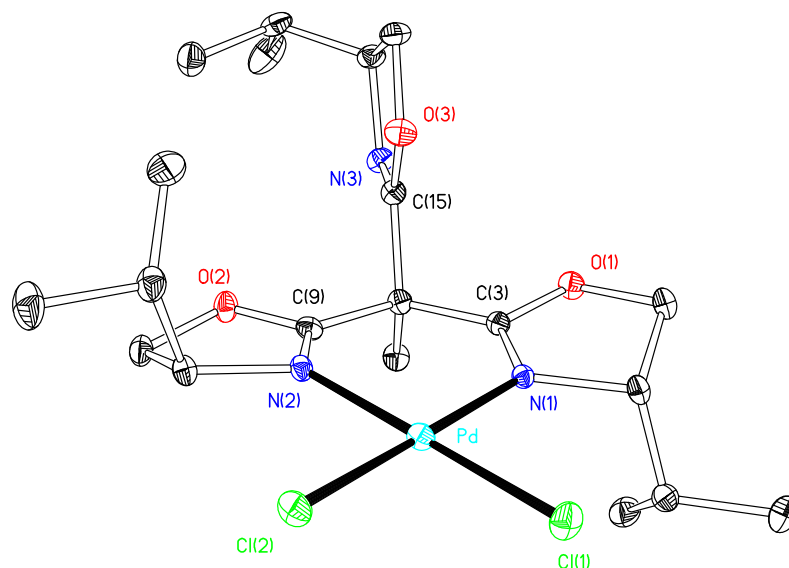


**Figure 3.1.1:** Thermal ellipsoid plot (25%) of  $[\text{PdCl}_2(\text{iPr-trisox})]$  **39**

Pd-N(1)	2.050(2)	Pd-N(2)	2.029(3)
Pd-Cl(1)	2.2864(9)	Pd-Cl(2)	2.2825(8)
N(1)-C(3)	1.272(4)	N(2)-C(9)	1.278(4)
N(3)-C(15)	1.256(4)		
Cl(1)-Pd-N(1)	92.31(8)	N(1)-Pd-N(2)	88.7(1)
N(2)-Pd-Cl(2)	91.84(8)	Cl(2)-Pd-Cl(1)	87.09(4)

**Table 3.1.1:** Selected bond lengths (Å) and angles (°) for complex  $[\text{PdCl}_2(\text{iPr-trisox})]$  **39**

Similarly, complex  $[\text{PdCl}_2(\text{Ph-trisox})]$  crystallised by slow diffusion of pentane into a solution of **40** in  $\text{CH}_2\text{Cl}_2$ . The structure of **40** is depicted in Figure 3.1.2. Selected bond lengths and angles are given in Table 3.1.2.

Pd-N(1)	2.030(2)	Pd-N(2)	2.041(2)
Pd-Cl(1)	2.2915(7)	Pd-Cl(2)	2.2606(8)
N(1)-C(1)	1.273(4)	N(2)-C(12)	1.283(4)
N(3)-C(21)	1.294(4)		
Cl(1)-Pd-N(1)	91.58(7)	N(1)-Pd-N(2)	89.42(10)
N(2)-Pd-Cl(2)	91.02(8)	Cl(2)-Pd-Cl(1)	88.07(3)

**Table 3.1.2:** Selected bond lengths (Å) and angles (°) for complex  $[\text{PdCl}_2(\text{Ph-trisox})]$  **40**



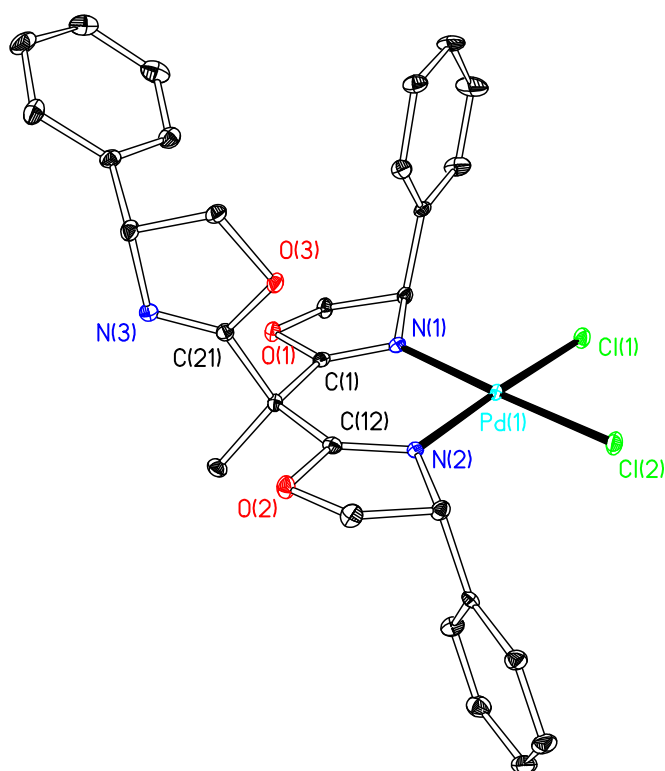


Figure 3.1.2: Thermal ellipsoid plot (25%) of [PdCl<sub>2</sub>(Ph-trisox)] **40**

In both complexes the geometry around the metal centre is distorted square planar, as expected for  $d^8$  palladium(II) complexes. The slight deformation is probably due to the steric repulsion of the chloro ligands and the isopropyl and phenyl substituents respectively.

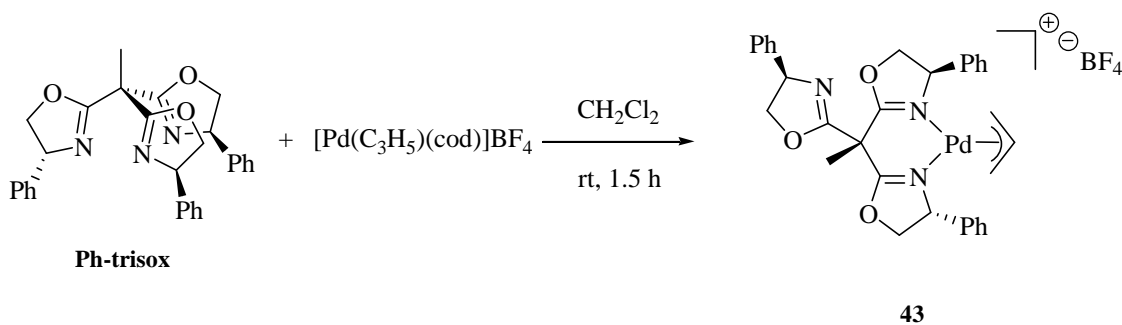
The trisoxazoline ligands adopt bidentate coordination, with the third oxazoline unit dangling, and the nitrogen donor pointing away from the metal centre. The free oxazoline ring is oriented perpendicularly to the plane defined by the six-membered metallacycle. The Pd-N and Pd-Cl bond lengths are in the range of those found for related structures.<sup>1</sup> As expected, the C=N bond length of the free oxazoline is slightly shorter than those in the coordinated oxazoline units (1.256(4) vs. 1.272(4) and 1.278(4) Å for **39** and 1.249(4) vs. 1.273(4) and 1.283(4) Å for **40**).

The infrared spectrum of [PdCl<sub>2</sub>(*i*Pr-trisox)] displays a vibrational band at 1660 cm<sup>-1</sup> which is assigned to the  $\nu_{\text{C=N}}$  stretching mode of the free oxazoline ring and an absorption at 1650 cm<sup>-1</sup> corresponding to the  $\nu_{\text{C=N}}$  stretching mode of the coordinated oxazoline units. In comparison, the  $\nu_{\text{C=N}}$  stretching frequency of free *i*Pr-trisox is 1660 cm<sup>-1</sup>. For complex **40**, only the band assigned to the  $\nu_{\text{C=N}}$  stretching mode of the coordinated oxazoline units is observed at 1655 cm<sup>-1</sup> (1665 cm<sup>-1</sup> for the  $\nu_{\text{C=N}}$  stretching mode of free Ph-trisox).

<sup>1</sup> A. El Hatimi, M. Gómez, S. Jansat, G. Muller, M. Font-Bardía, X. Solans, *J. Chem. Soc., Dalton Trans.* **1998**, 4229.

## 2. A $[Pd^{II}(\text{allyl})(\text{trisox})]$ complex

Reaction of palladium allyl derivatives with our most commonly used tripod *i*Pr-trisox yielded oily products. We then decided to focus on the phenyl-substituted trisoxazoline derivative Ph-trisox in order to obtain crystalline complexes. Reaction of commercially available  $[Pd(\eta^3\text{-C}_3\text{H}_5)\text{Cl}]_2$  with Ph-trisox in dichloromethane followed by the addition of one equivalent of silver tetrafluoroborate did not lead to the expected compound. The desired  $(\eta^3\text{-allyl})$ palladium complex was prepared from  $[Pd(\eta^3\text{-C}_3\text{H}_5)(\text{cod})]\text{BF}_4$  (cod = cyclooctadiene). The latter was obtained by reaction of the corresponding  $[Pd(\eta^3\text{-C}_3\text{H}_5)\text{Cl}]_2$  dimer with cyclooctadiene and silver tetrafluoroborate in good yields according to the procedure of White *et al.*<sup>2</sup> Reaction of  $[Pd(\eta^3\text{-C}_3\text{H}_5)(\text{cod})]\text{BF}_4$  with Ph-trisox in dichloromethane gave the expected corresponding allyl complex **43** (Scheme 3.1.2).



**Scheme 3.1.2:** Synthesis of  $[Pd(\eta^3\text{-C}_3\text{H}_5)(\text{Ph-trisox})]\text{BF}_4$  **43**

Suitable crystals for an X-ray diffraction study were obtained by slow diffusion of pentane into a solution of complex **43** in dichloromethane. The molecular structure is displayed in Figure 3.1.3 and selected bond lengths and angles are given in Table 3.1.3. For clarity, only a single orientation of the allyl ligand is shown, corresponding to the major isomer.

<sup>2</sup> D. A. White, *Inorg. Synth.* **1972**, 13, 55.

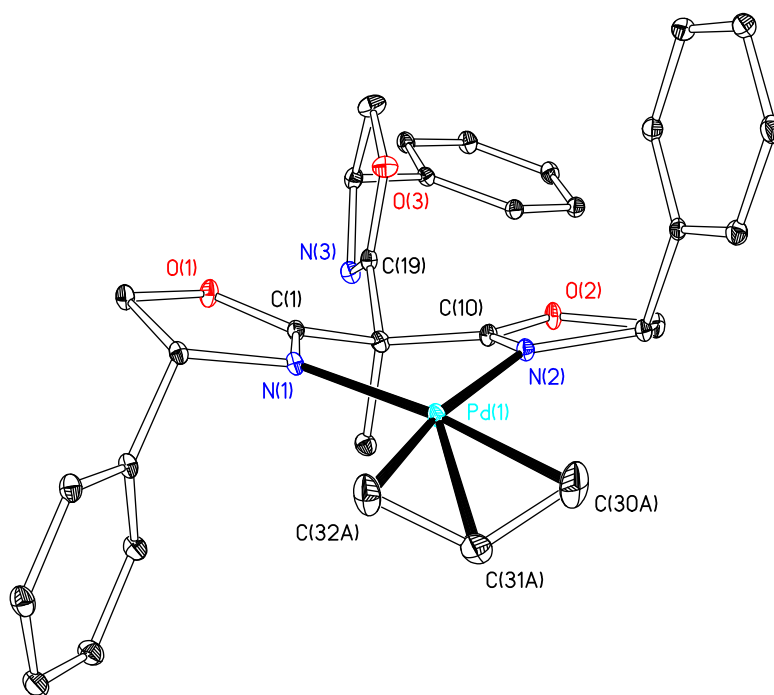


**Figure 3.1.3:** Thermal ellipsoid plot (25%) of  $[\text{Pd}(\eta^3\text{-C}_3\text{H}_5)(\text{Ph-trisox})]\text{BF}_4$  **43**  
Hydrogen atoms and the counteranion are omitted for clarity

Pd-N(1)	2.104(2)	Pd-N(2)	2.102(2)
Pd-C(32)	2.120(3)	Pd-C(30)	2.131(3)
N(1)-C(1)	1.279(3)	N(2)-C(10)	1.274(3)
N(3)-C(19)	1.264(3)	C(32)-C(31)	1.405(5)
C(30)-C(31)	1.345(5)		
C(32)-Pd-N(1)	102.16(9)	N(1)-Pd-N(2)	88.14(7)
N(2)-Pd-C(30)	100.85(10)	C(32)-Pd-C(30)	68.87(12)
C(32)-C(31)-C(30)	121.86(4)		

**Table 3.1.3:** Selected bond lengths (Å) and angles (°) for complex  $[\text{Pd}(\eta^3\text{-C}_3\text{H}_5)(\text{Ph-trisox})]\text{BF}_4$  **43**

The palladium atom adopts a planar coordination geometry with the  $\pi$ -allyl ligand and two of the three oxazoline rings of the ligand being coordinated. As expected for  $[\text{Pd}^{\text{II}}(\text{allyl})]$  complexes of this type,<sup>3,4</sup> the coordination geometry of **43** is pseudo-square planar with the four coordination sites occupied by the two nitrogen donors and the allylic termini C(32) and C(30). As for the dichloropalladium derivatives **39-42**, the third oxazoline unit is dangling with the

<sup>3</sup> a) A. Albinati, C. Ammann, P. S. Pregosin, H. Rüegger, *Organometallics* **1990**, *9*, 1826; b) A. Albinati, R. W. Kunz, C. Ammann, P. S. Pregosin, *Organometallics* **1991**, *10*, 1800; c) P. von Matt, G. C. Lloyd-Jones, A. B. E. Minidis, A. Pfaltz, L. Macko, M. Neuburger, M. Zehnder, H. Rüegger, P. S. Pregosin, *Helv. Chim. Acta* **1995**, *78*, 265.

<sup>4</sup> a) L. S. Hegedus, B. Åkermark, D. J. Olson, O. P. Anderson, K. Zetterberg, *J. Am. Chem. Soc.* **1982**, *104*, 697; b) N. W. Murrall, A. J. Welch, *J. Organomet. Chem.* **1986**, *301*, 109; c) A. Togni, G. Rihs, P. S. Pregosin, C. Ammann, *Helv. Chim. Acta* **1990**, *73*, 723.

nitrogen donor pointing away from the palladium centre. The free oxazoline ring is oriented perpendicularly to the plane defined by the six-membered metallacycle. The Pd-N and Pd-C bond lengths are within the range found for related complexes reported in the literature.<sup>5</sup> Here again, as expected, the C=N bond length of the free oxazoline is slightly shorter than those in the coordinated oxazoline units (1.264(3) vs. 1.279(3) and 1.274(3) Å).

The six-membered chelate ring adopts a slightly twisted boat conformation. A disorder in the central C-atom (C(31)) of the  $\pi$ -allyl ligand is found in the crystal structure of the complex with a relative occupancy of about 2:1. This indicates a mixture of the two diastereomers in that ratio, resulting of the reduction in the  $C_2$  symmetry of the coordinated bisoxazoline due to the presence of the third uncoordinated heterocycle. In the major isomer, the allyl group is orientated with the central C-H allylic bond pointing in the same direction as the axial methyl group (see Figure 3.1.3 where the structure of the major isomer is depicted).

The infrared spectrum of  $[\text{Pd}(\eta^3\text{-C}_3\text{H}_5)(\text{Ph-trisox})]\text{BF}_4$  displays a vibrational band at 1658  $\text{cm}^{-1}$  which is assigned to the  $\nu_{\text{C=N}}$  stretching mode of the coordinated oxazoline units (1665  $\text{cm}^{-1}$  for the  $\nu_{\text{C=N}}$  stretching mode of free Ph-trisox). The absorption from the  $\nu_{\text{C=N}}$  stretching mode of the free heterocycle is not observed.

### 3. $[\text{Pd}^0(\text{trisox})(\text{alkene})]$ complexes

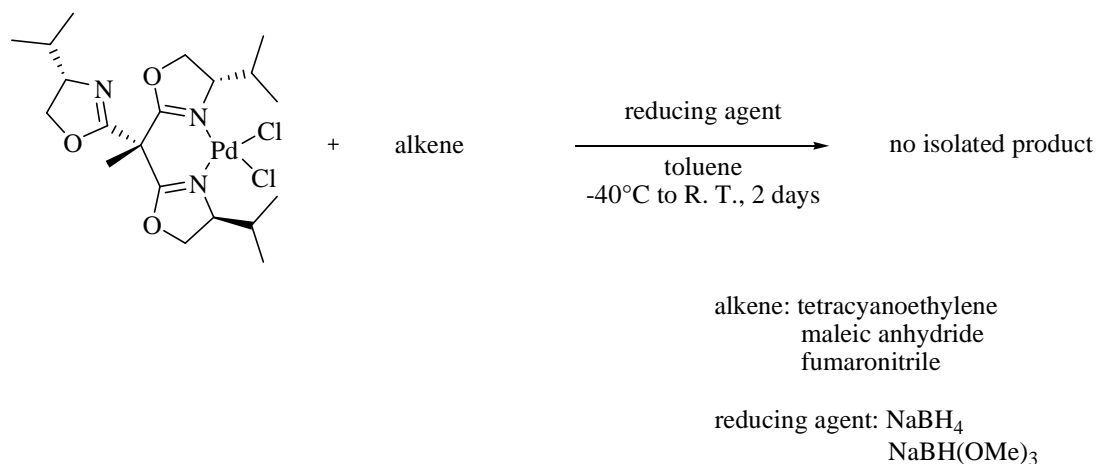
Having explored the coordination chemistry of the trisoxazolines with palladium(II), we then turned our attention to zero-valent palladium complexes. Compared to the extensive work on phosphine- $\eta^2$ -alkene palladium(0) complexes, there are only few well defined  $[\text{Pd}^0(\eta^2\text{-alkene})]$  complexes that contain ancillary nitrogen donor ligands.<sup>6</sup> In particular, we note that there is no report of structurally characterized Pd(0) complexes containing oxazoline-based ligands.

Palladium(0) compounds are generally either formed *in situ* by reduction of a suitable palladium(II) precursor, or by starting from a zero-valent palladium precursor complex

<sup>5</sup> a) O. Hoarau, H. Ait-Haddou, J.-C. Daran, D. Cramailere, G. G. A. Balavoine, *Organometallics* **1999**, *18*, 4718; b) M. Kehnder, M. Neuburger, P. von Matt, A. Pfaltz, *Acta Cryst.* **1995**, *C51*, 1109.

<sup>6</sup> a) F. Ozawa, T. Ito, Y. Nakamura, A. Yamamoto, *J. Organomet. Chem.* **1979**, *168*, 375; b) K. J. Cavell, D. J. Stufkens, K. Vrieze, *Inorg. Chim. Acta* **1981**, *47*, 67; c) B. Crociani, F. Di Bianca, P. Uguagliati, L. Canovese, A. Berton, *J. Chem. Soc., Dalton Trans.* **1991**, 71; d) B. Milani, A. Anzilutti, L. Vicentini, A. Sessanta o Santi, E. Zangrando, S. Geremia, G. Mestroni, *Organometallics* **1997**, *16*, 5064; e) R. A. Klein, P. Witte, R. Van Belzen, J. Fraanje, K. Goubitz, M. Numan, H. Schenk, J. M. Ernsting, C. J. Elsevier, *Eur. J. Inorg. Chem.* **1998**, 319; f) M. W. van Laren, C. J. Elsevier, *Angew. Chem. Int. Ed.* **1999**, *38*, 3715; *Angew. Chem.* **1999**, *111*, 3926; g) C. Boriello, M. L. Ferrara, I. Orabona, A. Panunzi, F. Ruffo, *J. Chem. Soc., Dalton Trans.* **2000**, 2545; h) A. M. Kluwer, C. J. Elsevier, M. Bühl, M. Lutz, A. L. Spek, *Angew. Chem. Int. Ed.* **2003**, *42*, 3501; *Angew. Chem.* **2003**, *115*, 3625; i) A. M. Kluwer, T. S. Koblenz, T. Jonischkeit, K. Woelk, C. J. Elsevier, *J. Am. Chem. Soc.* **2005**, *127*, 15470; j) J. J. de Pater, D. S. Tromp, D. M. Tooke, A. L. Spek, B.-J. Deelman, G. van Koten, C. J. Elsevier, *Organometallics* **2005**, *24*, 6411.

containing labile ligands. Attempts to reduce the  $[\text{PdCl}_2(\text{trisox})]$  complexes described in the previous sections did not lead to the isolation of the expected palladium(0) complexes (Scheme 3.1.3).



**Scheme 3.1.3:** Attempts to reduce  $[\text{PdCl}_2(i\text{Pr-trisox})]$

Reduction of **39** in the presence of an olefin was carried out by using either sodium borohydride or sodium trimethoxyborohydride as reducing agent.<sup>7</sup> The reaction led to the formation of brown solids.  $^1\text{H}$  NMR spectra of these compounds showed the presence of an impure complex and all attempts at recrystallisation resulted in decomposition.

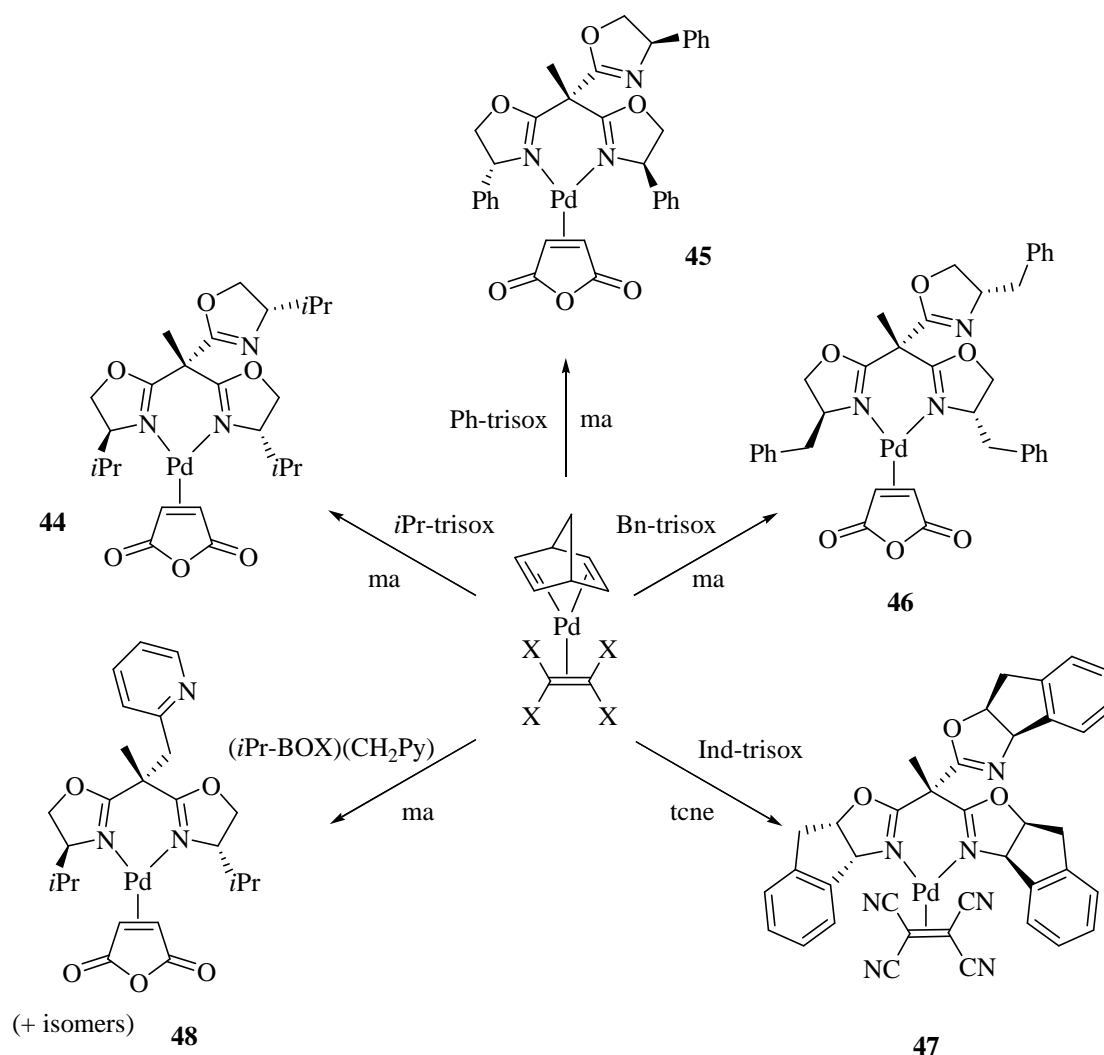
Considering these results, we decided to try the alternative synthetic route, starting from zero-valent palladium complexes. The  $\text{Pd}(0)$  precursor was chosen based on interesting results reported by Elsevier *et al.* in which mixed alkene complexes were used as precursors for the synthesis of palladium(0) species.<sup>6f</sup> The stability of these different mixed olefin complexes is based on the appropriate combination of electron donating and electron withdrawing olefin ligands.<sup>8</sup>

Palladium(0) precursors of the general formula  $[\text{Pd}(\text{nbd})(\text{alkene})]$  (nbd = norbornadiene; alkene = maleic anhydride or tetracyanoethylene) were synthesised, norbornadiene being the electron rich olefin and maleic anhydride or tetracyanoethylene being the electron poor olefins. A number of palladium(0) complexes with different ligands, including a potentially tridentate pyridine-bisoxazoline ligand, and alkenes were synthesised using these precursors. Complexes **44-48** were obtained by substitution of the norbornadiene ligand by the respective tripod ligand

<sup>7</sup> A. J. Blacker, M. L. Clarke, M. S. Loft, M. F. Mahon, M. E. Humphries, J. M. J. Williams, *Chem. Eur. J.* **2000**, *6*, 353.

<sup>8</sup> K. Ito, F. Ueda, K. Hirai, Y. Ishii, *Chem. Lett.* **1977**, 877.

in tetrahydrofuran and were isolated as highly air sensitive yellow powders in 50 -75% yield (Scheme 3.1.4).



**Scheme 3.1.4:** Synthesis of palladium(0) complexes of type [Pd(alkene)(tripod)] **44-48**  
 (nbd = norbornadiene, ma = maleic anhydride, tcne = tetracyanoethylene).

For  $d^{10}$  palladium(0) complexes, two different molecular geometries can be expected. The first one is a trigonal planar geometry with the trisoxazoline acting as a bidentate ligand. The second molecular geometry possible is tetrahedral with the three nitrogen donors of the facial tridentate ligand coordinated to the metal centre. Crystallisation by slow diffusion of pentane into a solution of **44** in diethylether gave suitable crystals for an X-ray diffraction study. The molecular structure is presented in Figure 3.1.4 and selected bond lengths and angles are given in Table 3.1.4.

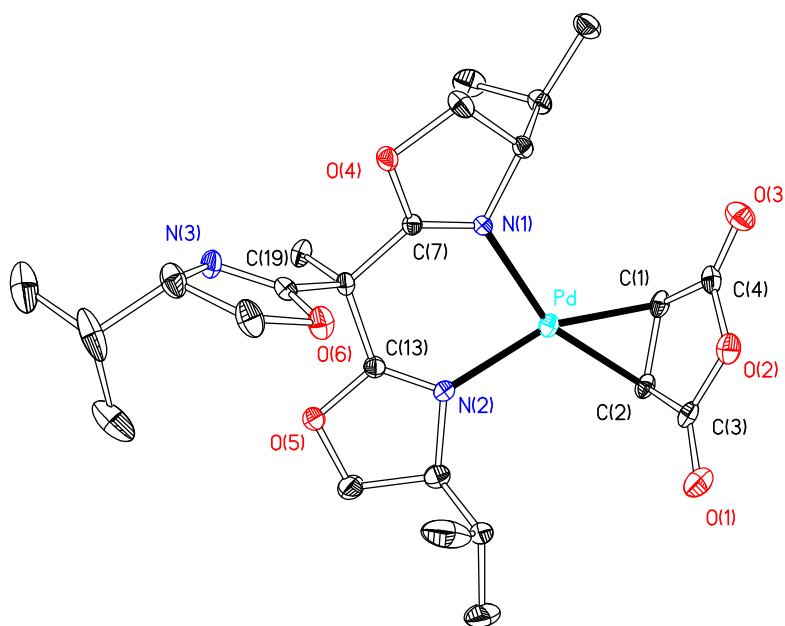


**Figure 3.1.4:** Thermal ellipsoid plot (25%) of [Pd(ma)(iPr-trisox)] **44**

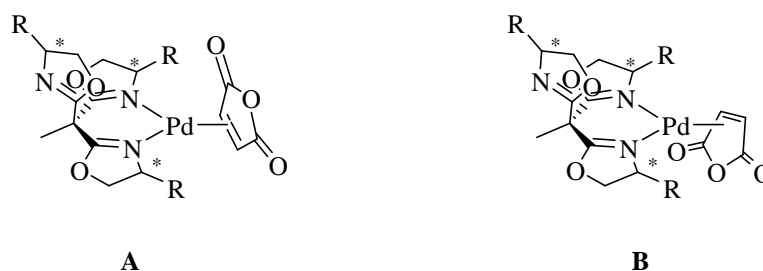
Pd-N(1)	2.127(5)	Pd-N(2)	2.115(4)
Pd-C(1)	2.107(7)	Pd-C(2)	2.082(6)
N(1)-C(7)	1.261(7)	N(2)-C(13)	1.261(7)
N(3)-C(19)	1.254(9)	C(1)-C(2)	1.448(9)
C(4)-O(3)	1.179(8)	C(3)-O(1)	1.212(9)
N(1)-Pd-N(2)	85.6(2)	N(2)-Pd-C(2)	116.9(2)
C(1)-Pd-N(1)	117.6(2)	C(1)-Pd-C(2)	40.4(2)
Torsion angle		C(3)-C(2)-C(1)-Pd	-98.4°

**Table 3.1.4:** Selected bond lengths (Å) and angles (°) for complex [Pd(ma)(iPr-trisox)] **44**

Complex **44** possesses Y-shaped trigonal planar geometry with the trisoxazoline ligand coordinated in a bidentate way whilst the third oxazoline unit is dangling with the nitrogen donor pointing away from the metal centre. Two nitrogen donor ligands are sufficient to stabilize the metal centre in its low oxidation state with maleic anhydride as co-ligand. The cyclic anhydride is oriented perpendicularly to the plane defined by the palladium atom and the two coordinated heterocycles in order to optimize the orbital overlapping between the  $\pi$ -orbital of the C=C bond and the  $d$  orbitals of the metal centre. The Pd-N (2.127(5) Å) and Pd-C (2.082(6) Å) bond lengths are in agreement with reported values for similar complexes that contain bidentate nitrogen-based ligands such as *t*BuDAB (3,6-diaza-2,2,7,7-tetramethyl-octa-3,5-diene).<sup>6j,9</sup> The N(1)-Pd-N(2) angle of 85.6(2)° is greater than those reported for related complexes (typically

<sup>9</sup> D. D. Ellis, A. L. Spek, *Acta Crystallogr. C* **2001**, 57, 235.

77.2 - 77.5°).<sup>10</sup> This increase of the bite angle is due to the six-membered chelate ring of a bidentate trisoxazoline compared to the values of five-membered rings described in the literature. As expected, upon coordination of the alkene an elongation of the C=C bond distance (1.448(9) Å) with respect to the free alkene (1.3322(9) Å) is observed.<sup>11</sup> Considering the presence of the third dangling oxazoline unit, two diastereomers can be formed: one with the central oxygen of the olefin pointing in the same direction as the free oxazoline unit (**A**) and one with the central oxygen of the olefin pointing in the opposite direction of the free heterocycle (**B**) (Scheme 3.1.5).



**Scheme 3.1.5:** The two possible diastereomers for complexes [Pd(ma)(trisox)] **44-46**

Notably although an equilibrium of these two diastereomers is observed in solution at ambient temperature, the crystals employed for the X-ray diffraction study of **44** consists only of one diastereomeric form.

Slow diffusion of pentane into a solution of [Pd(ma)(Ph-trisox)] in dichloromethane gave suitable crystals for X-ray diffraction. In the crystals of the phenyl substituted complex **45** the opposite diastereomer (**B**) is found exclusively. Apart from that, the molecular structure appears similar to that of **44**. However, the quality of the data was only sufficient to unequivocally establish the molecular connectivity and configuration, but did not allow a more detailed appreciation of the structure.

The infrared spectra of complexes **44-46** displayed the vibrational bands assigned to the  $\nu_{C=N}$  stretching mode of the free oxazoline ring and of the coordinated oxazoline units (Table 3.1.5). In case of complex **48**, the infrared spectrum (KBr-Pellet) also showed the presence of one free and one coordinated oxazoline unit indicating the formation of a 7-membered metallacycle. Absorptions at 1786-1794  $\text{cm}^{-1}$  and 1722-1727  $\text{cm}^{-1}$  were assigned to the  $\nu_{C=O}$  stretching mode of the anhydride (1784  $\text{cm}^{-1}$  for the free maleic anhydride).

<sup>10</sup> a) T. Schleis, J. Heinemann, T. P. Spaniol, R. Mülhaupt, J. Okuda, *Inorg. Chem. Commun.* **1998**, *1*, 431; b) M. L. Ferrara, F. Giordana, I. Orabona, A. Panunzi, F. Ruffo, *Eur. J. Inorg. Chem.* **1999**, 1939.

<sup>11</sup> M. Lutz, *Acta Crystallogr. Sect. E* **2001**, *57*, o1136.



	V <sub>C=N</sub>	V <sub>C=N</sub>	V <sub>C=O</sub>	V <sub>C=N</sub>
	dangling oxazoline	coordinated oxazolines		tripodal ligand
<b>44</b>	1660	1650	1786, 1722	1660
<b>45</b>	1662	1655	1798, 1727	1665
<b>46</b>	1662	1655	1793, 1724	1664
<b>48</b>	1664	1653	1794, 1723	1663

**Table 3.1.5:** Selected  $\nu_{C=O}$  and  $\nu_{C=N}$  stretching mode ( $\text{cm}^{-1}$ ) of complexes [Pd(ma)(tripod)] **44-46** and **48** and  $\nu_{C=N}$  stretching mode ( $\text{cm}^{-1}$ ) of the corresponding tripodal ligand

#### 4. Conclusion

Trisoxazoline-based palladium complexes in the oxidation states (0) and (II) were successfully synthesized. They were obtained starting from the appropriate palladium precursors. For each family of complexes, [PdCl<sub>2</sub>(triso)], [Pd(allyl)(triso)] and [Pd(alkene)(tripod)], at least one compound could be structurally characterised. It has been shown that, in the solid state, trisoxazolines act as bidentate ligands with the third dangling oxazoline unit oriented perpendicularly to the plane defined by the two ligating heterocycles. This  $\kappa^2$ -coordination of the trisoxazoline ligands was also confirmed by infrared spectroscopy.

We were then interested in the behaviour of these complexes in solution. It has been observed, in the <sup>1</sup>H NMR spectra at room or high temperature, that dynamic exchange between the three binding sites occurs. The next part of this chapter describes our investigations into the fluxional behaviour of the C<sub>3</sub>-symmetric ligands.

## II. Dynamic behaviour of triso-based palladium complexes in solution

### 1. [Pd<sup>II</sup>Cl<sub>2</sub>(triso)] complexes

The <sup>1</sup>H NMR spectra of [PdCl<sub>2</sub>(triso)] complexes described in the first part of this chapter were recorded at 296 K. They are consistent with C<sub>1</sub> symmetry compared to the C<sub>3</sub> symmetry observed in those from the free trisoxazolines. We obtained good quality <sup>15</sup>N NMR spectra by direct detection of the heteronuclei on a 600 MHz NMR spectrometer. It was possible to completely assign the signals in the <sup>1</sup>H and <sup>13</sup>C NMR spectra of the coordinated oxazolines and the non-coordinated oxazoline by combined 2D <sup>1</sup>H-<sup>15</sup>N and <sup>1</sup>H-<sup>13</sup>C NMR experiments. For complexes **39-42**, the <sup>15</sup>N nuclei of the coordinated oxazoline rings resonate at  $\delta = 160 - 167$  and appear as two singlets due to their diastereotopicity. The signal assigned to the dangling oxazoline arm is observed at  $\delta = 238 - 240$ . In complex **41**, for example, the <sup>15</sup>N nuclei of the coordinated oxazoline rings resonate at 161.3 and 162.2 ppm and the signal assigned to the free oxazoline unit is observed at 239.9 ppm. In comparison, the <sup>15</sup>N nuclei of the C<sub>3</sub>-symmetric free

ligand (Bn-trisox) resonate at 234.0 ppm. The  $^1\text{H}$ - $^{15}\text{N}$  correlated spectrum of complex **41** is shown in Figure 3.2.1 with the directly recorded 1D  $^{15}\text{N}$  NMR spectrum displayed along the F1-axis.

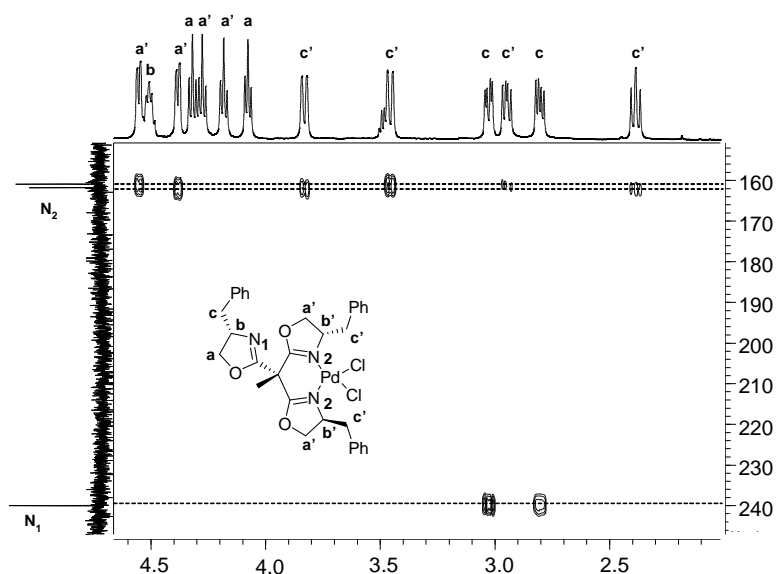


**Figure 3.2.1:** 2D  $^1\text{H}$ - $^{15}\text{N}$  NMR correlated experiment (HMBC) from complex **41** in  $\text{CDCl}_3$

As indicated above, the  $^1\text{H}$  NMR spectrum of **39** at 296 K is consistent with the molecular structure established for the crystalline state. Separated sets of signals, which are attributable to the protons of the three different isopropyl groups of the oxazoline units, indicate the loss of local threefold symmetry for the tripod ligand. The same loss of degeneracy of the three oxazoline units is observed in the  $^{13}\text{C}$  NMR spectra (75 MHz, 296 K) and the  $^{15}\text{N}$  NMR spectrum (60 MHz, 296 K). Upon increasing the temperature to 373 K coalescence occurs. The two doublets for the  $-\text{CH}(\text{CH}_3)_2$  isopropyl protons observed in the high temperature limiting spectrum, representing effective  $C_3$  symmetry, are consistent with a fast exchange between ligating and non-ligating oxazoline rings (Figure 3.2.2).

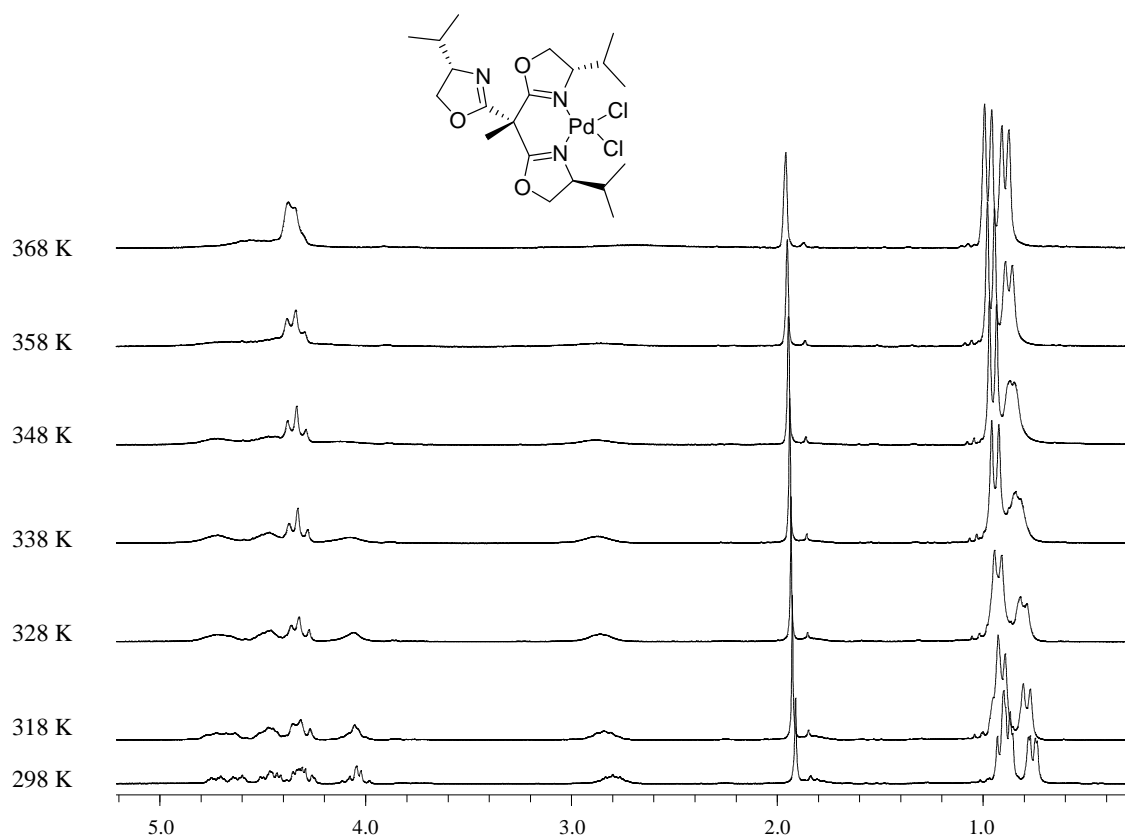


**Figure 3.2.2:** Variable temperature  $^1\text{H}$  NMR of complex  $[\text{PdCl}_2(\text{iPr-trisox})]$  **39** in 1,1,2,2-tetrachloroethane- $d_2$  (400 MHz)

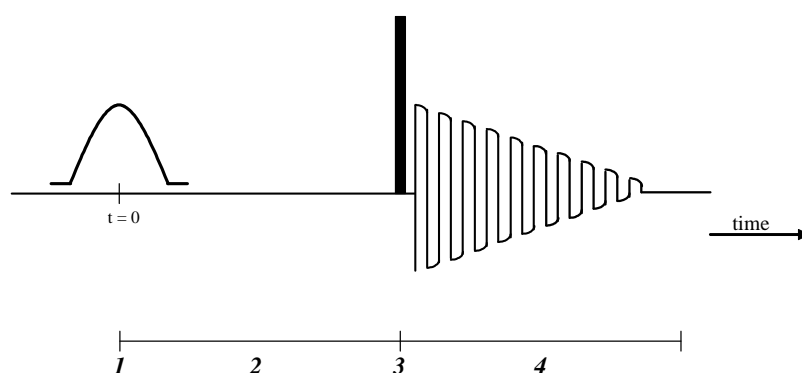
The effective threefold symmetry found for complex **39** at higher temperature was also observed for complexes **40-42**. These observations indicate the presence of a fluxional process of the trisox ligands with increasing temperature. Two substitution mechanisms can be involved in this fluxional process: either an associative or a dissociative mechanism. Both differ in their entropy of activation which would be positive for a dissociative mechanism and negative for the associative case. In order to quantitatively study this exchange of the ligating arms and to gain insight into the mechanism of this process, a systematic series of magnetisation transfer experiments have been carried out.

a. Principle of the magnetisation transfer

Magnetisation transfer is a method for determining kinetics of chemical exchange by perturbing the magnetisation of nuclei in a particular site or sites and following the rate at which magnetic equilibrium is restored. The most common perturbations are saturation and inversion and the corresponding techniques are often called “saturation transfer” and “selective inversion

recovery". The magnetisation transfer NMR technique<sup>12</sup> has become a popular method for measuring rates of chemical exchange processes, in particular for systems of biological importance.<sup>13</sup> Furthermore, this method often provides more detailed information about the exchange pathways than the classical line shape analysis.

To determine the kinetics of exchange of the ligating arms on the metal centre we were interested in the selective inversion transfer method. To explain the principle of the inversion transfer, one may consider two nuclei, A and B, with  $J_{AB} = 0$  Hz and for both spin = 1/2. The inversion transfer experiment consists in the selective inversion of the spin population of a nucleus, here the one called A, using a 180° shaped pulse. After variable delays, a non selective 90° pulse is applied (Scheme 3.2.1).



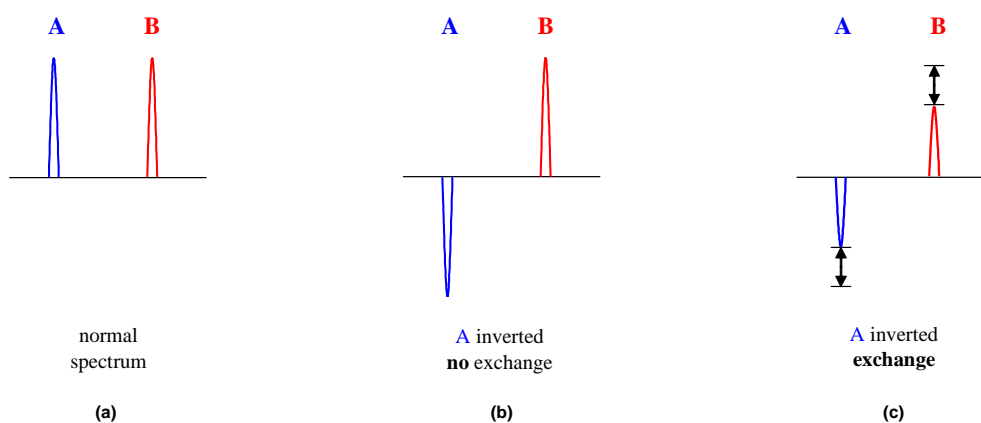
**Scheme 3.2.1:** Inversion transfer experiment

In Scheme 3.2.1, position 1 represents the selective 180° shaped pulse<sup>14</sup> which is applied to A, 2 indicates the delay between the selective and the non selective pulse ( $5 \cdot 10^{-4}$  s to 5 s), position 3 is the non selective 90° pulse and 4 represents the acquisition. The changes observed in the <sup>1</sup>H NMR spectrum after inversion transfer are depicted in Scheme 3.2.2.

<sup>12</sup> a) S. Forsén, R.A. Hoffman, *J. Chem. Phys.* **1963**, *39*, 2892; b) S. Forsén, R.A. Hoffman, *J. Chem. Phys.* **1964**, *40*, 1189; c) R.A. Hoffman, S. Forsén, *J. Chem. Phys.* **1966**, *45*, 2049; d) J. R. Alger, J.H. Prestegard, *J. Magn. Reson.* **1977**, *27*, 137; e) G. A. Morris, R. Freeman, *J. Magn. Reson.* **1978**, *29*, 433.

<sup>13</sup> a) K. Ugurbil, R. G. Shulman, T. R. Brown, „Biological Applications of Magnetic Resonance“ (R. G. Shulman, Ed.), Academic Press, New-York, **1979**, 537; b) D. G. Gardian, G. K. Radda, T. R. Brown, E. M. Chance, M. J. Dawson, D. R. Wilkie, *Biochem. J.* **1981**, *194*, 215; c) K. M. Brindle, *Prog. NMR Spectrosc.* **1988**, *20*, 257; d) J. G. Sheldon, S.-P. Williams, A. M. Fulton, K. M. Brindle, *Proc. Natl. Acad. Sci. USA* **1996**, *93*, 6399; e) M. S. Sanford, J. A. Love, R. H. Grubbs, *J. Am. Chem. Soc.* **2001**, *123*, 6543; f) J. S. Owen, J. A. Labinger, J. E. Bercaw, *J. Am. Chem. Soc.* **2004**, *126*, 8247; g) H. Wadepohl, U. Kohl, M. Bittner, H. Köppel, *Organometallics* **2005**, *24*, 2097; h) L. M. Klingensmith, E. R. Strieter, T. E. Barder, S. L. Buchwald, *Organometallics* **2006**, *25*, 82; i) J. Zhou, P. C. M. Van Zijl, *Prog. NMR Spectros.* **2006**, *48*, 109.

<sup>14</sup> See Chapter 6.



**Scheme 3.2.2:** Changes observed in the  $^1\text{H}$  NMR spectrum after selective inversion

Selective inversion of the spin population of A generates an inverted signal for A in the  $^1\text{H}$  spectrum (b). If there is no chemical exchange between A and B, the signals are of the same intensity in case (b) as in case (a). Variation of the absolute intensities of the signals in the  $^1\text{H}$  NMR spectrum is observed in case of chemical exchange of nuclei A and B (c). Increasing the delay between the selective  $180^\circ$  shaped pulse and the non selective  $90^\circ$  pulse leads to an increase of the absolute intensity of the signal of A whereas the absolute intensity of the signal of B first decreases and then increases.

The magnetisation transfer experiment makes it possible to directly monitor the exchange of the different sites involved in the process. This method has been used to determine the activation parameters of the fluxional exchange of the ligands in the  $[\text{PdCl}_2(\text{trisox})]$  complexes. Complexes **40** and **41** could not be used for this study due to overlapping signals in the  $^1\text{H}$  spectra. We therefore turned our attention to complexes **39** and **42** and the next two paragraphs, respectively, describe the results.

b. Experimental determination of the activation parameters for the fluxional process in complex **39**

With the aim to monitor the exchange of the protons between the coordinated oxazolines and the non-coordinated oxazoline, it turned out that the most interesting signals for our study of complex **39** were protons **a** and **a'**, ( $-\text{CHMe}_2$ ) of the coordinated oxazolines and proton **b**, ( $-\text{CHMe}_2$ ) of the non-coordinated oxazoline (Figure 3.2.3).

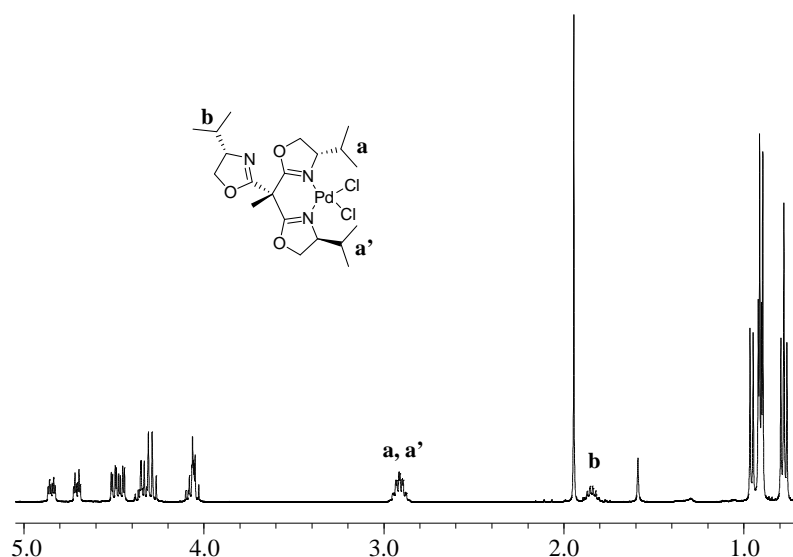


**Figure 3.2.3:**  $^1\text{H}$  NMR spectrum of  $[\text{PdCl}_2(\text{iPr-trisox})]$  **39** in 1,1,2,2-tetrachloroethane- $d_2$  at 296 K (400 MHz)

In a series of experiments carried out with **39** in 1,1,2,2-tetrachloroethane- $d_2$ , the protons of the coordinated oxazolines (**a**) were selectively inverted with a shaped pulse, followed by monitoring of the time evolution of the intensities in the two sites **a/a'** and **b**. In Figure 3.2.4 an example of the time evolution of the intensities in the two sites at 302 K is shown.

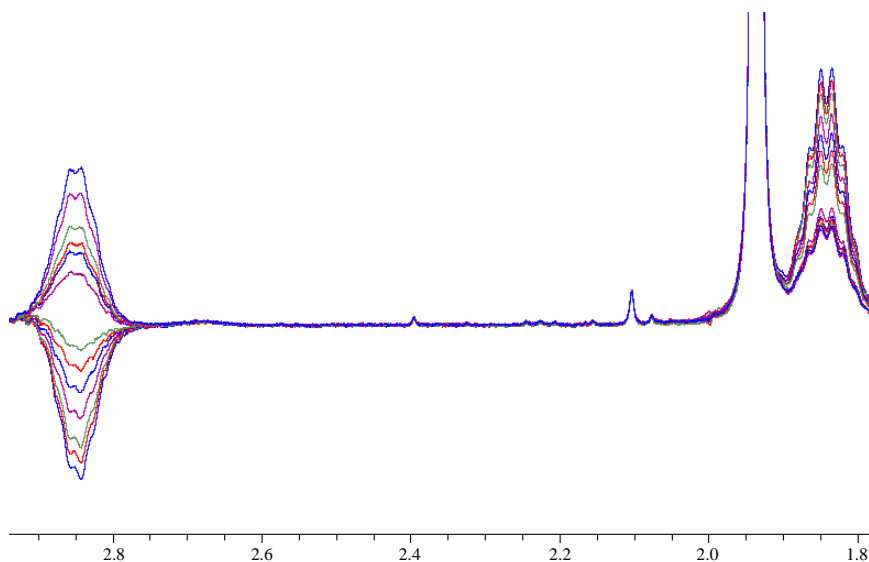


**Figure 3.2.4:** Time dependence of the magnetisation of the inverted site **a/a'** (left) and the one connected to it by chemical exchange **b** (right) at 302 K (in 1,1,2,2-tetrachloroethane- $d_2$ , 400 MHz)

Evolution of the absolute intensities of the signals can be measured as a function of the delay (36 measurements between  $5.10^{-4}$  s and 5 s) and as a function of the temperature (between 302 K and 318 K). 1,4-dimethoxybenzene was used as internal standard to determine the

absolute intensities. The results of experiments in which magnetisation of protons **a** was inverted are shown in Figure 3.2.5.

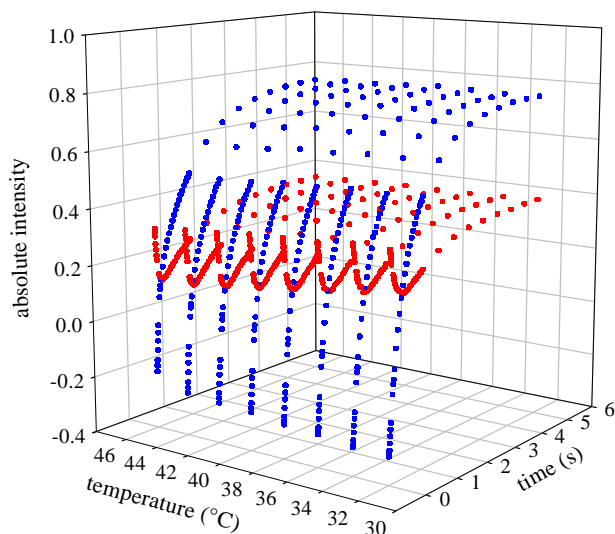


**Figure 3.2.5:** Time evolution of the magnetisation in the two sites (exponential traces, coordinated oxazolines **a**, **a'**; other traces, non coordinated oxazoline **b**) after selective inversion of the coordinated oxazolines resonance. Data are represented in a 3D representation as a function of the temperature

T (K)	$k_{\text{chem}_a}$	$k_{\text{chem}_b}$	Combined data $k_{\text{chem}}$
302	3.19	2.63	2.91
304	3.96	3.23	3.59
306	4.77	3.90	4.34
308	5.58	4.74	5.16
310	6.87	5.78	6.32
312	8.19	6.98	7.58
314	9.57	8.46	9.01
316	11.52	10.07	10.79
318	13.71	11.93	12.82

**Table 3.2.1:** Rate constants  $k_{\text{chem}}$  ( $\text{s}^{-1}$ ) for the fluxional process in complex **39** in 1,1,2,2-tetrachloroethane- $d_2$

Varying the temperature, the time dependence of the magnetisation in the two exchanging sites after inversion of protons **a** was fitted to the appropriate sets of equations derived from the McConnell equations.<sup>15,16,17</sup> Fits of the theoretical curves to the experimental data gave the NMR spectroscopic rate constants  $k_{\text{NMR}_a}$  and  $k_{\text{NMR}_b}$  for the fluxional exchange. It was found, as expected for our system due to the overlapping of **a** and **a'**, that  $k_{\text{NMR}_b} \approx 2 \times k_{\text{NMR}_a}$ . Taking the

<sup>15</sup> H. M. McConnell, *J. Chem. Phys.* **1958**, 28, 430.

<sup>16</sup> J.J. Led, H. Gesmar, *J. Magn. Reson.* **1982**, 49, 444.

<sup>17</sup> See Chapter 5.

statistical factors for the fluxional exchange of the three sites into account,  $k_{\text{NMR}}$  was converted into the chemical rate constants  $k_{\text{chem}_a}$  and  $k_{\text{chem}_b}$  using the relation between  $k_{\text{NMR}}$  and  $k_{\text{chem}}$  for  $A_2B$  systems where A is inverted ( $k_{\text{chem}_a} = 3 \times k_{\text{NMR}_a}$  and  $k_{\text{chem}_b} = 3/2 k_{\text{NMR}_b}$ ) (Table 3.2.1).<sup>18</sup>

The Eyring plot resulting from the measured rate constants is shown in Figure 3.2.6.

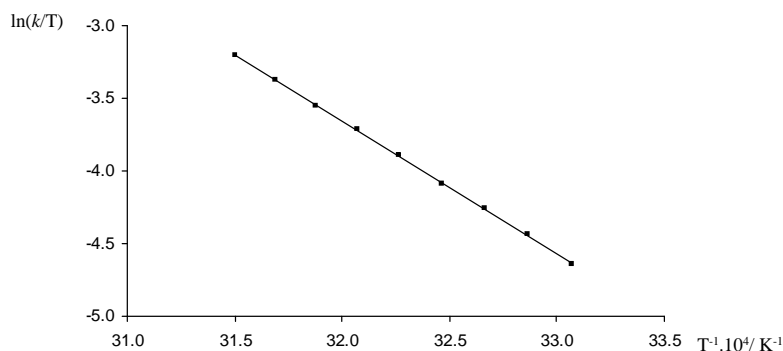


Figure 3.2.6: Eyring plot for the data reported in Table 3.2.1 ( $k_{\text{chem}}$ )

The analysis of the Eyring plot allows the determination of the activation parameters of the fluxional process of the ligand in  $[\text{PdCl}_2(i\text{Pr-trisox})]$ . An enthalpy of activation for the fluxional process of  $\Delta H^\ddagger = 75.6 \pm 0.5 \text{ kJ.mol}^{-1}$  and an entropy of activation of  $\Delta S^\ddagger = 14.0 \pm 1.5 \text{ J.mol}^{-1}$  have been found. To confirm the previously quoted activation parameters, the corresponding data from another series of magnetisation transfer experiments have been analysed.

c. Experimental determination of the activation parameters for the fluxional process in complex **42**

To study the fluxional process in **42**, the exchange of the protons between the coordinated oxazolines and the non-coordinated oxazoline was monitored. Regarding the  $^1\text{H}$  NMR spectrum of complex **42** (Figure 3.2.7), it turned out that the most convenient signals for our study were the ones of protons **a** and **b** (respectively one proton of the  $\text{CH}_2$  group of the indanyl substituent) of the coordinated oxazolines. The corresponding proton **c** of the non-coordinated oxazoline is overlapping with the other proton of the  $\text{CH}_2$  group of the indanyl substituent **c'**.

<sup>18</sup> M. L. H. Green, L.-L. Wong, A. Sella, *Organometallics* **1992**, *11*, 2660.



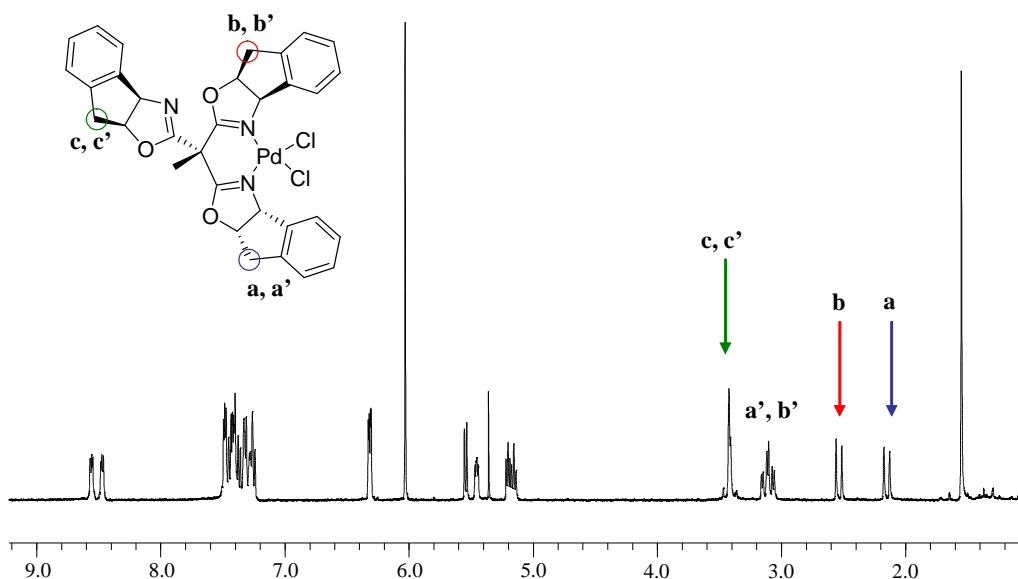


**Figure 3.2.7:**  $^1\text{H}$  NMR spectrum of  $[\text{PdCl}_2(\text{Ind-trisox})]$  **42** in 1,1,2,2-tetrachloroethane- $d_2$  at 296 K (400 MHz)

In a series of experiments carried out with **42** in 1,1,2,2-tetrachloroethane- $d_2$ , the proton of one of the coordinated oxazolines **a** was selectively inverted with a shaped pulse, followed by monitoring the time evolution of the intensities in the two sites **a** and **b**. To confirm these results, proton **b** was selectively inverted with a shaped pulse, followed by monitoring of the time evolution of the intensities in the two sites **a** and **b**. Evolution of the absolute intensities of the signals was measured as a function of the delay (33 measurements between  $5 \cdot 10^{-4}$  s and 5 s) and as a function of the temperature (between 323 K and 331 K in the presence of 1,4-dimethoxybenzene as internal standard). The results are displayed in Figure 3.2.8.

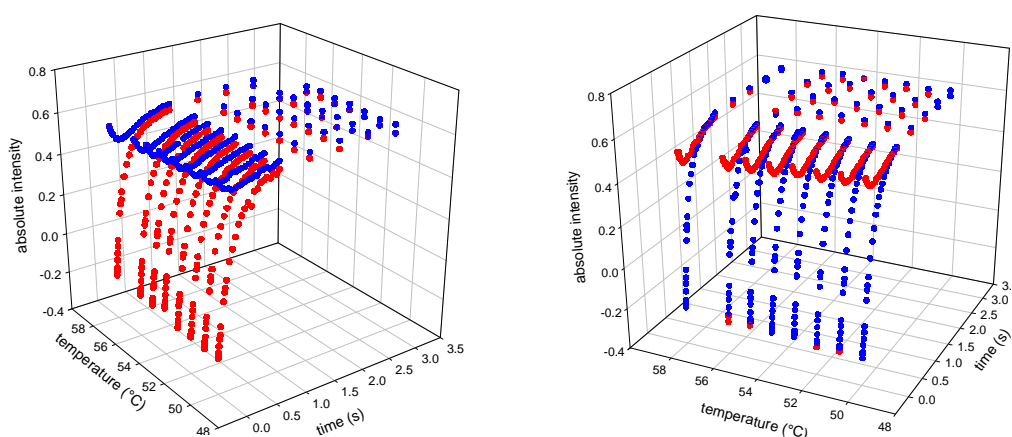


**Figure 3.2.8:** Time evolution of the magnetisation in the different sites after selective inversion of the coordinated oxazolines resonance **a** (left) and **b** (right). Data are represented in a 3D representation as a function of the temperature

For the different temperatures studied, the time dependence of the magnetisation in the exchanging sites after inversion of proton **a** and inversion of proton **b** was fitted to the appropriate sets of equations derived from the McConnell equations. Fits of the theoretical curves to the experimental data gave the NMR spectroscopic rate constants  $k_{\text{NMR}_a}$  and  $k_{\text{NMR}_b}$  for the fluxional exchange. It was found, as expected, that  $k_{\text{NMR}_a}$  and  $k_{\text{NMR}_b}$  are equal. Taking the statistical factors for the fluxional exchange of the three sites into account,  $k_{\text{NMR}}$  was then converted into the chemical rate constants  $k_{\text{chem}_a}$  and  $k_{\text{chem}_b}$  using the relation between  $k_{\text{NMR}}$  and  $k_{\text{chem}}$  for ABC systems where A or B are inverted ( $k_{\text{chem}_a} = 3 \times k_{\text{NMR}_a}$  and  $k_{\text{chem}_b} = 3 \times k_{\text{NMR}_b}$ ) (Table 3.2.2).<sup>18</sup>

T (K)	$k_{\text{chem}_a}$	$k_{\text{chem}_b}$	Combined data $k_{\text{chem}}$
323	2.54	2.65	2.59
324	2.73	2.76	2.75
325	2.93	3.07	3.00
326	3.35	3.33	3.34
327	3.59	3.54	3.57
328	3.89	4.20	4.05
329	4.36	4.30	4.33
331	5.25	5.06	5.16

**Table 3.2.2:** Rate constants  $k_{\text{chem}}$  ( $\text{s}^{-1}$ ) for the fluxional process in complex **42** in 1,1,2,2-tetrachloroethane- $d_2$

The Eyring plot resulting from the rate constants obtained from inversion of the coordinated oxazoline sites is shown in Figure 3.2.9.

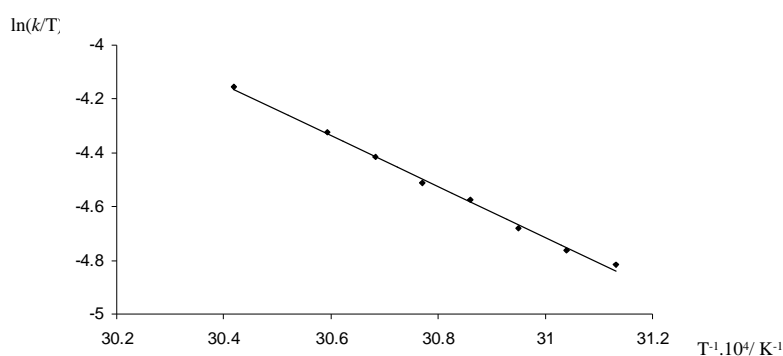


**Figure 3.2.9:** Eyring plot for the data reported in Table 3.2.1 ( $k_{\text{chem}}$ )

The analysis of the Eyring plot enables us to determine the activation parameters of the fluxional process of the ligand in  $[\text{PdCl}_2(\text{Ind-trisox})]$ . An enthalpy of activation for the fluxional process of  $\Delta H^\ddagger = 79.4 \pm 2.0 \text{ kJ} \cdot \text{mol}^{-1}$  and an entropy of activation  $\Delta S^\ddagger = 9.3 \pm 6.0 \text{ J} \cdot \text{mol}^{-1}$  have been found. These results are discussed in the next part.

d. Solution dynamics of complexes 39-42

As previously stated, either an associative or a dissociative ligand interchange mechanism could be suggested for the dynamic behaviour of the complexes in solution. Values of the activation parameters for the exchange process determined using magnetisation transfer experiments enable us to gain insight into the mechanism. The results are summarised in Table 3.2.3.

	<b>39</b>	<b>42</b>
$\Delta H^\ddagger$ (kJ.mol <sup>-1</sup> )	75.6 ± 0.5	79.4 ± 2.0
$\Delta S^\ddagger$ (J.mol <sup>-1</sup> )	14.0 ± 1.5	9.3 ± 6.0
$\Delta G^\ddagger_{298K}$ (kJ.mol <sup>-1</sup> )	71.4 ± 0.6	76.4 ± 2.8

**Table 3.2.3:** Activation parameters for the dynamic exchange of coordinated and free oxazoline rings in complexes **39** and **42**

Whereas the calculated enthalpy values are as expected for such a dynamic process, the small activation entropy values indicate neither an associative nor a dominantly dissociative substitution mechanism. A reasonable intimate mechanism for the exchange between coordinating and non-coordinating oxazolines may resemble an interchange process. Given the mechanistic work carried out for substitutions at square-planar Pd(II) complexes,<sup>19</sup> we assume that the interchange has slightly associative character ( $I_a$ -mechanism), which implies the transient formation of a pentacoordinated palladium(II) complex in the transition state. This type of mechanism via pentacoordination has been invoked by Vrieze *et al* for the case of tridentate  $N,N,N$ -type ligand.<sup>20</sup>

We note that fluxional processes with potentially tridentate ligands have been encountered with terpyridine, bisoxazoline-phenylphosphonite or bisoxazoline-pyridine (Pybox) ligands.<sup>21</sup>

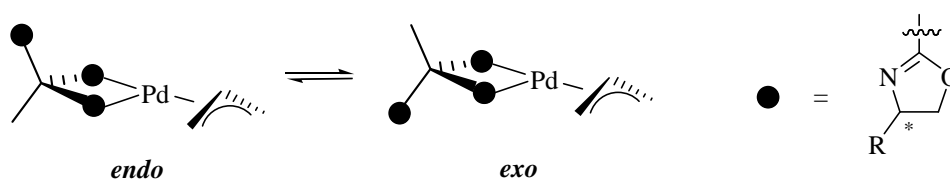
<sup>19</sup> a) J. B. Goddard, F. Basolo, *Inorg. Chem.* **1968**, 7, 936; b) L. A. P. Kane-Maguire, G. Thomas, *J. Chem. Soc., Dalton Trans.* **1975**, 19, 1890. Studies published more recently include: c) T. Shi, L. I. Elding, *Inorg. Chem.* **1996**, 35, 735; d) T. Shi, L. I. Elding, *Inorg. Chem.* **1997**, 36, 528; e) Z. D. Bugarčić, G. Liehr, R. van Eldik, *J. Chem. Soc., Dalton Trans.* **2002**, 951.

<sup>20</sup> R. E. Rülke, J. M. Ernsting, A. L. Spek, C. J. Elsevier, P. W. N. M. van Leeuwen, K. Vrieze, *Inorg. Chem.* **1993**, 32, 5769.

<sup>21</sup> a) P. Wehman, R. E. Rülke, V. E. Kaasjager, P. C. J. Kamer, H. Kooijman, A. L. Spek, C. J. Elsevier, K. Vrieze, P. W. N. M. Van Leeuwen, *J. Chem. Soc., Chem. Commun.* **1995**, 331; b) G. Zhu, M. Terry, X. Zhang, *Tetrahedron Lett.* **1996**, 37, 4475; c) P. J. Heard, C. Jones, *J. Chem. Soc., Dalton Trans.* **1997**, 1083; d) P. Braunstein, F. Naud, A. Dedieu, M.-M. Rohmer, A. DeCian, S. J. Rettig, *Organometallics* **2001**, 20, 2966.

## 2. The $[Pd^{II}(\text{allyl})(\text{Ph-trisox})]$ complex

In the  $^1\text{H}$  NMR spectrum of complex **43** at room temperature, only three, well-defined signals for the oxazoline protons are observed indicating fast exchange between the three heterocycles as well as between the *exo* and *endo* diastereomers, *exo* being defined as the central C-H allylic bond pointing in the same direction as the axial methyl group (Scheme 3.2.3).<sup>22</sup> Formally, an apparent  $180^\circ$  rotation of the  $\eta^3$ -allyl ligand around its bond axis to the central metal interchanges an isomer of structure *exo* into the isomer of structure *endo*.



**Scheme 3.2.3:** The two possible *exo* and *endo* diastereomers

Five signals are observed for the allyl moiety as expected for a non-symmetrical  $\pi$ -allyl ligand (Figure 3.2.10), the partial assignment being based on a  $^1\text{H}$  NOESY experiment. In Figure 3.2.10, according to the accepted nomenclature of the planar allyl ligand,  $H_S$  and  $H_A$  respectively refer to the *syn* and *anti* protons in direct relation to the central hydrogen atom termed  $H_C$ .

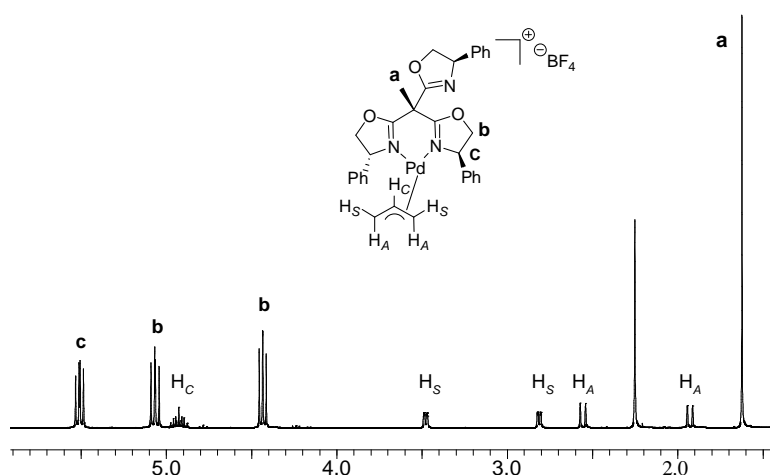
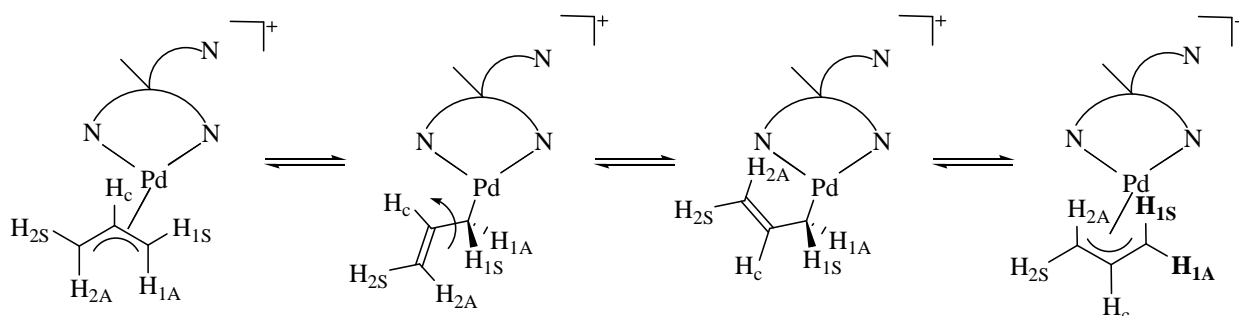


**Figure 3.2.10:**  $^1\text{H}$  NMR of complex  $[\text{Pd}(\eta^3\text{-allyl})(\text{Ph-trisox})]\text{BF}_4$  **43** in chloroform- $d_1$  at 296 K (400 MHz)

The  $^1\text{H}$  NOESY experiment shows, in addition to the negative phase non-diagonal NOE cross-peaks, weak EXSY signals between *syn* and *anti* protons, indicating slow exchange

<sup>22</sup> The terms *exo* and *endo* were introduced by Faller *et al.* for the description of diastereomeric  $\pi$ -allyl complexes: a) R. D. Adams, D. F. Chodosh, J. W. Faller, A. M. Rosan, *J. Am. Chem. Soc.* **1979**, *101*, 2570; b) J. W. Faller, K.-H. Chao, *J. Am. Chem. Soc.* **1983**, *105*, 3893.

between  $\eta^3$ -allyl and  $\eta^1$ -allyl forms. Indeed the  $\pi$ - $\sigma$ - $\pi$  isomerisation, well described in the literature,<sup>23</sup> is the only way of exchange for the *syn* and *anti* protons (Scheme 3.2.4).



**Scheme 3.2.4:**  $\pi$ - $\sigma$ - $\pi$  isomerisation explaining the exchange between *syn* and *anti* protons in the allyl termini

A series of variable temperature  $^1\text{H}$  NMR experiments were performed between 296 K and 373 K. They indicate no spectral changes for the allyl proton resonances, neither between the pairs of the *syn* or *anti* protons nor cross exchange among them. As previously observed for other non-symmetrical allyl complexes, this is consistent with the stereochemical rigidity of the allyl-Pd fragment on the time scale of the experiments, in other words, it is not affected by the interchange of the oxazoline coordination as well as the (possibly concomitant) interconversion of *exo* and *endo* diastereomers.<sup>24</sup>

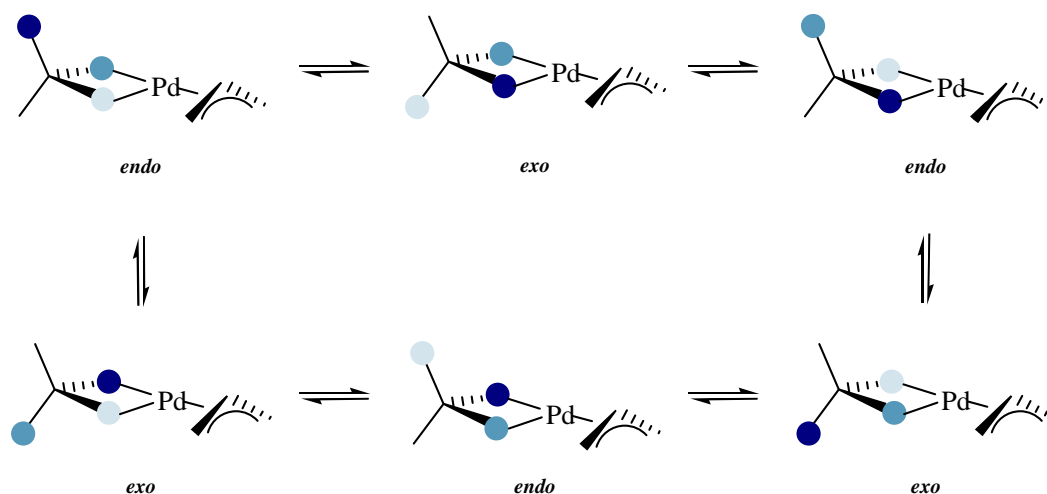
In order to quantify the latter, a low temperature  $^1\text{H}$  NMR study was carried out. Coalescence of the trisoxazoline ligand resonances occurred at 198 K, however, the low temperature limit was not attained at 190 K (in dichloromethane- $d_2$ ). Although the exchange of the three oxazolines was not completely frozen, an estimate of the activation barrier  $\Delta G^\ddagger$  for the oxazoline exchange of *ca.* 55  $\text{kJ}\cdot\text{mol}^{-1}$  may be derived. At low temperature, the resonance pattern of the ligand was thus consistent with the bidentate *N,N* chelation observed in the solid state. Notably, the signals of the allyl fragment began to broaden at 190 K, presumably owing to the slowing down of the *exo/endo* exchange, however, complete decoalescence was not obtained.

The stereochemical rigidity of the allyl-Pd fragment on the VT-NMR timescale and the observation that the oxazoline exchange and the *exo/endo* interconversion are associated with similarly low activation barriers may indicate that both are mechanistically coupled, that is to say

<sup>23</sup> a) J. W. Faller, M. E. Thomsen, M. J. Mattina, *J. Am. Chem. Soc.* **1971**, *93*, 2642; b) J. W. Faller, M. T. Tully, *J. Am. Chem. Soc.* **1972**, *94*, 2676; c) E. Cesarotti, M. Grassi, L. Prati, F. Demartin, *J. Organomet. Chem.* **1989**, *370*, 407 ; d) S. Hansson, P.-O. Norrby, M. P. T. Sjögren, B. Åkermark, M. E. Cucciolito, F. Giordano, A. Vitagliano, *Organometallics* **1993**, *12*, 4940; e) C. Breutel, P. S. Pregosin, R. Salzmann, A. Togni, *J. Am. Chem. Soc.* **1994**, *116*, 4067 ; f) A. Gogoll, J. Örnebro, H. Grennberg, J.-E. Bäckvall, *J. Am. Chem. Soc.* **1994**, *116*, 3631.

<sup>24</sup> M. A. Pericas, C. Puigjamer, A. Riera, A. Vidal-Ferran, M. Gomez, F. Jimenez, G. Muller, M. Rocamora, *Chem. Eur. J.* **2002**, *8*, 4164 and references cited therein.

that the trisox fluxional process and the reorientation of the allyl-Pd unit occur by the same route. A possible pathway based on an oxazoline walkabout is proposed in Scheme 3.2.5.



**Scheme 3.2.5:** Possible exchange pathway, based on a stereospecific interchange of the oxazolines

### 3. $[Pd^0(alkene)(trisox)]$ complexes

#### a. VT-NMR spectroscopic study of complexes **44-46**

$^1H$  NMR spectra of all complexes recorded at 296 K represent a dynamic exchange regime for the trisox ligand as well as the equilibrium between the two diastereomers due to the different orientation of the  $\pi$ -bonded maleic anhydride ligand relative to the pendant oxazoline arm (see Scheme 3.1.5). The protons of the maleic anhydride give rise to two different resonances because the cyclic anhydride is oriented perpendicularly to the plane defined by the palladium atom and the two coordinated heterocycles (see Chapter 3, I.3). The signals of the protons of the alkene ligand are shifted to lower frequency with respect to the free olefin and the alkene CH carbon resonances observed in the region of 39.8-41.4 ppm are strongly shifted to higher field with respect to the free alkene (Table 3.2.4).

	$^1H$ NMR		$^{13}C$ NMR		
	$H_A$	$H_B$	CO		CH
<b>44</b>	3.69	3.74	172.3	172.8	40.4
<b>45</b>	2.92	3.30	171.9	172.7	41.4
<b>46</b>	2.78	3.13	172.8	173.6	39.8
free alkene	7.05		164.6		136.8

**Table 3.2.4:** Selected  $^1H$  and  $^{13}C$  NMR data in ppm for the alkene ligand in complexes **44-46**

The NMR chemical shifts listed in Table 3.2.4 are in the range usually observed for other zero-valent  $[\text{ML}_n(\text{alkene})]$  palladium and platinum complexes.<sup>25</sup>

Upon lowering the temperature, the fluxional processes are frozen for complexes **44-46** and different sets of resonances attributable to the two possible diastereomers are observed. Variable temperature  $^1\text{H}$  NMR spectra were recorded between 296 K and 213 K for complex **45**, and the low-temperature limiting spectrum (213.2 K) is consistent with the freezing up of the diastereomers interconversion and the ratio was found to be 1:1.1 (Figure 3.2.11).

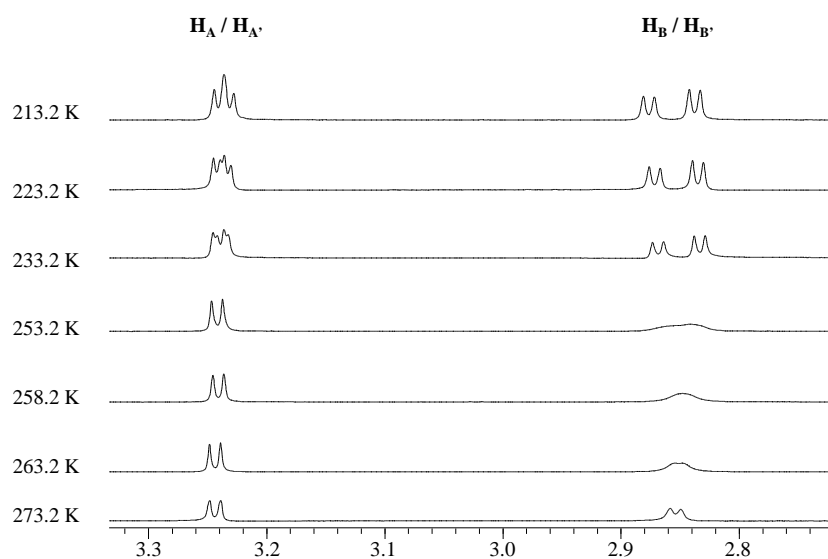


**Figure 3.2.11:** Variable temperature  $^1\text{H}$  NMR of complex  $[\text{Pd}(\text{ma})(\text{Ph-trisox})]$  **45** in dichloromethane- $d_2$  (400 MHz). Only the signals from the protons of maleic anhydride are shown

It was possible to determine the activation barrier of the process using the relation between the coalescence temperature and the free activation entropy:

$$\Delta G^\ddagger = R \cdot T_c \cdot [22.96 + \ln(T_c/\Delta\nu)]$$

$T_c$ : coalescence temperature

$\Delta\nu$ : difference, in Hertz, between the two signals ( $\text{H}_A/\text{H}_{A'}$  and  $\text{H}_B/\text{H}_{B'}$ ) when the fluxional process is frozen

The activation barrier values obtained with this method are summarised in Table 3.2.5.

<sup>25</sup> a) K. J. Cavell, D. J. Stufkens, K. Vrieze, *Inorg. Chim. Acta* **1980**, *47*, 67; b) R. Van Asselt, C. J. Elsevier, W. J. Smeets, A. L. Spek, *Inorg. Chem.* **1994**, *33*, 1521; c) R. Fernández-Gálan, F. A. Jalón, B. R. Manzano, J. Rodríguez de la Fuente, *Organometallics* **1997**, *16*, 3758.

$\Delta\nu$ (Hz)	$T_c$ (K)	$\Delta G^\ddagger$ (kJ.mol <sup>-1</sup> )	Nuclei studied
3.7	236.2	53.2	H <sub>A</sub> /H <sub>A'</sub>
16.7	260.7	55.7	H <sub>B</sub> /H <sub>B'</sub>

**Table 3.2.5:** Activation barrier values for complex **45**

The isomer interconversion may, in principle be caused by either an olefin rotation or a decoordination-coordination process that involves the alkene and/or the ligand. The  $\Delta G^\ddagger$  value measured for complex **45** is 54.5 kJ.mol<sup>-1</sup>.  $\Delta G^\ddagger$  values reported in the literature for alkene rotation are usually *ca.* 60-70 kJ.mol<sup>-1</sup>,<sup>26</sup> however energy barriers of 50 kJ.mol<sup>-1</sup> have also been observed.<sup>24b</sup> In the case of complex **45**, it is therefore difficult to derive the exact mechanism.

b. VT-NMR spectroscopic study of complex **47**

In the case of complex **47**, which contains tetracyanoethylene as  $\pi$ -bonded alkene, the resonance pattern of the oxazoline protons is consistent with effective  $C_3$  symmetry and thus rapid exchange between the three heterocycles. Lowering the temperature leads to coalescence at 243 K and to the non-symmetrical low temperature limiting spectrum at 198 K. The relative instability of the complex in solution did not allow us to gain more insight into the fluxional process of the ligand. Indeed, it was not possible to carry out magnetisation transfer experiments due to the long time needed to collect the data, more than fifteen hours, during which complex **47** decomposed. However, the complex was stable enough to measure different variable temperature <sup>1</sup>H NMR spectra at lower temperature. A simulation of the dynamic NMR spectra was carried out using gNMR software in order to determine the activation barrier of the fluxional process involved. In Figure 3.2.12 a simulation of the proton resonance of the  $CH_2$  group in the indanyl substituent of the ligand at 223 K is represented.

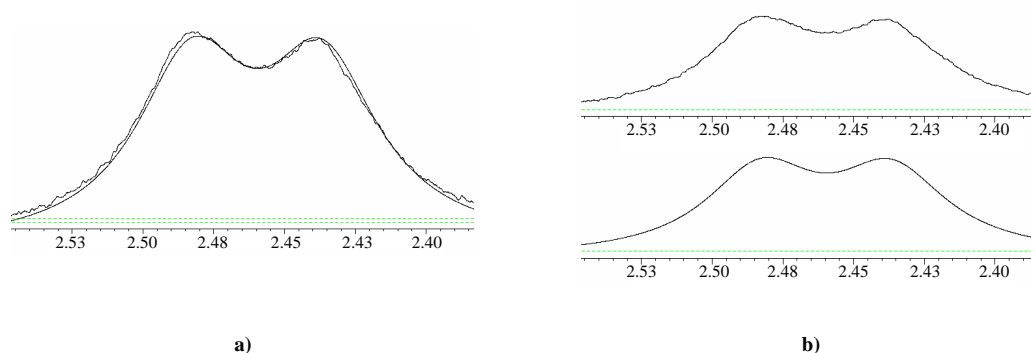


**Figure 3.2.12:** Simulation of the dynamic NMR spectrum of complex **47** at 223 K in dichloromethane-*d*<sub>2</sub> (400 MHz) using the gNMR software: a) overlapping spectra; b) top = experimental spectrum, bottom = simulated spectrum

<sup>26</sup> R. Fernandez-Galan, F. A. Jalon, B. R. Manzano, J. Rodriguez-de la Fuente, *Organometallics* **1997**, *16*, 3758.



Simulation of the experimental spectra gave the NMR spectroscopic rate constant  $k_{\text{NMR}}$  for the fluxional exchange.  $k_{\text{NMR}}$  was then converted into the chemical rate constant using the relation  $k_{\text{chem}} = 3 k_{\text{NMR}}$  (Table 3.2.6).

T (K)	228	226	223	220	217	214	211
$k_{\text{NMR}}$	65	52	35	33	17	8	4
$k_{\text{chem}}$	195	156	105	99	51	24	12

**Table 3.2.6:** Rate constant  $k_{\text{NMR}}$  and  $k_{\text{chem}}$  for the fluxional process in complex **47** in dichloromethane- $d_2$

The analysis of the Eyring plot, resulting from the rate constant values given in Table 3.2.6, enabled us to determine the activation barrier of the fluxional process of the ligand in  $[\text{Pd}(\text{tcne})(\text{Ind-trisox})]$ :  $\Delta G^\ddagger_{298\text{K}} = 42 \pm 5 \text{ kJ.mol}^{-1}$ .

The fact that the activation barrier is lower than for complexes **44-46** indicates that the fluxional process of the ligand is facilitated in the latter case.

### c. VT-NMR spectroscopic study of complex **48**

Whereas the trisox-Pd complexes **44-47** contain threefold symmetrical tripods, complex **48** contains a bisoxazoline ligand to which a 2-pyridylmethyl sidearm has been added. This renders the ligand completely non-symmetrical and thus there are potentially three species which differ in the way the ligand is coordinated to the metal center. Apart from an isomer with two oxazoline units bound to the metal, there are two closely related but diastereomeric forms with one oxazoline ring and the pyridyl arm bound to the metal. Whereas the  $^1\text{H}$  NMR spectrum recorded at 296 K represents an intermediate dynamic regime, the exchange between the different diastereomers was frozen out at 218 K.

A 1:1 equilibrium mixture of the bisoxazoline complex and the two forms of the oxazolin-pyridine isomer are observed. The oxazoline-pyridine isomers possess near-identical overlapping resonance patterns and therefore they were treated as one single species in the analysis of the dynamic process. The fact that the  $\pi$ -coordinated maleic anhydride can adopt two possible orientations with respect to the pendant arm renders the situation more complex. By means of a variable temperature  $^1\text{H}$  NMR study the high temperature limit for these exchange processes between a total of six diastereomers was attained (Figure 3.2.13).

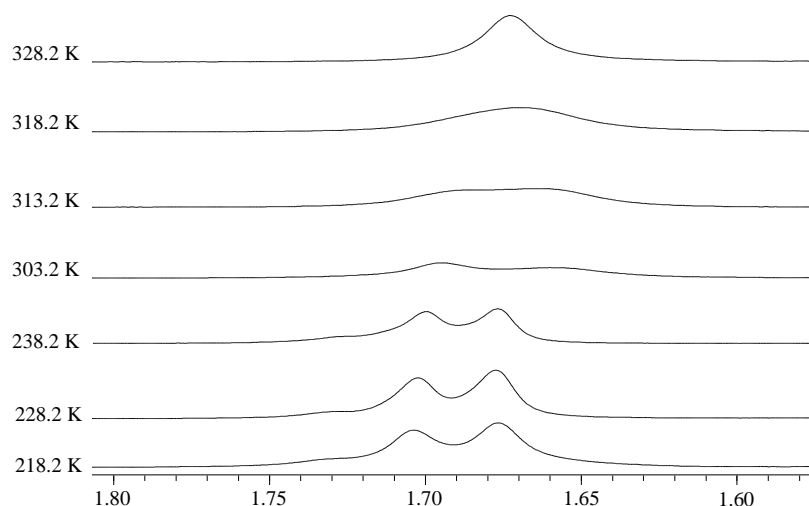


**Figure 3.2.13:** Variable temperature  $^1\text{H}$  NMR of complex **48** in dichloromethane- $d_2$  (600 MHz). The resonances of the protons of the apical methyl group of the tripod are shown

An effective free enthalpy of activation for the overall process of bisoxazoline/oxazolin-pyridine exchange of  $\Delta G^\ddagger_{315\text{K}} \approx 63 \text{ kJ}\cdot\text{mol}^{-1}$  was estimated with  $T_c = 315 \text{ K}$  and  $\Delta\nu = 107.7 \text{ Hz}$ .

#### 4. Conclusion

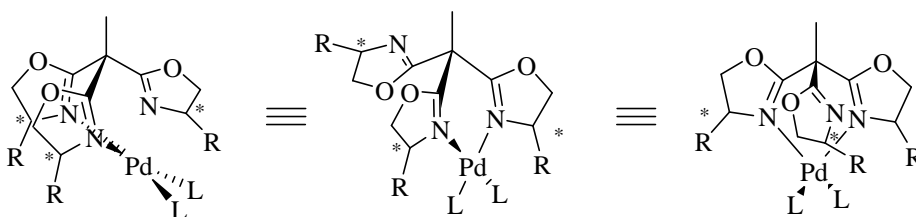
The behaviour of the palladium complexes in solution has been studied. It has been observed that there is a dynamic exchange between the three binding sites either at room or at variable temperature, depending on the type of complex studied. We were able to determine the activation parameters of the exchange between coordinating and non-coordinating oxazolines for the palladium(II) chloride complexes by carrying out magnetisation transfer experiments. Regarding the values obtained, we assume that the substitution mechanism has a slightly associative character. In case of the palladium(II) allyl complex, we found that both the interchange of the oxazoline coordination and the interconversion of the *exo* and *endo* diastereomers may be concomitant. Palladium(0) complexes have shown fluxional behaviour in solution already at room temperature. It was possible to give an estimate of the activation barriers for the fluxional processes observed for the five complexes studied. The next part of this chapter reports the results of the asymmetric allylic substitution, chosen to study the activity and selectivity of the highly symmetric trisoxazolines.

### III. Palladium-catalysed asymmetric allylic substitution

#### 1. The test reaction

As analysed in the Chapter 1, octahedral complexes are associated to threefold rotational symmetry in the same way that square planar complexes (or tetrahedral complexes) are associated to  $C_2$  symmetry. However we could expect a favourable situation with tridentate highly symmetrical ligands in square planar environment when the complex displays fluxional behaviour.

In the preceding part of this chapter we have shown that the Pd(II) and Pd(0) complexes undergo fluxional processes. Thus, in the square planar complexes chemical exchange between the different  $\kappa^2$ -coordinated species takes place and the non-coordinated sidearm may play a direct or indirect role at some earlier or later stage in the catalytic cycle.<sup>27</sup> Such an exchange which induces an equilibrium between identical species for the highly symmetrical trisoxazolines is schematically shown in Scheme 3.3.1.



**Scheme 3.3.1:** Dynamic exchange between the three symmetry related square planar Pd(II) complexes bearing  $\kappa^2$ -chelating  $C_3$ -symmetric trisoxazoline ligands

The palladium-catalysed allylic substitution is a catalytic reaction which involves active species with square planar coordination geometry. Thus, this catalysis may be viewed as a good test reaction to understand the effect of tridentate  $C_3$ -symmetric ligands on catalytic reactions with intermediates having a bidentate coordination mode.

For that purpose trisoxazolines will be used in this model reaction. In addition a direct comparison with the corresponding 1,1-bis(oxazoliny)ethane and other functionalised bisoxazolines will help us to shed light upon the role of threefold rotational symmetry as well as the role of the third oxazoline arm.

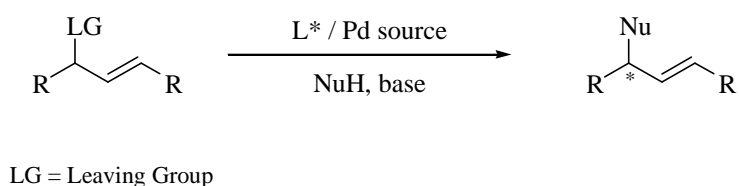
<sup>27</sup> a) H. Brunner, J. Kraus, H.-J. Lautenschlager, *Monatsh. Chemie* **1988**, *119*, 1161; b) H. Brunner, H.-J. Lautenschlager, *Synthesis* **1989**, 706; c) H. Brunner, H.-J. Lautenschlager, W. A. König, R. Krebber, *Chem. Ber.* **1990**, *123*, 847.

## 2. Palladium-catalysed asymmetric allylic substitution: general aspects

### a. Introduction

In the field of organic synthesis, the discovery of the Wacker process in 1956 was the starting point of the increasing interest for palladium chemistry. The first  $\pi$ -allyl/Pd complex was reported in 1959<sup>28</sup> and only six years later its application in C-C bond forming substitution reactions was discovered by Tsuji *et al.*<sup>29</sup> First attempts to achieve enantioselectivity with the help of a chiral ligand, and using a stoichiometric allylic substitution, were described in 1973 by Trost and coworkers.<sup>30</sup> Since the successful report of catalytic asymmetric allylic alkylation ('AAA') in 1977 it took almost 20 years of research until effective catalytic systems based on chiral ligands were developed.<sup>31</sup> The palladium-catalysed allylic substitution has now emerged as one of the most versatile asymmetric transformations.

Among asymmetric bond forming reactions, the metal-catalysed asymmetric allylic substitution is remarkable for several reasons (Scheme 3.3.2).<sup>32</sup>



**Scheme 3.3.2:** General scheme for catalytic asymmetric allylic substitution

Notably, an asymmetric allylic substitution reaction can form many different kinds of bonds using the same catalyst: the nucleophilic centre may be N, O, S, C, H *etc.*, giving access to C-N, C-O, C-S, C-C, C-H *etc.* bonds. Depending on the metal and/or the nucleophile, the reaction may proceed by an inversion or retention mechanism.

### b. Mechanism

The generally accepted catalytic cycle of the asymmetric allylic substitution reaction is depicted in Scheme 3.3.3.

<sup>28</sup> J. Smid, W. Hafner, *Angew. Chem.* **1959**, 71, 284.

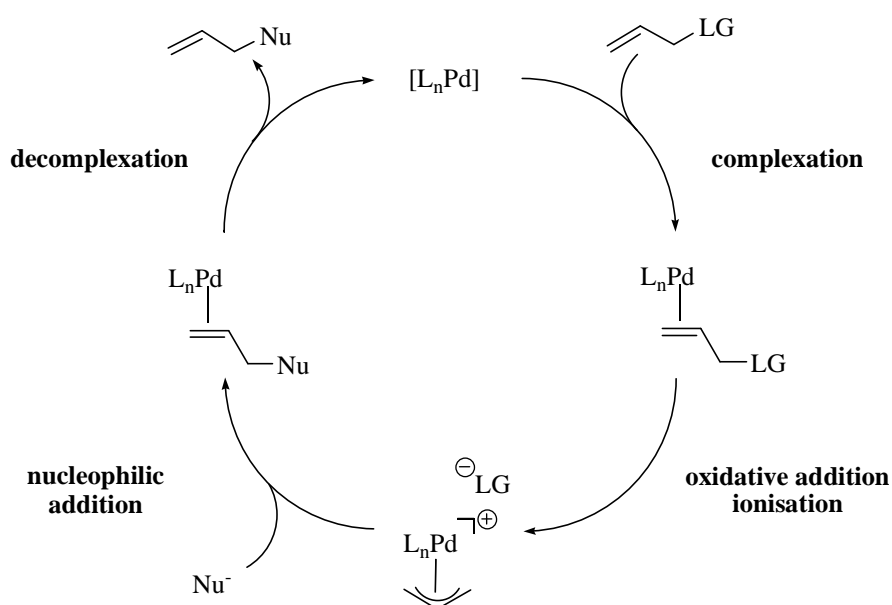
<sup>29</sup> J. Tsuji, H. Takahashi, A. Miyake, *Tetrahedron Lett.* **1965**, 4387.

<sup>30</sup> B. M. Trost, T. J. Dietsche, *J. Am. Chem. Soc.* **1973**, 95, 8200.

<sup>31</sup> B. M. Trost, P. E. Strege, *J. Am. Chem. Soc.* **1977**, 99, 1649.

<sup>32</sup> a) B. M. Trost, D. L. van Vranken, *Chem. Rev.* **1996**, 96, 395; b) A. Pfaltz, M. Lautens, In *Comprehensive Asymmetric Catalysis II*, Eds: E. N. Jacobsen, A. Pfaltz, H. Yamamoto, Springer: Berlin, **1999**, chap. 24, 833; c) B. M. Trost, C. B. Lee, In *Catalytic Asymmetric Synthesis II*, Ed.: I. Ojima, Wiley-VCH: New-York, **2000**, chap. 8E, 593; d) B. M. Trost, M. L. Crawley, *Chem. Rev.* **2003**, 103, 2921; e) B. M. Trost, *J. Org. Chem.* **2004**, 69, 5813.

Complexation of the substrate to the palladium(0) active species is the first step of this catalytic cycle. The initial complexation step is reversible and therefore palladium can interconvert between the two  $\pi$  faces of the olefin. The second step is the formation of the cationic  $\pi$ -allyl complexes after oxidative addition/ionisation. Structurally, the  $\pi$ -allylpalladium intermediate is a square planar 16-electron complex consisting of a ligand and a coordinated allyl moiety.<sup>33</sup> These  $\eta^3$ -bound  $\pi$ -allylpalladium complexes are in equilibrium with the corresponding  $\eta^1$  derivatives (see Scheme 3.2.4). It has to be noted that the rate of the  $\pi$ - $\sigma$ - $\pi$  isomerisation is increased in the presence of an external ligand such as halide.<sup>34</sup> The ionisation step is followed by the nucleophilic addition leading to the formation of a palladium(0)-product complex. The nature of each of these three steps ultimately determines the overall stereochemical event. Finally decomplexation of the olefin affords the product and regenerates the Pd(0) active species.

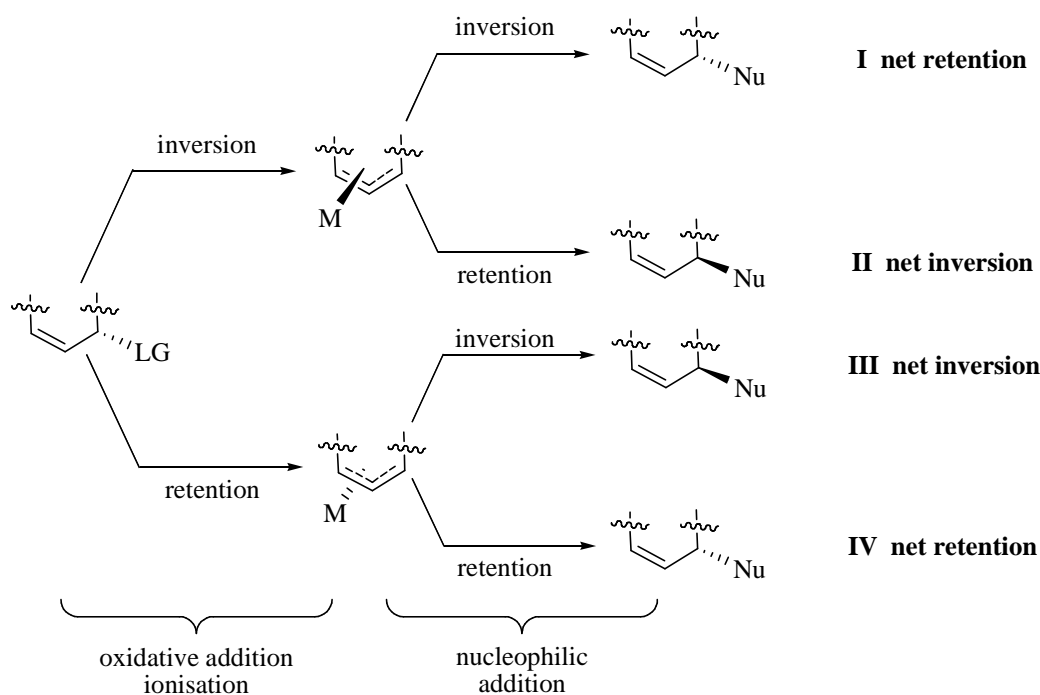


**Scheme 3.3.3:** Palladium-catalysed allylic substitution catalytic cycle (L = ligand, LG = living group)

If the process has an odd number of inversions of stereochemistry (or retentions), this overall process leads to a compound with inversion of configuration. On the other hand, a retention can result either from a double retention or a double inversion path (Scheme 3.3.4).

<sup>33</sup> S. A. Godleski, *Organometallics* **1984**, *3*, 21.

<sup>34</sup> a) U. Burkhardt, M. Baumann, A. Togni, *Tetrahedron: Asymmetry* **1997**, *8*, 155; b) T. Cantat, E. Genin, C. Giroud, G. Meyer, A. Jutand, *J. Organomet. Chem.* **2003**, *687*, 365.



**Scheme 3.3.4:** Overall stereochemistry for the asymmetric allylic substitution

Mechanistic work has demonstrated that the ionisation of the palladium-substrate complex occurs with inversion of configuration.<sup>35</sup> In that case, one can think of this step as an  $S_N2$ -like displacement of the leaving group by the incoming palladium “nucleophile”. The outcome of the process after the nucleophilic addition depends on the nature of the nucleophile. Use of “hard” nucleophiles, defined as those derived from conjugate acids whose  $pK_a$  greater than 25, implies coordination of the nucleophile to the metal followed by reductive elimination. This leads to retention of configuration after the nucleophilic addition giving the product with net inversion of stereochemistry. On the other hand, addition of “soft” nucleophiles, defined as those derived from conjugate acids with  $pK_a$  lower than 25, occurs with inversion of configuration. This step is also considered to be  $S_N2$  like with palladium(II) displaced. To summarise, palladium complexes associated to “soft” nucleophiles afford products with net retention (**I** from Scheme 3.3.4) and combined with “hard” nucleophiles afford products with net inversion (**II** from Scheme 3.3.4).

Because ionisation and nucleophilic attack occur in an antiperiplanar fashion for Pd-catalysed asymmetric allylic substitution, both bond breaking and making events occur outside the coordination sphere of the metal and thus on the opposite face from the chirality control

<sup>35</sup> a) B. M. Trost, L. Weber, *J. Am. Chem. Soc.* **1975**, *97*, 1611; b) B. M. Trost, T. R. Verhoeven, *J. Am. Chem. Soc.* **1976**, *98*, 630; c) T. Hayashi, T. Hagihara, M. Konishi, M. Kumada, *J. Am. Chem. Soc.* **1983**, *105*, 7767; d) J. C. Fiaud, L. Y. Legros, *J. Org. Chem.* **1987**, *52*, 1907; e) I. Stary, J. Zajicek, P. Kocovsky, *Tetrahedron* **1992**, *48*, 7229.

element. Despite this potential obstacle, a wide range of chiral ligands have been employed with success.

### c. Catalysts

Among the factors which contribute to high stereoselectivity in asymmetric transformations, the steric, electronic and symmetric properties of the reagents may play a role. All these factors are needed to be considered in the design of new ligands.

The  $C_2$ -symmetrical ligands BINAP,<sup>36</sup> DIOP<sup>31</sup> and CHIRAPHOS<sup>37</sup> which have proven to be very efficient in asymmetric hydrogenation afforded only modest success in asymmetric allylic alkylation. Nevertheless, many other classes of ligands have shown excellent selectivities in asymmetric allylic substitution reactions. Selected classes of ligands that have proven to be efficient in the palladium-catalysed AAA are depicted in Figure 3.3.1.

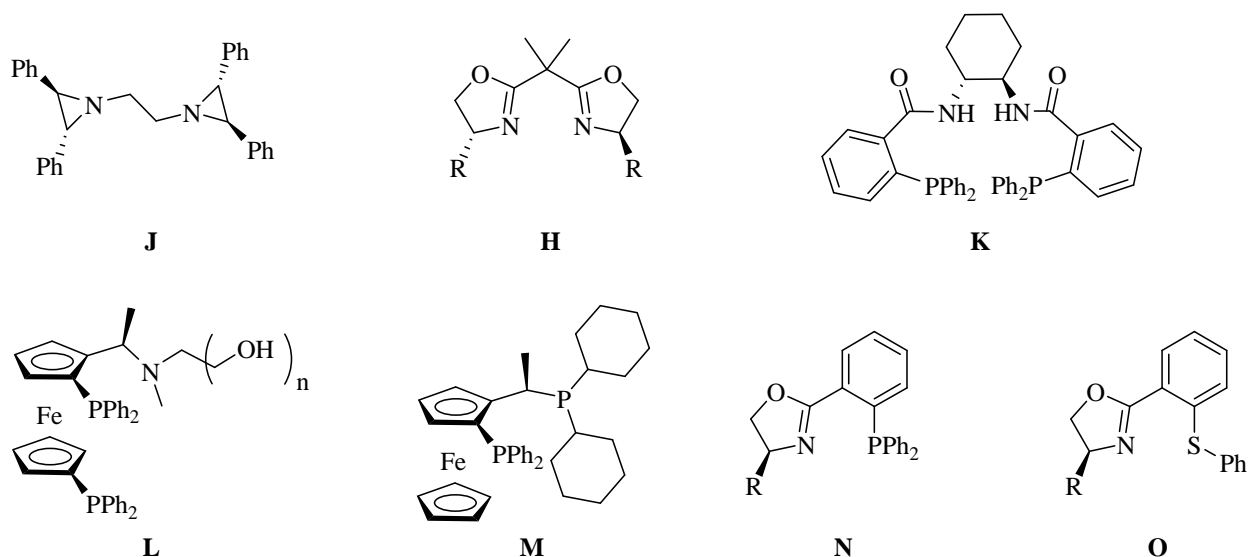


Figure 3.3.1: Some examples of chiral ligands applied in allylic alkylation

$C_2$ -symmetric diamine ligands (**J**)<sup>38</sup> and bisoxazoline ligands (**H**)<sup>39</sup> have both shown good chiral induction. Chiral diphosphine ligands displaying a large bite angle (such as **K**) have been widely applied in AAA and have been the objects of study in mechanistic work.<sup>40</sup> However for this catalysis,  $C_2$  symmetry is not required to achieve high levels of enantioselectivity.

<sup>36</sup> a) B. M. Trost, D. J. Murphy, *Organometallics* **1985**, *4*, 1143; b) P. S. Pregosin, H. Ruegger, R. Salzmann, A. Albinati, F. Lianza, R. W. Kunz, *Organometallics* **1994**, *13*, 83.

<sup>37</sup> P. R. Auburn, P. B. Mackenzie, B. Bosnich, *J. Am. Chem. Soc.* **1985**, *107*, 2033.

<sup>38</sup> P. G. Andersson, A. Harden, D. Tanner, P. D. Norrby, *Chem. Eur. J.* **1995**, *1*, 12.

<sup>39</sup> A. Pfatz, *Acc. Chem. Res.* **1993**, *26*, 339.

<sup>40</sup> a) B. M. Trost, D. L. van Vranken, *Angew. Chem. Int. Ed. Engl.* **1992**, *31*, 228; *Angew. Chem.* **1992**, *104*, 194; b) B. M. Trost, B. Breit, S. Peukert, J. Zambrano, J. W. Ziller, *Angew. Chem. Int. Ed. Engl.* **1995**, *34*, 2386; *Angew. Chem.* **1995**, *107*, 2577; c) B. M. Trost, M. R. Machacek, A. Aponick, *Acc. Chem. Res.* **2006**, *39*, 747.

Ferrocenyl-based ligands, such as (**L**), employing a chiral arm scaffold to extend the chiral environment for the approaching nucleophile were also successfully applied in the AAA<sup>41</sup> and ferrocenyl ligands such as Josiphos (**M**) also impart excellent selectivities in certain cases.<sup>42</sup> Knowing that the different properties of the donor atoms are transmitted to the allylic substrate through the metal, ligands with electronically differentiated bidentate scaffolds such as **N**<sup>43</sup> or **O**<sup>44</sup> were applied in AAA and induced high enantioselectivity even with less common substrates.

Many other metals (Mo,<sup>45</sup> Ir,<sup>46</sup> W,<sup>47</sup> Cu,<sup>48</sup> Rh,<sup>49</sup> Ru<sup>50</sup>, Ni,<sup>51</sup> Pt<sup>52</sup>) also catalyse allylic alkylation and may involved different stereochemical courses as palladium. For example, Mo-catalysed AAA involved a net retention of stereochemistry but by a double retention pathway (**IV** from Scheme 3.3.4).<sup>45</sup>

### 3. Trisox/palladium catalysts in allylic substitutions

#### a. Experimental conditions

Different classes of allylic substitutions can be carried out enantioselectively with chiral palladium-based catalysts depending on the type of substrate and nucleophile chosen. In this short part our experimental conditions are discussed.

---

<sup>41</sup> a) T. Hayashi, A. Yamamoto, Y. Ito, T. Hagihara, *Tetrahedron Lett.* **1986**, 27, 191; b) T. Hayashi, *Pure Appl. Chem.* **1988**, 60, 7.

<sup>42</sup> A. Togni, C. Breutel, A. Schnyder, F. Spindler, H. Landert, A. Tijani, *J. Am. Chem. Soc.* **1994**, 116, 4062.

<sup>43</sup> a) P. Von Matt, O. Loiseleur, G. Koch, A. Pfaltz, C. Lefeber, T. Feucht, G. Helmchen, *Tetrahedron: Asymmetry* **1994**, 5, 573; b) J. Sprinz, M. Kiefer, G. Helmchen, M. Reggelin, G. Huttner, O. Walter, L. Zsolnai, *Tetrahedron Lett.* **1994**, 35, 1523; c) J. M. J. Williams, *Synlett* **1996**, 705; d) G. Helmchen, *J. Organomet. Chem.* **1999**, 576, 203; e) G. Helmchen, A. Pfaltz, *Acc. Chem. Res.* **2000**, 33, 336.

<sup>44</sup> a) J. V. Allen, S. J. Coote, G. J. Dawson, C. G. Frost, C. J. Martin, J. M. J. Williams, *J. Chem. Soc., Perkin Trans. 1* **1994**, 15, 2065; b) D. A. Evans, K. R. Campos, J. S. Tedrow, F. E. Michael, M. R. Gagne, *J. Am. Chem. Soc.* **2000**, 122, 7905; c) O. G. Mancheno, J. Priego, S. Cabrera, R. G. Arrayas, T. Llamas, J. C. Carretero, *J. Org. Chem.* **2003**, 68, 3679.

<sup>45</sup> a) B. M. Trost, I. Hachiya, *J. Am. Chem. Soc.* **1998**, 120, 1104; b) F. Glorius, A. Pfaltz, *Org. Lett.* **1999**, 1, 141; c) B. M. Trost, K. Dogra, M. Franzini, *J. Am. Chem. Soc.* **2004**, 126, 1944; d) O. Belda, C. Moberg, *Acc. Chem. Res.* **2004**, 37, 159; e) D. L. Hughes, G. C. Lloyd-Jones, S. W. Krska, L. Gouriou, V. D. Bonnet, K. Jack, Y. Sun, D. J. Mathre, R. A. Reamer, *Proc. Natl. Acad. Sci. U.S.A.* **2004**, 101, 5379.

<sup>46</sup> a) R. Takeuchi, N. Ue, K. Tanabe, K. Yamashita, N. Shiga, *J. Am. Chem. Soc.* **2001**, 123, 952; b) B. Bartels, G. Helmchen, *Chem. Commun.* **1999**, 741; c) G. Helmchen, A. Dahnz, P. Dübon, M. Schelwies, R. Weihofen, *Chem. Commun.* **2007**, 675.

<sup>47</sup> G. C. Lloyd-Jones, A. Pfaltz, *Angew. Chem. Int. Ed. Engl.* **1995**, 34, 462; *Angew. Chem.* **1995**, 107, 534.

<sup>48</sup> a) A. W. Van Zijl, L. A. Arnold, A. J. Minnaard, B. L. Feringa, *Adv. Synth. Catal.* **2004**, 346, 413; b) H. Yorimitsu, K. Oshima, *Angew. Chem. Int. Ed.* **2005**, 44, 4435; *Angew. Chem.* **2005**, 117, 4509 c) A. Alexakis, C. Malan, L. Lea, K. Tissot-Croset, D. Polet, C. Falcicola, *Chimia* **2006**, 60, 124;

<sup>49</sup> P. A. Evans, D. K. Leaky, *Chemtracts* **2003**, 16, 567.

<sup>50</sup> a) B. M. Trost, P. L. Fraisse, Z. T. Ball, *Angew. Chem. Int. Ed.* **2002**, 41, 1059; *Angew. Chem.* **2002**, 114, 1101; b) Y. Matsushita, K. Omitsuka, T. Kondo, T. Mitsudo, S. Takahashimi, *J. Am. Chem. Soc.* **2001**, 123, 10405.

<sup>51</sup> G. Consiglio, A. Indolese, *J. Organomet. Chem.* **1991**, 417, C36.

<sup>52</sup> J. M. Brown, J. E. McIntyre, *J. Chem. Soc., Perkin Trans. 2* **1985**, 961.



### Choice of the substrate

In the literature numerous substrates, precursors of the  $\pi$ -allylpalladium complexes, have been reported. Racemic allylic acetates are the most common employed substrates and Figure 3.3.2 gives an overview of some symmetric (top) and asymmetric substrates (bottom).

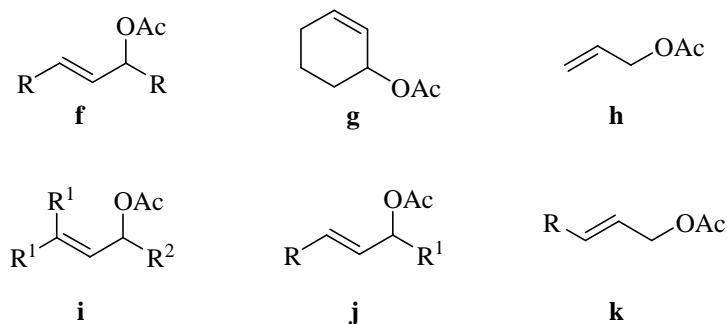
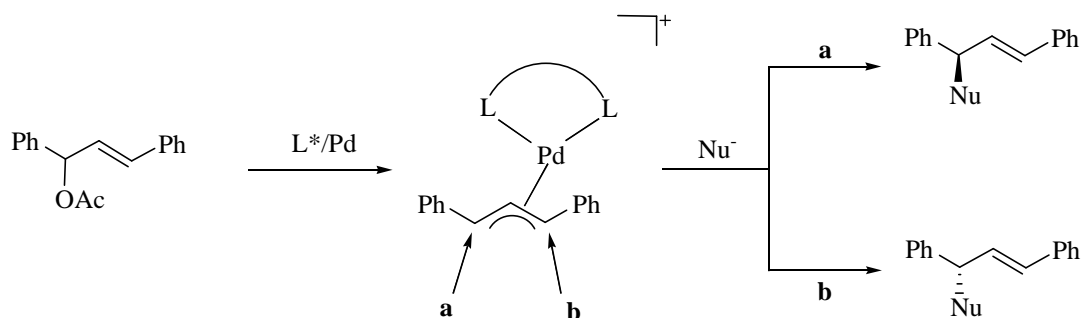


**Figure 3.3.2:** Examples of symmetric (**f-h**) and asymmetric (**i-k**) allylic acetates

Trying to find a highly regioselective catalyst is not the aim of our study, therefore we turned our attention to symmetric allylic acetates and more precisely to the most commonly used substrate in allylic alkylation, *rac*-1,3-diphenylprop-2-enyl acetate (**f-1** with R = Ph). Oxidative addition / ionisation in that case lead to the formation of allylic termini with two equivalent positions where the nucleophilic attack can occur for catalysts bearing a  $C_2$ -symmetric ligand. The two possible enantiomers that can be obtained after AAA of **f-1** with a nucleophile are shown in Scheme 3.3.5.

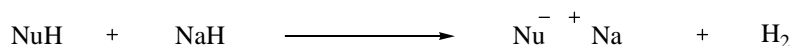


**Scheme 3.3.5:** Asymmetric allylic alkylation of *rac*-1,3-diphenylprop-2-enyl acetate

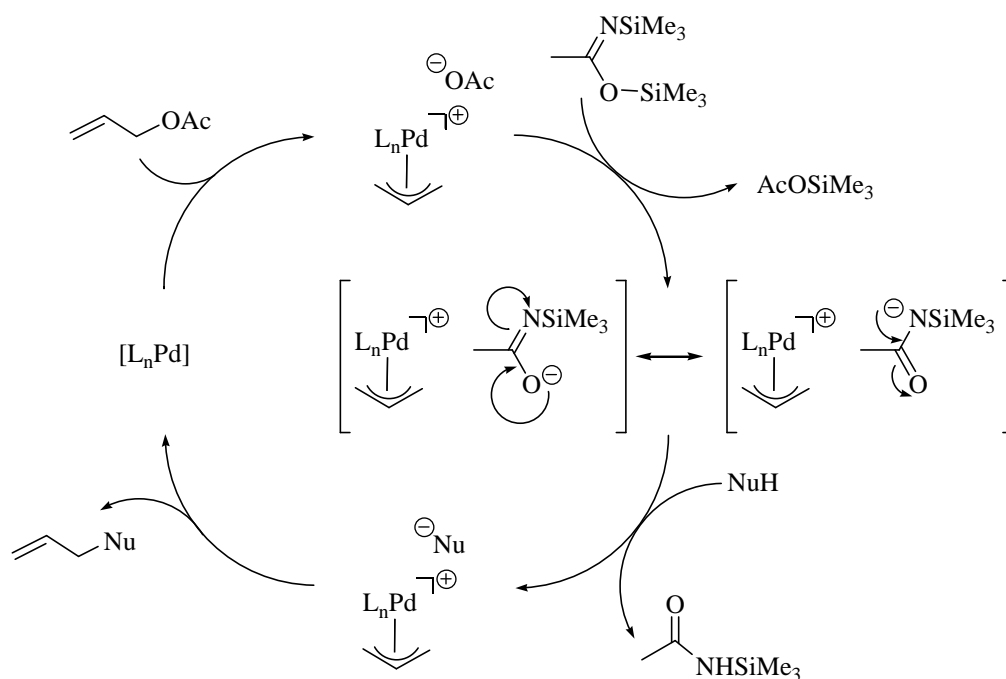
### Choice of the nucleophile

Asymmetric allylic substitution enables the formation of C-C, C-N, C-O, C-H... bonds, depending on the nucleophile employed *e.g.* malonate, amine, and sodium borohydride. To make the comparison with results published in the literature possible, C-C bond formation was the object of our study with the “soft” nucleophile dimethyl malonate.

There are two possible ways to generate the carbanion  $\text{Nu}^-$ . In the classical pathway the nucleophile is preformed by an acid-base reaction:



The carbanion can also be generated *in situ* under the catalytic conditions using *N,O*-bis-trimethylsilylacetamide (BSA) as base precursor.<sup>53</sup> The formation of the carbanion probably occurs through the mechanism depicted in Scheme 3.3.6. The oxidative addition of the allylic acetate affords a cationic  $\pi$ -allylpalladium complex. The nucleophilic substitution of the acetate on the BSA generates the *N*-trimethylsilylacetamide anion as well as the trimethylsilyl acetate by-product. The third step of the cycle is an acid-base reaction between  $\text{NuH}$  and *N*-trimethylsilylacetamide giving the carbanion. Finally the intermolecular nucleophilic attack on the  $\pi$ -allyl yields the product and regenerates the palladium(0) active species.



**Scheme 3.3.6:** Mechanism of the formation of the nucleophile by reaction with BSA

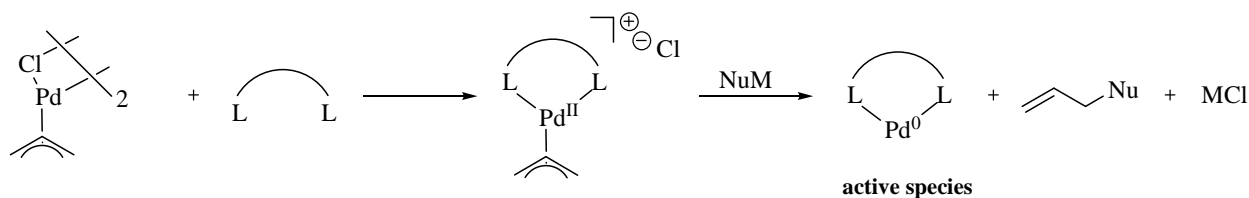
This method to generate the carbanion presents several advantages: i) the carbanion is formed *in situ* during the catalysis; ii) BSA is soluble in most of the solvents and allows the variation of the reaction conditions, *e.g.* use of dichloromethane as a solvent; iii) the concentration of the nucleophile relative to that of the catalyst remains constant and this can be significant for the selectivity. In our studies the second of the protocols described has been used to generate the carbanion.

<sup>53</sup> B. M. Trost, D. J. Murphy, *Organometallics* **1985**, *4*, 1143.

### Palladium source

The zerovalent  $\text{Pd}^0(\text{dba})_2$  complex (dba = dibenzylidene acetone) combined with diphosphine ligands is often used as palladium source in asymmetric catalytic allylic alkylations. The  $[\text{Pd}^0\text{P}_2]$  catalyst is generated by substitution of the labile dba ligand by the diphosphine. However, Amatore *et al.* have shown that sometimes the substitution is not always complete and the dba ligand may still coordinate to the metal centre and may thus influence the selectivity of the reaction.<sup>54</sup>

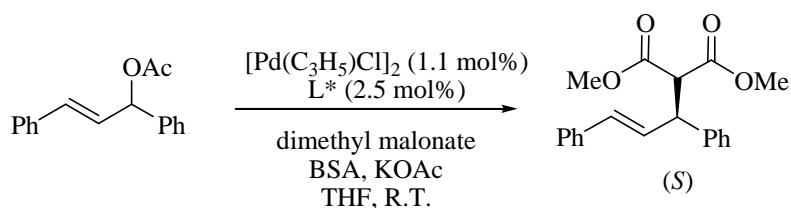
With the  $[\text{Pd}(\eta^3\text{-C}_3\text{H}_5)\text{Cl}]_2$  dimer in the presence of the ligand the  $[\text{Pd}^0\text{L}_2]$  active species is generated *in situ* after reduction of the palladium(II). The reduction occurs in the presence of the first equivalent of nucleophile (Scheme 3.3.7).



**Scheme 3.3.7:** Formation of the active species starting from the  $[\text{Pd}(\eta^3\text{-C}_3\text{H}_5)\text{Cl}]_2$  dimer

#### b. Preliminary results

Pfaltz and coworkers previously investigated this reaction with the well established bisoxazoline as stereodirecting ligands and this particular system therefore provided the point of reference for our work. The allylic alkylation of *rac*-1,3-diphenylprop-2-enyl acetate with dimethyl malonate as a nucleophile in the presence of BSA was carried out using the catalytic systems prepared *in situ* by addition of the ligand to the palladium allyl chloride dimer  $[\text{PdCl}(\eta^3\text{-C}_3\text{H}_5)]_2$  precursor (Scheme 3.3.8).<sup>55</sup>



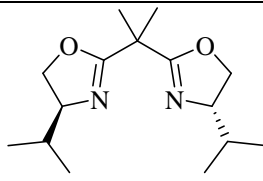
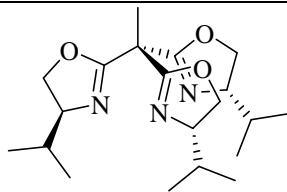
**Scheme 3.3.8:** General scheme for the palladium-catalysed allylic alkylation of *rac*-1,3-diphenylprop-2-enyl acetate

<sup>54</sup> C. Amatore, A. Jutand, F. Khalil, M. M'Barki, L. Mottier, *Organometallics* **1993**, *12*, 3168.

<sup>55</sup> B. M. Strickner, *J. Am. Chem. Soc.* **1983**, *105*, 568.

After 1.5 hours at 50°C in tetrahydrofuran to generate the catalytic precursor, the reaction mixture was cooled down to room temperature before starting the catalysis. Using 2.2 mol% of palladium and ligand *i*Pr-BOX, an enantiomeric excess of 89% and 89% isolated yield were obtained after three days in reasonably good agreement with Pfaltz' results.<sup>56</sup> Under the same conditions, the analogous catalyst with *i*Pr-trisox as stereodirecting ligand gave an ee value of 95% and 90% yield (Table 3.3.1).

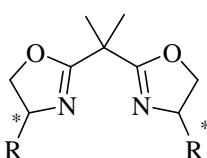
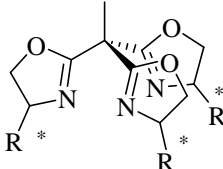
These first results indicated higher selectivity for the trisox-based catalyst and possibly similar activity for both systems. The modular strategy of the ligand design enabled us to synthesise three highly symmetric trisoxazolines: Bn-trisox, Ph-trisox and Ind-trisox. A similar comparative study was then investigated with the different BOX/trisox couple available.

		
	<i>i</i> Pr-BOX	<i>i</i> Pr-trisox
Yield (%)	89	90
ee (%)	89	95

**Table 3.3.1:** Results of asymmetric allylic alkylation with *i*Pr-BOX and *i*Pr-trisox

### c. Trisoxazoline vs bisoxazoline

The analogous comparative study with the other oxazoline derivatives shows that the trisoxazoline-based catalysts generally induce a better enantioselectivity compared to their bisoxazoline analogues (Table 3.3.2). This behaviour appears to be independent of the substituent as shown in Table 3.3.2.

					
Entry	R	Yield (%)	ee (%)	Yield (%)	ee (%)
1	( <i>S</i> )- <i>i</i> Pr	89	89	90	95
2	( <i>R</i> )-Ph	7	-72	28	-88
3	( <i>S</i> )-Bn	88	83	92	88
4	(4 <i>R</i> ,5 <i>S</i> )-Ind	13	-93	95	-98

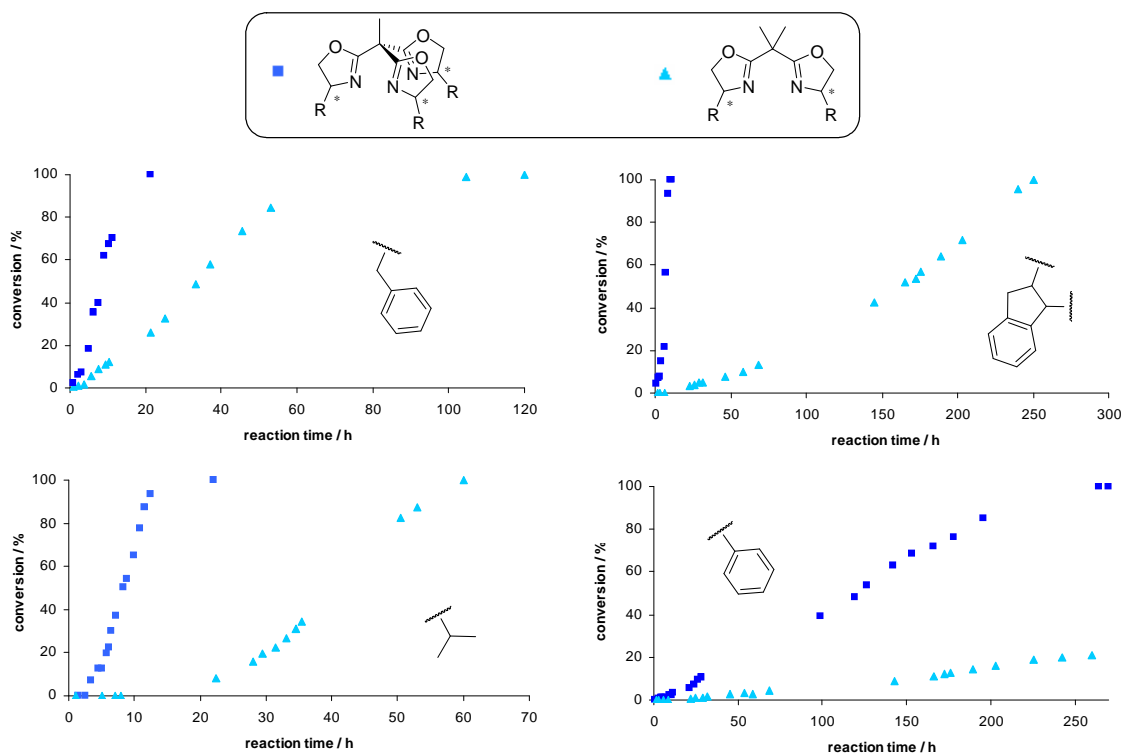
**Table 3.3.2** Results of asymmetric allylic alkylation with the different bisoxazolines and trisoxazolines

<sup>56</sup> P. von Matt, G. C. Lloyd-Jones, A. B. E. Minidis, A. Pfaltz, L. Macko, M. Neuburger, M. Zehnder, H. Rügger, P. S. Pregosin, *Helv. Chim. Acta* **1995**, 78, 265.

Concerning the yields, for the oxazolines bearing the isopropyl (entry 1) and benzyl (entry 3) substituents both catalytic systems seem to lead to the same conversion after three days reaction. For the oxazolines with phenyl (entry 2) or indanyl (entry 4) substituents the trisox/Pd systems are clearly superior.

The catalyst bearing the Ind-trisox ligand, *i.e.* with the lowest internal degrees of freedom, displays the highest selectivity and activity. Rigidity of the chiral environment around the palladium centre could explain this superiority.

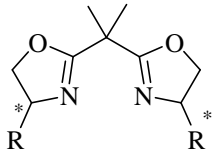
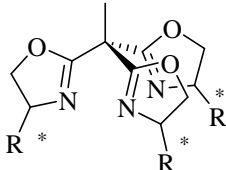
Kinetic studies have been carried out in order to obtain more insight. The catalytic conversions with the BOX and trisox ligands from Table 3.3.2 have been monitored by gas chromatography. The evolution of the conversion as a function of time for the four different BOX/trisox couple is depicted in Figure 3.3.3.



**Figure 3.3.3:** Comparison of the conversion curves for the trisox/Pd systems (■) and the corresponding bisoxazoline/Pd systems (▲)

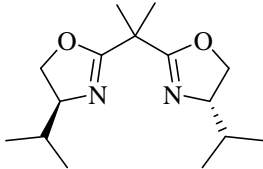
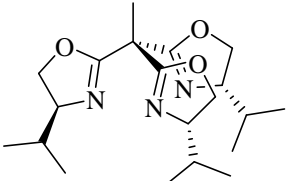
BOX/Pd complexes require longer induction periods than their corresponding trisox/Pd catalysts. The most notable observation is the rate acceleration with the tripods compared to the BOX ligands for all substitution patterns. The turn-over frequencies (TOFs) derived from the quasilinear section in the conversion curves are displayed in Table 3.3.3. The rate of the reaction

is strongly dependent on the substituent of the respective ligand. The *i*Pr substituent yields the most active BOX-derivative whereas the indanyl substituent leads to the highest rate for the trisox-based catalysts. With *i*Pr, Ph and Bn-based ligands the TOFs differ by a factor of four in favour of the tripod, whilst a 64-fold acceleration was found for the indanyl-derivative.

			TOF ratio trisox/BOX
( <i>S</i> )- <i>i</i> Pr	1.37	5.02	3.7
( <i>R</i> )-Ph	0.05	0.2	4.0
( <i>S</i> )-Bn	0.91	3.73	4.1
(4 <i>R</i> ,5 <i>S</i> )-Ind	0.19	12.2	64.2

**Table 3.3.3:** Turn-over frequencies TOF (h<sup>-1</sup>) derived from the conversion curves shown in Figure 3.3.3

Moreover, the efficiency of the BOX and trisox ligands were compared in the allylic amination of *rac*-1,3-diphenylprop-2-enyl acetate. Only the oxazoline derivatives with isopropyl substituents were investigated. The general reaction scheme and results are displayed in Table 3.3.4.

		
Yield (%)	16	68
ee (%)	53	63

**Table 3.3.4:** Results of allylic amination with *i*Pr-BOX/Pd and *i*Pr-trisox/Pd catalysts

Again, the trisox-based catalyst shows higher activity and selectivity confirming that the trisoxazoline derivatives lead to superior catalysts compared to the bisoxazolines.

The third oxazoline arm may play a direct or indirect role at some earlier or later stage during the catalysis. To see the influence of the third heterocycle on the efficiency of the catalysts, a series of catalysts bearing oxazoline derivatives as stereodirecting ligands have been investigated.

d. Extension of the study to functionalised bisoxazolines

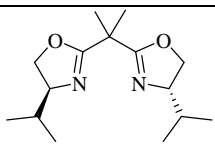
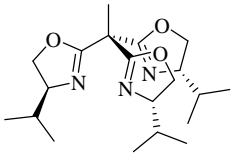
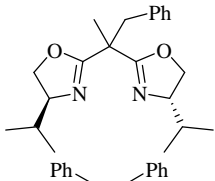
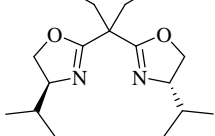
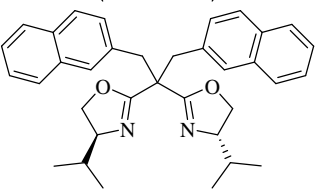
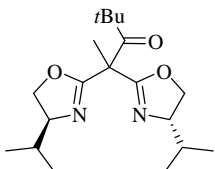
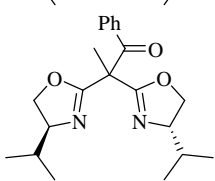
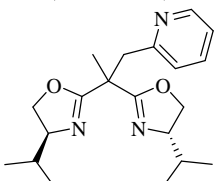
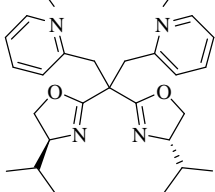
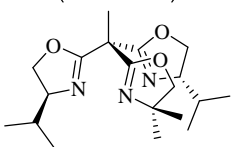
A series of modified bisoxazoline ligands containing potentially coordinating or non-coordinating “sidearms” at the apical position were synthesised following literature procedures.<sup>57</sup> Additionally, several dually functionalized  $C_2$  symmetric systems which are readily obtained from the bis(oxazolinyl)methane, were also synthesised.<sup>58</sup> For practical reasons only oxazoline derivatives with the isopropyl substituents were prepared. The results of the asymmetric allylic alkylations are summarised in Table 3.3.5 as well as the previously discussed results for the *iPr*-BOX/*iPr*-trisox couple (entries 1-2).

Increasing the steric bulk on the bridging carbon atom gives better ee's compared to the BOX ligand however yields are significantly lower (entries 3-5). The two functionalised-bisoxazoline derivatives with ketone-based arms induce the same enantioselectivity as the trisoxazoline probably due to steric hindrance, but give rise to lower yields than *iPr*-BOX and *iPr*-trisox (entries 6-7). In contrast, the introduction of the pyridylmethyl sidearm does not affect the yield but the ee value drops to 66% (entry 8). This is probably due to the presence of three isomeric active species, two of them coordinated by an achiral pyridine and an oxazoline. The same trend is followed with the introduction of a second pyridylmethyl sidearm (entry 9). In this case the observed ee value (3%) can be rationalised by four interchanging active species: bisoxazoline, oxazoline-pyridine (two diastereomers) and bispyridine. Finally the alkylation catalyst with the  $C_1$ -symmetric trisoxazoline, containing an achiral oxazoline unit, displays a slightly lower ee value than the  $C_3$ -symmetric catalyst (91% vs. 95%) (entry 10). For possible explanations, see chapter 4 and the copper-catalysed amination reaction.

To summarise, the highest yields were obtained from ligands that contain a potentially donating heteroatom as sidearm, with ligands that contain nitrogen donors displaying slightly higher activity than oxygen donors. The enantioselectivity of the product is also affected by the nature of the sidearm. Ligands with no heteroatom-containing sidearms usually give lower yield and moderate to good enantiomeric excesses depending on the bulkiness of the substituents.

<sup>57</sup> a) J. Zhou, M. C. Ye, Y. Tang, *J. Comb. Chem.* **2004**, *6*, 301; b) M. Honma, T. Sawada, Y. Fujisawa, M. Utsugi, H. Wanatabe, A. Umino, T. Matsamura, T. Hagihara, M. Takano, M. Nakada, *J. Am. Chem. Soc.* **2003**, *125*, 2860.

<sup>58</sup> M. Seitz, C. Capacchione, S. Bellemin-Lapponnaz, H. Wadepohl, B. D. Ward, L. H. Gade, *Dalton Trans.* **2006**, 193.

Entry	Ligand	Yield (%)	ee (%)	
1		<i>i</i> Pr-BOX	89	89
2		<i>i</i> Pr-trisox	90	95
3		<b>P</b>	15	86
4		<b>Q</b>	51	94
5		<b>R</b>	63	93
6		<b>S</b>	74	95
7		<b>T</b>	68	95
8		<b>U</b>	93	66
9		<b>V</b>	84	3
10		<b>W</b>	67	91

**Table 3.3.5:** Results of asymmetric allylic alkylation with different oxazoline derivatives



To further explore this influence, a comparative kinetic study of the catalytic conversion with two representative non-symmetric side-arm-functionalised ligands (-CO*t*Bu, entry 6 and -CH<sub>2</sub>Py, entry 8) has been carried out and compared with the results obtained for *i*Pr-BOX and *i*Pr-trisox systems (Figure 3.3.4).

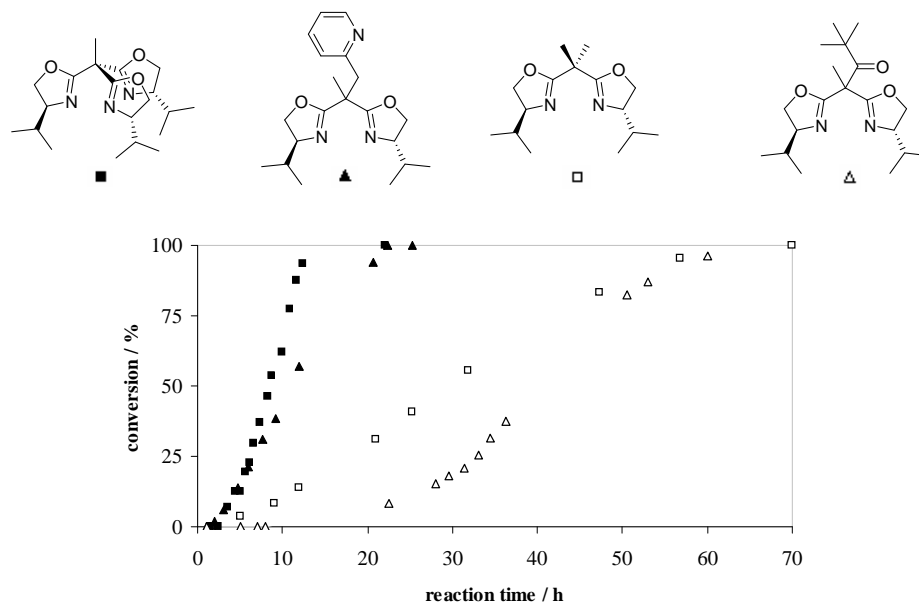


Figure 3.3.4: Comparison of the conversion curves for four catalyst systems

This study confirms that the introduction of a donating sidearm leads to rate enhancement; the best catalytic activity being reached with the trisoxazoline ligand *i*Pr-trisox.

#### 4. Conclusion

The mechanism of palladium-catalysed allylic alkylation involves four steps: after coordination of the substrate to the palladium(0) species, an oxidative addition/ionisation sequence results in the formation of the  $\pi$ -allyl palladium(II) complex; the nucleophile then externally attacks the  $\pi$ -allyl intermediate giving rise to a palladium(0) species bearing the product which is displaced by way of substitution through another substrate molecule.

Since our catalytic systems were prepared *in situ* from palladium(II) allyl chloride and the trisox ligand, the first step in the formation of the active catalyst involves the reduction of the palladium(II) precursor by a nucleophilic attack by the malonate. The observation of an induction period in the conversion curves is thus not surprising. Introduction of an additional donor function in the stereodirecting ligand generally resulted not only in a rate enhancement but

also in the reduction of this induction period. The observed overall rate acceleration might be due to the ability of the additional donating group to induce the formation of the palladium(0) species both in the initial generation of the active species as well as in the product/substrate exchange step at the end of the catalytic cycle. This mechanistic aspect, as well as the symmetry-related simplification of the reaction network for the catalysts bearing  $C_3$ -chiral tripods, may be at the root of the superior performance of the trisox-systems.

## - Chapter 4 -

<b>I. Introduction.....</b>	<b>111</b>
1. Asymmetric Lewis acid copper-based catalysis .....	111
2. Problem set and aims of the study .....	113
<b>II. Highly symmetric trisoxazolines in enantioselective copper(II) Lewis acid catalysis</b>	<b>114</b>
1. From bisoxazoline/copper(II) to trisoxazoline/copper(II) catalysts .....	114
2. Model reactions.....	117
a. Mannich reaction .....	117
b. $\alpha$ -amination reaction .....	118
3. Influence of the third oxazoline unit on the catalyst loading.....	119
a. Reaction conditions.....	119
b. Trisoxazolines in the asymmetric Mannich reaction .....	120
c. Trisoxazolines in the asymmetric $\alpha$ -amination reaction.....	121
d. The active catalyst: bidentate coordination mode of the trisoxazoline.....	123
4. Conclusion .....	124
<b>III. Stereochemical consequences of threefold symmetry.....</b>	<b>124</b>
1. Introduction: Inverting chiral centres in $C_2$ and $C_3$ symmetric stereodirecting tripod ligands.....	124
2. Effect of the inversion of one of the chiral centres in BOX and trisox ligands.....	127
a. Catalytic $\alpha$ -amination of ethyl 2-methylacetoacetate.....	127
b. Active species and consideration of “first coordination sphere” symmetry .....	128
c. Crystal structure of a copper(II) complex with $C_1$ -chiral ( $R,S,S$ )-Ph-trisox .....	129
d. A steady state kinetic model for the behaviour	

---

of the stereochemically mixed ( <i>R,S,S</i> )-Ph-trisox/copper catalyst.....	130
3. Effect of the combination of chiral and achiral oxazolines in $C_1$ -symmetric tripods.....	134
a. Desymmetrisation of $C_3$ -symmetric trisox and dicoordinate isomers generated.....	134
b. Catalytic $\alpha$ -amination of ethyl 2-methylacetoacetate with the stereochemically “mixed” trisox/copper catalysts .....	136
c. Estimate of the relative amounts of catalytic species for $Ph_2$ -dm-trisox/copper and $Ph$ -dm <sub>2</sub> -trisox/copper catalysts.....	138
4. Conclusion .....	139

This chapter is devoted to the application of the trisoxazolines in copper(II) chemistry. The first part concentrates on generalities about enantioselective copper-catalysed Lewis acid reactions and on the description of the aim of the work. The study of the influence of the catalyst loading on the activity and selectivity is presented in the following part. Finally, threefold vs. twofold symmetry in asymmetric catalysis is discussed by comparing the catalytic performance of BOX- and trisox- containing copper(II) Lewis acid.

## I. Introduction

### I. Asymmetric Lewis acid copper-based catalysis

Many carbon-carbon or carbon-nitrogen bond-forming reactions are subject to Lewis acid-promoted rate acceleration.<sup>1</sup> Cycloadditions, conjugate additions and aldol reactions are representative examples of such Lewis acid activations. If the Lewis acid complex is chiral, it may control the stereochemical outcome of the process. Electrophilic activation of carbonyl compounds by metal-centred chiral Lewis acids is an efficient method for the enantioselective catalysis of nucleophile-electrophile reactions. Different transition metals have been applied in Lewis acid-promoted catalytic reactions.<sup>2</sup> Among them, copper(II) is an efficient Lewis acid and therefore has been the focus of great interest. The Irving-Williams series for divalent ions in the first transition series indicates that Cu(II) forms the most stable ligand/metal complexes and dissociation of the chelating chiral ligand in such complexes is negligible. The order of the stability  $\text{Mn(II)} < \text{Fe(II)} < \text{Co(II)} < \text{Ni(II)} < \mathbf{\text{Cu(II)}} > \text{Zn(II)}$  has been found to be independent on the nature of the coordinated ligand or on the number of ligand molecules involved.<sup>3</sup> The order of stability is directly correlated with the second ionisation potentials and ionic radii. Copper(II) displays a disposition to form square planar or elongated tetragonal complexes. For copper complexes bearing bidentate chelating ligands coordination of a bidentate substrate is thus favoured in the equatorial plane with the counterion being a weakly or non-coordinating ligand.<sup>4</sup> Jahn-Teller distortion in the  $d^9$  complex elongates the remaining apical sites where the

---

<sup>1</sup> M. Santelli, J.-M. Pons, In *Lewis Acids and Selectivity in Organic Synthesis*, CRC Press: New York, **1996**.

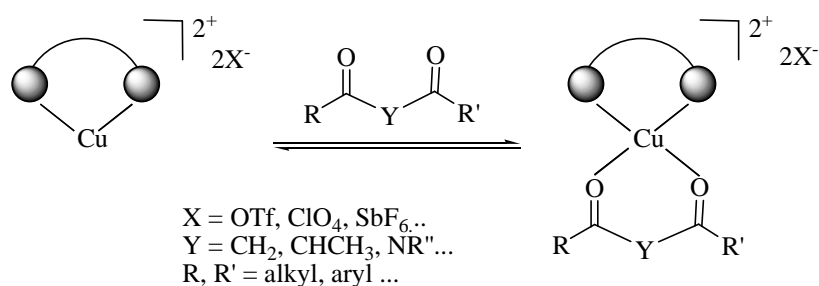
<sup>2</sup> See for example: a) S. Kobayashi, *Pure Appl. Chem.* **1998**, *70*, 1019; b) B. Bosnich, *Aldrichimica Acta* **1998**, *31*, 76; c) S. Kobayashi, K. Manabe, *Acc. Chem. Res.* **2002**, *35*, 209; d) A. Corma, H. Garcia, *Chem. Rev.* **2002**, *102*, 3837; e) A. Yanagisawa, In *Modern Aldol Reactions*, Ed.: R. Mahrwald, Wiley-VCH, **2004**, Vol. 2, 1; f) J. S. Johnson, D. A. Nicewicz, In *Modern Aldol Reactions*, Ed.: R. Mahrwald, Wiley-VCH, **2004**, Vol. 2, 69; g) Y. Yamashita, S. Kobayashi, In *Modern Aldol Reactions* Ed.: R. Mahrwald, Wiley-VCH, **2004**, Vol. 2, 167; h) R. F. R. Jazzar, E. P. Kündig, In *Ruthenium in Organic Synthesis*, Ed.: S.-I. Muharashi, Wiley-VCH, **2004**, 257.

<sup>3</sup> H. Irving, R. J. P. Williams, *J. Chem. Soc.* **1953**, 3192.

<sup>4</sup> B. J. Hathaway, D. E. Billing, *Coord. Chem. Rev.* **1970**, *5*, 143.

counteranion may (or may not) reside. These considerations act jointly to provide well-defined complexes that may exhibit excellent properties as catalysts.

In the field of chiral copper(II)-based Lewis acid catalysis, the catalyst, in general, consists of a cation coordinated to an optically active bidentate ligand to give a chiral complex with at least one vacant site suitable for coordination and activation of the reagent. The substrates generally used in these catalysis are often capable of chelating to the chiral Lewis acidic metal complex (Scheme 4.1.1).



**Scheme 4.1.1:** Lewis acid catalysts possessing two vacant Lewis acid sites for the coordination of the chelating substrate

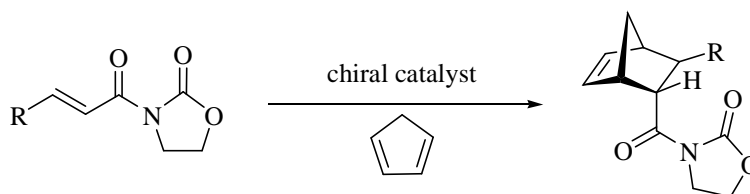
This chelating-assisted catalysis is applied in various types of reactions and transformations. Among these processes, those catalysed with chiral metal(II) complexes frequently reach enantioselectivities greater than 90%.<sup>5</sup> An important outcome of the chelation criterion is that the analysis of the catalyst-substrate complex usually leads to an unambiguous prediction of the sense of asymmetric induction. To induce a good level of enantioselection, the coordinated reagent should be suitably oriented to favour a selective attack to one specific face.

$C_2$ -symmetric bisoxazolines are among the most popular classes of chiral ligands satisfying the various requirements needed for good face selectivity. Corey *et al* first demonstrated that this class of ligands combined with Mn(II) and Fe(III) leads to effective chiral Lewis acid catalysts for Diels-Alder reactions.<sup>6</sup> The versatility of chiral bisoxazoline/copper(II) complexes in such reactions has been first illustrated in 1993 by Evans *et al*.<sup>7</sup> They reported that [Cu(*t*Bu-BOX)](OTf)<sub>2</sub> complex acts as an effective chiral Lewis acid for the Diels-Alder reaction described in Scheme 4.1.2.

<sup>5</sup> a) D. A. Evans, T. Rovis, J. S. Johnson, *Pure Appl. Chem.* **1999**, *71*, 1407; b) *Lewis Acids in Organic Synthesis*, Ed.: H. Yamamoto, Wiley-VCH: New York, **2000**, Vols. 1 and 2; c) S. Kobayashi, Y. Mori, Y. Yamashita, In *Comprehensive Coordination Chemistry II* **2004**, *9*, 399.

<sup>6</sup> a) E. J. Corey, N. Imai, H.-Y. Zhang, *J. Am. Chem. Soc.* **1991**, *113*, 728; b) E. J. Corey, K. Ishihara, *Tetrahedron Lett.* **1992**, *33*, 6807.

<sup>7</sup> D. A. Evans, S. J. Miller, T. Lectka, *J. Am. Chem. Soc.* **1993**, *115*, 6460.



**Scheme 4.1.2:** Diels-Alder reaction of a 2-oxazolidinone derivative with cyclopentadiene

From these investigations it appears that copper(II) triflate is uniquely effective in delivering cycloadducts in high diastereo- and enantiomeric excesses ( $-78^{\circ}\text{C}$ ,  $> 98\%$  ee) out of the ten metal triflates tested at the time.<sup>8</sup> Since then,  $C_2$ -symmetric bisoxazolines, including those immobilised on heterogeneous media,<sup>9</sup> have proven to be efficient ligands in Lewis acid copper-catalysed reactions yielding valuable enantiomerically enriched compounds.<sup>5,10</sup>

During the course of the studies reported in the literature it has been observed that the isolation of the  $[\text{Cu}(\text{BOX})]^{2+}$  precursors is not a prerequisite for their success as enantioselective catalysts. They can efficiently be prepared *in situ*: when the chiral bisoxazoline ligand is mixed with an inorganic copper salt in an organic solvent, a chiral BOX/metal complex is usually instantaneously formed, which is the precatalyst of the reaction in question. Therefore, any structural information is important to understand the arrangement at the metal centre of the molecules involved in the reaction and in the stereochemical outcome. Work to date has revealed that bisoxazoline/copper complexes provide a rigid square planar template with a defined chiral environment.

## 2. Problem set and aims of the study

Similar to palladium chemistry described in the previous section we expected a favourable effect of highly symmetrical trisoxazolines on the catalyst performance in square planar copper(II) complexes undergoing fluxional processes. The substitutional lability of the copper(II) complexes promotes this fluxionality. Thus, in the square planar complexes chemical exchange between the symmetry-equivalent  $\kappa^2$ -coordinated species takes place, with the non-coordinated sidearm playing a direct or indirect role at some stage in the catalytic reaction. The expected interconverting key intermediates are represented in Figure 4.1.1.

<sup>8</sup> D. A. Evans, S. J. Miller, T. Lectka, P. von Matt, *J. Am. Chem. Soc.* **1999**, *121*, 7569.

<sup>9</sup> D. Rechavi, M. Lemaire, *Chem. Rev.* **2002**, *102*, 3467.

<sup>10</sup> a) A. K. Ghosh, P. Mathivanan, J. Capiello, *Tetrahedron: Asymmetry* **1998**, *9*, 1; b) K. A. Jørgensen, M. Johannsen, S. Yao, H. Audrain, J. Thorhauge, *Acc. Chem. Res.* **1999**, *32*, 605; c) J. S. Johnson, D. A. Evans, *Acc. Chem. Res.* **2000**, *33*, 325; d) G. Desimoni, G. Faita, K. A. Jørgensen, *Chem. Rev.* **2006**, *106*, 3561.

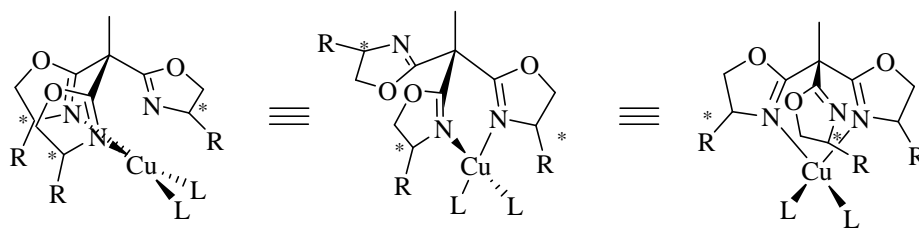


**Figure 4.1.1:** The three symmetry-equivalent square planar Cu(II) complexes bearing  $\kappa^2$ -chelating  $C_3$ -symmetric trisoxazoline ligands

The application of trisoxazoline ligands in Lewis acid copper-catalysed reactions is aimed to see if the use of these tridentate ligands may solve a limitation encountered with the bisoxazoline-based catalysts: the high catalyst loadings required. To that end trisoxazolines have been used in two model reactions, an asymmetric  $\alpha$ -amination and a Mannich reaction. A direct comparison with the corresponding 2,2-bis(oxazolanyl)propane ligands will help us to find out whether the third donating arm influences the activity and/or the stereoselective outcome of catalysis carried out with lower catalyst loadings. This concept and the results obtained are described in the following part.

Finally, the conceptual differences in exploiting twofold and threefold rotational symmetry in the design of chiral ligands for asymmetric catalysis have been addressed in a comparative study of the catalytic performance with BOX and trisox containing copper(II) catalysts. The results of this study are discussed in the last part of this chapter.

## II. Highly symmetric trisoxazolines in enantioselective copper(II) Lewis acid catalysis

### 1. From bisoxazoline/copper(II) to trisoxazoline/copper(II) catalysts

Some bisoxazoline ligands are commercially available, such as (*R*)- and (*S*)-Ph-BOX as well as (*S*)-*t*Bu-BOX. These bisoxazolines belong to the most widely used ligands in the literature and their catalytic performance is a testimony to the efficiency of 4-aryl- and 4-alkyl-substituted BOX-based catalysts.

After formation of the bisoxazoline/copper(II) complex, the next step is coordination of the dicarbonyl substrate compound to the catalyst. It is generally accepted that the dicarbonyl compound utilizes both carbonyl functionalities for coordination to the copper centre. BOX/copper(II) catalysts have proven to be highly efficient for the addition reactions to dicarbonyl compounds and for the reactions where the latter act as pro-nucleophile. This is probably because the Lewis acidity of copper(II) is optimal for this class of substrates and



because the bidentate coordination of the dicarbonyl compound to the metal centre leads to a chiral environment with efficient shielding of one of the carbonyl faces. The latter is illustrated in Figure 4.2.1 for a  $[\text{Cu}((S)\text{-}t\text{Bu-BOX})(\text{dicarbonyl})]^{2+}$  species.

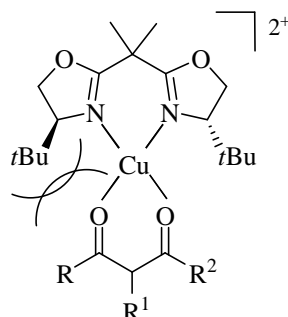
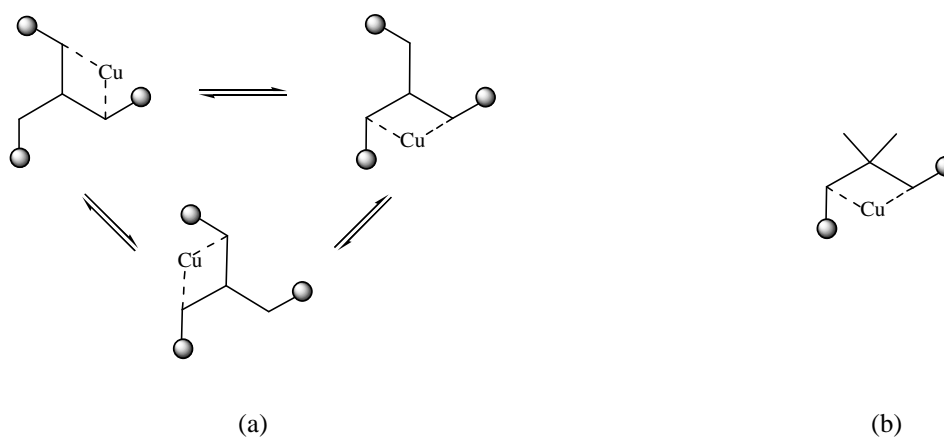


**Figure 4.2.1:** Coordination of the dicarbonyl substrate to copper(II): one of the approach is blocked by the *t*Bu group

In Figure 4.2.1 the *upper* face of “left” carbonyl functionality is shielded by the *tert*-butyl group and therefore the nucleophilic/electrophilic attack occurs from the back of the dicarbonyl compound. Thus, BOX/copper(II) catalysts provide a chiral environment at the Lewis acidic centre leading to highly selective reactions.

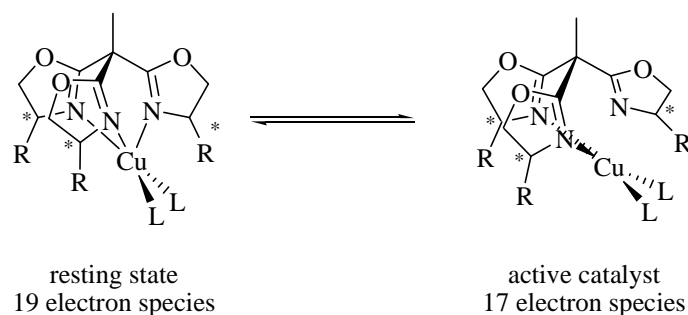
Based on the high stereoselectivity observed for the bisoxazoline-based Lewis acid catalysts, the trisoxazoline-based complexes may act as selective catalysts. The conceptual approach in which the high rotational symmetry of the chiral trisoxazoline renders the reversible pathways leading to the active catalyst equivalent has been presented above (see Figure 4.1.1). The three active species bearing a ligand with a bidentate coordination mode have a similar chiral environment at the Lewis acidic centre to that of the BOX/copper catalysts (Scheme 4.2.1).



**Scheme 4.2.1:** Dynamic exchange between the three catalytic active species (a); the copper/bisoxazoline catalyst (b)

A possible facial coordination by a chiral tridentate ligand was thought to stabilise the resting state of the copper complexes. The additional oxazoline ligation is expected to deactivate the complexes in their Lewis acidity as shown in a theoretical study on BOX/copper(II) catalysts.<sup>11</sup> Jørgensen *et al.* calculated the energy of the LUMO orbital of the 17 electron  $[\text{Cu}(\text{BOX})(\text{substrate})]^{2+}$  and the 19 electron  $[\text{Cu}(\text{BOX})(\text{substrate})(\text{CH}_3\text{CN})]^{2+}$  complexes. An important factor for the reactivity of  $[\text{Cu}(\text{BOX})(\text{substrate})]^{2+}$  complexes is the energy of the LUMO orbital which is the orbital responsible for the interaction with the HOMO of the incoming electron rich reagent. For the 19 electron complex possessing a third nitrogen donor it has been found that the dicarbonyl is less reactive, as the LUMO was found to be 1.04 eV higher in energy than for the 17 electron complex. Moreover, the Cu-O bond of the reacting carbonyl oxygen atom was found to be longer in the 19 electron complex. This bond length change shows that the carbonyl functionality of the substrate is less coordinated to the Lewis acidic centre. This accounts for higher LUMO energy and thus for the reduced activity of the 19 electron complex compared to the 17 electron complex.

Therefore the transformation of the resting state into the active 17 electron Cu(II) species necessitates the decooordination of an oxazoline unit and the opening up of the system (Scheme 4.2.2). This required "hemilability"<sup>12</sup> is provided stereoelectronically by the strong dynamic Jahn-Teller effect of the  $d^9$  Cu(II) centre.



**Scheme 4.2.2:** Coordination/decoordination equilibrium between the proposed resting and active states of the trisox/copper catalysts

<sup>11</sup> J. Thorhauge, M. Roberson, R. G. Hazell, K. A. Jørgensen, *Chem. Eur. J.* **2002**, *8*, 1888.

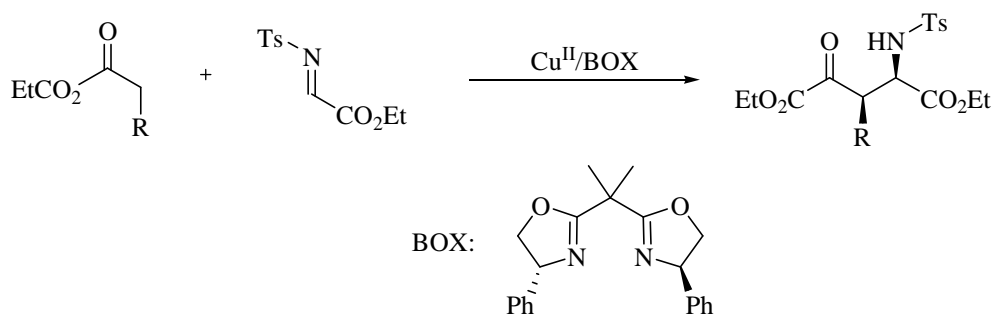
<sup>12</sup> P. Braunstein, F. Naud, *Angew. Chem. Int. Ed.* **2001**, *40*, 680; *Angew. Chem.* **2001**, *113*, 702.

## 2. Model reactions

Based on results published by Jørgensen and coworkers with bisoxazoline/copper(II) Lewis acid catalysed the asymmetric  $\alpha$ -amination and Mannich reactions were chosen as test reactions.

### a. Mannich reaction

The Mannich reaction is an effective carbon-carbon bond-forming process for the construction of nitrogen containing compounds.<sup>13</sup> This reaction has been employed numerous times successfully as a key step in natural product synthesis as well as in medicinal chemistry.<sup>14</sup> The first catalytic enantioselective Mannich-type reaction was reported in 1997 by Kobayashi *et al.* using chiral zirconium/BINOL complexes as catalysts.<sup>15</sup> In 2001, Jørgensen and coworkers disclosed a highly enantioselective catalytic direct Mannich reaction where 2-ketoesters were treated with *N*-protected  $\alpha$ -iminoesters in the presence of bisoxazoline/copper(II) complexes (Scheme 4.2.3).<sup>16</sup>



**Scheme 4.2.3:** Diastereo- and enantioselective direct Mannich reaction of activated carbonyl compounds with  $\alpha$ -iminoesters catalysed by a chiral Lewis acid

Lewis acid-catalysed reaction of 2-ketoesters with *N*-tosyl  $\alpha$ -iminoesters gave enantiomeric excesses up to 97% using the chiral [Cu(Ph-BOX)](OTf)<sub>2</sub> complex. The reaction allowed the formation of highly functionalised 4-oxo-glutamic acid ester derivatives which could be converted into highly functionalised optically active  $\alpha$ -amino- $\gamma$ -lactones.<sup>16</sup>

In 2003, the group of Jørgensen reported the use of  $\beta$ -ketoesters as pro-nucleophiles in the catalytic asymmetric direct Mannich reaction with an activated *N*-tosyl  $\alpha$ -iminoester. This

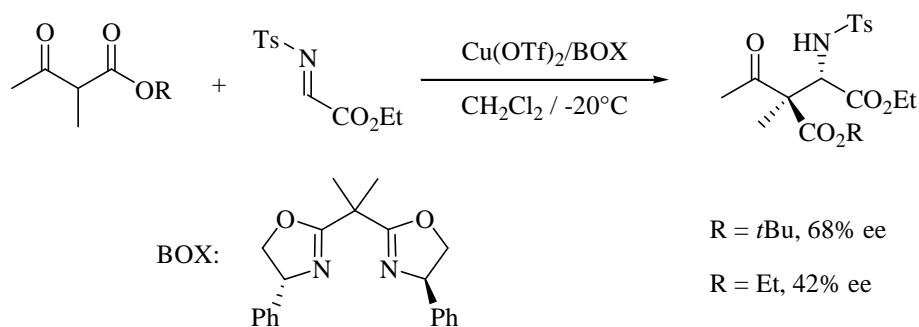
<sup>13</sup> a) S. Kobayashi, H. Ishitani, *Chem. Rev.* **1999**, 99, 1069; b) A. Córdova, *Acc. Chem. Res.* **2004**, 37, 102.

<sup>14</sup> a) E. F. Kleinmann, In *Comprehensive Organic Synthesis*, Eds: B. M. Trost, I. Fleming, Pergamon Press: New York, **1991**, Vol. 2, chap. 4.1; b) M. Arend, B. Westermann, N. Risch, *Angew. Chem. Int. Ed.* **1998**, 37, 1044; *Angew. Chem.* **1998**, 110, 1096; c) S. Denmark, O. J.-C. Nicaise, In *Comprehensive Asymmetric Catalysis*, Eds.: E. N. Jacobsen, A. Pfaltz, H. Yamamoto, Springer: Berlin, **1999**, Vol. 2, 93.

<sup>15</sup> H. Ishitani, M. Ueno, S. Kobayashi, *J. Am. Chem. Soc.* **1997**, 119, 7153.

<sup>16</sup> K. Juhl, N. Gathergood, K. A. Jørgensen, *Angew. Chem. Int. Ed.* **2001**, 40, 2995; *Angew. Chem.* **2001**, 113, 3083.

new chiral Lewis acid-catalysed reaction is an easy entry to the formation of chiral quaternary carbon centres. Moreover the utility of this catalysis could be enhanced by the development of a diastereoselective decarboxylation reaction of the Mannich adducts providing an attractive approach to optically active  $\gamma$ -keto  $\alpha$ -amino acid derivatives. The direct asymmetric Mannich reaction of  $\beta$ -ketoesters with an activated *N*-tosyl  $\alpha$ -iminoester described by Jørgensen *et al.* is depicted in Scheme 4.2.4.<sup>17</sup>



**Scheme 4.2.4:** Diastereo- and enantioselective direct Mannich reaction of  $\beta$ -ketoesters with  $\alpha$ -iminoesters catalysed by a chiral Lewis acid

It was found that the size of the alkoxy moiety of the  $\beta$ -ketoesters is critical. In order to obtain high enantioselectivities, the *tert*-butyl ester moiety was required, while the corresponding ethyl esters gave only low to moderate selectivities of 22–42% in the presence of 10 mol% of [Cu(Ph-BOX)](OTf)<sub>2</sub>. It was therefore interesting to choose the latter nucleophile for the Mannich reaction catalysed by [Cu(trisox)]<sup>2+</sup>, to try to optimise the reaction conditions and to find out whether high selectivities with this less selective substrate could be obtained.

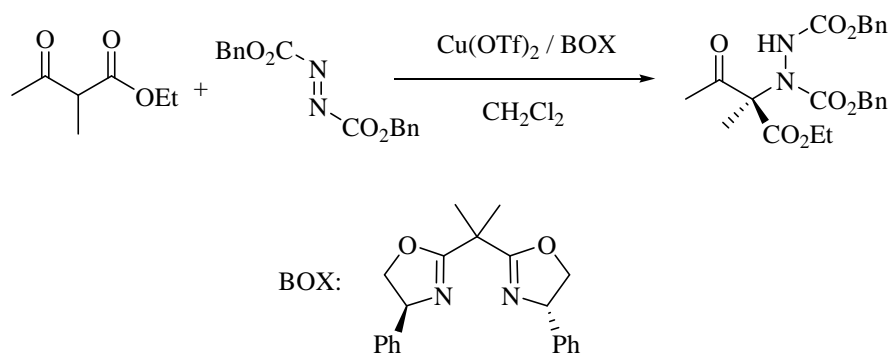
#### b. $\alpha$ -amination reaction

As a second model reaction the direct  $\alpha$ -amination of  $\alpha$ -substituted  $\beta$ -ketoesters with azodicarboxylates which forms enantioselectively carbon-nitrogen bonds has been chosen. This reaction is of interest for the synthesis of  $\beta$ -hydroxy- $\alpha$ -amino acids such as oxazolidinone derivatives, and is a simple procedure for the formation of an asymmetric carbon centre attached to a nitrogen atom.<sup>18</sup> An efficient bisoxazoline/copper(II) catalysed version has been reported recently by Jørgensen and coworkers. They disclosed the first direct  $\alpha$ -amination of  $\beta$ -ketoesters

<sup>17</sup> M. Marigo, A. Kjærsgaard, K. Juhl, N. Gathergood, K. A. Jørgensen, *Chem. Eur. J.* **2003**, *9*, 2359. This type of reaction was first developed by: D. A. Evans, S. G. Nelson, *J. Am. Chem. Soc.* **1997**, *119*, 6452.

<sup>18</sup> For a review on asymmetric  $\alpha$ -amination reactions see: J.-P. Genet, C. Greck, D. Lavergne, In *Modern Amination Methods*, Ed: A. Ricci, Wiley-VCH: Weinheim, **2000**, chap. 3.

catalysed by a chiral Lewis acid complex with azodicarboxylate derivatives as nitrogen fragment source (Scheme 4.2.5).<sup>19</sup>



**Scheme 4.2.5:** Enantioselective direct  $\alpha$ -amination of ethyl 2-methylacetoacetate with dibenzyl azodicarboxylate catalysed by  $[\text{Cu}(\text{Ph-BOX})](\text{OTf})_2$

High yields and excellent enantioselectivities were observed using 2,2-bis[(4*S*)-4-phenyloxazolin-2-yl]propane (Ph-BOX) as ancillary ligand. Originally performed in the presence of 10 mol% of catalyst, they observed that the reaction proceeds with catalyst loadings of 0.2 - 1 mol% without loss in selectivity (Table 4.2.1). However further reduction of the catalyst loading led to a significant drop in the stereoselectivity of the transformation.

Catalyst loading (mol%)	Yield (%)	ee (%)
10	98	98
1	92	98
0.5	91	96
0.2	91	96
0.05	65	55

**Table 4.2.1:** Variation of the catalyst loadings in the enantioselective direct  $\alpha$ -amination of ethyl 2-methylacetoacetate with dibenzyl azodicarboxylate

### 3. Influence of the third oxazoline unit on the catalyst loading

#### a. Reaction conditions

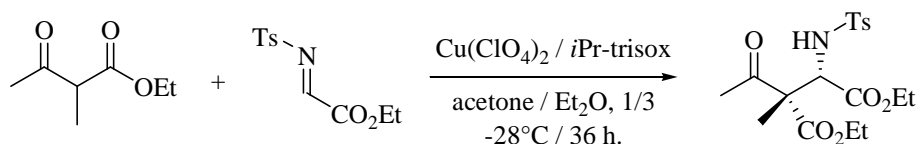
The  $[\text{Cu}(\text{triso})]^{2+}$  precursors have been efficiently prepared *in situ* by reacting the desired copper(II) salt with the trisoxazoline ligand in the organic solvent chosen for the catalysis. The reactions do not require any special precautions and have been carried out in air illustrating the practical applicability of the process.

<sup>19</sup> M. Marigo, K. Juhl, K. A. Jørgensen, *Angew. Chem. Int. Ed.* **2003**, 42, 1367, *Angew. Chem.* **2003**, 115, 1405.

The different solutions containing the catalyst precursors with variable catalyst loadings have been prepared from a mother solution and the same procedure was followed for the Mannich reaction and for the  $\alpha$ -amination reaction. The homogeneous stock solutions containing the copper(II) salt and the desired ligand have been stirred under air for 30 min. Successive aliquots have been then taken to obtain the desired catalyst loading for each run.

b. Trisoxazolines in the asymmetric Mannich reaction

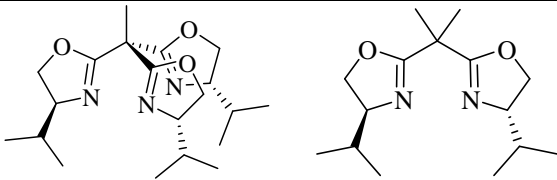
The Mannich reaction of ethyl 2-methylacetoacetate with an activated *N*-tosyl  $\alpha$ -imino ester was first investigated. After optimization of the reaction conditions, the Mannich reaction catalysed by the  $[\text{Cu}(i\text{Pr-trisox})]^{2+}$  catalyst afforded high activity and selectivity. The best catalyst efficiency has been found using the copper(II) perchlorate salt in a 1/3 mixture of acetone and diethyl ether at  $-28^\circ\text{C}$  (Scheme 4.2.6).



**Scheme 4.2.6:** Enantioselective Mannich reaction of ethyl 2-methylacetoacetate with *N*-tosyl  $\alpha$ -imino methyl ester catalysed by  $[\text{Cu}(i\text{Pr-trisox})](\text{ClO}_4)_2$

With a ligand/metal ratio of 1.5 and using 10 mol% of catalyst the reaction proceeds in good yield (84%). The diastereoselectivity, measured by HPLC, is at *ca.* syn/anti = 13/87. The  $[\text{Cu}(i\text{Pr-trisox})](\text{ClO}_4)_2$  precursor gives the reaction product with an excellent ee of 90% (enantiomeric excess of the major diastereomer).

Using the reaction conditions described above, the evolution of the catalytic efficiency when decreasing the catalyst loadings has been investigated. This study has been carried out in the presence of 10, 1, 0.1 and 0.01 mol% of  $[\text{Cu}(i\text{Pr-trisox})](\text{ClO}_4)_2$ . As a direct comparison the same stepwise reduction of the catalyst loading has been investigated in the presence of  $[\text{Cu}(i\text{Pr-BOX})](\text{ClO}_4)_2$ . The results are summarised in Table 4.2.2.

					
		<i>iPr-trisox</i>		<i>iPr-BOX</i>	
Catalyst loading (mol%)	Yield (%)	ee (%)	Yield (%)	ee (%)	
10	84	90	84	84	
1	75	89	70	84	
0.1	59	91	56	80	
0.01	36	90	35	66	

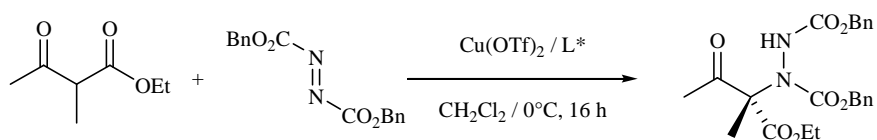
**Table 4.2.2:** Variation of the catalyst loadings in the enantioselective Mannich reaction of ethyl 2-methylacetoacetate with *N*-tosyl  $\alpha$ -imino methyl ester catalysed by [Cu(*iPr-trisox*)](ClO<sub>4</sub>)<sub>2</sub> and [Cu(*BOX*)](ClO<sub>4</sub>)<sub>2</sub>

Upon reduction of the catalyst loading by a factor of 10<sup>3</sup>, that is to say in the presence of only 0.01 mol% of catalyst, the enantioselectivity remains unchanged with the [Cu(*iPr-trisox*)](ClO<sub>4</sub>)<sub>2</sub> catalyst (90% ee). Throughout the dilution series, the diastereoselectivity remains constant. With the bisoxazoline ligand and in the presence of 10 mol% of catalyst, 84% ee (84% yield) is observed showing lower selectivity compared to the corresponding trisoxazoline-based system. For the *BOX*-based systems, reducing the catalyst loading leads to a decrease of the stereoselectivity. From 84% ee in the presence 10 and 1 mol% of catalyst loading the enantiomeric excess drops to 80% ee at catalyst concentration of 0.1 mol% and more dramatically to 66% ee at catalyst concentration of 0.01 mol%.

### c. Trisoxazolines in the asymmetric $\alpha$ -amination reaction

The  $\alpha$ -amination reaction of ethyl 2-methylacetoacetate with dibenzyl azodicarboxylate as nitrogen source has subsequently been the focus of our interest. Jørgensen and coworkers have shown that high yields and excellent enantioselectivities can be obtained in the presence of 10 mol% of [Cu(Ph-*BOX*)](OTf)<sub>2</sub> and that the reaction proceeds without loss in selectivity with a catalyst loading of 0.2 mol% (further decrease of the catalyst concentration induces lower selectivity, see Table 4.2.1). The concept of stereoelectronic hemilability of the divalent copper(II) has been tested by exploring this catalysis with the corresponding trisoxazoline ligand.

Influence of the variation of the catalyst loadings on the outcome of the reaction have been investigated for both [Cu(Ph-*BOX*)](OTf)<sub>2</sub> and [Cu(Ph-*trisox*)](OTf)<sub>2</sub> catalysts to make a direct comparison of the catalytic efficiencies. The reactions were carried out under air in dichloromethane at 0°C over 16 hours and with a ligand/metal ratio of 1.2 (Scheme 4.2.7).



**Scheme 4.2.7:** Enantioselective  $\alpha$ -amination reaction of ethyl 2-methylacetoacetate with dibenzyl azodicarboxylate catalysed by  $[\text{Cu}(\text{Ph-trisox})](\text{OTf})_2$  and  $[\text{Cu}(\text{Ph-BOX})](\text{OTf})_2$

Catalyst loadings going from 10 to 0.01 mol% have been surveyed during the course of the study and the activities and selectivities observed upon successive reduction of the catalyst loading are summarised in Table 4.2.3.

Ph-trisox		Ph-BOX		
Catalyst loading (mol%)	Yield (%)	ee (%)	Yield (%)	ee (%)
10	97	99	98	98
1	91	99	93	98
0.1	72	99	72	55
0.01	49	48	41	15

**Table 4.2.3:** Variation of the catalyst loading in the enantioselective  $\alpha$ -amination reaction of ethyl 2-methylacetoacetate with dibenzyl azodicarboxylate catalysed by  $[\text{Cu}(\text{Ph-trisox})](\text{OTf})_2$  and  $[\text{Cu}(\text{Ph-BOX})](\text{OTf})_2$

Using 10 mol% of the tripodal system  $[\text{Cu}(\text{Ph-trisox})](\text{OTf})_2$ , an enantiomeric excess of 99% is observed for the reaction of ethyl 2-methylacetoacetate with dibenzyl azodicarboxylate and the product is obtained with 97% yield. Decreasing the amount of catalyst to 0.1 mol% affects moderately the yield and does not affect the enantioselectivity. However, further reduction of the catalyst loading by a factor of 10 leads to a significant decrease in enantioselectivity for this reaction. Concerning the bisoxazoline-based catalyst for 10 and 1 mol% catalyst loading the system displays the same activity and selectivity as the one of the corresponding tridentate ligand. Nevertheless, already with 0.1 mol% of catalyst a decrease in both activity and stereoselectivity is observed. More dramatic is the drop of the selectivity when the reaction is carried out with 0.01 mol% of catalyst.

Comparing the outcome of both Mannich reaction and  $\alpha$ -amination reaction after variation of the catalyst loadings indicates that the difference between tridentate- and bidentate-based catalysts is less significant in the latter reaction. The influence of the third oxazoline donor is less pronounced in the  $\alpha$ -amination reaction.



d. The active catalyst: bidentate coordination mode of the trisoxazoline

A considerable number of copper complexes bearing facially coordinated tripodal nitrogen donor ligands have been structurally characterized. Copper(II) complexes with facial coordination of  $C_{3v}$ -symmetrical tris(pyrazolyl)methane ligand<sup>20</sup> and tris(2-pyridyl)methane ligand<sup>21</sup> have been characterized by X-ray diffraction. However the opening up of these systems, as postulated for the transformation of the resting state into the active species, is rarely observed. Direct evidence for the assumption of a partially decoordinated trisoxazoline ligand in the active state of the catalyst has been obtained in our group by Guido Marconi. Crystallisation of the reaction intermediate which results from the reaction of a  $[\text{Cu}(\text{trisox})]^{2+}$  precursor with deprotonated ethyl 2-methylacetoacetate gave single crystals of  $[\text{Cu}(i\text{Pr-trisox})(\kappa^2\text{-}O,O'\text{-MeCOCHCOOEt})](\text{BF}_4)$  as well as of the analogous and isomorphous perchlorate salt. The molecular structure of the tetrafluoroborate salt in the solid state is depicted in Figure 4.2.3.

Two of the oxazoline groups of the *iPr*-trisox ligand are coordinated to the central copper atom whilst the third oxazoline unit is dangling with the nitrogen donor pointing away from the metal centre.<sup>22</sup> The geometry of the complex is square pyramidal with a fluorine atom of the  $\text{BF}_4$ -counterion occupying the apical position. The six-membered metallacycles formed by the copper centre and the deprotonated  $\beta$ -ketoester, and by the metal and the bisoxazoline unit lie within one molecular plane. There are two possibilities for the coordination of the substrate (ketone and the ester functionalities could bind in the opposite fashion), however, in the solid state only one diastereoisomer has been observed.

Given this arrangement of substrate and ligand as well as the coordination of the counterion, it appears likely that electrophilic attack on the metallated  $\beta$ -ketoester occurs on the face which is liberated by the decoordination of the hemilabile third oxazoline.<sup>17</sup> This would lead to products having the correct absolute stereochemistry, as observed in the Mannich addition. However, the substitutional lability of the copper(II) complexes, and thus the possibility of rapid equilibria, limits the usefulness of interpretations based on X-ray structural data.

---

<sup>20</sup> a) K. Fujisawa, T. Ono, H. Aoki, Y. Ishikawa, Y. Miyashita, K. Okamoto, H. Nakazawa, H. Higashimura, *Inorg. Chem. Commun.* **2004**, 7, 330; b) D. L. Reger, C. A. Little, M. D. Smith, G. J. Long, *Inorg. Chem.* **2002**, 41, 4453; c) D. Martini, M. Pelli, C. Pettinari, B. W. Skelton, A. H. White, *Inorg. Chim. Acta* **2002**, 333, 72.

<sup>21</sup> a) M. Kodera, Y. Tachi, T. Kita, H. Kobushi, Y. Sumi, K. Kano, M. Shiro, M. Koikawa, T. Tokii, M. Ohba, H. Okawa, *Inorg. Chem.* **2000**, 39, 226; b) M. Kodera, Y. Kajita, Y. Tachi, K. Kano, *Inorg. Chem.* **2003**, 42, 1193; c) P. J. Arnold, S. C. Davies, J. R. Dilworth, M. C. Durrant, D. V. Griffiths, D. L. Hughes, R. L. Richards, P. C. Sharpe, *Dalton Trans.* **2001**, 736; d) T. Astley, P. J. Ellis, H. C. Freeman, M. A. Hitchman, F. Richard Keene, E. R. T. Tiekink, *J. Chem. Soc., Dalton Trans.* **1995**, 595.

<sup>22</sup> In this copper(II) complex, the bidentate coordination mode of the trisoxazoline, with the nitrogen donor of the free unit pointing away from the metal centre, is similar to that of the ligand in palladium(II) and palladium(0) complexes (see chapter 3)

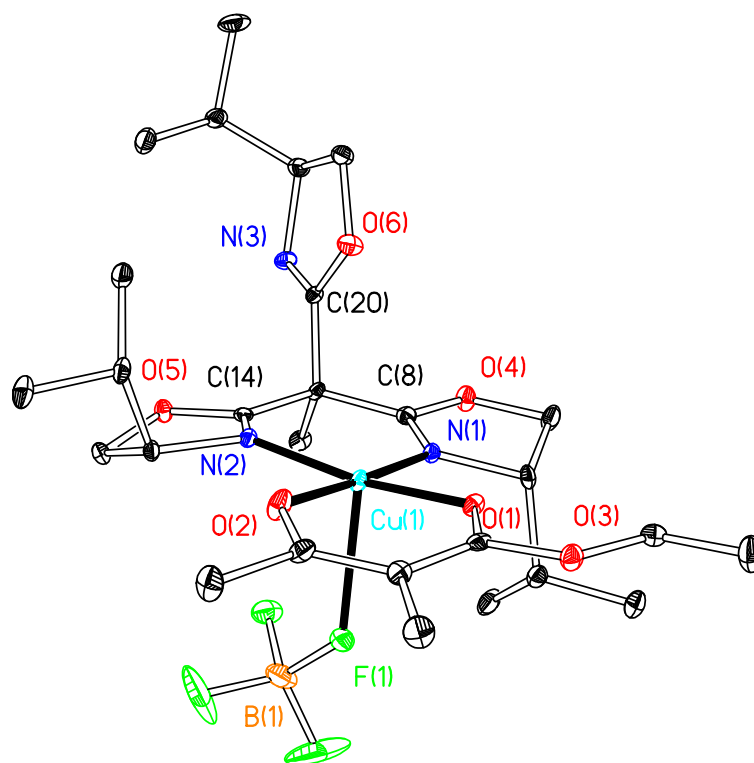


**Figure 4.2.3:** Thermal ellipsoid plot (25%) of  $[\text{Cu}(\text{iPr-trisox})(\kappa^2\text{-O},\text{O}'\text{-MeCOCHCOEt})](\text{BF}_4)$

#### 4. Conclusion

It has been shown that  $C_3$ -symmetric trisoxazolines form highly efficient enantioselective copper(II) Lewis acid catalysts which are based on the concept of a stereoelectronic hemilability of the divalent copper. The trisoxazoline, dynamically coordinated to the copper(II), is thought to stabilise the resting state by (weak) coordination of the third donor.<sup>23</sup> The opening-up of the system generates the 17 electron active species. In a direct comparison with the analogous bisoxazoline systems, the tripod/copper catalysts have proven to be more efficient in the enantioselective Mannich reaction as well as the enantioselective  $\alpha$ -amination of prochiral  $\beta$ -ketoesters.

### III. Stereochemical consequences of threefold symmetry

#### 1. Introduction: Inverting chiral centres in $C_2$ and $C_3$ symmetric stereodirecting ligands

In the last section we have seen that  $C_3$ -symmetric trisox ligands allow the reduction of the catalyst loading compared to  $C_2$ -symmetric BOX ligands but the enantioselectivity is not greatly influenced by the addition of the third dangling arm (for 10 and 1 mol% catalyst). This is

<sup>23</sup> Stereochemical models are based on this concept. See for example: a) M.-C. Ye, J. Zhou, Y. Tang, *J. Org. Chem.* **2006**, *71*, 3576; b) R. Rasappan, M. Hager, A. Gissibl, O. Reiser, *Org. Lett.* **2006**, *8*, 6099.

expected by considering the proposed model of the active species based on a partially decoordinated tripod. At first sight one could conclude that  $C_3$ -symmetric trisox behave as a  $C_2$ -symmetric bisoxazoline in terms of enantioselectivity. However, from the point of view of ligand design there is a remarkable difference between  $C_2$ - and  $C_3$ -chiral podands which becomes apparent when one chiral element (*e.g.* a chiral centre) out of  $n$  ( $n = 2,3$  respectively) is inverted, while leaving all other structural features unchanged. The rotational symmetry is thus destroyed: whereas the inversion of a chiral centre in a  $C_2$ -symmetrical chelate ligand will generate a *meso*-structure, *i.e.* an achiral ligand possessing mirror symmetry ( $C_s$ ), the same process carried out for one of the three ligand arms of a  $C_3$ -chiral tripod will leave the system chiral and  $C_1$ -symmetrical (Figure 4.3.1).

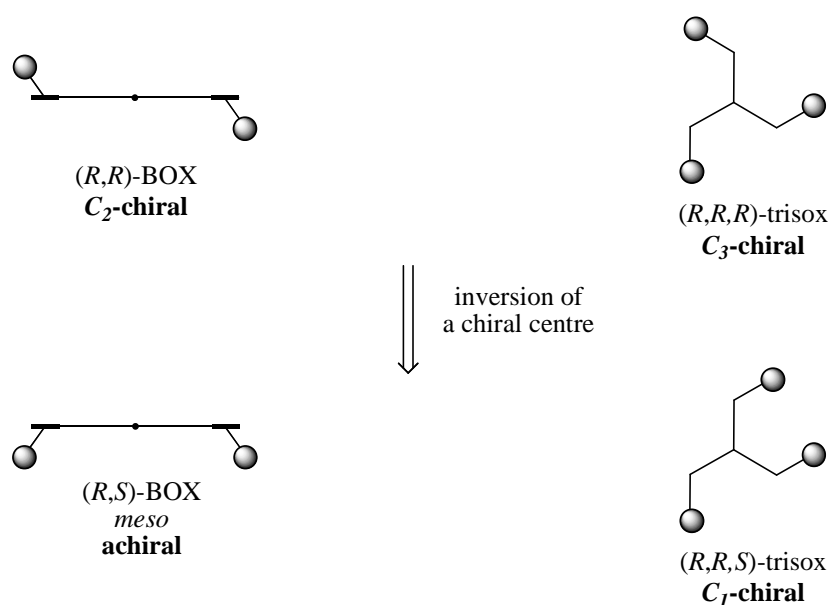


**Figure 4.3.1:** Transformation of a  $C_2$ -chiral chelate (left) and a  $C_3$ -chiral podand (right) upon inversion of the configuration at a chiral ligand arm

The modular nature of BOX and trisox ligands allows for a systematic investigation of the implications that such an inversion has on the stereoselective outcome of the catalysis. The ligands employed in this work are represented in Figure 4.3.2.

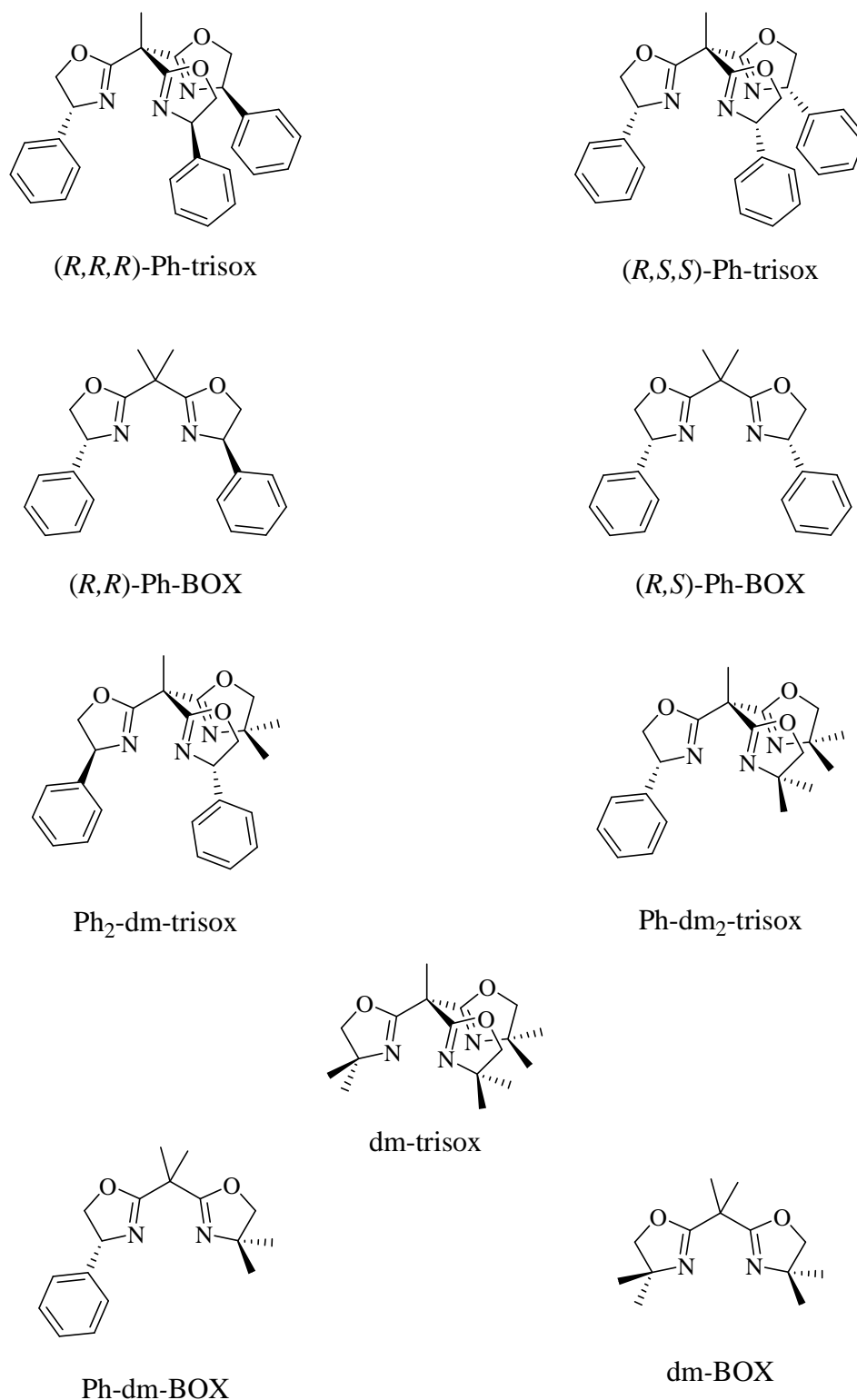


**Figure 4.3.2:** Overview of the bis- and trisoxazoline ligands employed in this study

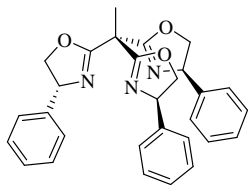
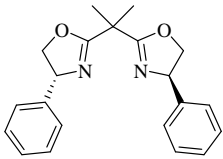
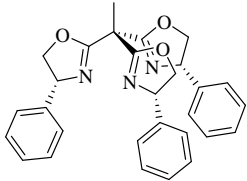
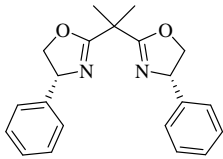
The effect on the catalytic performance is investigated by direct comparison of  $C_3$ -symmetrical (*R,R,R*)-Ph-trisox with  $C_1$ -symmetrical (*R,S,S*)-Ph-trisox and the pair of bisoxazoline ligands (*R,R*)-Ph-BOX and (*R,S*)-Ph-BOX. In addition, the combination of chiral and achiral podand arms has been investigated in a comparative study of Ph<sub>2</sub>-dm-trisox and Ph-

dm<sub>2</sub>-trisox with the bidentate Ph-dm-BOX, the latter representing a *minimal structure* in asymmetric oxazoline/copper(II) catalysis. The  $\alpha$ -amination of a  $\beta$ -ketoester by dibenzyl azodicarboxylate previously developed has been chosen as test reaction for this study.

## 2. Effect of the inversion of one of the chiral centres in BOX and trisox ligands

### a. Catalytic $\alpha$ -amination of ethyl 2-methylacetoacetate

The test reaction introduced above has been carried out using (*R,R,R*)-Ph-trisox and (*R,S,S*)-Ph-trisox as stereodirecting podands as well as the bisoxazolines (*R,R*)-Ph-BOX and (*R,S*)-Ph-BOX. The results of the catalytic runs performed with 1 mol% of catalyst are summarised in Table 4.3.1.

				
	( <i>R,R,R</i> )-Ph-trisox	( <i>R,R</i> )-Ph-BOX	( <i>R,S,S</i> )-Ph-trisox	( <i>R,S</i> )-Ph-BOX
ee (%)	99	98	-41	0
Yield (%)	91	93	94	88

**Table 4.3.1:**  $\alpha$ -amination of ethyl 2-methylacetoacetate with dibenzyl azodicarboxylate with 1 mol% of catalyst

The selectivity of the transformation catalysed by copper(II) complexes of (*R,R,R*)-Ph-trisox and the chelating (*R,R*)-Ph-BOX is almost identical. This is as expected based on the proposed model of the active catalyst that contains a partially decoordinated podand. In it, the dangling oxazoline ring adopts a remote orientation (see next part), and the trisox system therefore effectively coordinates like the corresponding bisoxazoline. Whereas the use of the *meso*-BOX ligand (*R,S*)-Ph-BOX leads to a racemic product, the catalyst formed with the stereochemically mixed *C*<sub>1</sub>-symmetrical (*R,S,S*)-Ph-trisox gives the reaction product with -41% ee. In this case a closer look at the real active species is required.

b. Active species and consideration of “first coordination sphere” symmetry

In the case of the  $C_1$ -chiral ( $R,S,S$ )-Ph-trisox, the interplay of three isomeric forms of dicoordinated trisox has to be considered, all three being catalytically active. These three diastereomeric catalysts, which are thought to be involved, are depicted in Figure 4.3.3.

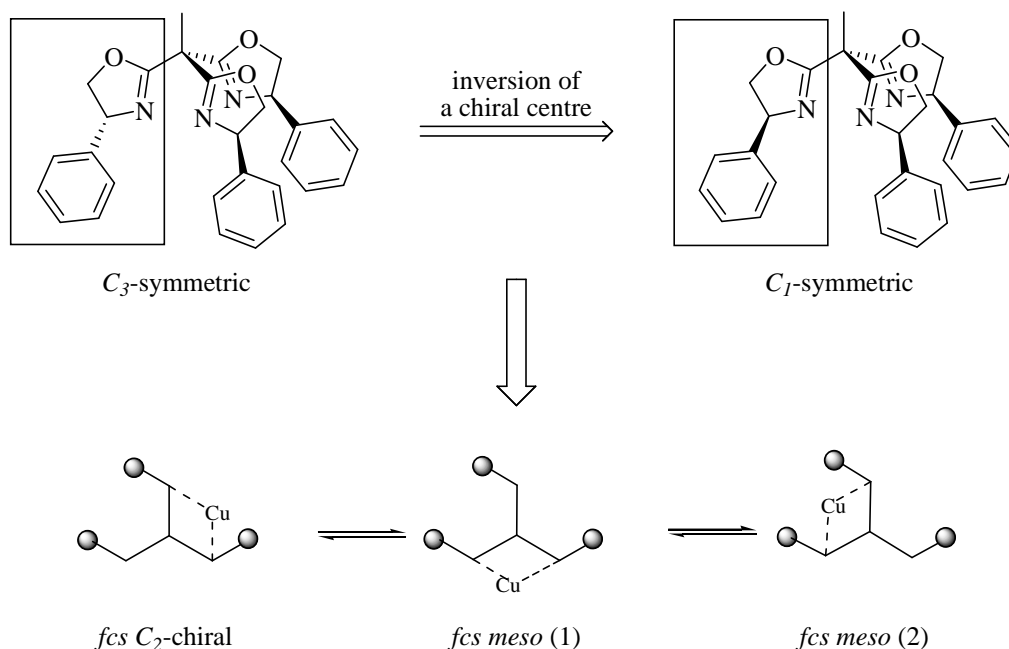


**Figure 4.3.3:** Effect of the inversion of a chiral centre in Ph-trisox (top) leading to an equilibrium between three diastereoisomeric active species in solution (bottom)

The local environment (*i.e.* the arrangement of the coordinated oxazoline rings) at the metal centre is the most important parameter in the discussion of the effect, which the formal inversion of one of the chiral centres in ( $R,S,S$ )-Ph-trisox has on the catalyst system. As is readily apparent, only one of the three isomers expected to be in equilibrium with each other, contains the metal centre in an essentially  $C_2$ -chiral BOX-like environment to be found for the three symmetry-equivalent species of the catalyst derived from the  $C_3$ -symmetrical derivative ( $R,R,R$ )-Ph-trisox. This local molecular shape and, specifically, the effective local symmetry of a coordinated ligand at a metal centre will be designated as first coordination sphere symmetry (**fcs** symmetry) and will play a key role in the following discussions.<sup>24</sup> The other two isomeric forms have a *fcs meso*-arrangement of the oxazoline substituents. Given the orientation and distance of the dangling ligand arm (see Figures 4.2.3 and 4.3.4), the catalytic behaviour of the latter two

<sup>24</sup> The term first coordination sphere (fcs) symmetry is introduced to designate the effective local symmetry of a coordinated ligand at a metal centre. This is meant to avoid confusion with the stereochemical term “local symmetry”, for which Mislow and Siegel have given a strict definition with reference to the symmetry of the whole molecule: K. Mislow, J. Siegel, *J. Am. Chem. Soc.* **1984**, *106*, 3319.

forms should be similar to that of the complex bearing the achiral ligand (*R,S*)-Ph-BOX. This line of argument is supported by structural data obtained for intermediates of the catalytic cycle with both the  $C_3$ - (see Chapter 4, II.3) and the  $C_1$ -chiral tripods. The crystal structure of the latter is discussed in the following part.

c. Crystal structure of a copper(II) complex with  $C_1$ -chiral (*R,S,S*)-Ph-trisox

The crystal structure of  $[\text{Cu}^{\text{II}}(\textit{iPr}\text{-trisox})(\kappa^2\text{-}O,O'\text{-MeCOCHCOOEt})]^+(\text{BF}_4^-)$  is depicted in figure 4.2.3. From the structure it is clear that the third oxazoline ring will have little influence upon the attack of an electrophile on the acylenolate (expected to approach from the left) and that the complex may therefore be effectively treated as a (substituted) bisoxazoline/Cu derivative.

It has also been possible to crystallise the stereochemically mixed  $C_1$ -trisox complex  $[\text{Cu}^{\text{II}}\{(\textit{R,S,S})\text{-Ph-trisox}\}(\kappa^2\text{-}O,O'\text{-MeCOCHCOOEt})(\text{H}_2\text{O})]^+(\text{ClO}_4^-)$  by a similar reaction of (*R,S,S*)-Ph-trisox/Cu with the deprotonated  $\beta$ -ketoester. The X-ray structure of this complex is depicted in figure 4.3.4 along with selected bond lengths and angles in Table 4.3.2.

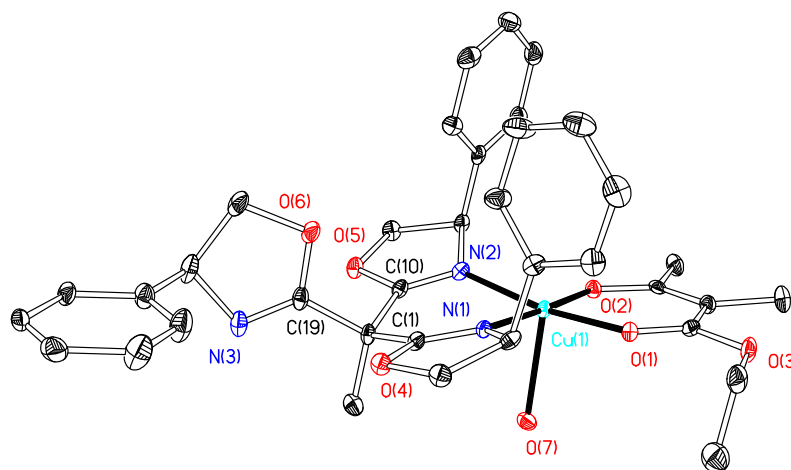


**Figure 4.3.4:** Thermal ellipsoid plot (25%) of  $[\text{Cu}^{\text{II}}\{(\textit{R,S,S})\text{-Ph-trisox}\}(\kappa^2\text{-}O,O'\text{-MeCOCHCOOEt})(\text{H}_2\text{O})]^+(\text{ClO}_4^-)$ . The counter-anion is omitted for clarity

Cu(1)-N(1)	1.973(4)	Cu(1)-N(2)	1.990(4)
Cu(1)-O(1)	1.921(4)	Cu(1)-O(2)	1.886(3)
Cu(1)-O(7)	2.293(4)		
N(1)-Cu(1)-N(2)	87.42(16)	N(1)-Cu(1)-O(2)	177.36(16)
N(1)-Cu(1)-O(1)	90.92(16)	N(2)-Cu(1)-O(1)	169.48(17)
N(2)-Cu(1)-O(2)	90.12(16)	O(1)-Cu(1)-O(2)	91.33(16)

**Table 4.3.2:** Selected bond lengths (Å) and angles (°) for complex of  $[\text{Cu}^{\text{II}}\{(\textit{R,S,S})\text{-Ph-trisox}\}(\kappa^2\text{-}O,O'\text{-MeCOCHCOOEt})(\text{H}_2\text{O})]^+(\text{ClO}_4^-)$

In this acylenolate complex, the trisox ligand adopts a bidentate coordination [Cu-N bonds lengths: 1.976(3) and 1.990(4) Å], the third oxazoline unit pointing away from the coordinated oxazoline rings and thus also generating an effective bisoxazoline/copper system. Similar to complex with the  $C_3$ -symmetric *i*Pr-trisox, the coordination geometry is square pyramidal with an oxygen atom of a water molecule occupying the apical position [Cu(1)-O(7) 2.293(4) Å].

As already discussed above, three stereochemically distinct ways of coordination of the trisox ligand are to be expected: one leading to an *fcc*  $C_2$ -symmetric species and two representing *fcc* achiral *meso* species (Figure 4.3.3). One of the two diastereomeric species with an *fcc meso* arrangement of the coordinated bisoxazoline unit crystallised, the one with the phenyl substituents of the coordinated oxazoline units located on the same side as the dangling free oxazoline ring.

d. A steady state kinetic model for the behaviour of the stereochemically mixed (*R,S,S*)-Ph-trisox/copper catalyst

In order to understand the observed enantiomeric excess for the catalytic  $\alpha$ -amination of ethyl 2-methylacetoacetate of 41%, the ratio of the three isomeric active species as well as their relative catalytic activity needs to be established. For this purpose a kinetic study was carried out using the different catalysts bearing (*R,R,R*)-Ph-trisox, (*R,S,S*)-Ph-trisox as well as (*R,R*)-Ph-BOX and (*R,S*)-Ph-BOX as stereodirecting ligands. The conversion curves under the standard catalytic conditions of 1 mol% of catalyst loading for the four catalysts are depicted in Figure 4.3.5.



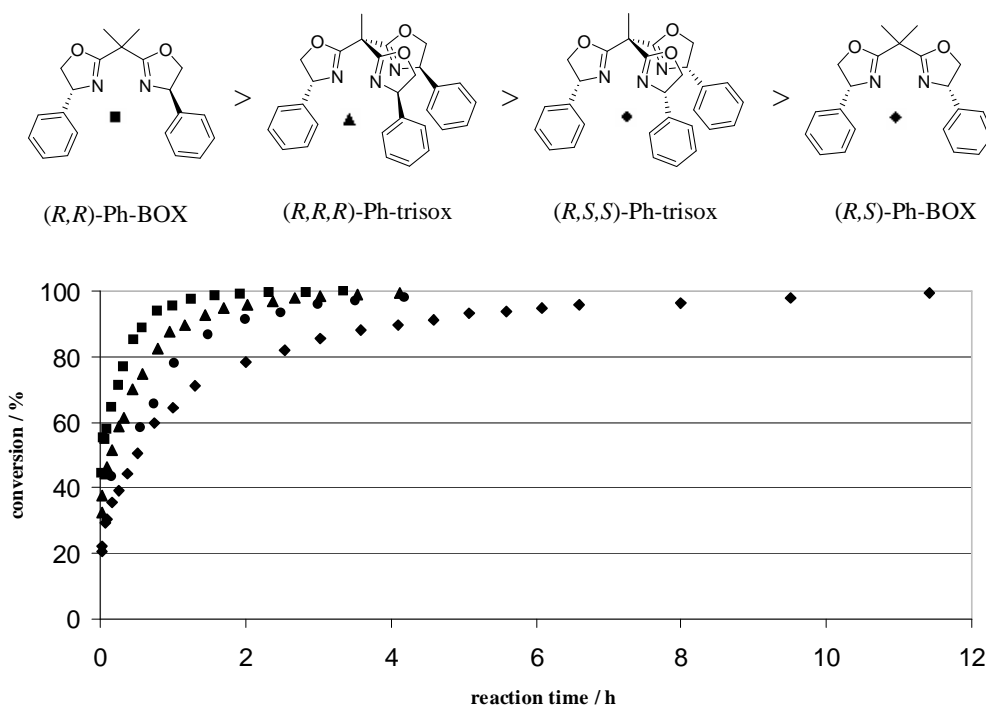


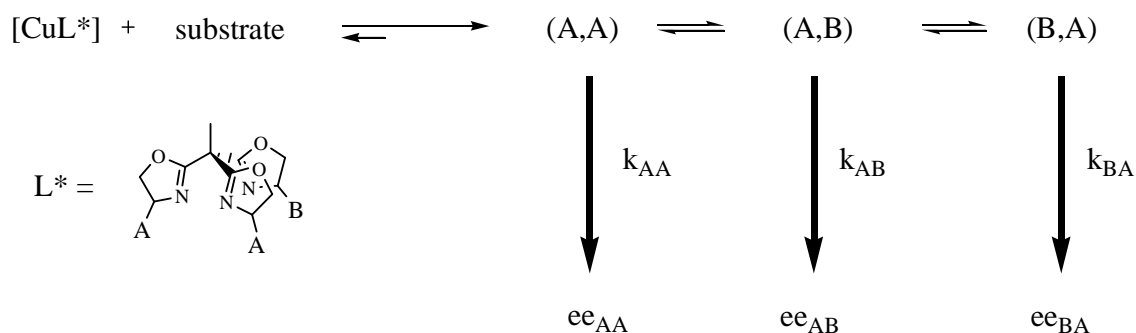
**Figure 4.3.5:** Conversion curves of the Cu-catalyzed  $\alpha$ -amination (1 mol% of catalyst loading) for the four catalysts bearing (R,R,R)-Ph-trisox, (R,S,S)-Ph-trisox as well as (R,R)-Ph-BOX and (R,S)-Ph-BOX

Whereas the (R,R)-Ph-BOX derivative displays the highest activity (first order rate constant derived from an exponential fitting analysis of the conversion curve:  $k_{RR} = 2.484 \text{ h}^{-1}$ ), the corresponding *meso*-system (R,S)-Ph-BOX proved to be the least active catalyst ( $k_{RS} = 0.756 \text{ h}^{-1}$ ). Since it is thought that the stereodirecting ligand in the active trisox/copper catalyst acts as a bidentate ligand and thus effectively corresponds to the BOX analogues, the behaviour of both the homo and heterochiral systems should be explicable in reasonable approximation using the kinetic data: The copper(II) catalyst bearing the  $C_3$ -chiral trisox ligand (R,R,R)-Ph-trisox possesses an activity ( $k_{RRR} = 1.638 \text{ h}^{-1}$ ) which is close to that of the  $C_2$ -chiral bisoxazoline whilst the activity of the catalytic system based on the heterochiral tripod lies between this value and the conversion rate of the *meso*-BOX catalyst ( $k_{RSS} = 1.074 \text{ h}^{-1}$ ). The latter may indeed be an indication that both the *fac*  $C_2$ -symmetric chiral isomer as well as the two *meso* forms may play a role in the transformation catalyzed by (R,S,S)-Ph-trisox/copper.

The behaviour of the “desymmetrised” trisox/Cu catalysts may be rationalised in terms of a general steady state kinetic model for the three possible active bisoxazoline-copper species which are expected to be in rapid exchange with each other in solution. This assumption is based on the well established substitutional lability of divalent copper complexes.

*General model for the catalysis with  $C_1$ -symmetric chiral tripods*

Given is a trisoxazoline in which two of the heterocycles bear a substituent A whilst the third substituent, B, is assumed to be different. This leads to three dicoordinate species in solution, in which the copper atom is either coordinated by two equally substituted oxazoline rings (A,A) or by a non-equal combination, (A,B) or (B,A). The two latter are diastereomers, however, since they differ only in terms of the orientation of the third, dangling oxazoline ring which is pointing away from the active centre, they may be assumed in reasonable approximation to be equivalent (both in terms of activity and stability). All three catalyst isomers will transform the substrate to a given product P with enantioselectivities of  $ee_{AA}$ ,  $ee_{AB}$  and  $ee_{BA}$  ( $ee_{AB} \approx ee_{BA}$ ) as shown in Scheme 4.3.1.



**Scheme 4.3.1:** Model scheme describing the behaviour of a  $C_1$ -symmetric trisox ligand in copper catalysis

Designating two enantiomers of the product as  $P_R$  and  $P_S$ , it is possible to express the rate of formation of these two products as a function of the different rate constants, selectivities and the proportions  $x_R$  and  $x_S$  of (A,A) that give respectively  $P_R$  or  $P_S$  as well as the proportions  $x_R'$  and  $x_S'$  of (A,B) and (B,A) that give respectively  $P_R$  or  $P_S$ , with  $P_R$  being assumed to be the major product:

$$\frac{dP_R}{dt} = x_R k_{AA} [(A, A)] + 2 x_R' k_{AB} [(A, B)]$$

$$\frac{dP_S}{dt} = x_S k_{AA} [(A, A)] + 2 x_S' k_{AB} [(A, B)]$$

In this simplified form, the properties of (A,B) and (B,A) are treated as equal. In that case, the ratio of the two rates of formation is:

$$\frac{dP_R}{dP_S} = \frac{(x_R k_{AA} [(A, A)] + 2 \cdot x_R' k_{AB} [(A, B)])}{(x_S k_{AA} [(A, A)] + 2 \cdot x_S' k_{AB} [(A, B)])}$$

Knowing that

and that

$$\begin{array}{ll} ee_{AA} = x_R - x_S & ee_{AB} = x_{R'} - x_{S'} \\ x_R + x_S = 1 & x_{R'} + x_{S'} = 1 \end{array}$$

the four proportions  $x_R$ ,  $x_S$ ,  $x_{R'}$  and  $x_{S'}$  can be expressed in terms of partial enantiomeric excesses ( $ee_{AA}$  and  $ee_{AB}$ ):

$$x_R = \frac{(1 + ee_{AA})}{2} \quad x_S = \frac{(1 - ee_{AA})}{2} \quad x_{R'} = \frac{(1 + ee_{AB})}{2} \quad x_{S'} = \frac{(1 - ee_{AB})}{2}$$

The composition of the total amount of catalytically active species is as follow:<sup>25</sup>

$$C_{(cat)} = [(A, A)] + 2[(A, B)]$$

Assuming steady state conditions gives the following expression for the observed ee-values:

$$ee = \frac{(k_{AA} [C_{cat} - 2 \cdot [(A, B)]] ee_{AA} + 2 \cdot k_{AB} ee_{AB} [(A, B)])}{(k_{AA} [C_{cat} - 2 \cdot [(A, B)]] + 2 \cdot k_{AB} [(A, B)])} \quad (eq.1)$$

This general equation could be applied to the different  $C_1$ -symmetric chiral trisoxazolines.

#### Application to the (R,S,S)-Ph-trisox/copper system

In the case of the (R,S,S)-Ph-trisox ligand, the “hetero-substituent” B is an stereochemically inverted A, *i.e.* B = -A (B = S, A = R) and the two species (A,B) and (B,A) possess the two *meso*-configurations. Consequently  $ee_{A,-A} \approx ee_{-A,A} \approx 0$ , which gives the simplified expression:

$$ee = \frac{(k_{AA} [C_{cat} - 2 \cdot [(A, -A)]] ee_{AA})}{(k_{AA} [C_{cat} - 2 \cdot [(A, -A)]] + 2 \cdot k_{A-A} [(A, -A)])} \quad (eq.2)$$

In order to apply this equation, the pseudo first order rate constants derived from the conversion curves discussed above for the different BOX and trisox copper systems may be employed. It is assumed that the (A,-A) and (-A,A) active species from the trisox-based catalyst have approximately the same activity as the *meso*-(A,-A)-BOX/Cu catalyst and that the (A,A) active (trisox-derived) species has the same activity as the (A,A)-BOX/Cu catalyst. Assuming furthermore, that the *meso* and  $C_2$ -symmetric active species give the same enantioselectivities as their corresponding BOX/copper catalysts, as implied by the data reported in the previous section, the relative concentrations and activities of the components of the (R,S,S)-Ph-trisox/copper may be estimated.

<sup>25</sup> To write this equation, the quantity of complex  $[CuL^*]^{2+}$  is assumed to be negligible; *i.e.* the equilibrium is shifted to the right (see Scheme 4.3.1).

In a first step the concentration of the *meso*-species, [(R,S)] is calculated by re-arranging equation 2:

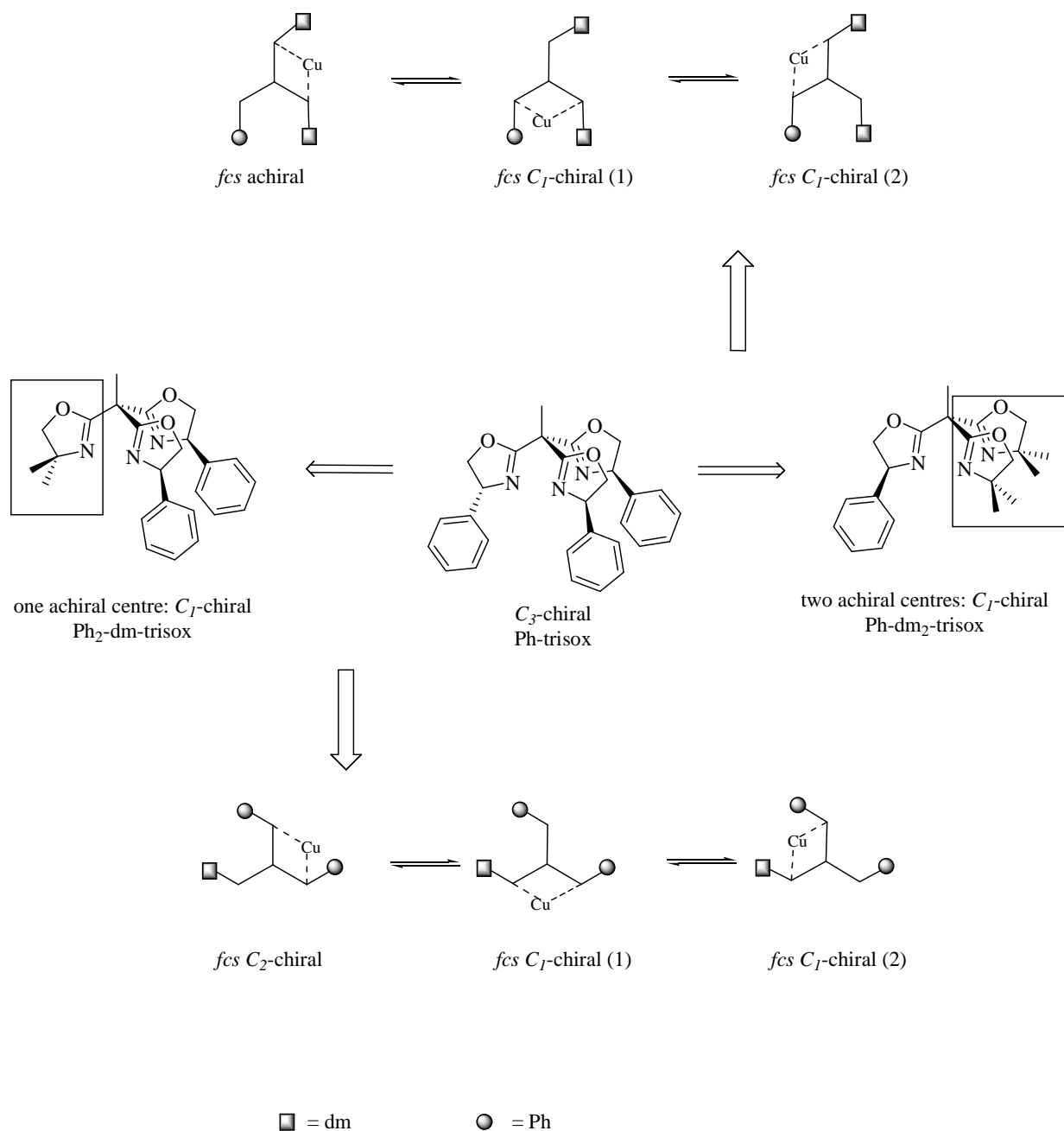
$$[(A, -A)] = \frac{1}{2} \frac{(k_{AA}(ee_{AA} - ee))}{(ee \cdot k_{A-A} + k_{AA}(ee_{AA} - ee))} C_{cat} \quad (eq.3)$$

Using the experimental value of  $ee = 41 \pm 1 \%$  and the catalyst concentration  $C_{cat}$  of 1.5  $\mu\text{mol/L}$  in equation 3 (as well as  $k_{A-A} = k_{RS} = 0.756$ ,  $k_{AA} = k_{RR} = 2.484 \text{ h}^{-1}$  and  $ee_{AA} = ee_{RR} = 0.98$  derived from the two BOX-systems) gives a concentration of  $0.615 \pm 0.005 \mu\text{mol/L}$  for each *meso* diastereomer (R,S) and (S,R) of the (R,S,S)-Ph-trisox-Cu catalyst and of  $0.270 \pm 0.005 \mu\text{mol/L}$  for the  $C_2$ -symmetric active species (S,S). This shows that the amount of each *meso* species is significantly greater than the proportion of the  $C_2$ -symmetric species and that the former therefore possesses slightly greater stability ( $\Delta G < 1 \text{ kcal.mol}^{-1}$ ). The greater amount of the *meso* isomers in the equilibrium of exchanging species could explain the observed preferred crystallisation of a catalyst-substrate intermediate with the (R,S,S)-Ph-trisox in which the two oxazoline units adopt a heterochiral relationship as demonstrated above. The domination of the *fcc meso* active species also explains the magnitude of the pseudo-first order rate constant found for the  $C_1$ -symmetric tripod. This is closer to that observed for the (R,S)-Ph-BOX-Cu than to the one of the  $C_2$ -symmetric bisoxazoline ( $k_{RSS} = 1.074$ ,  $k_{RS} = 0.756$  and  $k_{RR} = 2.484 \text{ h}^{-1}$ ).

### 3. Effect of the combination of chiral and achiral oxazolines in $C_1$ -symmetric tripods

#### a. Desymmetrisation of $C_3$ -symmetric trisox and dicoordinate isomers generated

The inversion of one chiral centre in a  $C_3$ -chiral tripod is one way of systematically distorting such a threefold symmetric species with the consequences for copper(II) Lewis acid catalysis discussed above. Another such operation is the successive replacement of chirally substituted oxazoline rings in a trisox system by achiral oxazolines. This transformation of the threefold symmetric chiral ligand Ph-trisox is schematically represented in Figure 4.3.6. Exchanging one 4-phenyloxazolin-2-yl unit by a 4,4'-dimethyloxazolin-2-yl unit results in the non-symmetrical tripod Ph<sub>2</sub>-dm-trisox and upon a similar replacement of a second oxazolinyl ring one arrives at Ph-dm<sub>2</sub>-trisox.

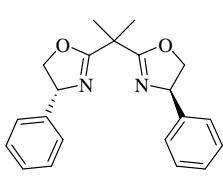
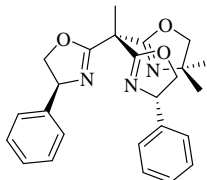
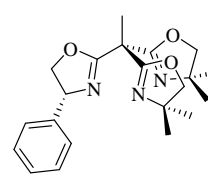
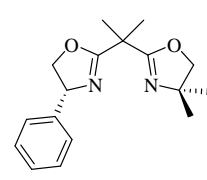


**Figure 4.3.6:** Successive replacement of chiral oxazoline units in a trisox system by achiral oxazoline rings (dm =dimethyl)

Figure 4.3.6 also shows the expected equilibria between the three diastereomeric dicoordinate copper(II) complexes which have different sets of *fcs* symmetries for the two non-symmetrical tripodal ligands. Whilst the Ph<sub>2</sub>-dm-trisox/copper system is composed of one isomer with *fcs* C<sub>2</sub> symmetry and two which are *fcs* chiral but unsymmetrical, the proposed equilibrium of the catalytic species derived from Ph-dm<sub>2</sub>-trisox comprises one *fcs* achiral and two unsymmetrical chiral species.

b. Catalytic  $\alpha$ -amination of ethyl 2-methylacetoacetate with the stereochemically “mixed” trisox/copper catalysts

The results of the  $\alpha$ -amination of ethyl 2-methylacetoacetate with dibenzyl azodicarboxylate with 1 mol% of catalyst using the copper(II) complexes of (*R,R*)-Ph-BOX, Ph<sub>2</sub>-dm-trisox, Ph-dm<sub>2</sub>-trisox as well as Ph-dm-BOX are summarized in Table 4.3.3.

				
	( <i>R,R</i> )-Ph-BOX	Ph <sub>2</sub> -dm-trisox	Ph-dm <sub>2</sub> -trisox	Ph-dm-BOX
ee (%)	98	-97	82	83
Yield (%)	93	90	73	85

**Table 4.3.3:**  $\alpha$ -amination of ethyl 2-methylacetoacetate with dibenzyl azodicarboxylate using 1 mol% of catalyst

It is notable that the replacement of one 4-phenyloxazolin-2-yl by a 4,4'-dimethyloxazolin-2-yl unit barely affects the catalyst performance (97% ee, 90% yield) and even the introduction of the second 4,4'-dimethyloxazolin-2-yl ring within the trisox system only leads to a reduction of the selectivity of the transformation to 82 % ee (1 mol% of cat.) and a lower yield due to a decreased catalytic activity. Remarkably, the bisoxazoline-copper catalyst bearing Ph-dm-BOX as the stereodirecting ligand generates the C-N coupling product with an enantiomeric excess of 83 % (88% ee for 10 mol% of catalyst). This catalyst with the bidentate ligand which only contains one chiral centre may therefore be viewed as possessing the *minimal catalyst structure* for efficient stereoselective catalysis of this transformation.

The relative activities of the copper(II) Lewis acid catalysts bearing the bisoxazolines Ph-BOX, Ph-dm-BOX and dm-BOX as well as the trisoxazolines Ph<sub>2</sub>-dm-trisox, Ph-dm<sub>2</sub>-trisox and dm-trisox were established in a kinetic study of the asymmetric C-N coupling under pseudo-first order conditions for the respective catalyst. The conversion curves are depicted in Figure 4.3.7 and display the general trend that the replacement of a 4-phenyloxazolin-2-yl by a 4,4'-dimethyloxazolin-2-yl unit leads to reduced activity.

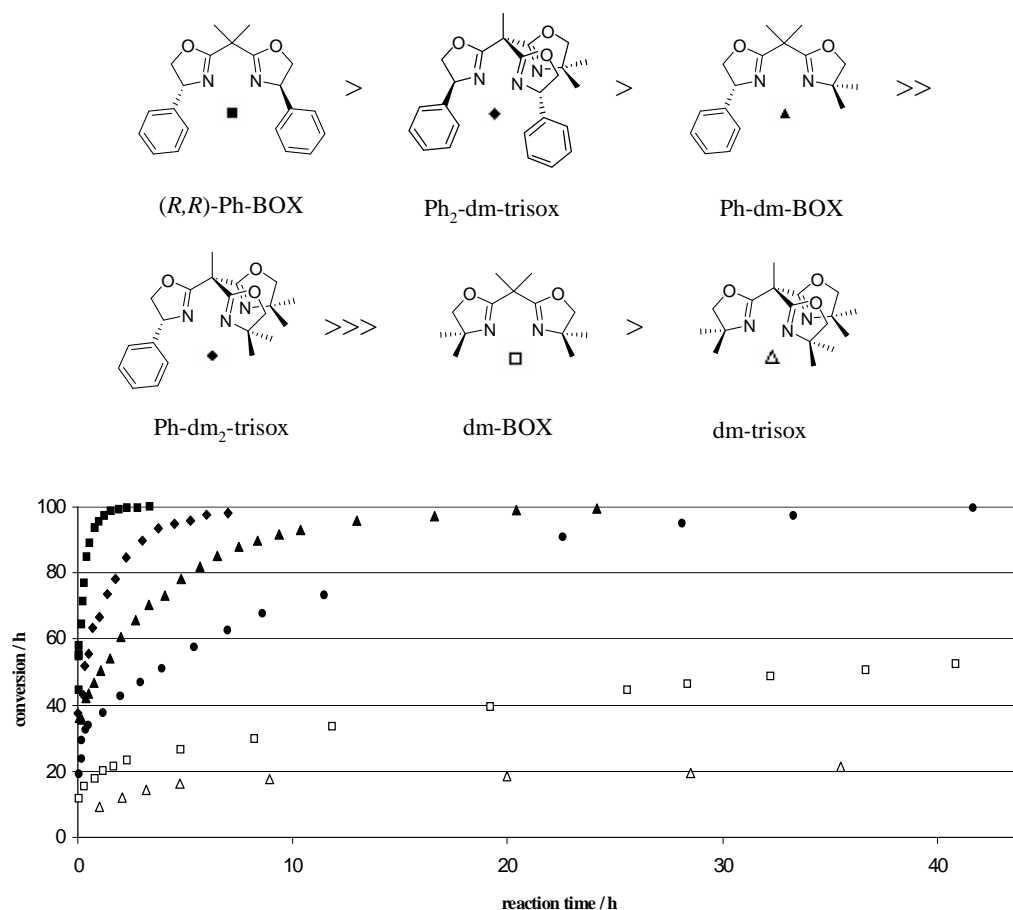


**Figure 4.3.7:** Asymmetric C-N coupling for the stereochemically “mixed” catalysts involving the bisoxazolines Ph-BOX, Ph-dm-BOX and dm-BOX as well as the trisoxazolines Ph<sub>2</sub>-dm-trisox, Ph-dm<sub>2</sub>-trisox and dm-trisox

In general, the ligands with two 4-phenyloxazolin-2-yl rings give rise to more active catalysts than the ones with one 4-phenyloxazolin-2-yl unit. The catalysts with the achiral ligands dm-BOX and dm-trisox possess very low activity and only incomplete conversion of the substrates is observed even after more than 40 h of reaction time. An exponential analysis of the conversion curves gives the pseudo-first order rate constants  $k_{AA}$  and  $k_{AB}$  in equation 1 (Table 4.3.4) and the relevant data for  $ee_{AA}$  and  $ee_{AB}$  for both systems are derived from the data listed in Table 4.3.3.

	( <i>R,R</i> )-Ph BOX	Ph <sub>2</sub> -dm trisox	Ph-dm BOX	Ph-dm <sub>2</sub> trisox	dm BOX	dm trisox
ee (%)	98	-97	83	82	0	0
k (h <sup>-1</sup> )	2.484	0.594	0.222	0.096	0.060	0.012

**Table 4.3.4:** Enantiomeric excesses and pseudo-first order rate constants of the asymmetric amination of ethyl 2-methylacetoacetate with dibenzyl azodicarboxylate with the copper(II) Lewis acid catalysts

- c. Estimate of the relative amounts of catalytic species for Ph<sub>2</sub>-dm-trisox/copper and Ph-dm<sub>2</sub>-trisox/copper catalysts

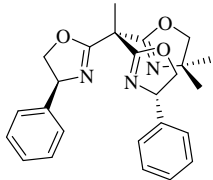
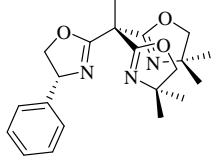
Equation 1 can be applied to the catalytic system with the *C*<sub>1</sub>-symmetric Ph<sub>2</sub>-dm-trisox, where A = *S* and B = dm and the quantity of the *fcc*-C<sub>1</sub> symmetric (A,B) = (Ph,dm) isomer can be expressed in equation 4 by rearrangement of equation 1:

$$[(A, B)] = \frac{(C_{cat} k_{AA} (ee_{AA} - ee))}{(2 \cdot k_{AB} (ee - ee_{AB}) + 2 \cdot k_{AA} (ee_{AA} - ee))} \quad (eq.4)$$

For the Ph-dm<sub>2</sub>-trisox/Cu catalyst, in which A is achiral and thus  $ee_{AA} \approx 0$ , concentration of mixed (A,B) is given by the simplified equation 5:

$$[(A, B)] = \frac{(C_{cat} k_{AA} ee)}{(2 \cdot k_{AB} ee_{AB} + 2 \cdot ee (k_{AA} - k_{AB}))} \quad (eq.5)$$

Numeric calculation of quantities of respective non-symmetrical (A,B) isomer is given in table 4.3.5 and shows that all three isomers relevant in exchange equilibrium are present in about equal amount.

		[(AA)] (%)	[(AB)] + [(BA)] (%)
 <b>Ph<sub>2</sub>-dm-trisox</b> A = <i>Ph</i> B = <i>dm</i>		56 ± 10	2 × 22 ± 10
 <b>Ph-dm<sub>2</sub>-trisox</b> A = <i>dm</i> B = <i>Ph</i>		18.4 ± 8	2 × 40.8 ± 8

**Table 4.3.5:** Estimated composition of the non-symmetrical A<sub>2</sub>B-trisox/copper(II) catalysts. The relative amounts of *fcc* C<sub>2</sub>-symmetric species are given in bold and those for *fcc* achiral species in italics.

Therefore, the relatively high enantioselectivity of the catalysts bearing the Ph<sub>2</sub>-dm-trisox and Ph-dm<sub>2</sub>-trisox is a consequence of the significantly greater activity of the species giving the best ee: *fcc*-C<sub>2</sub>-symmetric (Ph,Ph) compared to *fcc*-C<sub>1</sub>-symmetric (Ph,dm) for Ph<sub>2</sub>-dm-trisox (11 times more active) and *fcc*-chiral (Ph,dm) compared to *fcc*-achiral (dm,dm) for Ph-dm<sub>2</sub>-trisox (19 times).



#### 4. Conclusion

The aim of this study was to shed some light onto the implications which the use of chiral tridentate podands may have in stereoselective catalysis as compared to the more established bidentate chelates. The different order of the rotational axis in symmetrical systems, whilst not affecting the principals of stereoselection by intermolecular interaction between substrate and catalyst, becomes apparent when the symmetry of the stereodirecting ligand is systematically reduced or modified. Here, the twofold rotational symmetry may in principle be mapped onto mirror-/centrosymmetry (as may play a role when chiral molecules adopt a conformation which renders their shape close to achiral) whilst such a scenario is not possible for chiral threefold symmetric systems. Regarding only the systems bearing ligated tripods, this study underscores the previous observations of superior performance of the catalysts bearing  $C_3$ -chiral stereodirecting ligands as compared to systems of lower symmetry (see Chapter 3). The simplified behaviour with regard to potential catalyst equilibria in solution along with the stereochemical non-ambiguity of the active catalytic species appear to play the principal underlying role in this trend.



# **GENERAL CONCLUSION**



The aim of this work was to study the effect of threefold rotational symmetry as well as the role of the third oxazoline arm on catalytic reactions with intermediates preferring a bidentate coordination mode. For that purpose, new  $C_1$ - and  $C_3$ -symmetric 1,1,1-tris(oxazoliny)ethane ligands have been synthesised and applied in several model reactions.

Chapter 1 provides an introduction to the chemistry of oxazoline-based ligands, especially to trisoxazoline ligands. The synthetic strategies of the latter are reviewed, along with their applications in asymmetric catalysis and molecular recognition.

Chapter 2 is dedicated to the synthesis of highly symmetrical chiral 1,1,1-tris(oxazoliny)ethane ligands bearing phenyl, benzyl or indanyl substituents. A description of the preparation of mixed bis- and trisoxazolines is also given. The last two parts of this chapter focus on the isomerisation of the brominated monooxazoline derivatives. It has been shown that the thermally induced rearrangement of the 2-bromooxazolines generates the corresponding  $\alpha$ -bromo-isocyanate derivatives. Reaction of the latter with phenylethylamine leads selectively to the *N*-cyclised aziridines or to the *O*-cyclised 2-aminooxazolines depending on reaction conditions.

In Chapter 3, the coordination chemistry of the trisoxazoline ligands with palladium is first described. We have been able to isolate stable palladium(II) chloride or allyl complexes by reacting the desired trisoxazoline ligand with respectively  $[\text{Pd}(\text{PhCN})_2\text{Cl}_2]$  and  $[\text{Pd}(\eta^3\text{-C}_3\text{H}_5)(\text{cod})]\text{BF}_4$  as precursor. A number of palladium(0) complexes with different ligands, including a potentially tridentate pyridine-bisoxazoline ligand, and alkenes have been successfully synthesised using the most adapted Pd(0) precursor, namely the  $[\text{Pd}(\text{alkene})(\text{nbd})]$  complex. The dynamic behaviour of these complexes in solution has then been studied and activation parameters have been determined. Both  $\pi$ -allyl-Pd(II) and Pd(0) complexes are fluxional at room temperature, *i.e.* under the conditions of the asymmetric allylic alkylations. In the last part of the chapter, the systematic comparison of the catalytic efficiency of trisox- and bisox-palladium systems in allylic substitution is described. We have demonstrated that the trisoxazoline-based complexes are superior catalysts in direct comparison to the corresponding bisoxazoline-based catalysts. By using various  $C_3$ -symmetric trisoxazolines, in addition to bisoxazolines that contain a hetero-sidearm, we have found that the use of potentially tridentate ligands in this reaction results in a rate enhancement and in an increase in enantioselectivity relative to the corresponding catalysts bearing purely bidentate stereodirecting ligands. The results show that the additional donor function appears to play a role in the product/substrate exchange step as well as in the initial generation of the active catalyst.

Finally, Chapter 4 describes the exploitation of the dynamic coordination of the trisoxazolines to copper (II) in two copper-catalysed asymmetric reactions. It has first been shown that  $C_3$ -symmetric trisoxazolines form highly efficient enantioselective copper(II) Lewis acid catalysts which are based on the concept of a stereoelectronic hemilability of the divalent copper. In a direct comparison with the analogous bisoxazoline systems, the trisox/copper catalysts have proven to be more efficient in an enantioselective Mannich reaction as well as an enantioselective  $\alpha$ -amination of prochiral  $\beta$ -ketoesters in presence of low catalyst loadings. Finally, the implications of the use of chiral tridentate podands in stereoselective catalysis compared to the ones of the more established bidentate chelates have been lightened. In addition, the study underscores the superior performance of the catalysts bearing  $C_3$ -chiral stereodirecting ligands as compared to systems of lower symmetry as observed in the palladium chemistry.

## - Chapter 5 -

<b>I. General methods and instrumentation .....</b>	<b>149</b>
1. Materials .....	149
2. Solvents.....	149
3. Nuclear Magnetic Resonance (NMR).....	150
4. Infra-red Spectroscopy.....	150
5. Mass Spectrometry.....	150
6. Elemental Analysis .....	151
7. Gas Chromatography .....	151
8. HPLC .....	151
9. X-Ray Crystallography .....	151
<b>II. Chapter 2 .....</b>	<b>152</b>
1. Bisoxazolines with identical oxazoline units.....	152
1,1-bis[(4 <i>S</i> )-4-benzyloxazolin-2-yl]ethane ( <b>2</b> ) .....	152
1,1-bis[(4 <i>R</i> , 5 <i>S</i> )-4,5-indanediylloxazolin-2-yl]ethane ( <b>4</b> ).....	153
2. 2H-oxazolines .....	153
(4 <i>R</i> , 5 <i>S</i> )-4,5-indanediylloxazoline ( <b>7</b> ).....	154
3. 2-bromooxazolines.....	154
2-bromo-4,4-dimethyloxazoline ( <b>8</b> ).....	154
(4 <i>S</i> )-2-bromo-4-isopropylloxazoline ( <b>9</b> ).....	155
(4 <i>S</i> )-2-bromo-4-benzyloxazoline ( <b>10</b> ) .....	155
(4 <i>R</i> )-2-bromo-4-phenyloxazoline ( <b>11</b> ).....	156
(4 <i>R</i> , 5 <i>S</i> )-2-bromo-4,5-indanediylloxazoline ( <b>12</b> ).....	156
4. C <sub>3</sub> -symmetric trisoxazolines .....	157
1,1,1-tris[(4 <i>R</i> )-4-phenyloxazolin-2-yl]ethane ( <b>13</b> ) .....	157
1,1,1-tris[(4 <i>S</i> )-4-benzyloxazolin-2-yl]ethane ( <b>14</b> ).....	157

1,1,1-tris[(4 <i>R</i> , 5 <i>S</i> )-4,5-indanediylloxazolin-2-yl]ethane ( <b>15</b> ) .....	158
5. C <sub>1</sub> -symmetric trisoxazolines .....	159
1-((4 <i>R</i> )-4-phenyloxazolin-2-yl)-1,1-di((4 <i>S</i> )-4-phenyloxazolin-2-yl)ethane ( <b>16</b> ) .....	159
1,1-Bis((4 <i>S</i> )-4-phenyloxazolin-2-yl)-1-(4,4-dimethyloxazolin-2-yl)ethane ( <b>17</b> ) .....	160
1-((4 <i>R</i> )-4-phenyloxazolin-2-yl)-1,1-di(4,4-dimethyloxazolin-2-yl)ethane ( <b>18</b> ) .....	160
6. Precursors of the non-symmetric bisoxazolines .....	161
2,2-dimethyl malonic acid ethyl monoester	
<i>N</i> -(( <i>S</i> )-2-hydroxy-1-phenylethyl) monoamide ( <b>19</b> ) .....	161
2,2-dimethyl malonic acid ethyl monoester	
<i>N</i> -(2-hydroxy-1,1-dimethylethyl) monoamide ( <b>20</b> ) .....	162
<i>N</i> -(( <i>S</i> )-2-hydroxy-1-phenylethyl)- <i>N</i> '-(( <i>R</i> )-2-	
hydroxy-1-phenylethyl)-dimethylmalonamide ( <b>21</b> ) .....	162
<i>N</i> -(( <i>R</i> )-2-hydroxy-1-phenylethyl)- <i>N</i> '-(2-	
hydroxy-1,1-dimethylethyl)-dimethylmalonamide ( <b>22</b> ) .....	163
7. Mixed bisoxazolines .....	163
1-((4 <i>R</i> )-4-phenyloxazolin-2-yl)-1-((4 <i>S</i> )-4-phenyloxazolin-2-yl)-1-methylethane ( <b>23</b> ) .....	163
1-((4 <i>R</i> )-4-phenyloxazolin-2-yl)-1-(4,4-dimethyloxazolin-2-yl)-1-methylethane ( <b>24</b> ) .....	164
8. Isocyanate derivatives .....	165
1-bromo-2-isocyanato-2-methylpropane ( <b>25</b> ) .....	165
(2 <i>S</i> )-1-bromo-2-isocyanato-3-methylbutane ( <b>26</b> ) .....	165
(1 <i>R</i> )-1-(2-bromo-1-isocyanatoethyl)benzene ( <b>27</b> ) .....	165
(1 <i>R</i> ,2 <i>R</i> )-2-bromo-1-isocyanato-2,3-dihydro-1 <i>H</i> -indene ( <b>28</b> ) .....	166
9. Urea .....	166
1-(( <i>S</i> )-2-bromo-1-isopropylethyl)-3-((1 <i>S</i> )-1-phenylethyl)urea ( <b>29</b> ) .....	166
10. Aziridines .....	167
2,2-dimethyl- <i>N</i> -(1-phenylethyl)aziridine-1-carboxamide ( <b>30</b> ) .....	167
(2 <i>S</i> )-2-isopropyl- <i>N</i> -((1 <i>S</i> )-1-phenylethyl)aziridine-1-carboxamide ( <b>31a</b> ) .....	167
(2 <i>S</i> )-2-isopropyl- <i>N</i> -(1-phenylethyl)aziridine-1-carboxamide ( <b>31a+b</b> ) .....	168
(2 <i>R</i> )-2-phenyl- <i>N</i> -((1 <i>S</i> )-1-phenylethyl)aziridine-1-carboxamide ( <b>32</b> ) .....	168
11. Hydrobromide salts of the 2-aminooxazolines .....	169
2-(1-phenylethylamino)-4,4-dimethyloxazoline hydrobromide ( <b>33</b> ) .....	169
(4 <i>S</i> )-2-((1 <i>R</i> )-1-phenylethylamino)-4-isopropylloxazoline hydrobromide ( <b>34a</b> ) .....	170
(4 <i>S</i> )-2-(1-phenylethylamino)-4-isopropylloxazoline hydrobromide ( <b>34a+b</b> ) .....	170
(4 <i>R</i> )-2-((1 <i>R</i> )-1-phenylethylamino)-4-phenyloxazoline hydrobromide ( <b>35</b> ) .....	171



12.	2-aminoxazolines .....	171
	2-(1-phenylethylamino)-4,4-dimethyloxazoline ( <b>36</b> ) .....	171
	(4 <i>S</i> )-2-((1 <i>R</i> )-1-phenylethylamino)-4-isopropylloxazoline ( <b>37a</b> ).....	171
	(4 <i>S</i> )-2-(1-phenylethylamino)-4-isopropylloxazoline ( <b>37a+b</b> ).....	172
	(4 <i>R</i> )-2-((1 <i>R</i> )-1-phenylethylamino)-4-phenylloxazoline ( <b>38</b> ).....	173
<b>III. Chapter 3 .....</b>		<b>173</b>
1.	Palladium(II)chloride complexes.....	173
	General Procedure.....	173
	(1,1,1-tris[(4 <i>S</i> )-4-isopropylloxazolin-2-yl]ethane)palladium(II) dichloride ( <b>39</b> ) .....	173
	(1,1,1-tris[(4 <i>R</i> )-4-phenylloxazolin-2-yl]ethane)palladium(II) dichloride ( <b>40</b> ) .....	174
	(1,1,1-tris[(4 <i>S</i> )-4-benzylloxazolin-2-yl]ethane)palladium(II) dichloride ( <b>41</b> ).....	175
	(1,1,1-tris[(4 <i>R</i> , 5 <i>S</i> )-4,5-indanediylloxazolin-2-yl]ethane)palladium(II) dichloride ( <b>42</b> ).....	175
2.	Palladium(II) allyl complex .....	176
	( $\eta^3$ -allyl)(1,1,1-tris[(4 <i>R</i> )-4-phenylloxazolin-2-yl]ethane)palladium(II) ( <b>43</b> ).....	176
3.	Palladium(0) complexes.....	177
	[Pd(ma)(triox)] complexes: General Procedure .....	177
	(1,1,1-tris[(4 <i>S</i> )-4-isopropylloxazolin-2-yl]ethane)(maleic anhydride)palladium(0) ( <b>44</b> )....	177
	(1,1,1-tris[(4 <i>R</i> )-4-phenylloxazolin-2-yl]ethane)(maleic anhydride)palladium(0) ( <b>45</b> ) .....	178
	(1,1,1-tris[(4 <i>S</i> )-4-benzylloxazolin-2-yl]ethane)(maleic anhydride)palladium(0) ( <b>46</b> ) .....	178
	(2,2-bis[(4 <i>S</i> )-4-isopropylloxazolin-2-yl]-1-(pyridin-2-yl)propane)(maleic anhydride) palladium(0) ( <b>48</b> ) .....	179
	(1,1,1-tris[(4 <i>R</i> ,5 <i>S</i> )-4,5-indanediylloxazolin-2-yl]ethane)(tetracyanoethylene) palladium(0) ( <b>47</b> ) .....	179
4.	Magnetisation transfer experiments.....	180
	Acquisition of the data .....	180
	Theoretical fit of the experimental data .....	182
5.	Asymmetric allylic alkylation.....	183
	General procedure .....	183
	Determination of enantiomeric excesses .....	183
	Kinetic studies.....	183
6.	Asymmetric allylic amination.....	184
	General procedure .....	184

---

Determination of enantiomeric excesses .....	184
<b>IV. Chapter 4 .....</b>	<b>184</b>
1. Copper(II) complex.....	184
[Cu(( <i>R,S,S</i> )-Ph-trisox)( $\beta$ -ketoester)](ClO <sub>4</sub> ) ( <b>49</b> ) .....	184
2. Asymmetric Mannich reaction.....	185
General procedure:.....	185
Determination of enantiomeric excesses .....	185
3. Asymmetric $\alpha$ -amination .....	185
General procedure:.....	185
Determination of enantiomeric excesses .....	186
Kinetic studies.....	186
<b>V. X-ray experimental data.....</b>	<b>187</b>

## I. General methods and instrumentation

### 1. Materials

All manipulations, except those indicated, were performed under a nitrogen atmosphere using standard Schlenk techniques and a glove box.

(*S*)-valinol, (*S*)-phenylalaninol and (*R*)-phenylglycinol were obtained by reduction of L-valine, L-phenylalanine and D-phenylglycine respectively.<sup>1</sup> The compounds 2,2-bis[(4*S*)-4-isopropylloxazolin-2-yl]-1-(pyridin-2-yl)propane (**U**),<sup>2</sup> 2,2-bis[(4*S*)-4-isopropylloxazolin-2-yl]-1-phenylpropane (**P**)<sup>2</sup> and 2,2-bis[(4*S*)-4-isopropylloxazolin-2-yl]-1,3-diphenylpropane (**Q**)<sup>3</sup> were synthesized according to literature procedures. 2,2-bis[(4*S*)-4-isopropylloxazolin-2-yl]-4,4-dimethylpentan-3-one (**S**), 2,2-bis[(4*S*)-4-isopropylloxazolin-2-yl]-1-phenylpropan-1-one (**T**), 2,2-bis[(4*S*)-4-isopropylloxazolin-2-yl]-1,3-di(naphth-2-yl)propane (**R**) and 2,2-bis[(4*S*)-4-isopropylloxazolin-2-yl]-1,3-di(pyridin-2-yl)propane (**V**) were obtained according to previously published protocols.<sup>4</sup> The *i*Pr-BOX, Ph-BOX, Bn-BOX, Ind-BOX and dm-BOX ligands were obtained by methylation of the corresponding 2,2-bis[oxazolin-2-yl]ethane. The trisoxazolines *i*Pr-trisox and dm-trisox were prepared following the procedures developed in our group.<sup>5</sup> The palladium precursors [(cod)Pd( $\eta^3$ -C<sub>3</sub>H<sub>5</sub>)]BF<sub>4</sub>,<sup>6</sup> [( $\eta^2$ , $\eta^2$ -nbd)( $\eta^2$ -ma)Pd]<sup>7</sup> and [( $\eta^2$ , $\eta^2$ -nbd)( $\eta^2$ -tcne)Pd]<sup>6</sup> were prepared according to published methods.

Ethyl 2-methylacetoacetate and dodecane are commercially available and were purified by bulb to bulb distillation prior to use. All other reagents were commercially available and used as received. All palladium(0) complexes synthesized were stored in the glove box.

### 2. Solvents

Solvents were predried over activated 4 Å molecular sieves and were refluxed over potassium (tetrahydrofuran, toluene and hexane), sodium/potassium alloy (pentane and diethyl ether) or calcium hydride (dichloromethane) under an argon atmosphere and collected by distillation.

<sup>1</sup> A. Abiko, S. Masamune, *Tetrahedron Lett.* **1992**, 33, 5517.

<sup>2</sup> J. Zhou, M. C. Ye, Y. Tang, *J. Comb. Chem.* **2004**, 6, 301.

<sup>3</sup> M. Honma, T. Sawada, Y. Fujisawa, M. Utsugi, H. Wanatabe, A. Umino, T. Matsamura, T. Hagihara, M. Takano, M. Nakada, *J. Am. Chem. Soc.* **2003**, 125, 2860.

<sup>4</sup> M. Seitz, C. Capacchione, S. Bellemin-Laponnaz, H. Wadepohl, B. D. Ward, L. H. Gade, *Dalton Trans.* **2006**, 193.

<sup>5</sup> a) S. Bellemin-Laponnaz, L. H. Gade, *Chem. Commun.* **2002**, 1286; b) S. Bellemin-Laponnaz, L. H. Gade, *Angew. Chem. Int. Ed.* **2002**, 41, 3473; *Angew. Chem.* **2002**, 114, 3623.

<sup>6</sup> D. A. White, *Inorg. Synth.* **1972**, 13, 55.

<sup>7</sup> A. M. Kluwer, C. J. Elsevier, M. Bühl, M. Lutz, A. L. Spek, *Angew. Chem. Int. Ed.* **2003**, 42, 3501; *Angew. Chem.* **2003**, 115, 3625.

Deuterated solvents were dried over calcium hydride ( $\text{CD}_2\text{Cl}_2$ ,  $\text{C}_2\text{D}_2\text{Cl}_4$  and  $\text{CDCl}_3$ ), distilled under reduced pressure and stored under argon in Teflon valve ampoules.

### 3. Nuclear Magnetic Resonance (NMR)

$^1\text{H}$  and  $^{13}\text{C}$  NMR spectra were recorded on the following spectrometers:

- Bruker DRX 200 ( $^1\text{H}$  200 MHz,  $^{13}\text{C}$  50 MHz),
- Bruker Avance 300 ( $^1\text{H}$  300 MHz,  $^{13}\text{C}$  75 MHz),
- Bruker Avance II 400 ( $^1\text{H}$  400 MHz,  $^{13}\text{C}$  100 MHz),
- Bruker Avance III 600 ( $^1\text{H}$  600 MHz,  $^{13}\text{C}$  150 MHz,  $^{15}\text{N}$  60 MHz).

$^1\text{H}$  and  $^{13}\text{C}$  assignments were confirmed when necessary with the use of DEPT-135 and two dimensional  $^1\text{H}$ - $^1\text{H}$  and  $^{13}\text{C}$ - $^1\text{H}$  NMR correlation experiments.  $^1\text{H}$  and  $^{13}\text{C}$  spectra were referenced internally to residual protio-solvent ( $^1\text{H}$ ) or solvent ( $^{13}\text{C}$ ) resonances, and are reported relative to tetramethylsilane ( $\delta = 0$  ppm).

$^{15}\text{N}$  NMR spectra were recorded on a Bruker Avance III 600 spectrometer equipped with a cryogenically cooled direct detection probe (QNP-cryoprobe<sup>TM</sup>, optimized for detection of  $^{31}\text{P}$ ,  $^{13}\text{C}$  and  $^{15}\text{N}$ ). The experimental parameters for the direct  $^{15}\text{N}$  detection were optimized with a 0.2 M solution of a non-enriched *N*-ligand titanium complex (ext. standard: liquid  $\text{NH}_3$ ). For routine direct  $^{15}\text{N}$  NMR detection concentrations of not less than 0.1 M are necessary. Selected parameters are: Puls-program: inverse gated decoupled; relaxation delay 6 sec;  $90^\circ$ - $^{15}\text{N}$ -puls (10  $\mu\text{sec}$ ); pre-acquisition delay 400  $\mu\text{sec}$ ; time domain 65K; sweep 500 ppm; acquisition time 1 sec; number of accumulations 5000.

Chemical shifts are quoted in  $\delta$ (ppm) and coupling constants in Hertz (Hz).

### 4. Infra-red Spectroscopy

Infrared spectra of KBr pellets were recorded on a Varian 3100 FT-IR spectrometer between 4000 and 250  $\text{cm}^{-1}$ . Infrared data are quoted in wavenumbers  $\nu$  ( $\text{cm}^{-1}$ ).

### 5. Mass Spectrometry

Mass spectra were recorded by the mass spectrometry services of the University of Strasbourg and of the University of Heidelberg,

## 6. Elemental Analysis

Elemental Analysis were carried out by the analytical services of the University of Strasbourg and of the University of Heidelberg.

## 7. Gas Chromatography

Gas chromatography analysis were obtained on a Finnigan Focus GC apparatus equipped with a capillary column (BPX5, 5 % phenyl, polysilphenylene-siloxane, nonpolar, 30 m x 0.25 mm x 0.5  $\mu\text{m}$ ):  $T_{\text{inj}} = 200^\circ\text{C}$ ,  $T_{\text{det}} = 220^\circ\text{C}$  (Flame Ionization Detector), carrier gas: He.

## 8. HPLC

Determinations of the enantiomeric excesses were carried out using a Kontron 2000 HPLC equipped with a Daicel Chiralcel OD column (0.46 x 25 cm) and a Thermo Finnigan Surveyor HPLC equipped with a Daicel Chiralcel AD-H column (0.46 cm x 25 cm) and the corresponding pre-column (0.40 cm x 1 cm). Eluant: hexane/isopropanol (ratio depending on the compound).

## 9. X-Ray Crystallography

Intensity data were collected at low temperature, in Strasbourg on a Nonius Kappa CCD diffractometer for compounds **39** and **44** and in Heidelberg on Bruker Smart 1000 CCD diffractometer for compounds **7**, **7 hydrolysed**, **13**, **14**, **28**, **31a**, **39**, **40**, **43**, **44** and **49**.

Data were corrected for Lorentz, polarization and absorption effects (semiempirical<sup>8</sup> or empirical<sup>9</sup>) in Heidelberg. The structures were solved using heavy atom or direct methods and refined by a full-matrix least squares procedure based on  $F^2$  with all measured unique reflections. All non-hydrogen atoms were given anisotropic displacement parameters. Hydrogen atoms were included at calculated positions and refined with a riding model.

The calculations were performed using the programs DIRDIF,<sup>10</sup> SIR,<sup>11</sup> SHELXS-86,<sup>12</sup> SHELXL-97<sup>13</sup> and OpenMoleN.<sup>14</sup> Graphical representations were drawn with XP.<sup>15</sup> Anisotropic displacement ellipsoids are scaled to 25% probability.

---

<sup>8</sup> G. M. Sheldrick, *SADABS-2004/1*, Bruker AXS, **2004**.

<sup>9</sup> N. Walker, D. Stuart, *Acta Cryst.*, **1983**, A39, 158.

<sup>10</sup> P. T. Beurskens, G. Beurskens, R. de Gelder, S. Garcia-Granda, R. O. Gould, R. Israel, J. M. M. Smits, *DIRDIF-99*, University of Nijmegen, The Netherlands, **1999**.

<sup>11</sup> M. C. Burla, M. Camalli, G. Cascarano, C. Giacovazzo, G. Polidori, R. Spagna, D. Viterbo, *J. Appl. Cryst.* **1989**, 22, 389.

<sup>12</sup> G. M. Sheldrick, *SHELXS-86*, University of Göttingen, **1986**; G. M. Sheldrick, *Acta Cryst.* **1990**, A46, 467.

<sup>13</sup> G. M. Sheldrick, *SHELXL-97*, University of Göttingen, **1997**.

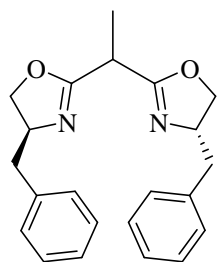
<sup>14</sup> OpenMoleN, Interactive Intelligent Structure Solution, Nonius B.V., Delft, **1997**.

## II. Chapter 2

### 1. Bisoxazolines with identical oxazoline units

1,1-bis[(4*R*)-4-phenyloxazolin-2-yl]ethane (**1**),<sup>16</sup> 1,1-bis[4,4-dimethyloxazolin-2-yl]ethane<sup>17</sup> and bis[(4*R*, 5*S*)-4,5-indanediyoaxolin-2-yl]methane (**3**)<sup>18</sup> were obtained according to procedures reported in the literature.

#### 1,1-bis[(4*S*)-4-benzyloxazolin-2-yl]ethane (**2**)



Diethyl methylmalonate (2.8 mL, 16.3 mmol) and (*S*)-phenylalaninol were added in a Schlenk flask. NaH (10 mg, 0.25 mmol; 60% dispersion in mineral oil) was then added under nitrogen to the flask which was sealed and heated to 130°C. After 16 h, the ethanol was removed under vacuum to leave a white solid pure enough to be used for the next step without further purification (5.9 g, 95%). To an ice-cooled solution of the dihydroxy diamide

prepared in the previous step (5.9 g, 15.4 mmol), triethylamine (17.2 mL, 123.2 mmol) and DMAP (188 mg, 1.54 mmol) in CH<sub>2</sub>Cl<sub>2</sub> (200 mL) a solution of TsCl (5.9 g, 30.8 mmol) in CH<sub>2</sub>Cl<sub>2</sub> (30 mL) was slowly added. The mixture was warmed to room temperature, stirred for three days and washed with a saturated aqueous solution of NH<sub>4</sub>Cl and brine. The organic phase was dried over Na<sub>2</sub>SO<sub>4</sub> and concentrated *in vacuo* to give a yellow oil. Purification by flash chromatography (CH<sub>2</sub>Cl<sub>2</sub>/MeOH/Et<sub>3</sub>N, 97/3/1) gave the desired product as a colorless oil (2.4 g, 45% yield).

<sup>1</sup>H NMR (200 MHz, CDCl<sub>3</sub>, 296 K) δ 1.46 (d, *J* = 7.2 Hz, 3H, CH<sub>3</sub>), 2.67 (dd, *J* = 8.5 Hz, 13.7 Hz, 2H, CH<sub>2</sub> Bn), 3.11 (dd, *J* = 5.0 Hz, 13.7 Hz, 2H, CH<sub>2</sub> Bn), 3.48 (q, *J* = 7.2 Hz, 1H, CH<sub>bridge</sub>), 4.00 (dd, *J* = 7.4 Hz, 8.3 Hz, 2H, CH<sub>2</sub> oxa), 4.20 (m, 2H, CH<sub>2</sub> oxa), 4.42 (m, 2H, CH<sub>oxa</sub>), 7.23 (m, 10 H, CH<sub>arom</sub>).

<sup>13</sup>C {<sup>1</sup>H} NMR (50 MHz, CDCl<sub>3</sub>, 296 K) δ 15.2 (CH<sub>3</sub>), 33.9 (CH<sub>bridge</sub>), 41.4 (CH<sub>2</sub> Bn), 67.2 (CH<sub>oxa</sub>), 72.1 (CH<sub>2</sub> oxa), 126.5, 128.5, 129.3 (C<sub>arom</sub>), 137.7 (C<sub>quat-arom</sub>), 166.1 (NCO).

FT-IR (KBr): ν 1661 cm<sup>-1</sup> (s, ν<sub>C=N</sub>).

MS (EI): *m/z* (%): 257.1 (100) [*M*-CH<sub>2</sub>Ph]<sup>+</sup> 348.2 (50) [*M*]<sup>+</sup>.

<sup>15</sup> SHELXTL, Bruker AXS GmbH, Karlsruhe, 1997.

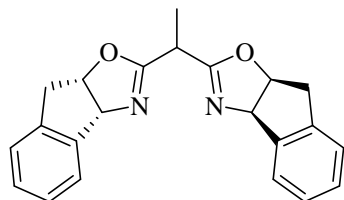
<sup>16</sup> J. Bourguignon, U. Bremberg, G. Dupas, K. Hallman, L. Hagberg, L. Hortala, V. Levacher, S. Lutsenko, E. Macedo, C. Moberg, G. Quéguiner, F. Rahm, *Tetrahedron* **2003**, *59*, 9583.

<sup>17</sup> S.E. Denmark, C. M. Stiff, *J. Org. Chem.* **2000**, *65*, 5875.

<sup>18</sup> D. M. Barnes, J. Ji, M. G. Fickes, M. A. Fitzgerald, S. A. King, H. E. Morton, F. A. Plagge, M. Preskill, S. H. Wagaw, S. J. Wittenberger, J. Zhang, *J. Am. Chem. Soc.* **2002**, *124*, 13097.

elemental analysis calcd (%) for C<sub>22</sub>H<sub>24</sub>N<sub>2</sub>O<sub>2</sub>: C 75.83, H 6.94, N 8.04; found: C 75.62, H 6.99, N 7.96.

### 1,1-bis[(4*R*, 5*S*)-4,5-indanediylloxazolin-2-yl]ethane (4)



A solution of LDA (0.9 mL, 2 M in THF/pentane, 1.8 mmol) was added dropwise to a solution of bis[(4*R*, 5*S*)-4,5-indanediylloxazolin-2-yl]methane (552 mg, 1.7 mmol) in THF (25 mL) at -78°C. The brown reaction mixture was allowed to warm to ambient temperature and stirred for an additional 0.5 h prior to the addition of methyl trifluoromethanesulfonate (0.20 mL, 1.8 mmol). The colorless solution was stirred for 12 h and was concentrated to dryness. The residue was redissolved in dichloromethane (60 mL) and washed with a saturated aqueous solution of NH<sub>4</sub>Cl (10 mL) and brine (10 mL). The organic extract was dried over Na<sub>2</sub>SO<sub>4</sub> and concentrated *in vacuo* to give a yellowish solid. Purification by flash chromatography (Hexane /EtOAc, 50/50) gave the desired product as a white solid (340 mg, 59% yield).

<sup>1</sup>H NMR (400 MHz, CD<sub>2</sub>Cl<sub>2</sub>, 296 K) δ 1.35 (d, *J* = 7.2 Hz, 3H, CH<sub>3</sub>), 3.03 (m, 2H, CH<sub>2</sub> Ind), 3.39 (m, 3H, CH<sub>2</sub> Ind, CH<sub>bridge</sub>), 5.30 (m, 2H, OCH<sub>oxa</sub>), 5.52 (d, *J* = 8.0 Hz, 2H, NCH<sub>oxa</sub>), 7.28 (m, 6H, CH<sub>arom</sub>), 7.45 (m, 2H, CH<sub>arom</sub>).

<sup>13</sup>C {<sup>1</sup>H}NMR (100 MHz, CD<sub>2</sub>Cl<sub>2</sub>, 296 K) δ 14.6 (CH<sub>3</sub>), 33.9 (CH<sub>bridge</sub>), 39.7 (CH<sub>2</sub> Ind), 76.6 (NCH<sub>oxa</sub>), 83.2 (OCH<sub>oxa</sub>), 125.3, 127.2, 128.3 (C<sub>arom</sub>), 139.9, 141.9 (C<sub>quat-arom</sub>), 165.6 (NCO).

FT-IR (KBr): ν 1653 cm<sup>-1</sup> (s, ν<sub>C=N</sub>).

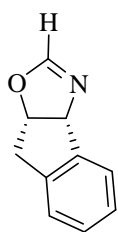
MS (EI): *m/z* (%): 344.4 (81) [M]<sup>+</sup>.

elemental analysis calcd (%) for C<sub>22</sub>H<sub>20</sub>N<sub>2</sub>O<sub>2</sub>: C 76.72, H 5.85, N 8.13; found: C 76.61, H 5.89, N 8.17.

## 2. 2*H*-oxazolines

(4*S*)-4-isopropylloxazoline, (4*R*)-4-phenylloxazoline (**6**) and (4*S*)-4-benzyloxazoline (**5**) were obtained by condensation of (*S*)-valinol, (*R*)-phenylglycinol and (*S*)-phenylalaninol respectively with the reagent dimethylformamide-dimethyl acetal (DMF-DMA) according to a procedure developed by Meyers *et al.*<sup>19</sup> 4,4-dimethylloxazoline was purchased from Acros.

<sup>19</sup> W. R. Leonard, J. L. Romine, A. I. Meyers, *J. Org. Chem.* **1991**, 56, 1961.

(4R, 5S)-4,5-indanediylloxazoline (7)

(1R, 2S)-*cis*-1-amino-2-indanol (2.24 g, 15 mmol) and DMF-DMA were combined without solvent. After the reaction mixture was stirred for 12 h, the volatiles were removed and the mixture was twice azeotropically concentrated by addition of 100 mL portions of hexane. *p*-Toluenesulfonic acid (10 mg) was added to the resultant formamidine and the mixture was diluted with hexane (125 mL), the round-bottom flask was fitted with a liquid/solid extraction apparatus containing 20 g of 4Å molecular sieves and refluxed for 3 days. The solution was washed with 10%  $\text{KHCO}_3$  (15 mL) and brine (15 mL). The organic extract was dried over  $\text{Na}_2\text{SO}_4$  and concentrated *in vacuo* to give the product as a white solid (1.82 g, 76%).

$^1\text{H}$  NMR ( $\text{CD}_2\text{Cl}_2$ , 200 MHz, 296 K)  $\delta$  3.25 (dd,  $J = 1.1$  Hz, 17.9 Hz, 1H,  $\text{CH}_2_{\text{Ind}}$ ), 3.50 (dd,  $J = 6.8$  Hz, 18.0 Hz, 1H,  $\text{CH}_2_{\text{Ind}}$ ), 5.29 (ddd,  $J = 1.7$  Hz, 6.9 Hz, 8.2 Hz, 1H,  $\text{OCH}_{\text{Oxa}}$ ), 5.55 (dd,  $J = 1.4$  Hz, 8.0 Hz, 1H,  $\text{NCH}_{\text{Oxa}}$ ), 6.80 (d,  $J = 1.6$  Hz, 1H,  $\text{OCHN}$ ), 7.28 (m, 3H,  $\text{CH}_{\text{arom}}$ ), 7.46 (m, 1H,  $\text{CH}_{\text{arom}}$ ).

$^{13}\text{C}$  { $^1\text{H}$ } NMR ( $\text{CD}_2\text{Cl}_2$ , 50 MHz, 296 K)  $\delta$  39.6 ( $\text{CH}_2$ ), 75.8 ( $\text{NCH}_{\text{Oxa}}$ ), 81.9 ( $\text{OCH}_{\text{Oxa}}$ ), 125.3, 127.3, 128.4 ( $\text{C}_{\text{arom}}$ ), 139.8, 142.0 ( $\text{C}_{\text{quat-arom}}$ ), 154.4 ( $\text{NCO}$ ).

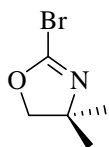
FT-IR (KBr)  $\nu$  1617  $\text{cm}^{-1}$  ( $\nu_{\text{C=N}}$ ).

MS (EI)  $m/z$  (%) 159.1 (66) [ $M$ ] $^+$ .

elemental analysis calcd (%) for  $\text{C}_{29}\text{H}_{27}\text{N}_3\text{O}_3$  (465.54): C 74.82, H 5.85, N 9.03; found: C 74.70, H 5.81, N 8.99.

### 3. 2-bromooxazolines

The 2-bromooxazolines were synthesized based on a procedure described in the literature.<sup>20</sup>

2-bromo-4,4-dimethyloxazoline (8)

*t*BuLi (21 mL, 1.5 M in pentane, 31.3 mmol) was added dropwise to a solution of 4,4-dimethyloxazoline (3 mL, 28.4 mmol) in anhydrous THF (150 mL) at  $-78^\circ\text{C}$ . The bright yellow solution of the anion was allowed to stir at  $-78^\circ\text{C}$  for an additional 0.5 h prior to the addition of 1,2-dibromo-1,1,2,2-tetrafluoroethane (3.8 mL, 31.3 mmol), was subsequently allowed to warm slowly to ambient temperature overnight, and then concentrated to about 5 mL. The brownish mixture was purified by a short bulb-to-bulb distillation to yield a colorless solution of the expected 2-bromooxazoline in THF (2.69 g of pure compound, 53%).

<sup>20</sup> A. I. Meyers, K. A. Novachek, *Tetrahedron Lett.* **1996**, 37, 1747



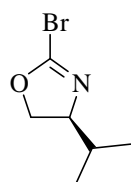
$^1\text{H}$  NMR ( $\text{CDCl}_3$ , 600 MHz, 296 K)  $\delta$  1.34 (s, 6H,  $\text{CH}_3$ ), 4.13 (s, 2H,  $\text{CH}_2$ ).

$^{13}\text{C}$  { $^1\text{H}$ } NMR ( $\text{CDCl}_3$ , 150 MHz, 296 K)  $\delta$  28.1 ( $\text{CH}_3$ ), 68.8 ( $\text{C}_{\text{quat methyl}}$ ), 81.8 ( $\text{CH}_2$ ), 141.2 (NCO).

$^{15}\text{N}$  NMR ( $\text{CDCl}_3$ , 60 MHz, 296 K)  $\delta$  252.6 (N).

HRMS (EI):  $m/z$  : calcd for  $\text{C}_5\text{H}_8\text{BrNO}$  ( $[M]^+$ ) 176.9789, found: 176.9800.

(4S)-2-bromo-4-isopropylloxazoline (9)



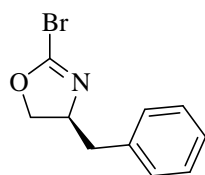
$t\text{BuLi}$  (17.9 mL, 30.4 M) was added dropwise to a solution of (4S)-4-isopropylloxazoline (3.12 g, 27.6 mmol) in anhydrous THF (150 mL) at  $-78^\circ\text{C}$ . The bright yellow solution of the anion was allowed to stir at  $-78^\circ\text{C}$  for an additional 0.5 h prior to the addition of 1,2-dibromo-1,1,2,2-tetrafluoroethane (3.6 mL, 30.4 mmol), was subsequently allowed to warm slowly to ambient temperature overnight, and then concentrated to about 5 mL. The brownish mixture was purified by a short bulb-to-bulb distillation to yield a colorless solution of the expected 2-bromooxazoline in THF (2.91 g of pure compound, 55%).

$^1\text{H}$  NMR ( $\text{CDCl}_3$ , 300 MHz, 296 K)  $\delta$  0.91 (d,  $J = 6.7$  Hz, 3H,  $\text{CH}_3$  isopropyl), 0.99 (d,  $J = 6.7$  Hz, 3H,  $\text{CH}_3$  isopropyl), 1.80 (m, 1H,  $\text{CH}$  isopropyl), 3.96 (m, 1H,  $\text{CH}_{\text{oxa}}$ ), 4.15 (pseudo-t,  $J = 8.2$  Hz, 1H,  $\text{CH}_2_{\text{oxa}}$ ), 4.45 (dd,  $J = 8.3$  Hz, 9.7 Hz, 1H,  $\text{CH}_2_{\text{oxa}}$ ).

$^{13}\text{C}$  { $^1\text{H}$ } NMR ( $\text{CDCl}_3$ , 75 MHz, 296 K)  $\delta$  18.4, 18.1 ( $\text{CH}_3$  isopropyl), 32.5 ( $\text{CH}$  isopropyl), 72.9 ( $\text{CH}_{\text{oxa}}$ ), 73.2 ( $\text{CH}_2_{\text{oxa}}$ ), 141.7 (NCO).

HRMS (EI):  $m/z$  : calcd for  $\text{C}_6\text{H}_{10}\text{BrNO}$  ( $[M]^+$ ) 190.9946, found: 190.9891.

(4S)-2-bromo-4-benzyloxazoline (10)



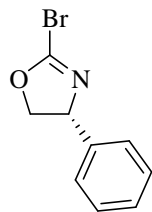
$t\text{BuLi}$  (3.6 mL, 1.5 M in pentane, 5.4 mmol) was added dropwise to a solution of (4S)-4-benzyloxazoline (784 mg, 4.9 mmol) in anhydrous THF (50 mL) at  $-90^\circ\text{C}$ . The bright yellow solution of the anion was allowed to stir at  $-90^\circ\text{C}$  for an additional 0.5 h prior to the addition of 1,2-dibromo-1,1,2,2-tetrafluoroethane (0.64 mL, 5.4 mmol), was subsequently allowed to warm slowly to ambient temperature overnight, and then concentrated to about 5 mL. The brownish mixture was purified by a short bulb-to-bulb distillation to yield a colorless solution of the expected 2-bromooxazoline in THF (634 mg of pure compound, 54%).

$^1\text{H}$  NMR ( $\text{CDCl}_3$ , 400 MHz, 296 K)  $\delta$  2.78 (dd,  $J = 8.0$  Hz, 13.9 Hz, 1H,  $\text{CH}_2_{\text{Bn}}$ ), 3.17 (dd,  $J = 5.3$  Hz, 13.8 Hz, 1H,  $\text{CH}_2_{\text{Bn}}$ ), 4.19 (dd,  $J = 7.1$  Hz, 7.8 Hz, 1H,  $\text{CH}_2_{\text{oxa}}$ ), 4.42 (dd,  $J = 8.1$  Hz, 9.4 Hz, 1H,  $\text{CH}_2_{\text{oxa}}$ ), 4.48 (m, 1H,  $\text{CH}_{\text{oxa}}$ ), 7.31 (m, 5H,  $\text{CH}_{\text{arom}}$ ).

$^{13}\text{C}$  { $^1\text{H}$ } NMR ( $\text{CDCl}_3$ , 100 MHz, 296 K)  $\delta$  41.1 ( $\text{CH}_2_{\text{Bn}}$ ), 67.9 ( $\text{CH}_{\text{oxa}}$ ), 74.5 ( $\text{CH}_2_{\text{oxa}}$ ), 126.8, 128.7, 129.2 ( $\text{CH}_{\text{arom}}$ ), 136.7 ( $\text{C}_{\text{quat-arom}}$ ), 142.7 (NCO).

HRMS (EI):  $m/z$  : calcd for  $\text{C}_{10}\text{H}_{10}\text{BrNO}$  ( $[M]^+$ ) 238.9946, found: 238.9953.

(4R)-2-bromo-4-phenyloxazoline (11)



*t*BuLi (3.9 mL, 1.7 M in pentane, 6.6 mmol) was added dropwise to a solution of (4R)-4-phenyloxazoline (890 mg, 6 mmol) in THF (100 mL) at  $-100^\circ\text{C}$ . The light brown solution of the anion was allowed to stir at  $-100^\circ\text{C}$  for an additional 0.5 h prior to the addition of 1,2-dibromo-1,1,2,2-tetrafluoroethane (0.8 mL, 6.7 mmol). The reaction mixture was then allowed to warm slowly to ambient

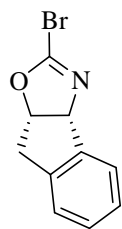
temperature overnight, and was concentrated to about 5 mL. The crude product was extracted from the reaction mixture with pentane (4 x 10 mL). The residue was purified by a short bulb-to-bulb distillation to yield a colorless solution of the expected 2-bromooxazoline in THF (453 mg of pure compound, 33%).

$^1\text{H}$  NMR ( $\text{CDCl}_3$ , 600 MHz, 296 K)  $\delta$  4.33 (pseudo-t,  $J = 8.3$  Hz, 1H,  $\text{CH}_2_{\text{oxa}}$ ), 4.82 (dd,  $J = 8.4$  Hz, 10.1 Hz, 1H,  $\text{CH}_2_{\text{oxa}}$ ), 5.27 (dd,  $J = 8.2$  Hz, 10.1 Hz, 1H,  $\text{CH}_{\text{oxa}}$ ), 7.25-7.42 (m, 5H,  $\text{CH}_{\text{arom}}$ ).

$^{13}\text{C}$  { $^1\text{H}$ } NMR ( $\text{CDCl}_3$ , 150 MHz, 296 K)  $\delta$  70.1 ( $\text{CH}_{\text{oxa}}$ ), 77.4 ( $\text{CH}_2_{\text{oxa}}$ ), 128.1, 128.9, 129.4 ( $\text{CH}_{\text{arom}}$ ), 140.4 ( $\text{C}_{\text{quat arom}}$ ), 143.5 (NCO).

HRMS (EI):  $m/z$  : calcd for  $\text{C}_9\text{H}_8\text{BrNO}$  ( $[M]^+$ ) 224.9789, found: 224.9740.

(4R, 5S)-2-bromo-4,5-indanediyoaxazoline (12)



*t*BuLi (3 mL, 1.5 M in pentane, 5.1 mmol) was added dropwise to a solution of (4R, 5S)-4,5-indanediyoaxazoline (736 mg, 4.6 mmol) in anhydrous THF (50 mL) at  $-85^\circ\text{C}$ . The bright yellow solution of the anion was allowed to stir at  $-85^\circ\text{C}$  for an additional 0.5 h prior to the addition of 1,2-dibromo-1,1,2,2-tetrafluoroethane (0.6 mL, 5.1 mmol), was subsequently allowed to warm slowly to ambient temperature

overnight, and then concentrated to dryness. The crude product was sublimed to yield the expected 2-bromooxazoline as a white solid (346 mg, 32%).

$^1\text{H}$  NMR ( $\text{CD}_2\text{Cl}_2$ , 400 MHz, 296 K)  $\delta$  3.38 (ddd,  $J = 18.3$  Hz, 1.0 Hz, 0.4 Hz, 1H,  $\text{CH}_2_{\text{Ind}}$ ) 3.52 (dd,  $J = 18.4$  Hz, 6.5 Hz, 1H,  $\text{CH}_2_{\text{Ind}}$ ) 5.56 (ddd,  $J = 7.9$  Hz, 6.5 Hz, 1.7 Hz, 1H,  $\text{OCH}_{\text{oxa}}$ ) 5.61 (d,  $J = 7.9$  Hz, 1H,  $\text{NCH}_{\text{oxa}}$ ) 7.34 (m, 3H,  $\text{CH}_{\text{arom}}$ ) 7.48 (m, 1H,  $\text{CH}_{\text{arom}}$ ).

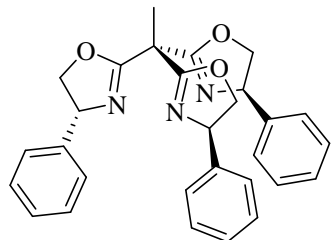
$^{13}\text{C}$  { $^1\text{H}$ } NMR ( $\text{CD}_2\text{Cl}_2$ , 100 MHz, 296 K)  $\delta$  39.3 ( $\text{CH}_2$ ), 76.9 ( $\text{NCH}_{\text{oxa}}$ ), 86.7 ( $\text{OCH}_{\text{oxa}}$ ), 125.3, 125.4, 127.6, 128.9 ( $\text{CH}_{\text{arom}}$ ), 139.6, 140.5 ( $\text{C}_{\text{quat-arom}}$ ), 150.4 (NCO).

$^{15}\text{N}$  NMR ( $\text{CD}_2\text{Cl}_2$ , 60 MHz, 296 K)  $\delta$  238.0 (N).

HRMS (FAB):  $m/z$  : calcd for  $C_{10}H_8BrNO$  ( $[M]^+$ ) 236.9789, found: 236.9782.

#### 4. $C_3$ -symmetric trisoxazolines

##### 1,1,1-tris[(4*R*)-4-phenyloxazolin-2-yl]ethane (13)



*t*BuLi (1.2 mL, 1.7 M in pentane, 2 mmol) was added dropwise to a solution of 1,1-bis[(4*R*)-4-phenyloxazolin-2-yl]ethane (535 mg, 1.8 mmol) in THF (60 mL) at  $-78^\circ\text{C}$ . The resulting yellow solution was stirred for an additional 30 minutes prior to the addition of 1.2 equivalent of (4*R*)-2-bromo-4-phenyloxazoline (453 mg, 2 mmol). The reaction mixture was allowed to warm slowly to room temperature for 12 h and then concentrated to remove the pentane and finally the Schlenk tube was sealed. The stirred solution was heated at  $70^\circ\text{C}$  for five days. The resulting orange solution was evaporated to dryness. The residue was redissolved in dichloromethane (100 mL) and washed with water (10 mL). The organic extract was dried over  $\text{Na}_2\text{SO}_4$  and concentrated *in vacuo* to give a yellow solid. Purification by crystallisation from  $\text{CH}_2\text{Cl}_2$ /pentane gave the desired product (470 mg, 60% yield).

$^1\text{H}$  NMR (200 MHz,  $\text{CDCl}_3$ , 296 K)  $\delta$  2.06 (s, 3H,  $\text{CH}_3$ ), 4.27 (dd,  $J = 7.8$  Hz, 8.3 Hz, 3H,  $\text{CH}_2_{\text{oxa}}$ ), 4.76 (dd,  $J = 8.3$  Hz, 10.1 Hz, 3H,  $\text{CH}_2_{\text{oxa}}$ ), 5.32 (dd,  $J = 7.7$  Hz, 10.1 Hz, 3H,  $\text{CH}_{\text{oxa}}$ ), 7.30 (m, 15H,  $\text{CH}_{\text{arom}}$ ).

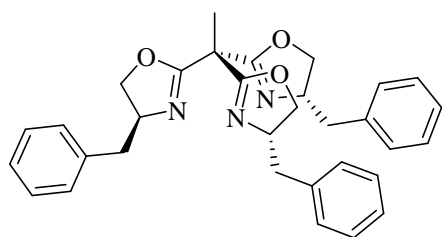
$^{13}\text{C}$  { $^1\text{H}$ } NMR (50 MHz,  $\text{CDCl}_3$ , 296 K)  $\delta$  21.4 ( $\text{CH}_3$ ), 45.2 ( $(\text{CH}_3)\text{C}(\text{oxa})_3$ ), 69.7 ( $\text{CH}_{\text{oxa}}$ ), 76.0 ( $\text{CH}_2_{\text{oxa}}$ ), 126.9, 127.6, 128.7 ( $\text{C}_{\text{arom}}$ ), 142.1 ( $\text{C}_{\text{quat-arom}}$ ), 166.1 (NCO).

FT-IR (KBr):  $\nu$  1665  $\text{cm}^{-1}$  (s,  $\nu_{\text{C=N}}$ ).

MS (EI):  $m/z$  (%): 465.7 (92)  $[M]^+$ .

elemental analysis calcd (%) for  $\text{C}_{29}\text{H}_{27}\text{N}_3\text{O}_3$ : C 74.82, H 5.85, N 9.03; found: C 74.70, H 5.81, N 8.99.

##### 1,1,1-tris[(4*S*)-4-benzyloxazolin-2-yl]ethane (14)



*t*BuLi (1.8 mL, 1.5 M in pentane, 2.6 mmol) was added dropwise to a solution of 1,1-bis[(4*S*)-4-benzyloxazolin-2-yl]ethane (768 mg, 2.2 mmol) in THF (80 mL) at  $-78^\circ\text{C}$ . The resulting yellow solution was stirred for an additional 30 minutes prior to the addition of 1.2 equivalents of (4*S*)-2-bromo-4-benzyloxazoline (634 mg, 2.6 mmol). The reaction mixture was allowed to warm slowly to room temperature for 12 hours and then concentrated to remove the

pentane and finally the Schlenk tube was sealed. The stirred solution was heated at 70°C for three days. The resulting orange solution was evaporated to dryness. The residue was redissolved in dichloromethane (100 mL) and washed with water (10 mL). The organic extract was dried over Na<sub>2</sub>SO<sub>4</sub> and concentrated *in vacuo* to give an orange oil. Purification by flash chromatography (CH<sub>2</sub>Cl<sub>2</sub>/MeOH/Et<sub>3</sub>N, 97/3/1) gave the desired product as a white solid (620 mg, 56% yield).

<sup>1</sup>H NMR (400 MHz, CDCl<sub>3</sub>, 296 K) δ 1.76 (s, 3H, CH<sub>3</sub>), 2.68 (dd, *J* = 8.5 Hz, 13.7 Hz, 3H, CH<sub>2</sub><sub>Bn</sub>), 3.11 (dd, *J* = 5.1 Hz, 13.7 Hz, 3H, CH<sub>2</sub><sub>Bn</sub>), 4.07 (dd, *J* = 6.9 Hz, 8.3 Hz, 3H, CH<sub>2</sub><sub>oxa</sub>), 4.23 (dd, *J* = 8.5 Hz, 9.0 Hz, 3H, CH<sub>2</sub><sub>oxa</sub>), 4.46 (m, 3H, CH<sub>oxa</sub>), 7.24 (m, 15H, CH<sub>arom</sub>).

<sup>13</sup>C {<sup>1</sup>H} NMR (100 MHz, CDCl<sub>3</sub>, 296 K) δ 20.9 (CH<sub>3</sub>), 41.2 (CH<sub>2</sub><sub>Bn</sub>), 44.6 ((CH<sub>3</sub>)C(oxa)<sub>3</sub>), 67.2 (CH<sub>oxa</sub>), 72.5 (CH<sub>2</sub><sub>oxa</sub>), 126.4, 128.4, 129.4 (C<sub>arom</sub>), 137.7 (C<sub>quat-arom</sub>), 165.0 (NCO).

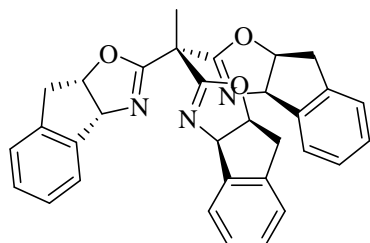
<sup>15</sup>N NMR (60 MHz, CDCl<sub>3</sub>, 296 K) δ 234 (N).

FT-IR (KBr): ν 1664 cm<sup>-1</sup> (s, ν<sub>C=N</sub>).

MS (FAB): *m/z* (%): 508.5 (100) [M]<sup>+</sup>.

elemental analysis calcd (%) for C<sub>32</sub>H<sub>33</sub>N<sub>3</sub>O<sub>3</sub>: C 75.71, H 6.55, N 8.28; found: C 75.55, H 6.52, N 8.33.

### 1,1,1-tris[(4*R*, 5*S*)-4,5-indanediylloxazolin-2-yl]ethane (15)



*t*BuLi (0.52 mL, 1.5 M in pentane, 0.77 mmol) was added dropwise to a solution of 1,1-bis[(4*R*, 5*S*)-4,5-indanediylloxazolin-2-yl]ethane (222 mg, 0.64 mmol) in toluene (60 mL) at -85°C. The resulting yellow solution was stirred for an additional 30 minutes prior to the addition of a solution of (4*R*, 5*S*)-2-bromo-4,5-indanediylloxazoline (346 mg, 1.45 mmol) in cold toluene (4 mL). The reaction mixture was allowed to warm slowly to room temperature for 12 h and then concentrated to remove the pentane and finally the Schlenk tube was sealed. The stirred solution was heated at 60°C for two days. The resulting orange solution was evaporated to dryness. The residue was redissolved in dichloromethane (100 mL) and washed with a saturated aqueous solution of NaHCO<sub>3</sub> (10 mL) and brine (10 mL). The organic extract was dried over Na<sub>2</sub>SO<sub>4</sub> and concentrated *in vacuo* to give an orange foam. Purification by flash chromatography (Hexane /EtOAc, 80/20) gave the desired product as a yellowish solid (100 mg, 31% yield).

<sup>1</sup>H NMR (400 MHz, CD<sub>2</sub>Cl<sub>2</sub>, 296 K) δ 1.60 (s, 3H, CH<sub>3</sub>), 3.04 (dd, *J* = 1.8 Hz, 18.0 Hz, 3H, CH<sub>2</sub><sub>ind</sub>), 3.33 (dd, *J* = 7.2 Hz, 18.1 Hz, 3H, CH<sub>2</sub><sub>ind</sub>), 5.29 (ddd, *J* = 2.1 Hz, 7.2 Hz, 8.0 Hz, 3H,

OCH<sub>oxa</sub>), 5.49 (d,  $J = 8.0$  Hz, 3H, NCH<sub>oxa</sub>) 7.25 (m, 9H, CH<sub>arom</sub>), 7.36 (d,  $J = 7.2$  Hz, 3H, CH<sub>arom</sub>).

<sup>13</sup>C {<sup>1</sup>H} NMR (100 MHz, CD<sub>2</sub>Cl<sub>2</sub>, 296 K)  $\delta$  21.3 (CH<sub>3</sub>), 22.4 ((CH<sub>3</sub>)C(oxa)<sub>3</sub>), 39.9 (CH<sub>2</sub> Ind), 76.9 (NCH<sub>oxa</sub>), 84.0 (OCH<sub>oxa</sub>), 125.5, 125.8, 127.5, 128.7 (C<sub>arom</sub>), 140.4, 141.9 (C<sub>quat-arom</sub>), 164.7 (NCO).

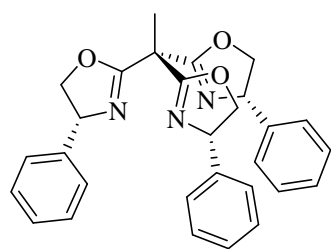
FT-IR (KBr):  $\nu$  1653 cm<sup>-1</sup> (s,  $\nu_{C=N}$ ).

MS (FAB):  $m/z$  (%): 502.4 (100) [M]<sup>+</sup>.

elemental analysis calcd (%) for C<sub>32</sub>H<sub>27</sub>N<sub>3</sub>O<sub>3</sub>: C 76.63, H 5.43, N 8.38; found: C 76.50, H 5.47, N 8.45.

### 5. C<sub>1</sub>-symmetric trisoxazolines

#### 1-((4R)-4-phenyloxazolin-2-yl)-1,1-di((4S)-4-phenyloxazolin-2-yl)ethane (**16**)



*t*BuLi (2 mL, 1.5 M in pentane, 3 mmol) was added dropwise to a solution of 1,1-bis[(4S)-4-phenyloxazolin-2-yl]ethane (794 mg, 2.5 mmol) in THF (80 mL) at -78°C. The resulting orange solution was stirred for an additional 30 minutes prior to the addition of 1.2 equivalent of (4R)-2-bromo-4-phenyloxazoline (673 mg, 3 mmol). The solution was allowed to warm slowly to room temperature for 12 hours and then concentrated to remove the pentane and finally the Schlenk tube was sealed. The stirred solution was heated at 70°C for five days. The resulting orange solution was evaporated to dryness. The residue was redissolved in dichloromethane (100 mL) and washed with water (10 mL). The organic extract was dried over Na<sub>2</sub>SO<sub>4</sub> and concentrated *in vacuo* to give an orange oil. Purification by flash chromatography (Hexane/EtOAc, 50/50) gave the desired product as a slightly orange solid (350 mg, 30% yield).

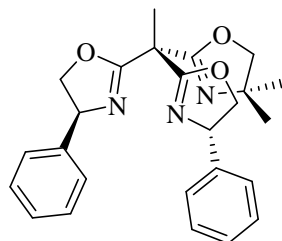
<sup>1</sup>H NMR (CDCl<sub>3</sub>, 400 MHz, 296 K)  $\delta$  1.38 (s, 3H, CH<sub>3</sub> oxa), 1.39 (s, 3H, CH<sub>3</sub> oxa), 2.04 (s, 3H, CH<sub>3</sub> apical), 4.11 (d,  $J = 8.0$  Hz, 1H, CH<sub>2</sub> methyl oxa), 4.13 (d,  $J = 8.0$  Hz, 1H, CH<sub>2</sub> methyl oxa), 4.26 (dd,  $J = 2.5$  Hz, 8.0 Hz, 1H, CH<sub>2</sub> phenyl oxa), 4.28 (dd,  $J = 2.4$  Hz, 7.9 Hz, 1H, CH<sub>2</sub> phenyl oxa), 4.78 (m, 2H, CH<sub>2</sub> phenyl oxa), 5.32 (dd,  $J = 7.7$  Hz, 9.8 Hz, 1H, CH oxa), 5.35 (dd,  $J = 7.6$  Hz, 10.0 Hz, 1H, CH oxa), 7.25-7.38 (m, 5H, CH<sub>arom</sub>).

<sup>13</sup>C {<sup>1</sup>H} NMR (CDCl<sub>3</sub>, 100 MHz, 296 K)  $\delta$  21.6 (CH<sub>3</sub> apical) 27.9 (CH<sub>3</sub> oxa), 44.8 ((CH<sub>3</sub>)C(oxa)<sub>3</sub>), 67.5 (C<sub>quat</sub> methyl oxa), 69.5 (CH), 75.8, 75.9 (CH<sub>2</sub> phenyl oxa), 79.8 (CH<sub>2</sub> methyl oxa), 126.8, 126.9, 127.4, 127.5, 128.5, 128.6 (CH<sub>arom</sub>), 142.2 (C<sub>quat</sub> arom), 163.0 (NCO methyl oxa), 166.2, 166.3 (NCO phenyl oxa).

HRMS (FAB):  $m/z$  : calcd for C<sub>29</sub>H<sub>28</sub>N<sub>3</sub>O<sub>3</sub> ([M+H]<sup>+</sup>) 466.2131, found: 466.2137.

elemental analysis calcd (%) C<sub>29</sub>H<sub>27</sub>N<sub>3</sub>O<sub>3</sub>: C 74.82, H 5.85, N 9.03; found: C 74.80, H 5.81, N 9.10.

1,1-Bis((4*S*)-4-phenyloxazolin-2-yl)-1-(4,4-dimethyloxazolin-2-yl)ethane (17)



*t*BuLi (4.4 mL, 1.5 M in pentane, 6.6 mmol) was added dropwise to a solution of 1,1-bis[(4*S*)-4-phenyloxazolin-2-yl]ethane (1.8 g, 5.5 mmol) in THF (100 mL) at -78°C. The resulting red solution was stirred for an additional 30 minutes prior to the addition of 1.2 equivalents of 2-bromo-4,4-dimethyloxazoline (1.17 mg, 6.6 mmol), was subsequently

allowed to warm slowly to room temperature for 12 hours and then concentrated to remove the pentane and finally the Schlenk tube was sealed. The stirred solution was heated at 70°C for four days. The resulting orange solution was evaporated to dryness. The residue was redissolved in dichloromethane (100 mL) and washed with water (10 mL). The organic extract was dried over Na<sub>2</sub>SO<sub>4</sub> and concentrated *in vacuo* to give an orange oil. Purification by flash chromatography (Hexane/EtOAc, 95/5 to 50/50) gave the desired product as a white solid (906 mg, 39% yield). <sup>1</sup>H NMR (CDCl<sub>3</sub>, 400 MHz, 296 K) δ 2.13 (s, 3H, CH<sub>3</sub>), 4.27-4.34 (m, 3H, CH<sub>2</sub>), 4.79-4.85 (m, 3H, CH<sub>2</sub>), 5.33-5.41 (m, 3H, CH), 7.25-7.42 (m, 15H, CH<sub>arom</sub>).

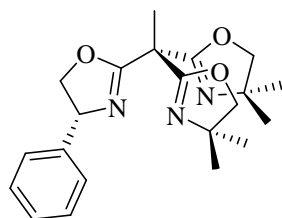
<sup>13</sup>C {<sup>1</sup>H} NMR (CDCl<sub>3</sub>, 100 MHz, 296 K) δ 21.7 (CH<sub>3</sub>), 45.1 ((CH<sub>3</sub>)C(oxa)<sub>3</sub>), 69.6, 69.6, 69.6 (CH), 75.9, 75.9, 76.0 (CH<sub>2</sub>), 126.8, 126.8, 126.9, 127.6, 127.6, 127.6, 128.6, 128.7, 128.7 (CH<sub>arom</sub>), 142.0, 142.1 (C<sub>quat arom</sub>), 165.9, 166.0, 166.1 (NCO).

FT-IR (KBr): ν 1654, 1677 cm<sup>-1</sup> (s, ν<sub>C=N</sub>).

HRMS (FAB): *m/z* : calcd for C<sub>25</sub>H<sub>28</sub>N<sub>3</sub>O<sub>3</sub> ([*M*+H]<sup>+</sup>) 418.2131, found: 418.2118.

elemental analysis calcd (%) C<sub>25</sub>H<sub>27</sub>N<sub>3</sub>O<sub>3</sub>: C 71.92, H 6.52, N 10.06; found: C 71.85, H 6.50, N 10.10.

1-((4*R*)-4-phenyloxazolin-2-yl)-1,1-di(4,4-dimethyloxazolin-2-yl)ethane (18)



*t*BuLi (1.7 mL, 1.5 M in pentane, 2.6 mmol) was added dropwise to a solution of 1,1-bis[(4,4-dimethyloxazolin-2-yl)]ethane (485 mg, 2.2 mmol) in THF (80 mL) at -78°C. The resulting bright yellow solution was stirred for an additional 30 minutes prior to the addition of 1.2 equivalents of (4*R*)-2-bromo-4-phenyloxazoline (588 mg, 2.6 mmol),

was subsequently allowed to warm slowly to room temperature for 12 hours and then concentrated to remove the pentane and finally the Schlenk tube was sealed. The stirred solution was heated at 75°C for five days. The resulting orange solution was evaporated to dryness. The

residue was redissolved in dichloromethane (100 mL) and washed with water (10 mL). The organic extract was dried over Na<sub>2</sub>SO<sub>4</sub> and concentrated *in vacuo* to give an orange oil. Purification by flash chromatography (Hexane/EtOAc, 50/50) gave the desired product as an orange oil (360 mg, 45% yield).

<sup>1</sup>H NMR (CDCl<sub>3</sub>, 400 MHz, 296 K)  $\delta$  1.30 (s, 3H, CH<sub>3</sub> oxa), 1.31 (s, 9H, CH<sub>3</sub> oxa), 1.91 (s, 3H, CH<sub>3</sub> apical), 4.00 (d, *J* = 8.0 Hz, 1H, CH<sub>2</sub> methyl oxa), 4.01 (d, *J* = 8.0 Hz, 1H, CH<sub>2</sub> methyl oxa), 4.04 (d, *J* = 8.0 Hz, 1H, CH<sub>2</sub> methyl oxa), 4.05 (d, *J* = 8.0 Hz, 1H, CH<sub>2</sub> methyl oxa), 4.17 (pseudo-t, *J* = 8.1 Hz, 1H, CH<sub>2</sub> phenyl oxa), 4.69 (dd, *J* = 8.4 Hz, 10.1 Hz, 1H, CH<sub>2</sub> phenyl oxa), 5.24 (dd, *J* = 8.4 Hz, 10.1 Hz, 1H, CH<sub>2</sub> phenyl oxa), 7.23-7.34 (m, 5H, CH<sub>arom</sub>).

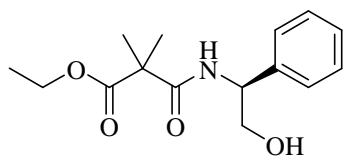
<sup>13</sup>C {<sup>1</sup>H} NMR (CDCl<sub>3</sub>, 100 MHz, 296 K)  $\delta$  21.8 (CH<sub>3</sub> apical) 27.8 (CH<sub>3</sub> oxa), 44.4 ((CH<sub>3</sub>)C(oxa)<sub>3</sub>), 67.3, 67.4 (C<sub>quat</sub> methyl oxa), 69.4 (CH), 75.8 (CH<sub>2</sub> phenyl oxa), 79.6, 79.7 (CH<sub>2</sub> methyl oxa), 126.8, 127.5, 128.5 (CH<sub>arom</sub>), 142.4 (C<sub>quat</sub> arom), 163.1, 163.2 (NCO<sub>methyl oxa</sub>), 166.4 (NCO<sub>phenyl oxa</sub>).

HRMS (FAB): *m/z* : calcd for C<sub>21</sub>H<sub>28</sub>N<sub>3</sub>O<sub>3</sub> ([*M*+H]<sup>+</sup>) 370.2131, found: 370.2135.

## 6. Precursors of the non-symmetric bisoxazolines

Monoethyl malonate was synthesised according to a procedure described by Strube.<sup>21</sup>

### 2,2-dimethyl malonic acid ethyl monoester *N*-((*S*)-2-hydroxy-1-phenylethyl) monoamide (19)



To a solution of monoethyl malonate (6.54 g, 41 mmol) in CH<sub>2</sub>Cl<sub>2</sub> (250 mL) DCC (9.3 g, 45 mmol) and HOBT (6.1 g, 45 mmol) were added under argon flow. After 2 hours stirring, (*S*)-phenylglycinol (6.1 g, 45 mmol) was added and the solution was

stirred at room temperature for 3 days. The reaction mixture was filtered through Celite to remove the DCU formed and washed with CH<sub>2</sub>Cl<sub>2</sub> (4 x 100 mL). The organic solution is washed with an aqueous solution of KHCO<sub>3</sub> 10% (350 mL), with H<sub>2</sub>O (300 mL) and with brine (300 mL) and is then dried over Na<sub>2</sub>SO<sub>4</sub>. Evaporation of the solvent gave the product as a white solid (9.8 g, 86% yield). The compound was used in the next step without further purification.

<sup>1</sup>H NMR (CDCl<sub>3</sub>, 400 MHz, 296 K)  $\delta$  1.31 (t, *J* = 7.1 Hz, 3H, CH<sub>3</sub> ethyl), 1.52 (s, 3H, CH<sub>3</sub> bridge), 1.53 (s, 3H, CH<sub>3</sub> bridge), 2.56 (br s, 1H, OH), 3.91 (pseudo-t, *J* = 3.9 Hz, 2H, CH<sub>2</sub> future oxa), 4.25 (q, *J* = 7.1 Hz, 2H, CH<sub>2</sub> ethyl), 5.10 (m, 1H, CH), 7.25 (d, *J* = 6.3 Hz, 1H, NH), 7.31-7.35 (m, 3H, CH<sub>arom</sub>), 7.39-7.42 (m, 2H, CH<sub>arom</sub>).

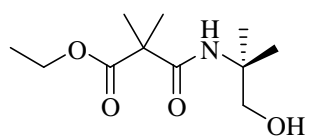
<sup>21</sup> R. E. Strube, *Org. Synth.* **1963**, *4*, 417.

$^{13}\text{C}$   $\{^1\text{H}\}$  NMR ( $\text{CDCl}_3$ , 100 MHz, 296 K)  $\delta$  13.9 ( $\text{CH}_3$  ethyl), 23.6, 23.8 ( $\text{CH}_3$  bridge), 49.9 ( $\text{C}_{\text{quat}}$  bridge), 55.9 ( $\text{CH}$ ), 61.7 ( $\text{CH}_2$  ethyl), 66.5 ( $\text{CH}_2$  future oxa), 126.5, 127.8, 128.8 ( $\text{C}_{\text{arom}}$ ), 138.9 ( $\text{C}_{\text{quat}}$  arom), 172.3 (OCO), 174.9 (NCO).

MS (FAB):  $m/z$  (%): 262.1 (11)  $[M-\text{OH}]^+$ , 280.1 (100)  $[M+\text{H}]^+$ .

HRMS (FAB):  $m/z$ : calcd for  $\text{C}_{15}\text{H}_{22}\text{NO}_4$  ( $[M+\text{H}]^+$ ) 280.1549, found: 280.1521.

### 2,2-dimethyl malonic acid ethyl monoester N-(2-hydroxy-1,1-dimethylethyl) monoamide (20)



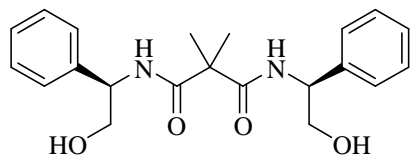
To a solution of monoethyl malonate (5.84 g, 36.5 mmol) in  $\text{CH}_2\text{Cl}_2$  (250 mL) DCC (8.3 g, 40.1 mmol) and HOBT (5.4 g, 40.1 mmol) were added under argon flow. After 2 hours stirring, 2-amino 2-methyl 1-propanol (3.6 g, 40.1 mmol) was added and the solution was stirred at room temperature for 3 days. The reaction mixture was filtered through Celite to remove the DCU formed and washed with  $\text{CH}_2\text{Cl}_2$  (4 x 80 mL). The organic solution is washed with an aqueous solution of  $\text{KHCO}_3$  10% (100 mL), with  $\text{H}_2\text{O}$  (100 mL) and with brine (100 mL) and is then dried over  $\text{Na}_2\text{SO}_4$ . After evaporation of the solvent the crude product was purified by flash chromatography (Hexane/EtOAc, 50/50) to give the product as a colorless oil (3.8 g, 45% yield).  $^1\text{H}$  NMR ( $\text{CDCl}_3$ , 400 MHz, 296 K)  $\delta$  1.26 (m, 9H,  $\text{CH}_3$  ethyl,  $\text{CH}_3$  future oxa), 1.41 (s, 6H,  $\text{CH}_3$  bridge), 3.56 (s, 2H,  $\text{CH}_2$  future oxa), 4.18 (q,  $J = 7.1$  Hz, 2H,  $\text{CH}_2$  ethyl), 4.33 (br s, 1H, OH), 6.48 (br s, 1H, NH).

$^{13}\text{C}$   $\{^1\text{H}\}$  NMR ( $\text{CDCl}_3$ , 100 MHz, 296 K)  $\delta$  14.0 ( $\text{CH}_3$  ethyl), 23.7 ( $\text{CH}_3$  bridge), 24.5 ( $\text{CH}_3$  future oxa), 50.0 ( $\text{C}_{\text{quat}}$  bridge), 56.0 ( $\text{C}_{\text{quat}}$  future oxa), 61.7 ( $\text{CH}_2$  ethyl), 70.3 ( $\text{CH}_2$  future oxa), 172.7 (NCO), 175.1 (OCO).

MS (FAB):  $m/z$  (%): 200.1 (12)  $[M-\text{CH}_2\text{OH}]^+$ , 214.1 (6)  $[M-\text{OH}]^+$ , 232.1 (100)  $[M+\text{H}]^+$ .

HRMS (FAB):  $m/z$ : calcd for  $\text{C}_{11}\text{H}_{22}\text{NO}_4$  ( $[M+\text{H}]^+$ ): 232.1549, found: 232.1559.

### N-((S)-2-hydroxy-1-phenylethyl)-N'-((R)-2-hydroxy-1-phenylethyl)-dimethylmalonamide (21)



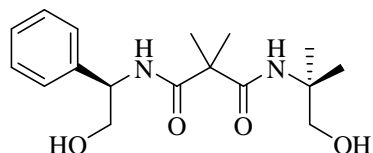
A solution of (*R*)-phenylglycinol (4.5 g, 32.5 mmol) and 2,2-dimethyl malonic acid ethyl monoester N-((*S*)-2-hydroxy-1-phenylethyl) monoamide (9.1 g, 32.5 mmol) in toluene (20 mL) was heated at  $110^\circ\text{C}$  for 2 days in the presence of a catalytic amount of NaH. The white precipitate obtained was filtered and washed with  $\text{Et}_2\text{O}$  (3 x 40 mL). Evaporation of the solvents gave the product as a white solid (5 g, 42% yield).



$^1\text{H}$  NMR (DMSO- $d_6$ , 200 MHz, 296 K)  $\delta$  1.37 (s, 3H,  $\text{CH}_3$  bridge), 1.39 (s, 3H,  $\text{CH}_3$  bridge), 3.37 (br s, 1H, OH), 3.59 (pseudo-t,  $J = 5.0$  Hz, 4H,  $\text{CH}_2$  future oxa), 4.89 (m, 2H, CH), 7.17-7.31 (m, 10H,  $\text{CH}_{\text{arom}}$ ), 7.25 (d,  $J = 7.8$  Hz, 2H, NH).

$^{13}\text{C}$   $\{^1\text{H}\}$  NMR (DMSO- $d_6$ , 50 MHz, 296 K)  $\delta$  23.1, 24.1 ( $\text{CH}_3$  bridge), 49.4 ( $\text{C}_{\text{quat}}$  bridge), 55.4 (CH), 64.4 ( $\text{CH}_2$  future oxa), 126.6, 126.8, 128.0 ( $\text{C}_{\text{arom}}$ ), 141.2 ( $\text{C}_{\text{quat}}$  arom), 172.7 (OCN).

### N-((R)-2-hydroxy-1-phenylethyl)-N'-(2-hydroxy-1,1-dimethylethyl)-dimethylmalonamide (22)



(*R*)-phenylglycinol (730 mg, 5.3 mmol) and 2,2-dimethyl malonic acid ethyl monoester *N*-(2-hydroxy-1,1-dimethylethyl) monoamide (1.23 g, 5.3 mmol) were heated at 110°C for 3 hours in the presence of catalytic amount of NaH. After evaporation of

the ethanol formed the crude product was purified by flash chromatography ( $\text{CH}_2\text{Cl}_2/\text{MeOH}$ , 95/5) to give the product as a colorless oil (943 mg, 55% yield).

$^1\text{H}$  NMR ( $\text{CDCl}_3$ , 400 MHz, 296 K)  $\delta$  1.22 (s, 3H,  $\text{CH}_3$  future oxa), 1.23 (s, 3H,  $\text{CH}_3$  future oxa), 1.44 (s, 3H,  $\text{CH}_3$  bridge), 1.46 (s, 3H,  $\text{CH}_3$  bridge), 3.48 (d,  $J = 11.5$  Hz, 1H,  $\text{CH}_2$  methyl side), 3.63 (d,  $J = 11.5$  Hz, 1H,  $\text{CH}_2$  methyl side), 3.79 (ddd,  $J = 1.0$  Hz, 4.0 Hz, 11.5 Hz, 1H,  $\text{CH}_2$  phenyl side), 3.88 (dd,  $J = 6.1$  Hz, 11.5 Hz, 1H,  $\text{CH}_2$  phenyl side), 5.03 (ddd,  $J = 4.1$  Hz, 6.5 Hz, 7.0 Hz, 1H, CH phenyl side), 6.51 (br s, 1H, NH methyl side), 7.11 (s,  $J = 7.3$  Hz, 1H, NH phenyl side) 7.23-7.35 (m, 5 H,  $\text{CH}_{\text{arom}}$ ).

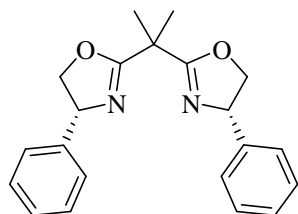
$^{13}\text{C}$   $\{^1\text{H}\}$  NMR ( $\text{CDCl}_3$ , 100 MHz, 296 K)  $\delta$  23.7, 23.8 ( $\text{CH}_3$  bridge), 24.0, 24.5 ( $\text{CH}_3$  future oxa), 50.0 ( $\text{C}_{\text{quat}}$  bridge), 55.7 ( $\text{C}_{\text{quat}}$  methyl side), 55.9 (CH), 66.2 ( $\text{CH}_2$  phenyl side), 69.6 ( $\text{CH}_2$  methyl side), 126.4, 128.0, 128.9 ( $\text{CH}_{\text{arom}}$ ), 138.7 ( $\text{C}_{\text{quat}}$  arom), 173.9, 174.0 (CO).

MS (FAB):  $m/z$  (%): 305.1 (36) [ $M\text{-OH}$ ] $^+$ , 323.2 (100) [ $M\text{+H}$ ] $^+$ .

HRMS (FAB):  $m/z$  : calcd for  $\text{C}_{17}\text{H}_{27}\text{N}_2\text{O}_4$  ( $[M\text{+H}]$ ) 323.1971, found: 323.2009.

## 7. Mixed bisoxazolines

### 1-((4R)-4-phenyloxazolin-2-yl)-1-((4S)-4-phenyloxazolin-2-yl)-1-methylethane (23)



To an ice-cooled solution of *N*-((*S*)-2-hydroxy-1-phenylethyl)-*N'*-((*R*)-2-hydroxy-1-phenylethyl)-dimethylmalonamide (4.8 g, 13 mmol), triethylamine (14.5 mL, 104 mmol) and DMAP (160 mg, 1.3 mmol) in  $\text{CH}_2\text{Cl}_2$  (200 mL) a solution of TsCl (5.4 g, 28.5 mmol) in  $\text{CH}_2\text{Cl}_2$  (30 mL) was slowly added. The mixture was warmed to room temperature, stirred for 10 days and washed with a saturated aqueous solution of  $\text{NH}_4\text{Cl}$  and brine. The organic phase was dried over  $\text{Na}_2\text{SO}_4$  and concentrated *in vacuo* to give a dark brown

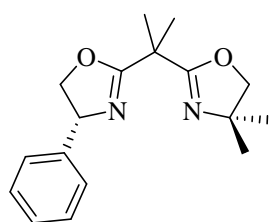
oil. Purification by flash chromatography (Hexane/EtOAc, 80/20) gave the desired product as a yellowish oil (3.7 g, 86% yield).

$^1\text{H}$  NMR ( $\text{CDCl}_3$ , 400 MHz, 296 K)  $\delta$  1.73 (s, 3H,  $\text{CH}_3$ ), 1.76 (s, 3H,  $\text{CH}_3$ ), 4.22 (pseudo-t,  $J = 8.1$  Hz, 2H,  $\text{CH}_2$ ), 4.72 (dd,  $J = 8.4$  Hz, 10.1 Hz, 2H,  $\text{CH}_2$ ), 5.28 (dd,  $J = 7.7$  Hz, 10.1 Hz, 2H,  $\text{CH}$ ), 7.25-7.35 (m, 10 H,  $\text{CH}_{\text{arom}}$ ).

$^{13}\text{C}$   $\{^1\text{H}\}$  NMR ( $\text{CDCl}_3$ , 100 MHz, 296 K)  $\delta$  24.4, 24.7 ( $\text{CH}_3$ ), 38.9 ( $\text{C}_{\text{quat bridge}}$ ), 69.5 ( $\text{CH}$ ), 75.5 ( $\text{CH}_2$ ), 126.6, 127.6, 128.7 ( $\text{CH}_{\text{arom}}$ ), 142.4 ( $\text{C}_{\text{quat arom}}$ ), 170.3 ( $\text{NCO}_{\text{phenyl oxa}}$ ).

HRMS (FAB):  $m/z$ : calcd for  $\text{C}_{21}\text{H}_{23}\text{N}_2\text{O}_2$  ( $[\text{M}+\text{H}]^+$ ) 335.1760, found: 335.1771.

1-((4R)-4-phenyloxazolin-2-yl)-1-(4,4-dimethyloxazolin-2-yl)-1-methylethane (24)



To a cooled solution ( $0^\circ\text{C}$ ) of N-((R)-2-hydroxy-1-phenylethyl)-N'-(2-hydroxy-1,1-dimethylethyl)-dimethylmalonamide (737 mg, 2.29 mmol) in  $\text{CH}_2\text{Cl}_2$  (150 mL) was added dropwise  $\text{SOCl}_2$  (0.80 mL, 10.9 mmol). The reaction mixture was stirred overnight at ambient temperature, cooled to  $0^\circ\text{C}$  and quenched by addition of aqueous  $\text{NaHCO}_3$

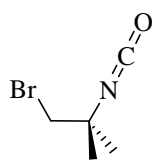
(65 mL). After an additional 5 min of stirring, the aqueous phase was separated and extracted with  $\text{CH}_2\text{Cl}_2$  (3 x 70 mL). The combined organic phases were dried over  $\text{Na}_2\text{SO}_4$  and the solvent was evaporated to give 800 mg of the chlorinated compound. The colorless oil was used directly without further purification. A solution of the chlorinated product (800 mg, 2.23 mmol) and  $\text{NaOH}$  (223 mg, 5.58 mmol) in ethanol (125 mL) was heated to reflux for 3 hours and then cooled to room temperature followed by evaporation of the solvent under reduced pressure. To the resulting crude product was added in  $\text{CH}_2\text{Cl}_2$  (50 mL) and a saturated aqueous solution of  $\text{NH}_4\text{Cl}$  (40 mL), the phases were separated and the aqueous layer was extracted with  $\text{CH}_2\text{Cl}_2$  (3 x 50 mL). The combined organic phases were dried over  $\text{Na}_2\text{SO}_4$  and the solvent was evaporated to give the oily yellowish crude product. Purification by flash chromatography (Hexane/EtOAc, 50/50) gave the product as a colorless oil (391 mg, 60% yield).

$^1\text{H}$  NMR ( $\text{CDCl}_3$ , 600 MHz, 296 K)  $\delta$  1.30 (s, 6H,  $\text{CH}_3_{\text{oxa}}$ ), 1.58 (s, 3H,  $\text{CH}_3_{\text{bridge}}$ ), 1.60 (s, 3H,  $\text{CH}_3_{\text{bridge}}$ ), 3.97 (s, 2H,  $\text{CH}_2_{\text{methyl oxa}}$ ), 4.11 (pseudo-t,  $J = 8.0$  Hz, 1H,  $\text{CH}_2_{\text{phenyl oxa}}$ ), 4.62 (dd,  $J = 8.4$  Hz, 10.1 Hz, 1H,  $\text{CH}_2_{\text{phenyl oxa}}$ ), 5.19 (dd,  $J = 7.6$  Hz, 10.1 Hz, 1H,  $\text{CH}_{\text{oxa}}$ ), 7.23-7.35 (m, 5H,  $\text{CH}_{\text{arom}}$ ).

$^{13}\text{C}$   $\{^1\text{H}\}$  NMR ( $\text{CDCl}_3$ , 150 MHz, 296 K)  $\delta$  24.4, 24.5 ( $\text{CH}_3_{\text{bridge}}$ ), 28.0, 28.1 ( $\text{CH}_3_{\text{oxa}}$ ), 38.5 ( $\text{C}_{\text{quat bridge}}$ ), 67.1 ( $\text{C}_{\text{quat methyl oxa}}$ ), 69.4 ( $\text{CH}$ ), 75.5 ( $\text{CH}_2_{\text{phenyl oxa}}$ ), 79.4 ( $\text{CH}_2_{\text{methyl oxa}}$ ), 126.6, 127.5, 128.6 ( $\text{CH}_{\text{arom}}$ ), 142.5 ( $\text{C}_{\text{quat arom}}$ ), 167.4 ( $\text{NCO}_{\text{methyl oxa}}$ ), 170.5 ( $\text{NCO}_{\text{phenyl oxa}}$ ).

HRMS (FAB):  $m/z$ : calcd for  $\text{C}_{17}\text{H}_{23}\text{N}_2\text{O}_2$  ( $[\text{M}+\text{H}]^+$ ) 287.1760, found: 287.1757.

## 8. Isocyanate derivatives

1-bromo-2-isocyanato-2-methylpropane (25)

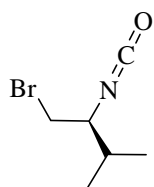
2-bromo-4,4-dimethyloxazoline in THF was heated at 65°C over 1 d. The resulting brown mixture was purified by bulb to bulb distillation to give the product as a colorless oil.

$^1\text{H}$  NMR ( $\text{CDCl}_3$ , 600 MHz, 296 K)  $\delta$  1.49 (s, 6H,  $\text{CH}_3$ ), 3.48 (s, 2H,  $\text{CH}_2$ ).

$^{13}\text{C}$  { $^1\text{H}$ } NMR ( $\text{CDCl}_3$ , 150 MHz, 296 K)  $\delta$  25.6 ( $\text{CH}_3$ ), 28.7 ( $\text{CH}_2$ ), 57.6 ( $\text{C}_{\text{quat}}$  methyl), 141.5 (NCO).

$^{15}\text{N}$  NMR ( $\text{CDCl}_3$ , 60 MHz, 296 K)  $\delta$  51.7 (NCO).

HRMS (EI):  $m/z$  : calcd for  $\text{C}_5\text{H}_8\text{BrNO}$  ( $[M]^+$ ) 176.9789, found: 176.9791.

(2S)-1-bromo-2-isocyanato-3-methylbutane (26)

(4S)-2-bromo-4-isopropyloxazoline in THF was heated at 95°C over 2 d. The resulting brown mixture was purified by bulb to bulb distillation to give a colorless oil.

$^1\text{H}$  NMR ( $\text{CDCl}_3$ , 600 MHz, 296 K)  $\delta$  0.99 (d,  $J = 6.7$  Hz, 3H,  $\text{CH}_3$  isopropyl), 1.01

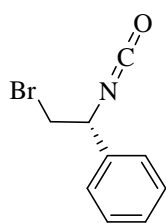
(d,  $J = 6.8$  Hz, 3H,  $\text{CH}_3$  isopropyl), 1.97 (m, 1H,  $\text{CH}$  isopropyl), 3.49 (m, 1H,  $\text{CH}_2$ ), 3.56 (m, 2H,  $\text{CH}_2$ , CH).

$^{13}\text{C}$  { $^1\text{H}$ } NMR ( $\text{CDCl}_3$ , 150 MHz, 296 K)  $\delta$  17.3 ( $\text{CH}_3$  isopropyl), 19.6 ( $\text{CH}_3$  isopropyl), 32.3 (CH isopropyl), 36.0 ( $\text{CH}_2$ ), 62.7 (CH), 124.0 (NCO).

$^{15}\text{N}$  NMR ( $\text{CDCl}_3$ , 60 MHz, 296 K)  $\delta$  35.5 (NCO)

FT-IR (KBr)  $\nu$  2265  $\text{cm}^{-1}$  (s,  $\nu_{\text{C=N}}$  isocyanate).

HRMS (EI):  $m/z$  : calcd for  $\text{C}_6\text{H}_{10}\text{BrNO}$  ( $[M]^+$ ) 190.9946, found: 190.9947.

(1R)-1-(2-bromo-1-isocyanatoethyl)benzene (27)

(4R)-2-bromo-4-phenyloxazoline in THF was heated at 95°C over 3 d. The resulting brown mixture was purified by bulb to bulb distillation to give a colorless oil.

$^1\text{H}$  NMR ( $\text{CDCl}_3$ , 300 MHz, 296 K)  $\delta$  3.55 (dd,  $J = 9.1$  Hz, 10.6 Hz, 1H,  $\text{CH}_2$  oxa),

3.66 (dd,  $J = 3.9$  Hz, 10.6 Hz, 1H,  $\text{CH}_2$  oxa), 4.95 (dd,  $J = 3.9$  Hz, 9.1 Hz, 1H,

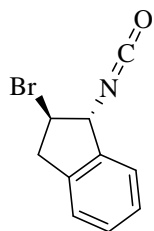
$\text{CH}_{\text{oxa}}$ ), 7.32-7.45 (m, 5H,  $\text{CH}_{\text{arom}}$ ).

$^{13}\text{C}$  { $^1\text{H}$ } NMR ( $\text{CDCl}_3$ , 75 MHz, 296 K)  $\delta$  38.5 ( $\text{CH}_2$  oxa), 60.5 ( $\text{CH}_{\text{oxa}}$ ), 126.1, 128.9, 129.0 (CH arom), 133.7 ( $\text{C}_{\text{quat}}$  arom), 138.0 (NCO).

FT-IR (KBr)  $\nu$  2265  $\text{cm}^{-1}$  (s,  $\nu_{\text{C}=\text{N}}$  isocyanate).

HRMS (EI):  $m/z$  : calcd for  $\text{C}_9\text{H}_8\text{BrNO}$  ( $[M]^+$ ) 224.9789, found: 224.9764.

(1R,2R)-2-bromo-1-isocyanato-2,3-dihydro-1H-indene (28)



Solid (4R, 5S)-2-bromo-4,5-indanediylloxazoline in a Schlenk at  $-78^\circ\text{C}$  was put at room temperature. Rearrangement occurred in the following 2 minutes.

$^1\text{H}$  NMR ( $\text{CD}_2\text{Cl}_2$ , 600 MHz, 296 K)  $\delta$  3.30 (dd,  $J = 8.3$  Hz, 16.0 Hz, 1H,  $\text{CH}_2$  Ind) 3.60 (dd,  $J = 7.3$  Hz, 16.0 Hz, 1H,  $\text{CH}_2$  Ind), 4.39 (dd,  $J = 7.5$  Hz, 15.4 Hz, 1H, BrCH), 5.22 (m, 1H, NCH) 7.29-7.42 (m, 4H,  $\text{CH}_{\text{arom}}$ ).

$^{13}\text{C}$  { $^1\text{H}$ } NMR ( $\text{CD}_2\text{Cl}_2$ , 150 MHz, 296 K)  $\delta$  40.7 ( $\text{CH}_2$ ), 52.8 (BrCH), 66.9 (NCH), 123.4, 124.6, 127.8, 129.1 ( $\text{CH}_{\text{arom}}$ ), 139.3, 139.8 ( $\text{C}_{\text{quat-arom}}$ ).

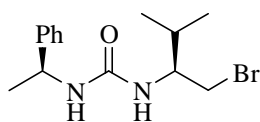
$^{15}\text{N}$  NMR ( $\text{CD}_2\text{Cl}_2$ , 60 MHz, 296 K)  $\delta$  36.0 (N).

FT-IR (KBr)  $\nu$  2257  $\text{cm}^{-1}$  (s,  $\nu_{\text{C}=\text{N}}$  isocyanate).

HRMS (FAB):  $m/z$  : calcd for  $\text{C}_{10}\text{H}_8\text{BrNO}$  ( $[M]^+$ ) 236.9789, found: 236.9796.

## 9. Urea

1-((S)-2-bromo-1-isopropylethyl)-3-((1S)-1-phenylethyl)urea (29)



To a solution of the (2S)-1-bromo-2-isocyanato-3-methylbutane in tetrahydrofuran- $d_8$  at  $-20^\circ\text{C}$  was added one equivalent of (S)-phenylethylamine. After 5 min the NMR spectroscopic data were collected at  $-20^\circ\text{C}$ .

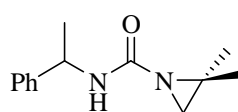
$^1\text{H}$  NMR (THF-  $d_8$ , 400 MHz, 253 K)  $\delta$  0.91 (*pseudo-t*,  $J = 6.9$  Hz, 6H,  $\text{CH}_3$  isopropyl), 1.36 (d,  $J = 6.9$  Hz, 3H,  $\text{CH}_3$  phenyl side), 1.83 (m, 1 H, CH isopropyl), 3.59-3.75 (m, 3H, CH bromine side,  $\text{CH}_2$ ), 4.94 (*pseudo-quint*,  $J = 7.0$  Hz, 1H, CH phenyl side), 5.86 (d,  $J = 8.2$  Hz, 1H, NH bromine side), 6.25 (d,  $J = 8.2$  Hz, 1H, NH phenyl side), 7.16-7.24 (m, 1H, CH arom), 7.27-7.36 (m, 4H, CH arom).

$^{13}\text{C}$  { $^1\text{H}$ } NMR (THF-  $d_8$ , 100 MHz, 253 K)  $\delta$  18.0, 19.0 ( $\text{CH}_3$  isopropyl), 22.8 ( $\text{CH}_3$  phenyl side), 30.3 (CH isopropyl), 38.5 ( $\text{CH}_2$ ), 48.9 (CH phenyl side), 54.8 (CH bromine side), 125.8, 126.5, 128.2, ( $\text{CH}_{\text{arom}}$ ), 145.5 ( $\text{C}_{\text{quat arom}}$ ), 157.2 (CO).

$^{15}\text{N}$  NMR (THF-  $d_8$ , 40 MHz, 253 K)  $\delta$  86.4 (NH bromine side), 94.1 (NH phenyl side).

## 10. Aziridines

### 2,2-dimethyl-*N*-(1-phenylethyl)aziridine-1-carboxamide (30)



To a solution of the 1-bromo-2-isocyanato-2-methylpropane (**25**) (521 mg, 2.9 mmol) in THF (25 mL) at  $-20^{\circ}\text{C}$  was added the phenylethylamine (0.38 mL, 2.9 mmol). The reaction mixture was stirred at  $-25^{\circ}\text{C}$  for 2.5 h and then cooled down to  $-40^{\circ}\text{C}$  prior to the addition of potassium *tert*-butoxide in solution in THF (2.9 mL, 2.9 mmol). The reaction mixture was then stirred overnight in the bath, quenched with water, extracted with  $\text{CH}_2\text{Cl}_2$  (3 x 25 mL) and dried over  $\text{Na}_2\text{SO}_4$ . After precipitation by adding pentane to the crude dissolved in  $\text{CH}_2\text{Cl}_2$ , the product was obtained as a white solid (318 mg, 50%).

$^1\text{H}$  NMR ( $\text{CDCl}_3$ , 400 MHz, 296 K)  $\delta$  1.20 (s, 3H,  $\text{CH}_3$  aziridine), 1.25 (s, 3H,  $\text{CH}_3$  aziridine), 1.48 (d,  $J = 6.9$  Hz, 3H,  $\text{CH}_3$  phenyl side), 2.08 (s, 2H,  $\text{CH}_2$ ), 4.98 (pseudo-qt,  $J = 7.0$  Hz, 1H, CH), 5.34 (br s, 1H, NH), 7.21-7.32 (m, 5H, CH arom).

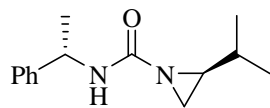
$^{13}\text{C}$  { $^1\text{H}$ } NMR ( $\text{CDCl}_3$ , 100 MHz, 296 K)  $\delta$  21.9 ( $\text{CH}_3$  phenyl side), 22.6 ( $\text{CH}_3$  aziridine), 37.2 ( $\text{CH}_2$ ), 41.4 ( $\text{C}_{\text{quat}}$  aziridine), 50.1 (CH), 126.2, 127.2, 128.6 (CH arom), 143.5 ( $\text{C}_{\text{quat}}$  arom), 162.4 (CO).

$^{15}\text{N}$  NMR ( $\text{CDCl}_3$ , 60 MHz, 296 K)  $\delta$  71.1 ( $\text{N}$  aziridine), 116.4 (NH).

FT-IR (KBr)  $\nu$  1642  $\text{cm}^{-1}$  (s,  $\nu$  aziridine), 3282  $\text{cm}^{-1}$  (s,  $\nu_{\text{NH}}$ ).

HRMS (FAB):  $m/z$  : calcd for  $\text{C}_{13}\text{H}_{19}\text{N}_2\text{O}$  ( $[\text{M}+\text{H}]^+$ ) 219.1497, found: 219.1407.

### (2*S*)-2-isopropyl-*N*-((1*S*)-1-phenylethyl)aziridine-1-carboxamide (31a)



To a solution of the (2*S*)-1-bromo-2-isocyanato-3-methylbutane (**26**) (508.1 mg, 2.6 mmol) in THF (25 mL) at  $-20^{\circ}\text{C}$  was added the (*S*)-phenylethylamine (0.34 mL, 2.6 mmol). The reaction mixture was stirred at  $-25^{\circ}\text{C}$  for 1.5 h and then cooled down to  $-40^{\circ}\text{C}$  prior to the addition of potassium *tert*-butoxide in solution in THF (2.6 mL, 2.6 mmol). The reaction mixture was then stirred over night in the bath, quenched with water, extracted with  $\text{Et}_2\text{O}$  (3 x 25 mL) and dried over  $\text{Na}_2\text{SO}_4$ . The crude was purified by flash chromatography (Hexane/ $\text{EtOAc}$ , 50/50) to yield a white solid (359 mg, 59% yield). Crystallisation from  $\text{CH}_2\text{Cl}_2$ /pentane gave white crystals suitable for X-ray diffraction.

$^1\text{H}$  NMR ( $\text{CDCl}_3$ , 600 MHz, 296 K)  $\delta$  0.95 (d,  $J = 6.8$  Hz, 3H,  $\text{CH}_3$  isopropyl), 1.04 (d,  $J = 6.7$  Hz, 3H,  $\text{CH}_3$  isopropyl), 1.41 (m, 1H, CH isopropyl), 1.49 (d,  $J = 6.9$  Hz, 3H,  $\text{CH}_3$  phenyl side), 1.85 (d,  $J = 4.1$  Hz, 1H,  $\text{CH}_2$ ), 2.08 (m, 1H, CH aziridine), 2.34 (d,  $J = 6.6$  Hz, 1H,  $\text{CH}_2$ ), 4.93 (pseudo-qt,  $J = 7.0$  Hz, 1H, CH phenyl side), 5.50 (br s, 1H, NH), 7.24-7.35 (m, 5H, CH arom).

$^{13}\text{C}$   $\{^1\text{H}\}$  NMR ( $\text{CDCl}_3$ , 150 MHz, 296 K)  $\delta$  19.1, 20.0 ( $\text{CH}_3$  isopropyl), 22.3 ( $\text{CH}_3$  phenyl side), 30.7 ( $\text{CH}_2$ ), 30.9 ( $\text{CH}$  isopropyl), 45.4 ( $\text{CH}$  aziridine), 50.1 ( $\text{CH}$  phenyl side), 125.9, 127.3, 128.7 ( $\text{CH}$  arom), 143.5 ( $\text{C}_{\text{quat}}$  arom), 164.5 ( $\text{CO}$ ).

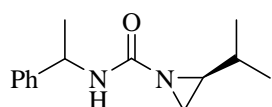
$^{15}\text{N}$  NMR ( $\text{CDCl}_3$ , 60 MHz, 296 K)  $\delta$  49.6 ( $N$  aziridine), 109.9 ( $\text{NH}$ ).

FT-IR (KBr)  $\nu$  1659  $\text{cm}^{-1}$  (s,  $\nu$  aziridine), 3343  $\text{cm}^{-1}$  (s,  $\nu_{\text{NH}}$ ).

MS (EI)  $m/z$  (%) 105.1 (100) [ethylbenzene] $^+$ , 232.2 (20) [ $M$ ] $^+$ .

elemental analysis calcd (%) for  $\text{C}_{14}\text{H}_{20}\text{N}_2\text{O}$  (232.32): C 72.38, H 8.68, N 12.06; Found: C 72.11, H 8.63, N 11.88.

(2S)-2-isopropyl-N-(1-phenylethyl)aziridine-1-carboxamide (31a+b)



To a solution of the (2S)-1-bromo-2-isocyanato-3-methylbutane (**26**) (775 mg, 4 mmol) in THF (25 mL) at  $-20^\circ\text{C}$  was added the phenylethylamine (0.34 mL, 2.6 mmol). The reaction mixture was stirred at  $-25^\circ\text{C}$  for 1.5 h and then cooled down to  $-40^\circ\text{C}$  prior to the addition of potassium *tert*-butoxide in solution in THF (2.6 mL, 2.6 mmol). The reaction mixture was then stirred overnight in the bath, over 48 h at room temperature, quenched with water, extracted with  $\text{Et}_2\text{O}$  (3 x 25 mL) and dried over  $\text{Na}_2\text{SO}_4$ . The crude was purified by flash chromatography (Hexane/EtOAc, 50/50) to yield a colorless oil (578 mg, 62% yield).

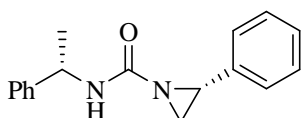
$^1\text{H}$  NMR ( $\text{CDCl}_3$ , 400 MHz, 296 K)  $\delta$  0.93 (d,  $J = 6.8$  Hz, 3H,  $\text{CH}_3$  isopropyl dia 1), 0.94 (d,  $J = 6.8$  Hz, 3H,  $\text{CH}_3$  isopropyl dia 2), 1.02 (d,  $J = 6.7$  Hz, 3H,  $\text{CH}_3$  isopropyl dia 1), 1.03 (d,  $J = 6.7$  Hz, 3H,  $\text{CH}_3$  isopropyl dia 2), 1.41 (m, 2H,  $\text{CH}$  isopropyl dia 1+2), 1.48 (d,  $J = 6.9$  Hz, 6H,  $\text{CH}_3$  phenyl side dia 1+2), 1.84 (d,  $J = 4.1$  Hz, 2H,  $\text{CH}_2$  dia 1+2), 2.08 (m, 1H,  $\text{CH}$  aziridine dia 1), 2.15 (m, 1H,  $\text{CH}$  aziridine dia 2), 2.29 (d,  $J = 6.6$  Hz, 1H,  $\text{CH}_2$  dia 2), 2.35 (d,  $J = 6.6$  Hz, 1H,  $\text{CH}_2$  dia 1), 4.92 (m, 2H,  $\text{CH}$  phenyl side dia 1+2), 5.50 (br s, 2H,  $\text{NH}$  dia 1+2), 7.23-7.35 (m, 10 H,  $\text{CH}$  arom dia 1+2).

$^{13}\text{C}$   $\{^1\text{H}\}$  NMR ( $\text{CDCl}_3$ , 100 MHz, 296 K)  $\delta$  19.1 ( $\text{CH}_3$  isopropyl dia 1+2), 20.0 ( $\text{CH}_3$  isopropyl dia 1+2), 22.1 ( $\text{CH}_3$  phenyl side dia 1), 22.3 ( $\text{CH}_3$  phenyl side dia 2), 30.7 ( $\text{CH}_2$  dia 1), 30.9 ( $\text{CH}$  isopropyl dia 1+2), 31.0 ( $\text{CH}_2$  dia 2), 45.1 ( $\text{CH}$  aziridine dia 2), 45.4 ( $\text{CH}$  aziridine dia 1), 50.1 ( $\text{CH}$  phenyl side dia 1+2), 125.9, 126.0, 127.3, 127.4, 128.7 ( $\text{CH}$  arom dia 1+2), 143.4 ( $\text{C}_{\text{quat}}$  arom dia 1), 143.5 ( $\text{C}_{\text{quat}}$  arom dia 2), 164.5 ( $\text{CO}$  dia 1+2).

FT-IR (KBr)  $\nu$  1658  $\text{cm}^{-1}$  (s,  $\nu$  aziridine), 3294  $\text{cm}^{-1}$  (s,  $\nu_{\text{NH}}$ ).

HRMS (FAB):  $m/z$  : calcd for  $\text{C}_{14}\text{H}_{21}\text{N}_2\text{O}$  ( $[M+\text{H}]^+$ ) 233.1654, found: 233.1662.

(2R)-2-phenyl-N-((1S)-1-phenylethyl)aziridine-1-carboxamide (32)



To a solution of the (1R)-1-(2-bromo-1-isocyanatoethyl)benzene (**27**) (141 mg, 0.6 mmol) in THF (15 mL) at  $-20^\circ\text{C}$  was added the

phenylethylamine (0.08 mL, 0.6 mmol). The reaction mixture was stirred at  $-25^{\circ}\text{C}$  for 2.5 h and then cooled down to  $-40^{\circ}\text{C}$  prior to the addition of potassium *tert*-butoxide in solution in THF (0.6 mL, 0.6 mmol). The reaction mixture was then stirred overnight in the bath, quenched with water, extracted with  $\text{CH}_2\text{Cl}_2$  (3 x 25 mL) and dried over  $\text{Na}_2\text{SO}_4$ . The crude was purified by flash chromatography (Hexane/EtOAc, 50/50) to yield a colorless solid (86 mg, 54% yield).

$^1\text{H}$  NMR ( $\text{CDCl}_3$ , 400 MHz, 296 K)  $\delta$  1.48 (d,  $J = 6.9$  Hz, 3H,  $\text{CH}_3$ ), 2.14 (d,  $J = 3.8$  Hz, 1H,  $\text{CH}_2$ ), 2.74 (d,  $J = 6.7$  Hz, 1H,  $\text{CH}_2$ ), 3.37 (dd,  $J = 3.9$  Hz,  $J = 6.7$  Hz, 1H,  $\text{CH}_{\text{aziridine}}$ ), 4.95 (m, 1H,  $\text{CH}$ ), 5.62 (d,  $J = 6.3$  Hz, 1H,  $\text{NH}$ ), 7.24-7.35 (m, 10H,  $\text{CH}_{\text{arom}}$ ).

$^{13}\text{C}$   $\{^1\text{H}\}$  NMR ( $\text{CDCl}_3$ , 100 MHz, 296 K)  $\delta$  22.0 ( $\text{CH}_3$ ), 35.1 ( $\text{CH}_2$ ), 40.3 ( $\text{CH}$ ), 50.2 ( $\text{CH}_{\text{aziridine}}$ ), 126.0, 126.2, 127.4, 127.7, 128.5, 128.7 ( $\text{CH}_{\text{arom}}$ ), 143.1 ( $\text{C}_{\text{quat arom}}$ ), 163.7 ( $\text{CO}$ ).

$^{15}\text{N}$  NMR ( $\text{CDCl}_3$ , 60 MHz, 296 K)  $\delta$  63.9 ( $N_{\text{aziridine}}$ ), 114.9 ( $\text{NH}$ ).

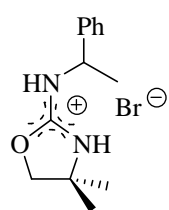
FT-IR (KBr)  $\nu$  1655  $\text{cm}^{-1}$  (s,  $\nu_{\text{aziridine}}$ ), 3356  $\text{cm}^{-1}$  (s,  $\nu_{\text{NH}}$ ).

HRMS (EI):  $m/z$ : calcd for  $\text{C}_{17}\text{H}_{18}\text{N}_2\text{O}$  ( $[M]^+$ ) 266.1419, found: 266.1415, calcd for  $\text{C}_8\text{H}_9\text{N}$  ( $[M-\text{CONHC}_8\text{H}_9]^+$ ) 119.0735, found: 119.0717.

### 11. Hydrobromide salts of the 2-aminooxazolines

General procedure to obtain the hydrobromide salts: To a solution of the desired isocyanate in THF was added 1-phenyl-1-ethylamine (1 equivalent) at room temperature. The mixture was stirred 3 h and the solvent was then evaporated *in vacuo*. The white foam obtained was used in the next step without further purification.  $^1\text{H}$  NMR spectra show complete conversion into the desired product without by-products.

#### 2-(1-phenylethylamino)-4,4-dimethyloxazoline hydrobromide (33)



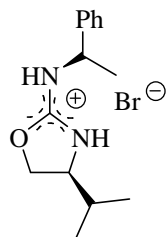
$^1\text{H}$  NMR ( $\text{CDCl}_3$ , 400 MHz, 296 K)  $\delta$  1.42 (s, 3H,  $\text{CH}_3$ ), 1.49 (s, 3H,  $\text{CH}_3$  ring) 1.61 (d,  $J = 7.0$  Hz, 3H,  $\text{CH}_3_{\text{ring}}$ ), 4.25 (d,  $J = 8.6$  Hz, 1H,  $\text{CH}_2$ ), 4.33 (d,  $J = 8.6$  Hz, 1H,  $\text{CH}_2$ ), 4.80 (q,  $J = 6.9$  Hz, 1H,  $\text{CH}$ ), 7.25-7.41 (m, 5H,  $\text{CH}_{\text{arom}}$ ).

$^{13}\text{C}$   $\{^1\text{H}\}$  NMR ( $\text{CDCl}_3$ , 100 MHz, 296 K)  $\delta$  23.3 ( $\text{CH}_3$ ), 26.9, 27.0 ( $\text{CH}_3_{\text{ring}}$ ), 53.7 ( $\text{CH}$ ), 60.0 ( $\text{C}_{\text{quat}}$ ), 81.6 ( $\text{CH}_2$ ), 125.7, 128.1, 129.0 ( $\text{CH}_{\text{arom}}$ ), 141.3 ( $\text{C}_{\text{quat arom}}$ ),

160.5 ( $\text{NCN}$ ).

$^{15}\text{N}$  ( $\text{CDCl}_3$ , 60 MHz, 296 K)  $\delta$  103.4 ( $\text{NH}$ ), 112.1 ( $\text{NH}_{\text{ring}}$ ).

MS (FAB):  $m/z$  (%): 817.1 (3)  $[(\text{AAH})_3\text{Br}_2]^+$ , 640.2 (5)  $[(\text{AAH})_2\text{Br}+\text{phenylethylamine}]^+$ , 517.1 (80)  $[(\text{AAH})_2\text{Br}]^+$ , 340.2 (30)  $[(\text{AAH})+\text{phenylethylamine}]^+$ , 219.2 (100)  $[(\text{AAH})]^+$ , 115.0 (100)  $[(\text{AAH})-\text{ethylbenzene}]^+$ , 100.0 (62)  $[(\text{AAH})-\text{phenylethylamine-isopropyl}]^+$  (AA = aminooxazoline, AAH = protonated aminooxazoline).

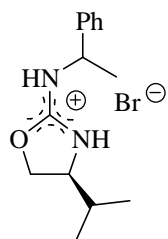
(4S)-2-((1R)-1-phenylethylamino)-4-isopropylloxazoline hydrobromide (34a)

$^1\text{H}$  NMR ( $\text{CDCl}_3$ , 600 MHz, 296 K)  $\delta$  0.94 (d,  $J = 6.8$  Hz, 3H,  $\text{CH}_3$  isopropyl), 1.02 (d,  $J = 6.7$  Hz, 3H,  $\text{CH}_3$  isopropyl), 1.60 (d,  $J = 7.0$  Hz, 3H,  $\text{CH}_3$ ), 1.85 (m, 1H,  $\text{CH}$  isopropyl), 3.89 (ddd,  $J = 6.7$  Hz, 8.7 Hz, 1H,  $\text{CH}$  ring), 4.38 (dd,  $J = 6.5$  Hz, 9.0 Hz, 1H,  $\text{CH}_2$ ), 4.62 (pseudo-t,  $J = 8.9$  Hz, 1H,  $\text{CH}_2$ ), 4.79 (q,  $J = 6.7$  Hz, 1H,  $\text{CH}$ ), 7.27-7.40 (m, 5H,  $\text{CH}$  arom).

$^{13}\text{C}$   $\{^1\text{H}\}$  NMR ( $\text{CDCl}_3$ , 150 MHz, 296 K)  $\delta$  17.8, 18.2 ( $\text{CH}_3$  isopropyl), 23.3 ( $\text{CH}_3$ ), 32.1 ( $\text{CH}$  isopropyl), 53.8 ( $\text{CH}$ ), 61.7 ( $\text{CH}$  ring), 73.8 ( $\text{CH}_2$ ), 125.8, 126.2, 128.1, 128.7, 129.0 ( $\text{CH}$  arom), 141.2 ( $\text{C}_{\text{quat}}$  arom), 161.5 (NCN).

$^{15}\text{N}$  ( $\text{CDCl}_3$ , 60 MHz, 296 K)  $\delta$  97.0 ( $\text{NH}$  ring), 101.3 ( $\text{NH}$  outside the ring).

MS (FAB):  $m/z$  (%): 668.2 (6)  $[(\text{AAH})_2\text{Br} + \text{phenylethylamine}]^+$ , 545.2 (10)  $[(\text{AAH})_2\text{Br}]^+$ , 465.3 (10)  $[(\text{AA})(\text{AAH})]^+$ , 354.2 (15)  $[(\text{AAH}) + \text{phenylethylamine}]^+$ , 233.1 (100)  $[(\text{AAH})]^+$ , 129.0 (35)  $[(\text{AAH}) - \text{ethylbenzene}]^+$ , 100.0 (28)  $[(\text{AAH}) - \text{phenylethylamine-isopropyl}]^+$  (AA = aminooxazoline, AAH = protonated aminooxazoline).

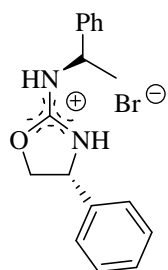
(4S)-2-(1-phenylethylamino)-4-isopropylloxazoline hydrobromide (34a+b)

$^1\text{H}$  NMR ( $\text{CDCl}_3$ , 600 MHz, 296 K)  $\delta$  0.93 (d,  $J = 6.8$  Hz, 3H,  $\text{CH}_3$  isopropyl dia 1), 0.99 (d,  $J = 6.7$  Hz, 3H,  $\text{CH}_3$  isopropyl dia 2), 1.01 (d,  $J = 6.7$  Hz, 3H,  $\text{CH}_3$  isopropyl dia 1), 1.08 (d,  $J = 6.7$  Hz, 3H,  $\text{CH}_3$  isopropyl dia 2), 1.66 (d,  $J = 6.9$  Hz, 6H,  $\text{CH}_3$  dia1+2), 1.82 (m, 1H,  $\text{CH}$  isopropyl dia 1), 1.89 (m, 1H,  $\text{CH}$  isopropyl dia 2), 3.95 (ddd,  $J = 6.8$  Hz, 8.6 Hz, 1H,  $\text{CH}$  ring dia 1), 4.01 (ddd,  $J = 6.8$  Hz, 8.6 Hz, 1H,  $\text{CH}$  ring dia 2), 4.35 (dd,  $J = 6.4$  Hz, 8.9 Hz, 1H,  $\text{CH}_2$  dia 1), 4.43 (dd,  $J = 6.5$  Hz, 8.9 Hz, 1H,  $\text{CH}_2$  dia 2), 4.66 (pseudo-t,  $J = 8.8$  Hz, 1H,  $\text{CH}_2$  dia 1), 4.75 (pseudo-t,  $J = 8.8$  Hz, 1H,  $\text{CH}_2$  dia 2), 4.48 (m, 2H,  $\text{CH}$  dia 1+2), 7.30-7.42 (m, 10H,  $\text{CH}$  arom dia 1+2).

$^{13}\text{C}$   $\{^1\text{H}\}$  NMR ( $\text{CDCl}_3$ , 150 MHz, 296 K)  $\delta$  17.6, 17.7, 17.9, 18.1 ( $\text{CH}_3$  isopropyl dia 1+2), 23.2 ( $\text{CH}_3$  dia 1), 23.3 ( $\text{CH}_3$  dia 2), 32.0 ( $\text{CH}$  isopropyl dia 1), 32.2 ( $\text{CH}$  isopropyl dia 2), 53.7 ( $\text{CH}$  dia 1+2), 61.7 ( $\text{CH}$  ring dia 1), 61.7 ( $\text{CH}$  ring dia 2), 73.6 ( $\text{CH}_2$  dia 1), 73.6 ( $\text{CH}_2$  dia 2), 125.6, 125.7, 128.0, 128.0, 128.9 ( $\text{CH}_{\text{arom}}$  dia 1+2), 141.2 ( $\text{C}_{\text{quat}}$  arom dia 1), 141.2 ( $\text{C}_{\text{quat}}$  arom dia 2), 161.4 (NCN dia 1), 161.5 (NCN dia 2).

$^{15}\text{N}$  ( $\text{CDCl}_3$ , 60 MHz, 296 K)  $\delta$  102.0 ( $\text{NH}$  outside the ring).

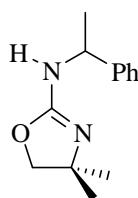


(4R)-2-((1R)-1-phenylethylamino)-4-phenyloxazoline hydrobromide (35)

$^1\text{H}$  NMR ( $\text{CDCl}_3$ , 400 MHz, 296 K)  $\delta$  1.70 (d,  $J = 6.9$  Hz, 3H,  $\text{CH}_3$ ), 4.34 (dd,  $J = 7.4$  Hz,  $J = 8.3$  Hz, 1H,  $\text{CH}_2$ ), 4.94 (m, 2H,  $\text{CH}_2$ , CH), 5.27 (dd,  $J = 7.4$  Hz, 8.7 Hz, 1H, CH ring), 7.24-7.26 (m, 2H, CH arom), 7.32-7.44 (m, 8H, CH arom).

$^{13}\text{C}$   $\{^1\text{H}\}$  NMR ( $\text{CDCl}_3$ , 100 MHz, 296 K)  $\delta$  23.6 ( $\text{CH}_3$ ), 53.6 (CH), 61.3 (CH ring), 76.9 ( $\text{CH}_2$ ), 125.8, 126.2, 127.8, 127.9, 128.8, 129.0 ( $\text{CH}_{\text{arom}}$ ), 141.8, 143.0 ( $\text{C}_{\text{quat arom}}$ ), 161.6 (NCN).

$^{15}\text{N}$  ( $\text{CDCl}_3$ , 60 MHz, 296 K)  $\delta$  99.9 (NH outside the ring).

**12. 2-aminoxazolines**2-(1-phenylethylamino)-4,4-dimethyloxazoline (36)

To a solution of the hydrobromide salt **33** (290 mg, 0.97 mmol) dissolved in THF at  $0^\circ\text{C}$  was added solid potassium *tert*-butoxide (131 mg, 1.16 mmol). The cloudy solution was stirred for 1.5 h, quenched with  $\text{H}_2\text{O}$  and extracted with  $\text{CH}_2\text{Cl}_2$ . The crude product was purified by flash chromatography (Hexane/EtOAc, 50/50) to yield 124 mg of a colorless solid (59%).

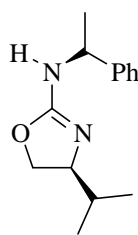
$^1\text{H}$  NMR ( $\text{CDCl}_3$ , 400 MHz, 296 K)  $\delta$  1.20 (s, 3H,  $\text{CH}_3$  oxa), 1.24 (s, 3H,  $\text{CH}_3$  oxa), 1.48 (d,  $J = 6.8$  Hz, 3H,  $\text{CH}_3$  phenyl side), 3.84 (d,  $J = 7.6$  Hz, 1H,  $\text{CH}_2$ ), 3.87 (d,  $J = 7.6$  Hz, 1H,  $\text{CH}_2$ ), 4.76 (q,  $J = 6.8$  Hz, 1H, CH), 7.20-7.30 (m, 5H, CH arom).

$^{13}\text{C}$   $\{^1\text{H}\}$  NMR ( $\text{CDCl}_3$ , 100 MHz, 296 K)  $\delta$  22.8 ( $\text{CH}_3$  phenyl side), 28.8 ( $\text{CH}_3$  oxa), 52.3 (CH), 65.1 ( $\text{C}_{\text{quat oxa}}$ ), 79.1 ( $\text{CH}_2$ ), 125.9, 127.1, 128.5 (CH arom), 143.9 ( $\text{C}_{\text{quat arom}}$ ), 158.3 (NCO).

$^{15}\text{N}$  NMR ( $\text{CDCl}_3$ , 60 MHz, 296 K)  $\delta$  77.6 (N), 176.7 (NH).

FT-IR (KBr)  $\nu$  1687  $\text{cm}^{-1}$  (s,  $\nu_{\text{C=N}}$ ).

HRMS (FAB):  $m/z$  : calcd for  $\text{C}_{13}\text{H}_{19}\text{N}_2\text{O}$  ( $[\text{M}+\text{H}]^+$ ) 219.1497, found: 219.1485.

(4S)-2-((1R)-1-phenylethylamino)-4-isopropyloxazoline (37a)

To a solution of the hydrobromide salt **34a** (501.2 mg, 1.6 mmol) dissolved in THF at  $0^\circ\text{C}$  was added solid potassium *tert*-butoxide (202 mg, 1.8 mmol). The cloudy solution was stirred for 1.5 h, quenched with  $\text{H}_2\text{O}$  and extracted with  $\text{CH}_2\text{Cl}_2$ . The crude product was purified by flash chromatography (Hexane/EtOAc, 50/50) to yield 210 mg of a yellowish oil (56%).

$^1\text{H}$  NMR ( $\text{CDCl}_3$ , 600 MHz, 296 K)  $\delta$  0.75 (d,  $J = 6.8$  Hz, 3H,  $\text{CH}_3$  isopropyl), 0.80 (d,  $J = 6.8$  Hz, 3H,  $\text{CH}_3$  isopropyl), 1.48 (d,  $J = 6.9$  Hz, 3H,  $\text{CH}_3$  phenyl side), 1.60 (m, 1H, CH isopropyl), 3.78 (m, 1H,

$CH_{\text{oxa}}$ ), 3.95 (dd,  $J = 6.3$  Hz, 8.0 Hz, 1H,  $CH_2$ ), 4.17 (dd,  $J = 8.1$  Hz, 8.8 Hz, 1H,  $CH_2$ ), 4.78 (q,  $J = 7.0$  Hz, 1H,  $CH_{\text{phenyl side}}$ ), 7.22-7.25 (m, 1H,  $CH_{\text{arom}}$ ), 7.29-7.34 (m, 4H,  $CH_{\text{arom}}$ ).

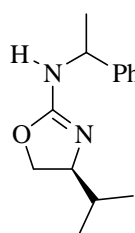
$^{13}\text{C}$   $\{^1\text{H}\}$  NMR ( $\text{CDCl}_3$ , 150 MHz, 296 K)  $\delta$  17.7, 18.4 ( $\text{CH}_3_{\text{isopropyl}}$ ), 23.2 ( $\text{CH}_3_{\text{phenyl side}}$ ), 33.1 ( $\text{CH}_{\text{isopropyl}}$ ), 52.4 ( $\text{CH}_{\text{phenyl side}}$ ), 70.2 ( $\text{CH}_2$ ,  $\text{CH}_{\text{oxa}}$ ), 125.9, 127.0, 128.4 ( $\text{CH}_{\text{arom}}$ ), 144.3 ( $\text{C}_{\text{quat arom}}$ ), 159.2 (NCO).

$^{15}\text{N}$  NMR ( $\text{CDCl}_3$ , 60 MHz, 296 K)  $\delta$  78.6 (N), 160.0 (NH).

FT-IR (KBr)  $\nu$  1672  $\text{cm}^{-1}$  (s,  $\nu_{\text{C=N}}$ ).

HRMS (FAB):  $m/z$  : calcd for  $\text{C}_{14}\text{H}_{21}\text{N}_2\text{O}$  ( $[M]^+$ ) 233.1654, found: 233.1643.

(4S)-2-(1-phenylethylamino)-4-isopropylloxazoline (**37a+b**)

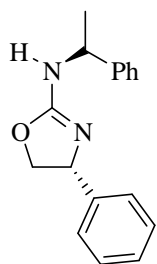


To a solution of the hydrobromide salt **34a+b** (848.4 mg, 2.7 mmol) dissolved in THF at 0°C was added solid potassium *tert*-butoxide (202 mg, 1.8 mmol). The cloudy solution was stirred for 1.5 h, quenched with  $\text{H}_2\text{O}$  and extracted with  $\text{CH}_2\text{Cl}_2$ . The crude product was purified by flash chromatography (Hexane/EtOAc, 50/50) to yield 389 mg of a colorless oil (62%).

$^1\text{H}$  NMR ( $\text{CDCl}_3$ , 400 MHz, 296 K)  $\delta$  0.81 (d,  $J = 6.7$  Hz, 3H,  $\text{CH}_3_{\text{isopropyl dia 1}}$ ), 0.86 (d,  $J = 6.8$  Hz, 3H,  $\text{CH}_3_{\text{isopropyl dia 1}}$ ), 0.90 (d,  $J = 6.8$  Hz, 3H,  $\text{CH}_3_{\text{isopropyl dia 2}}$ ), 0.98 (d,  $J = 6.8$  Hz, 3H,  $\text{CH}_3_{\text{isopropyl dia 2}}$ ), 1.53 (d,  $J = 6.9$  Hz, 3H,  $\text{CH}_3_{\text{phenyl side dia 1}}$ ), 1.57 (d,  $J = 6.8$  Hz, 3H,  $\text{CH}_3_{\text{phenyl side dia 2}}$ ), 1.65 (qd,  $J = 6.6$  Hz, 13.3 Hz, 1H,  $\text{CH}_{\text{isopropyl dia 1}}$ ), 1.77 (qd,  $J = 6.6$  Hz,  $J = 13.2$  Hz, 1H,  $\text{CH}_{\text{isopropyl dia 2}}$ ), 3.85 (m, 2H,  $\text{CH}_{\text{oxa dia 1+2}}$ ), 3.98 (dd,  $J = 6.6$  Hz, 7.8 Hz, 2H,  $\text{CH}_2_{\text{dia 1+2}}$ ), 4.24 (m, 2H,  $\text{CH}_2_{\text{dia 1+2}}$ ), 4.83 (q,  $J = 6.8$  Hz, 2H,  $\text{CH}_{\text{phenyl side dia 1+2}}$ ), 7.22-7.25 (m, 2H,  $\text{CH}_{\text{arom dia 1+2}}$ ), 7.34-7.39 (m, 8H,  $\text{CH}_{\text{arom dia 1+2}}$ );  $^{13}\text{C}$   $\{^1\text{H}\}$  NMR ( $\text{CDCl}_3$ , 150 MHz, 296 K)  $\delta$  17.7 ( $\text{CH}_3_{\text{isopropyl dia 1+2}}$ ), 18.4 ( $\text{CH}_3_{\text{isopropyl dia 1}}$ ), 18.7 ( $\text{CH}_3_{\text{isopropyl dia 2}}$ ), 22.8 ( $\text{CH}_3_{\text{phenyl side dia 2}}$ ), 23.2 ( $\text{CH}_3_{\text{phenyl side dia 1}}$ ), 30.9 ( $\text{CH}_{\text{isopropyl dia 1}}$ ), 33.1 ( $\text{CH}_{\text{isopropyl dia 2}}$ ), 52.4 ( $\text{CH}_{\text{phenyl side dia 1}}$ ), 52.5 ( $\text{CH}_{\text{phenyl side dia 2}}$ ), 70.1 ( $\text{CH}_{\text{ring dia 1+2}}$ ), 70.3 ( $\text{CH}_2_{\text{dia 1+2}}$ ), 125.6, 125.9, 127.0, 127.2, 128.4, 128.6 ( $\text{CH}_{\text{arom}}$ ), 143.3 ( $\text{C}_{\text{quat arom dia 2}}$ ), 144.9 ( $\text{C}_{\text{quat arom dia 1}}$ ), 159.2 (NCO  $_{\text{dia 2}}$ ), 159.4 (NCO  $_{\text{dia 1}}$ ).

FT-IR (KBr)  $\nu$  1676  $\text{cm}^{-1}$  (s,  $\nu_{\text{C=N}}$ ).

HRMS (EI):  $m/z$  : calcd for  $\text{C}_{14}\text{H}_{20}\text{N}_2\text{O}$  ( $[M]^+$ ) 232.1576, found: 232.1576.

(4R)-2-((1R)-1-phenylethylamino)-4-phenyloxazoline (38)

To a solution of the hydrobromide salt **35** (257.7 mg, 0.74 mmol) dissolved in THF at 0°C was added solid potassium *tert*-butoxide (202 mg, 1.8 mmol). The cloudy solution was stirred for 1.5 h, quenched with H<sub>2</sub>O and extracted with CH<sub>2</sub>Cl<sub>2</sub>. The crude product was purified by flash chromatography (Hexane/EtOAc, 50/50) to yield 95 mg of a yellowish solid (48%).

<sup>1</sup>H NMR (CDCl<sub>3</sub>, 400 MHz, 296 K) 1.61 (d, *J* = 6.8 Hz, 3H, CH<sub>3</sub>), 4.06 (pseudo-t, *J* = 7.5 Hz, 1H, CH<sub>2</sub>), 4.63 (pseudo-t, *J* = 8.5 Hz, 1H, CH<sub>2</sub>), 4.95 (q, *J* = 6.7 Hz, 1H, CH), 5.14 (dd, *J* = 7.7 Hz, 8.5 Hz, 1H, CH<sub>ring</sub>), 7.30-7.41 (m, 10 H, CH<sub>arom</sub>).

<sup>13</sup>C {<sup>1</sup>H} NMR (CDCl<sub>3</sub>, 100 MHz, 296 K) δ 22.9 (CH<sub>3</sub>), 52.6 (CH), 67.9 (CH<sub>oxa</sub>), 75.06 (CH<sub>2</sub>), 125.9, 126.5, 127.3, 128.5, 128.6 (CH<sub>arom</sub>), 144.8, 144.0 (C<sub>quat arom</sub>), 160.7 (NCO).

<sup>15</sup>N NMR (CDCl<sub>3</sub>, 60 MHz, 296 K) δ 79.8 (N).

FT-IR (KBr) ν 1686 cm<sup>-1</sup> (s, ν<sub>C=N</sub>).

HRMS (EI): *m/z* : calcd for C<sub>17</sub>H<sub>18</sub>N<sub>2</sub>O ([M]<sup>+</sup>) 266.1419, found: 266.1432

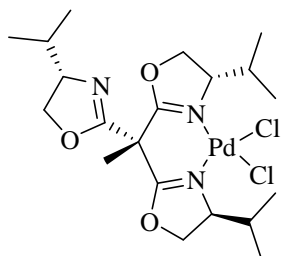
### III. Chapter 3

#### 1. Palladium(II)chloride complexes

##### General Procedure<sup>22</sup>

Bis(benzonitrile)palladium(II) dichloride (0.142 mmol) and [trisox] (0.149 mmol) were dissolved in CH<sub>2</sub>Cl<sub>2</sub> (1 mL). The reaction mixture was stirred for 90 min at room temperature and pentane was added (8 mL) to form an orange precipitate. The crude product was washed twice with pentane (8 mL) and dried *in vacuo* to give the complex as an orange powder.

##### (1,1,1-tris[(4S)-4-isopropylloxazolin-2-yl]ethane)palladium(II) dichloride (39)



Yield: 85%. Crystallisation from CH<sub>2</sub>Cl<sub>2</sub>/Et<sub>2</sub>O gave orange crystals suitable for X-ray diffraction.

<sup>1</sup>H NMR (300 MHz, CDCl<sub>3</sub>, 296 K) δ 0.74 (m, 6H, CH(CH<sub>3</sub>)<sub>2</sub>, 2 C), 0.87 (m, 9H, CH(CH<sub>3</sub>)<sub>2</sub>, 2 C, 1 F), 0.92 (d, *J* = 6.8 Hz, 3H, CH(CH<sub>3</sub>)<sub>2</sub>, F), 1.81 (m, 1H, CH(CH<sub>3</sub>)<sub>2</sub>, F), 1.91 (s, 3H, CH<sub>3</sub> apical), 2.87 (m, 2H,

<sup>22</sup> S. E. Denmark, R. A. Stavenger, A.-M. Faucher, J. P. Edwards, *J. Org. Chem.* **1997**, *62*, 3375.

$CH(CH_3)_2$ , C), 4.03 (m, 2H,  $CH_2$  oxa, F), 4.27 (m, 3H,  $CH_2$  oxa, C,  $CH_{oxa}$ , F), 4.44 (m, 2H,  $CH_2$  oxa, C), 4.66 (m, 1H,  $CH_{oxa}$ , C), 4.81 (m, 1H,  $CH_{oxa}$ , C).

$^{13}C$  { $^1H$ } NMR (75 MHz,  $CDCl_3$ , 296 K)  $\delta$  13.1, 13.6, 17.8, 18.3, 18.5, 18.6 ( $CH(CH_3)_2$ ), 22.5 ( $CH_3$  apical), 29.3, 29.7 ( $CH(CH_3)_2$ , C), 32.1 ( $CH(CH_3)_2$ , F), 45.2 ( $(CH_3)C(oxa)_3$ ), 69.3, 69.6 ( $CH_2$  oxa, C), 70.0, 70.4 ( $CH_{oxa}$ , C), 71.5 ( $CH_2$  oxa, F), 72.0 ( $CH_{oxa}$ , F), 160.1 (NCO, F), 165.8, 166.7 (NCO, C).

$^{15}N$  (60 MHz,  $CDCl_3$ , 296 K)  $\delta$  160.2 161.2 (N, C) 239.9 (N, F) (C = coordinated oxazoline, F = free oxazoline).

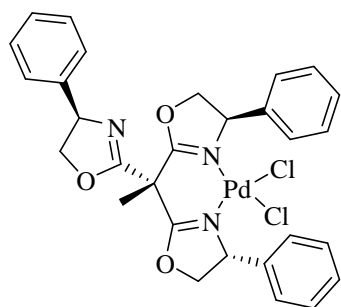
FT-IR (KBr):  $\nu$  1660  $cm^{-1}$  (s,  $\nu_{C=N}$  free oxazoline), 1650  $cm^{-1}$  (s,  $\nu_{C=N}$  coordinated oxazoline).

HRMS (ESI):  $m/z$  : calcd for  $C_{20}H_{33}Cl_2N_3NaO_3Pd$  ( $[M+Na]^+$ ) 564.084, found: 564.084; calcd for  $C_{40}H_{66}Cl_4N_6NaO_6Pd_2$  ( $[2M+Na]^+$ ) 1105.174, found: 1105.177.

elemental analysis calcd (%) for  $C_{20}H_{33}Cl_2N_3O_3Pd$ : C 44.42, H 6.15, N 7.77; found: C 44.28, H 6.27, N 7.67.

(1,1,1-tris[(4*R*)-4-phenyloxazolin-2-yl]ethane)palladium(II) dichloride (40)

Yield: 89%. Crystallisation from  $CH_2Cl_2$ /pentane gave orange crystals suitable for X-ray diffraction.



$^1H$  NMR (600 MHz,  $CDCl_3$ , 296 K)  $\delta$  2.27 (s, 3H,  $CH_3$ ), 4.36 (pseudo-t,  $J = 8.4$  Hz, 1H,  $CH_{2oxa}$ , F), 4.58-4.61 (m, 2H,  $CH_{2oxa}$ , C), 4.75 (pseudo-t,  $J = 8.9$  Hz, 1H,  $CH_{2oxa}$ , C), 4.80 (pseudo-t,  $J = 9.2$  Hz, 1H,  $CH_{2oxa}$ , C), 4.90 (dd,  $J = 8.6$  Hz, 10.2 Hz, 1H,  $CH_{2oxa}$ , F), 5.40 (dd,  $J = 8.3$  Hz, 10.1 Hz, 1H,  $CH_{oxa}$ , F), 5.91 (dd,  $J = 2.3$  Hz,

9.0 Hz, 1H,  $CH_{oxa}$ , C), 6.08 (dd,  $J = 3.5$  Hz, 9.6 Hz, 1H,  $CH_{oxa}$ , C), 7.25-7.27 (m, 3H,  $CH_{arom}$ ), 7.32-7.40 (m, 15H,  $CH_{arom}$ ).

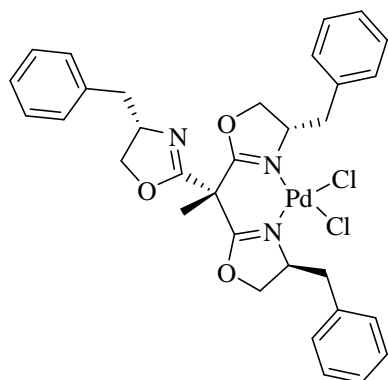
$^{13}C$  { $^1H$ } NMR (150 MHz,  $CDCl_3$ , 296 K)  $\delta$  22.4 ( $CH_3$ ), 45.6 ( $(CH_3)C(oxa)_3$ ), 68.5 ( $CH_{oxa}$ , C), 68.7 ( $CH_{oxa}$ , C) 69.7 ( $CH_{oxa}$ , F), 76.7 ( $CH_{2oxa}$ , F), 76.9 ( $CH_{2oxa}$ , F), 77.3 ( $CH_{2oxa}$ , C), 77.4 ( $CH_{2oxa}$ , C), 126.1, 126.6, 126.8 ( $C_{arom}$ , F), 128.3, 128.4, 128.5, 128.9, 129.0, 129.1 ( $C_{arom}$ , C), 139.4, 139.5 ( $C_{quat-arom}$ , C), 140.5 ( $C_{quat-arom}$ , F), 161.8 (NCO, NC), 167.1, 168.0 (NCO, C).

$^{15}N$  (60 MHz,  $CDCl_3$ , 296 K)  $\delta$  160.8 161.6 (N, C) 239.9 (N, F), (C = coordinated oxazoline, F = free oxazoline).

FT-IR (KBr):  $\nu$  1655  $cm^{-1}$  (s,  $\nu_{C=N}$ ).

HRMS (ESI):  $m/z$  : calcd for  $C_{29}H_{27}N_3O_3Pd$  ( $[M-2Cl]^+$ ) 570.103, found: 570.110.

elemental analysis calcd (%) for  $C_{29}H_{27}Cl_2N_3O_3Pd$ : C 54.18, H 4.23, N 6.54; found: C 53.01, H 4.29, N 6.60.

(1,1,1-tris[(4*S*)-4-benzyloxazolin-2-yl]ethane)palladium(II) dichloride (41)

Yield: 68%.

$^1\text{H}$  NMR (600 MHz,  $\text{CDCl}_3$ , 296 K)  $\delta$  1.55 (s, 3H,  $\text{CH}_3$ ), 2.37 (pseudo-t,  $J = 11.2$  Hz, 1H,  $\text{CH}_2_{\text{Bn}}$ , C), 2.79 (dd,  $J = 7.4$  Hz, 13.9 Hz, 1H,  $\text{CH}_2_{\text{Bn}}$ , F), 2.93 (dd,  $J = 8.5$  Hz, 13.4 Hz, 1H,  $\text{CH}_2_{\text{Bn}}$ , C), 3.01 (dd,  $J = 5.3$  Hz, 13.8 Hz, 1H,  $\text{CH}_2_{\text{Bn}}$ , F), 3.44 (dd,  $J = 1.4$  Hz, 13.8 Hz, 1H,  $\text{CH}_2_{\text{Bn}}$ , C), 3.82 (dd,  $J = 1.6$  Hz, 13.2 Hz, 1H,  $\text{CH}_2_{\text{Bn}}$ , C), 4.06 (pseudo-t,  $J = 8.1$  Hz, 1H,  $\text{CH}_2_{\text{oxa}}$ , F), 4.17 (pseudo-t,  $J = 8.6$  Hz, 1H,  $\text{CH}_2_{\text{oxa}}$ , C), 4.26 (pseudo-t,  $J = 8.8$  Hz, 1H,  $\text{CH}_2_{\text{oxa}}$ , C), 4.30 (pseudo-t,  $J = 9.1$  Hz, 1H,  $\text{CH}_2_{\text{oxa}}$ , F), 4.37 (dd,  $J = 1.9$  Hz, 8.9 Hz, 1H,  $\text{CH}_2_{\text{oxa}}$ , C), 4.49 (m, 1H,  $\text{CH}_{\text{oxa}}$ , F), 4.54 (dd,  $J = 1.6$  Hz, 8.8 Hz, 1H,  $\text{CH}_2_{\text{oxa}}$ , C), 5.04 (m, 1H,  $\text{CH}_{\text{oxa}}$ , C), 5.10 (m, 1H,  $\text{CH}_{\text{oxa}}$ , C), 7.19-7.24 (m, 4H,  $\text{CH}_{\text{arom}}$ ), 7.28-7.35 (m, 9 H,  $\text{CH}_{\text{arom}}$ ), 7.45 (m, 2H,  $\text{CH}_{\text{arom}}$ ).

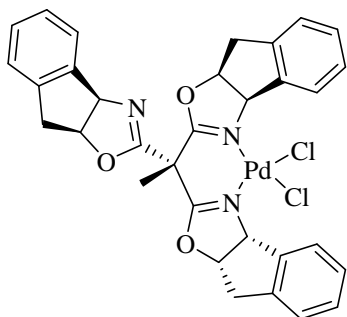
$^{13}\text{C}$  { $^1\text{H}$ } NMR (150 MHz,  $\text{CDCl}_3$ , 296 K)  $\delta$  20.9 ( $\text{CH}_3$ ), 39.2, 39.4 ( $\text{CH}_2_{\text{Bn}}$ , C) 40.6 ( $\text{CH}_2_{\text{Bn}}$ , F) 45.0 ( $(\text{CH}_3)\text{C}(\text{oxa})_3$ ), 66.2 ( $\text{CH}_{\text{oxa}}$ , C), 67.1 ( $\text{CH}_{\text{oxa}}$ , F) 67.2 ( $\text{CH}_{\text{oxa}}$ , C), 72.8, 72.9 ( $\text{CH}_2_{\text{oxa}}$ , C), 73.3 ( $\text{CH}_2_{\text{oxa}}$ , F), 126.8, 127.1, 1267.3 ( $\text{C}_{\text{arom}}$ , F), 128.6, 128.7, 128.8, 129.7, 129.8, 130.1 ( $\text{C}_{\text{arom}}$ , C), 135.4, 135.9 ( $\text{C}_{\text{quat-arom}}$ , C), 136.5 ( $\text{C}_{\text{quat-arom}}$ , F), 161.0 (NCO, F), 166.6, 166.8 (NCO, C).

$^{15}\text{N}$  (60 MHz,  $\text{CDCl}_3$ , 296 K)  $\delta$  161.3, 162.2 (N, C), 239.9 (N, F), (C= coordinated oxazoline, F= free oxazoline).

FT-IR (KBr):  $\nu$  1655  $\text{cm}^{-1}$  (s,  $\nu_{\text{C=N}}$ ).

HRMS (FAB):  $m/z$  : calcd for  $\text{C}_{32}\text{H}_{33}\text{N}_3\text{O}_3\text{Pd}$  ( $[\text{M}-2\text{Cl}]^+$ ) 613.156, found: 613.151

elemental analysis calcd (%) for  $\text{C}_{32}\text{H}_{33}\text{Cl}_2\text{N}_3\text{O}_3\text{Pd}$ : C 56.11, H 4.86, N 6.13; found: C 56.04, H 4.80, N 6.19.

(1,1,1-tris[(4*R*, 5*S*)-4,5-indanediylloxazolin-2-yl]ethane)palladium(II) dichloride (42)

Yield: 73%.

$^1\text{H}$  NMR (400 MHz, 1,1,2,2-tetrachloroethane- $d_2$ , 296 K)  $\delta$  1.50 (s, 3H,  $\text{CH}_3$ ), 2.09 (d,  $J = 18.2$  Hz, 1H,  $\text{CH}_2_{\text{Ind}}$ , C), 2.48 (d,  $J = 18.6$  Hz, 1H,  $\text{CH}_2_{\text{Ind}}$ , C), 3.03 (dd,  $J = 6.8$  Hz, 18.2 Hz, 1H,  $\text{CH}_2_{\text{Ind}}$ , C), 3.08 (dd,  $J = 5.8$  Hz, 17.8 Hz, 1H,  $\text{CH}_2_{\text{Ind}}$ , C), 3.37 (m, 2H,  $\text{CH}_2_{\text{Ind}}$ , F), 5.11 (ddd,  $J = 1.4$  Hz, 5.8 Hz, 7.2 Hz, 1H,  $\text{OCH}_{\text{oxa}}$ , C), 5.15 (dd,  $J = 5.7$  Hz, 7.2 Hz, 1H,  $\text{OCH}_{\text{oxa}}$ , C), 5.41 (dd,  $J = 5.9$  Hz, 7.3 Hz, 1H,  $\text{OCH}_{\text{oxa}}$ , F), 5.49 (d,  $J = 7.6$  Hz, 1H,  $\text{NCH}_{\text{oxa}}$ , F), 6.25 (d,  $J = 6.8$  Hz, 1H,  $\text{NCH}_{\text{oxa}}$ , C), 6.26 (d,  $J = 6.5$  Hz, 1H,  $\text{NCH}_{\text{oxa}}$ , C), 7.16-7.46 (m, 10 H,  $\text{CH}_{\text{arom}}$ ), 8.41 (m, 1H,  $\text{CH}_{\text{arom}}$ ), 8.50 (m, 1H,  $\text{CH}_{\text{arom}}$ ).

$^{13}\text{C}$   $\{^1\text{H}\}$  NMR (100 MHz, 1,1,2,2-tetrachloroethane- $d_2$ , 296 K)  $\delta$  20.8 ( $\text{CH}_3$ ), 37.3, 38.8, ( $\text{CH}_2$  ind), 45.2 ( $(\text{CH}_3)\text{Coxa}_3$ ), 73.3, 74.0 ( $\text{NCH}_{\text{oxa}}$ , C), 76.4 ( $\text{NCH}_{\text{oxa}}$ , F), 85.1, 86.7, ( $\text{OCH}_{\text{oxa}}$ , C), 87.8, ( $\text{OCH}_{\text{oxa}}$ , F), 124.9, 125.0, 125.3, 125.7, 127.6, 127.9, 128.0, 128.1, 128.3, 128.9, 129.7, 129.9 ( $\text{CH}_{\text{arom}}$ ), 138.2, 138.5, 138.5, 138.6 ( $\text{C}_{\text{quat-arom}}$ , C), 139.5, 140.5 ( $\text{C}_{\text{quat-arom}}$ , F), 160.3 ( $\text{NCO}$ , F), 166.6, 167.6 ( $\text{NCO}$ , C).

$^{15}\text{N}$  (60 MHz, 1,1,2,2-tetrachloroethane- $d_2$ , 296 K)  $\delta$  161.5, 162.8 (N, C), 238.3 (N, F) (C= coordinated oxazoline, F= free oxazoline).

FT-IR (KBr):  $\nu$  1653  $\text{cm}^{-1}$  (s,  $\nu_{\text{C=N}}$  free oxazoline), 1649  $\text{cm}^{-1}$  (s,  $\nu_{\text{C=N}}$  coordinated oxazoline).

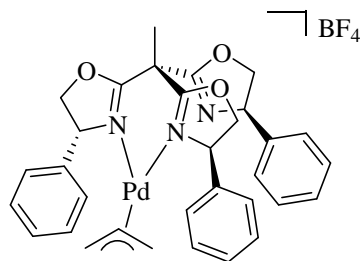
HRMS (ESI):  $m/z$  : calcd for  $\text{C}_{32}\text{H}_{27}\text{Cl}_2\text{N}_3\text{NaO}_3\text{Pd}$  ( $[\text{M}+\text{Na}]^+$ ) 701.891, found: 701.035; calcd for  $\text{C}_{32}\text{H}_{27}\text{ClN}_3\text{O}_3\text{Pd}$  ( $[\text{M}-\text{Cl}]^+$ ) 642.078, found: 642.077.

elemental analysis calcd (%) for  $\text{C}_{32}\text{H}_{27}\text{Cl}_2\text{N}_3\text{O}_3\text{Pd}$ : C 56.61, H 4.01, N 6.19; found: C 56.70, H 4.18, N 6.10.

## 2. Palladium(II) allyl complex

The palladium(II) complex was obtained following a procedure described in the literature.<sup>23</sup>

### ( $\eta^3$ -allyl)(1,1,1-tris[(4R)-4-phenyloxazolin-2-yl]ethane)palladium(II) (43)



Ph-trisox (65 mg, 0.14 mmol) in dry  $\text{CH}_2\text{Cl}_2$  (2 mL) was added to a solution of  $[(\text{cod})\text{Pd}(\eta^3\text{-C}_3\text{H}_5)]\text{BF}_4$  (47.3 mg, 0.14 mmol) in dry  $\text{CH}_2\text{Cl}_2$  (1 mL). The reaction mixture was stirred for 45 min, filtered through Celite and washed with  $\text{CH}_2\text{Cl}_2$  (2 x 1 mL). The solvents were evaporated to give a white powder which was washed twice with pentane (5 mL) and dried under vacuum to

yield the complex (50 mg, 52%). Suitable crystals for an X-ray diffraction study were obtained by slow diffusion of pentane into a solution of the complex in  $\text{CH}_2\text{Cl}_2$ .

$^1\text{H}$  NMR (400 MHz,  $\text{CDCl}_3$ , 296 K)  $\delta$  1.89 (d,  $J = 12.5$  Hz, 1H,  $\text{H}_{\text{A allyl}}$ ), 2.22 (s, 3H,  $\text{CH}_3$ ), 2.52 (d,  $J = 12.6$  Hz, 1H,  $\text{H}_{\text{A allyl}}$ ), 2.78 (dd,  $J = 2.0$  Hz, 7.0 Hz, 1H,  $\text{H}_{\text{S allyl}}$ ), 3.44 (d,  $J = 6.9$  Hz, 1H,  $\text{H}_{\text{A allyl}}$ ), 4.40 (pseudo-t,  $J = 8.3$  Hz, 3H,  $\text{CH}_2_{\text{oxa}}$ ), 4.89 (m, 1H,  $\text{H}_{\text{C allyl}}$ ), 5.03 (dd,  $J = 8.7$  Hz, 10.4 Hz, 3H,  $\text{CH}_2_{\text{oxa}}$ ), 5.47 (dd,  $J = 7.9$  Hz, 10.4 Hz, 3H,  $\text{CH}_{\text{oxa}}$ ), 7.33 (m, 15H,  $\text{CH}_{\text{arom}}$ ).

$^{13}\text{C}$   $\{^1\text{H}\}$  NMR (100 MHz,  $\text{CDCl}_3$ , 296 K)  $\delta$  20.8 ( $\text{CH}_3$ ), 45.9 ( $(\text{CH}_3)\text{C}(\text{oxa})_3$ ), 61.1 ( $\text{C}_1$  allyl,  $\text{C}_3$  allyl), 71.6 ( $\text{CH}_{\text{oxa}}$ ), 77.0 ( $\text{CH}_2_{\text{oxa}}$ ), 115.6 ( $\text{C}_2$  allyl), 127.0, 128.6, 129.2 ( $\text{C}_{\text{arom}}$ ), 140.2 ( $\text{C}_{\text{quat-arom}}$ ), 167.6 ( $\text{NCO}$ ).

<sup>23</sup> D. Franco, M. Gomez, F. Jiménez, G. Muller, M. Rocamora, M. A. Maestro, J. Mahia, *Organometallics* **2004**, *23*, 3197.

FT-IR (KBr):  $\nu$  1658  $\text{cm}^{-1}$  (s,  $\nu_{\text{C=N}}$ ).

MS (FAB):  $m/z$  (%): 612.1 (100) [ $M\text{-BF}_4$ ] $^+$ .

elemental analysis calcd (%) for  $\text{C}_{32}\text{H}_{32}\text{N}_3\text{O}_3\text{PdBF}_4$  with  $\text{CH}_2\text{Cl}_2$ : C 50.51, H 4.37, N 5.35; found: C 50.47, H 4.32, N 5.41.

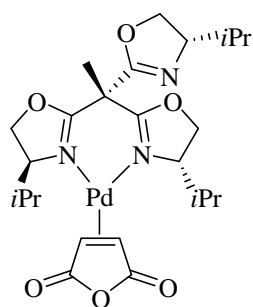
### 3. Palladium(0) complexes

#### [Pd(ma)(trisox)] complexes: General Procedure

Trisox (0.54 mmol) in dry THF (3 mL) was added to a solution of  $[(\eta^2, \eta^2\text{-nbd})(\eta^2\text{-ma})\text{Pd}^0]$ <sup>24</sup> (0.54 mmol) in dry THF (4 mL). After stirring for 15 min, the reaction mixture was filtered through Celite and concentrated under reduced pressure to 2 mL. Pentane (10 mL) was then added to the solution, after which a yellow powder was obtained. The crude solid was washed with pentane (3 x 7 mL) and dried *in vacuo* to give the complex as a yellow powder.

#### (1,1,1-tris[(4*S*)-4-isopropylloxazolin-2-yl]ethane)(maleic anhydride)palladium(0) (44)

Yield: 54%. Crystallization from  $\text{Et}_2\text{O}$ /pentane gave yellow crystals



suitable for an X-ray diffraction study.

$^1\text{H}$  NMR (300 MHz,  $\text{CDCl}_3$ , 296 K)  $\delta$  0.81 (d,  $J = 6.8$  Hz, 9H,  $\text{CH}(\text{CH}_3)_2$ ), 0.96 (d,  $J = 7.0$  Hz, 9H,  $\text{CH}(\text{CH}_3)_2$ ), 1.85 (s, 3H,  $\text{CH}_3$  apical), 2.23 (br m, 3H,  $\text{CH}(\text{CH}_3)_2$ ), 3.69 (d,  $J = 3.7$  Hz, 1H,  $\text{C}_4\text{H}_2\text{O}_3$ ), 3.74 (d,  $J = 3.7$  Hz, 1H,  $\text{C}_4\text{H}_2\text{O}_3$ ), 4.20 (m, 6H,  $\text{CH}_2$  oxa), 4.33 (m, 3H,  $\text{CH}_{\text{oxa}}$ ).

$^{13}\text{C}$  { $^1\text{H}$ } NMR (75 MHz,  $\text{CDCl}_3$ , 296 K)  $\delta$  14.8 ( $\text{CH}(\text{CH}_3)_2$ ), 18.4 ( $\text{CH}(\text{CH}_3)_2$ ), 21.9 ( $\text{CH}_3$  apical), 30.5 ( $\text{CH}(\text{CH}_3)_2$ ), 38.9 ( $\text{CH}_{\text{ma}}$ ), 40.4 ( $\text{CH}_{\text{ma}}$ ), 44.6 ( $(\text{CH}_3)\text{C}(\text{oxa})_3$ ), 69.5 ( $\text{CH}_{\text{oxa}}$ ), 72.8 ( $\text{CH}_2$  oxa), 164.3 (NCO), 172.3 ( $\text{C}_{\text{quat ma}}$ ), 172.8 ( $\text{C}_{\text{quat ma}}$ ).

FT-IR (KBr):  $\nu$  1786, 1722  $\text{cm}^{-1}$  ( $\nu_{\text{C=O}}$ ), 1660  $\text{cm}^{-1}$  ( $\nu_{\text{C=N}}$ , free oxazoline), 1650  $\text{cm}^{-1}$  ( $\nu_{\text{C=N}}$ , coordinated oxazoline).

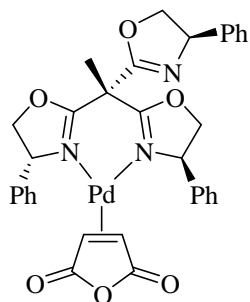
HRMS (ESI):  $m/z$  : calcd for  $\text{C}_{24}\text{H}_{35}\text{N}_3\text{NaO}_6\text{Pd}$  ( $[M+\text{Na}]^+$ ) 590.146, found: 590.162; calcd for  $\text{C}_{48}\text{H}_{70}\text{N}_6\text{NaO}_{12}\text{Pd}_2$  ( $[2M+\text{Na}]^+$ ) 1157.302, found: 1157.329.

elemental analysis calcd (%) for  $\text{C}_{24}\text{H}_{35}\text{Cl}_2\text{N}_3\text{O}_6\text{Pd}$ : C 50.75, H 6.21, N 7.40; found: C 50.86, H 6.19, N 7.37.

<sup>24</sup> A. M. Kluwer, C. J. Elsevier, M. Bühl, M. Lutz, A. L. Spek, *Angew. Chem.* **2003**, *115*, 3625; *Angew. Chem. Int. Ed.* **2003**, *42*, 3501

(1,1,1-tris[(4R)-4-phenyloxazolin-2-yl]ethane)(maleic anhydride)palladium(0) (45)

Yield: 75%.



$^1\text{H}$  NMR (600 MHz,  $\text{CD}_2\text{Cl}_2$ , 296 K)  $\delta$  2.16 (s, 3H,  $\text{CH}_3$ ), 2.92 (d,  $J = 3.9$  Hz, 1H,  $\text{C}_4\text{H}_2\text{O}_3$ ), 3.30 (d,  $J = 3.8$  Hz, 1H,  $\text{C}_4\text{H}_2\text{O}_3$ ), 4.46 (br s, 3H,  $\text{CH}_2$  oxa), 4.86 (pseudo-t,  $J = 9.2$  Hz, 3H,  $\text{CH}_2$  oxa), 5.40 (dd,  $J = 6.7$  Hz, 10.1 Hz, 3H,  $\text{CH}_{\text{oxa}}$ ), 7.33-7.48 (m, 15H,  $\text{CH}_{\text{arom}}$ ).

$^{13}\text{C}$  { $^1\text{H}$ } NMR (150 MHz,  $\text{CD}_2\text{Cl}_2$ , 296 K)  $\delta$  22.2 ( $\text{CH}_3$ ), 38.9 ( $\text{CH}_{\text{ma}}$ ), 41.4 ( $\text{CH}_{\text{ma}}$ ), 45.6 ( $(\text{CH}_3)\text{C}(\text{oxa})_3$ ), 76.2 ( $\text{CH}_2$  oxa), 76.6 ( $\text{CH}_2$  oxa), 76.7 ( $\text{CH}_{\text{oxa}}$ ),

127.0, 127.2, 127.9, 128.7, 129.1 ( $\text{C}_{\text{arom}}$ ), 140.7 ( $\text{C}_{\text{quat-arom}}$ ), 166.5 (NCO), 171.9 ( $\text{C}_{\text{quat ma}}$ ), 172.7 ( $\text{C}_{\text{quat ma}}$ ).

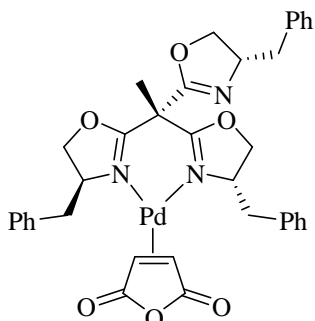
FT-IR (KBr)  $\nu$  1798, 1727  $\text{cm}^{-1}$  ( $\nu_{\text{C=O}}$ ), 1662  $\text{cm}^{-1}$  ( $\nu_{\text{C=N}}$ , free oxazoline), 1655  $\text{cm}^{-1}$  ( $\nu_{\text{C=N}}$ , coordinated oxazoline).

HRMS (FAB):  $m/z$  : calcd for  $\text{C}_{29}\text{H}_{27}\text{N}_3\text{O}_3\text{Pd}$  ( $[\text{M-ma}]^+$ ) 571.109, found: 571.114.

elemental analysis calcd (%) for  $\text{C}_{33}\text{H}_{29}\text{N}_3\text{O}_6\text{Pd}$ : C 59.16, H 4.36, N 6.27; found: C 58.02, H 4.32, N 6.35.

(1,1,1-tris[(4S)-4-benzyloxazolin-2-yl]ethane)(maleic anhydride)palladium(0) (46)

Yield: 56%.



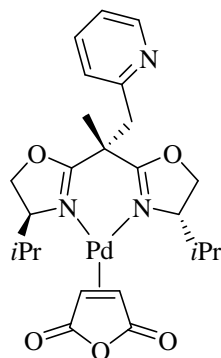
$^1\text{H}$  NMR (400 MHz,  $\text{CD}_2\text{Cl}_2$ , 296 K)  $\delta$  1.53 (s, 3H,  $\text{CH}_3$ ), 2.78 (dd,  $J = 8.1$  Hz, 13.2 Hz, 2H,  $\text{CH}_2$  Bn), 1H,  $\text{C}_4\text{H}_2\text{O}_3$ ), 3.13 (br m, 2H,  $\text{CH}_2$  Bn), 1H,  $\text{C}_4\text{H}_2\text{O}_3$ ) 3.87 (br m, 2H,  $\text{CH}_2$  Bn), 4.14 (br m, 3H,  $\text{CH}_2$  oxa), 4.27 (pseudo-t,  $J = 8.8$  Hz, 3H,  $\text{CH}_2$  oxa), 4.51 (m, 3H,  $\text{CH}_{\text{oxa}}$ ), 7.22-7.34 (m, 15H,  $\text{CH}_{\text{arom}}$ ).

$^{13}\text{C}$  { $^1\text{H}$ } NMR (100 MHz,  $\text{CD}_2\text{Cl}_2$ , 296 K)  $\delta$  21.8 ( $\text{CH}_3$ ), 39.8 ( $\text{CH}_{\text{ma}}$ ), 40.5 ( $\text{CH}_2$  Bn), 41.2 ( $\text{CH}_{\text{ma}}$ ), 45.0 ( $(\text{CH}_3)\text{C}(\text{oxa})_3$ ), 68.2 ( $\text{CH}_{\text{oxa}}$ ), 72.8 ( $\text{CH}_2$  oxa), 127.1, 128.9, 130.2 ( $\text{C}_{\text{arom}}$ ), 139.8 ( $\text{C}_{\text{quat-arom}}$ ), 164.4 (NCO), 172.8 ( $\text{C}_{\text{quat ma}}$ ), 173.6 ( $\text{C}_{\text{quat ma}}$ ).

FT-IR (KBr):  $\nu$  1793, 1724  $\text{cm}^{-1}$  ( $\nu_{\text{C=O}}$ ), 1662  $\text{cm}^{-1}$  ( $\nu_{\text{C=N}}$ , free oxazoline), 1655  $\text{cm}^{-1}$  ( $\nu_{\text{C=N}}$ , coordinated oxazoline).

HRMS (FAB):  $m/z$  : calcd for  $\text{C}_{32}\text{H}_{33}\text{N}_3\text{O}_3\text{Pd}$  ( $[\text{M-ma}]^+$ ) 613.156, found: 613.162.



(2,2-bis[(4S)-4-isopropylloxazolin-2-yl]-1-(pyridin-2-yl)propane)(maleic anhydride)palladium(0)(48)

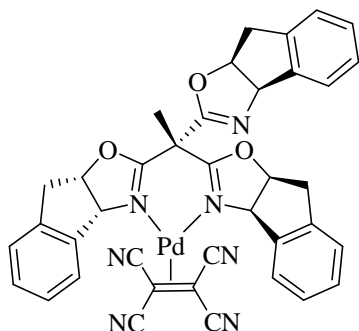
Yield: 69%.

$^1\text{H}$  NMR (600 MHz,  $\text{CD}_2\text{Cl}_2$ , 296 K)  $\delta$  0.48-0.53 (m, 2H,  $\text{CH}(\text{CH}_3)_2$ ), 0.74-0.98 (m, 10H,  $\text{CH}(\text{CH}_3)_2$ ), 1.71, 1.73 (s, 3H,  $\text{CH}_3$  apical), 2.33 (br m, 1H,  $\text{CH}(\text{CH}_3)_2$ ), 2.45 (br m, 1H,  $\text{CH}(\text{CH}_3)_2$ ), 3.43 (d,  $J = 15.2$  Hz, 1H,  $\text{CH}_2$  Py), 3.52 (d,  $J = 16.1$  Hz, 1H,  $\text{CH}_2$  Py), 3.60-3.68 (m, 2H,  $\text{C}_4\text{H}_2\text{O}_3$ ), 4.02-4.32 (m, 6H,  $\text{CH}_2$  oxa,  $\text{CH}_{\text{oxa}}$ ), 7.11 (m, 2H,  $\text{CH}_{\text{arom}}$ ), 7.61 (m, 1H,  $\text{CH}_{\text{arom}}$ ), 8.41 (m, 1H,  $\text{CH}_{\text{arom}}$ ).

(+ isomers)  $^{13}\text{C}$  { $^1\text{H}$ } NMR (150 MHz,  $\text{CD}_2\text{Cl}_2$ , 296 K)  $\delta$  13.6, 13.8, 18.4 ( $\text{CH}(\text{CH}_3)_2$ ), 26.1 ( $\text{CH}_3$  apical), 29.1, 29.6 ( $\text{CH}(\text{CH}_3)_2$ ), 37.5, 39.3 ( $\text{CH}_{\text{ma}}$ ), 43.9 ( $\text{CH}_2$  Bn), 42.7 ( $(\text{CH}_3)\text{C}(\text{oxa})_3$ ), 67.8, 68.2 ( $\text{CH}_{\text{oxa}}$ ), 72.2 ( $\text{CH}_2$  oxa), 121.6, 122.8, 136.0 ( $\text{C}_{\text{arom}}$ ), 156.3 ( $\text{C}_{\text{quat-arom}}$ ), 169.1 (NCO), 172.8, 173.8 ( $\text{C}_{\text{quat ma}}$ ).

FT-IR (KBr):  $\nu$  1794, 1723  $\text{cm}^{-1}$  ( $\nu_{\text{C=O}}$ ), 1664  $\text{cm}^{-1}$  ( $\nu_{\text{C=N}}$ , free oxazoline), 1653  $\text{cm}^{-1}$  ( $\nu_{\text{C=N}}$  coordinated oxazoline).

HRMS (FAB):  $m/z$ : calcd for  $\text{C}_{20}\text{H}_{29}\text{N}_3\text{O}_2\text{Pd}$  ( $[\text{M-ma}]^+$ ) 419.130, found: 449.131.

(1,1,1-tris[(4R,5S)-4,5-indanediylloxazolin-2-yl]ethane)(tetracyanoethylene)palladium(0) (47)

Ind-trisox (105 mg, 0.21 mmol) in THF (2 mL) was added to a solution of  $[(\eta^2, \eta^2\text{-nbd})(\eta^2\text{-tcne})\text{Pd}]$  (68 mg, 0.21 mmol) in THF (2 mL). After stirring for 2 h, the reaction mixture was filtered through Celite and concentrated under reduced pressure to 2 mL. Pentane (10 mL) was then added to the solution, after which a yellow powder was obtained. The crude solid was washed three times with pentane (7 mL) and dried *in vacuo* to yield 70 mg (50%) of the complex as a yellow powder.

$^1\text{H}$  NMR (400 MHz,  $\text{CD}_2\text{Cl}_2$ , 296 K)  $\delta$  1.60 (s, 3H,  $\text{CH}_3$ ), 2.77 (d,  $J = 18.0$  Hz, 3H,  $\text{CH}_2$  Ind), 3.28 (dd,  $J = 6.4$  Hz, 18.3 Hz, 3H,  $\text{CH}_2$  Ind), 5.40 (pseudo-t,  $J = 6.6$  Hz, 3H,  $\text{OCH}_{\text{oxa}}$ ), 5.66 (d,  $J = 7.4$  Hz, 3H,  $\text{NCH}_{\text{oxa}}$ ), 7.28 (m, 3H,  $\text{CH}_{\text{arom}}$ ), 7.38 (m, 6H,  $\text{CH}_{\text{arom}}$ ); 7.73 (m, 3H,  $\text{CH}_{\text{arom}}$ ).

$^{13}\text{C}$  NMR (100 MHz,  $\text{CD}_2\text{Cl}_2$ , 296 K)  $\delta$  20.6 ( $\text{CH}_3$ ), 38.6 ( $\text{CH}_2$  Ind), 45.6 ( $(\text{CH}_3)\text{C}(\text{oxa})_3$ ), 77.8 ( $\text{NCH}_{\text{oxa}}$ ), 86.9 ( $\text{OCH}_{\text{oxa}}$ ), 114.6, 115.0 ( $\text{C}_{\text{tcne}}$ ), 125.7, 126.2, 128.3, 129.8 ( $\text{C}_{\text{arom}}$ ), 139.3, 139.6 ( $\text{C}_{\text{quat-arom}}$ ), 159.7 (NCO).

$^1\text{H}$  NMR (400 MHz,  $\text{CD}_2\text{Cl}_2$ , 203 K)  $\delta$  1.54 (s, 3H,  $\text{CH}_3$ ), 1.88 (d,  $J = 18.2$  Hz, 1H,  $\text{CH}_2$  Ind), 2.42 (d,  $J = 18.3$  Hz, 1H,  $\text{CH}_2$  Ind), 3.01 (dd,  $J = 6.8$  Hz, 18.4 Hz, 1H,  $\text{CH}_2$  Ind), 3.18 (dd,  $J = 5.2$  Hz,

18.3 Hz, 1H,  $CH_2$  Ind), 3.38 (d,  $J = 18.4$  Hz, 1H,  $CH_2$  Ind), 3.46 (dd,  $J = 5.7$  Hz, 19.2 Hz, 1H,  $CH_2$  Ind), 5.14 (pseudo-t,  $J = 7.0$  Hz, 1H,  $OCH_{\text{oxa}}$ ), 5.36 (pseudo-t,  $J = 6.1$  Hz, 1H,  $OCH_{\text{oxa}}$ ), 5.53 (d,  $J = 7.8$  Hz, 1H,  $NCH_{\text{oxa}}$ ), 5.58 (d,  $J = 7.0$  Hz, 1H,  $NCH_{\text{oxa}}$ ), 5.61 (pseudo-t,  $J = 6.4$  Hz, 1H,  $OCH_{\text{oxa}}$ ), 5.76 (d,  $J = 7.2$  Hz, 1H,  $NCH_{\text{oxa}}$ ), 7.35 (m, 10 H,  $CH_{\text{arom}}$ ), 7.76 (d,  $J = 7.8$  Hz, 1H,  $CH_{\text{arom}}$ ); 7.87 (d,  $J = 7.5$  Hz, 1H,  $CH_{\text{arom}}$ ).

$^{13}\text{C}$  NMR (100 MHz,  $\text{CD}_2\text{Cl}_2$ , 203 K)  $\delta$  20.6 ( $\text{CH}_3$ ), 37.1, 37.4, 38.1, 38.4 ( $\text{CH}_2$  Ind), 44.3 ( $(\text{CH}_3)\text{C}(\text{oxa})_3$ ), 76.0, 77.0 ( $\text{NCH}_{\text{oxa}}$ ), 77.7, 84.0, 86.7, ( $\text{OCH}_{\text{oxa}}$ ), 87.0, ( $\text{NCH}_{\text{oxa}}$ ), 113.8, 114.4 ( $\text{C}_{\text{tcne}}$ ), 124.8, 125.1, 127.6, 129.5 ( $\text{C}_{\text{arom}}$ ), 137.5, 138.9 ( $\text{C}_{\text{quat-arom}}$ ), 160.2, 168.0 (NCO).

FT-IR (KBr):  $\nu$  1653  $\text{cm}^{-1}$  ( $\nu_{\text{C=N}}$ , coordinated oxazoline), 1649  $\text{cm}^{-1}$  ( $\nu_{\text{C=N}}$ , free oxazoline).

HRMS (FAB):  $m/z$  : calcd for  $\text{C}_{32}\text{H}_{27}\text{N}_3\text{O}_3\text{Pd}$  ( $[\text{M-tcne}]^+$ ) 607.109, found: 607.115; calcd for  $\text{C}_{38}\text{H}_{27}\text{N}_7\text{O}_3\text{Pd}$  ( $[\text{M}]^+$ ) 735.121, found: 735.129.

#### 4. Magnetisation transfer experiments

##### Acquisition of the data

The magnetisation transfer experiments were carried out on a Bruker Avance II 400 spectrometer. To invert selectively the desired signal a selective shaped pulse was employed. The two major parameters defining the selective pulse, sp1 and p11, have been optimised manually (sp1 = power of the excitation, p11 = width of the excitation).

##### *Pulse program*

For both study, the pulse program employed (t1ir\_car) was as followed:

```
1 ze
2 d1
  4u pl0:f1
  p11:sp1:f1 ph1:r
  vd
  p1 ph2
  go=2 ph31
  d11 wr #0 if #0 ivd
  lo to 1 times td1
exit
```

```
ph1=0 2
ph2=0 0 2 2 1 1 3 3
ph31=0 0 2 2 1 1 3 3
```

```
;p11 : f1 channel - power level for pulse (default)
;p1 : f1 channel - 90 degree high power pulse
```

```

;p2 : f1 channel - 180 degree high power pulse
;d1 : relaxation delay; 1-5 * T1
;d11: delay for disk I/O           [30 msec]
;vd : variable delay, taken from vd-list
;NS: 8 * n
;DS: 4
;td1: number of experiments = number of delays in vd-list

```

### Acquisition parameters

The relevant acquisition parameters are summarised in Table 5.3.1.

	<b>39</b>	<b>42</b>
<b>General</b>		
PULPROG	t1ir_car	t1ir_car
TD	16384	16384
NS	8	8
DS	0	0
SWH (Hz)	30.78.82	30.78.82
AQ (s)	2.6608117	2.6608117
RG	128	228
DW ( $\mu$ s)	162.400	162.400
DE ( $\mu$ s)	6.50	6.50
D1 (s)	10.000	10.000
D11 (s)	0.0300	0.0300
P2 ( $\mu$ s)	30.00	30.00
VDLIST	carole	carole
<b>Channel f1</b>		
NUC1	1H	1H
P1 ( $\mu$ s)	10.00	10.00
P11 ( $\mu$ s)	35000.00	88666.70
PL1 (dB)	-4.80	-4.80
PL1W (W)	19.72301865	19.72301865
SF01 (MHz)	399.8911325	399.8911325
SP1 (dB)	55.00	46.18
SP1W (W)	0.00002065	0.00015739
SPNAM1	Gaus1.1000	Re-burp_car
SPOAL1	0.500	0.500
SPOFFS1 (Hz)	0.00	0.00

**Table 5.3.1:** Important acquisition paramaters

In Figure 5.3.1 is depicted the graphical edit of the pulse program used for complex **39**.

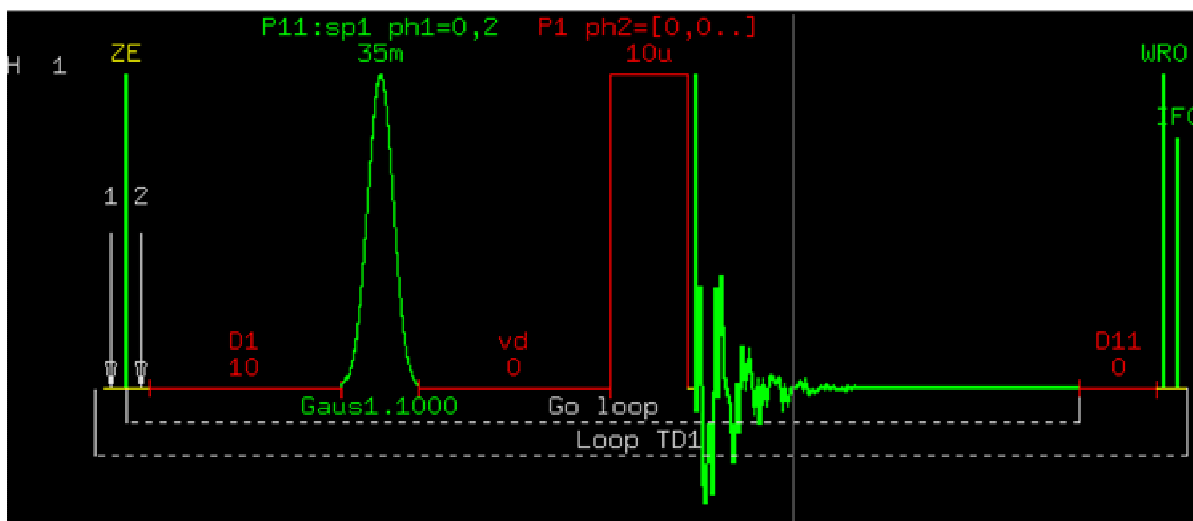


Figure 5.3.1: Graphical edit of the pulse program (study of complex **39**)

In Figure 5.3.2 is depicted the graphical edit of the pulse program used for complex **42**.

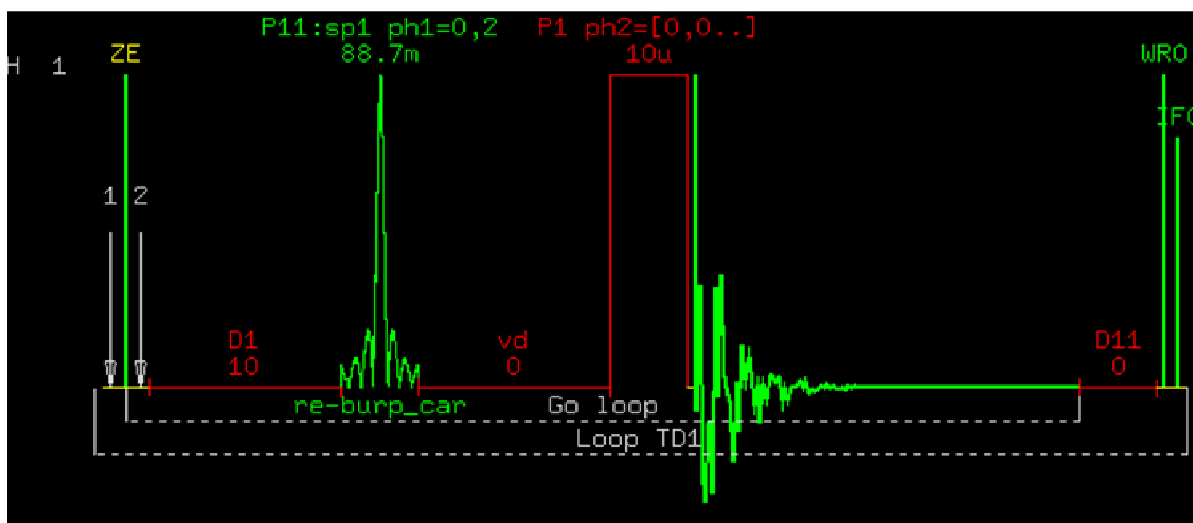


Figure 5.3.2: Graphical edit of the pulse program (study of complex **42**)

### Theoretical fit of the experimental data

Varying the temperature, the time dependence of the magnetisation in the two exchanging sites after inversion of the desired proton was fitted to the appropriate sets of equations derived from the McConnell equations.<sup>25,26</sup> The fits of the experimental data with derived McConnell

<sup>25</sup> H. M. McConnell, *J. Chem. Phys.* **1958**, 28, 430.

<sup>26</sup> J.J. Led, H. Gesmar, *J. Magn. Reson.* **1982**, 49, 444.

equations were carried out using the software SigmaPlot.<sup>27</sup> Fits of the theoretical curves to the experimental data gave the NMR spectroscopic rate constants  $k_{\text{NMR}}$  which are summarised in Table 3.2.1 for complex **39** and in Table 3.2.2 for complex **42** of Chapter 3.

### 5. Asymmetric allylic alkylation

Allylic acetate was prepared by acetylation of the corresponding commercially available allylic alcohol with acetic anhydride.<sup>28</sup>

#### General procedure

A degassed solution of  $[\text{Pd}(\eta^3\text{-C}_3\text{H}_5)\text{Cl}]_2$  (6.4  $\mu\text{mol}$ , 1.1 mol%) and ligand (14.5  $\mu\text{mol}$ , 2.5 mol%) in 0.7 mL THF was stirred at 50°C for 1.5 h. After cooling down to room temperature, *rac*-1,3-diphenylprop-2-enyl acetate (147 mg, 0.58 mmol) in THF (2.2 mL), dimethyl malonate (0.2 mL, 1.75 mmol), *N,O*-bis(trimethylsilyl)acetamide-BSA- (0.4 mL, 1.75 mmol) and a few milligrams of potassium acetate were added. The reaction mixture was stirred at room temperature. After the desired reaction time the reaction mixture was diluted with  $\text{CH}_2\text{Cl}_2$ , washed with a saturated aqueous solution of ammonium chloride and the organic extract was dried over  $\text{Na}_2\text{SO}_4$ . The residue was purified by flash chromatography (EtOAc/ Hexane, 90/10) to yield a colorless oil. Yields and ee-values are the average of at least 2 corroborating runs.

#### Determination of enantiomeric excesses

The ee-values of the product were determined by HPLC using a Daicel Chiralpak AD-H column. HPLC method: Hexane/*i*PrOH 95/5, 1 mL/min,  $t_{\text{R}1}$  = 14.6 min,  $t_{\text{R}2}$  = 20.5 min, detection at 260, 254 and 250 nm.

The absolute configuration was assigned by comparing the observed value of the optical rotation with literature data.<sup>29</sup>

#### Kinetic studies

The comparative studies of the catalytic activities were conducted for each experiment using palladium catalysts prepared *in situ* by reacting the respective ligand with the  $[\text{Pd}(\eta^3\text{-C}_3\text{H}_5)\text{Cl}]_2$  dimer at 50°C for 1.5 h in THF. The catalytic allylic alkylations were carried out at room temperature. The progress of the reaction was monitored by measuring the appearance of the product by GC, using dodecane as internal standard.

<sup>27</sup> The files are saved on a DVD and are available for more informations.

<sup>28</sup> I. D. G. Watson, S.A Styler, A. K. Yudin, *J. Am. Chem. Soc.* **2004**, *126*, 5086.

<sup>29</sup> J. Sprinz, G. Helmchen, *Tetrahedron Lett.* **1993**, *34*, 1769.

GC method:  $T_{inj} = 200^{\circ}\text{C}$ ,  $T_{det} = 250^{\circ}\text{C}$ , 20 mL/min He flow, splitless, temperature program:  $90^{\circ}\text{C}$ , 1 min,  $30^{\circ}\text{C}/\text{min}$  up to  $250^{\circ}\text{C}$ ,  $250^{\circ}\text{C}$ , 10 min;  $t_{R \text{ dodecane}} = 4.1 \text{ min}$ ,  $t_{R \text{ product}} = 13.3 \text{ min}$ .

## 6. Asymmetric allylic amination

### General procedure

A degassed solution of  $[\text{Pd}(\eta^3\text{-C}_3\text{H}_5)\text{Cl}]_2$  (6.4  $\mu\text{mol}$ , 1.1 mol-%) and ligand (14.5  $\mu\text{mol}$ , 2.5 mol-%) in 0.7 mL THF was stirred at  $50^{\circ}\text{C}$  for 15 min. Subsequently, *rac*-1,3-diphenylprop-2-enyl acetate (147 mg, 0.58 mmol) in THF (2.2 mL) and morpholine (35  $\mu\text{L}$ , 0.40 mmol) were added. The reaction mixture was stirred 5 days at  $50^{\circ}\text{C}$  and worked out by quenching with aqueous ammonium chloride, extracting the organic compound with  $\text{CH}_2\text{Cl}_2$  and drying with  $\text{Na}_2\text{SO}_4$ . The residue was purified by flash chromatography ( $\text{Et}_2\text{O}/\text{Pentane}$ , 1/1) to yield a colorless oil. Yields and ee-values are the average of at least 2 corroborating runs.

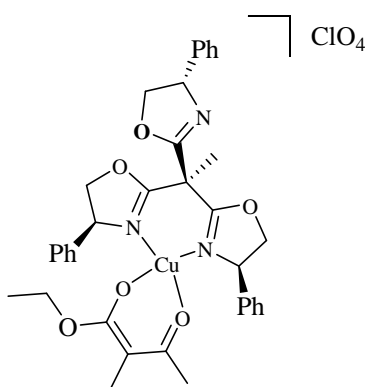
### Determination of enantiomeric excesses

The ee-values of the product was determined by HPLC using a Daicel Chiralpak OD column. HPLC method: Hexane/*i*PrOH 99/1, 1 mL/min,  $t_{R1} = 5.6 \text{ min}$ ,  $t_{R2} = 9.5 \text{ min}$ , detection at 265, 257 and 250 nm.

## IV. Chapter 4

### 1. Copper(II) complex

#### $[\text{Cu}((R,S,S)\text{-Ph-trisox})(\beta\text{-ketoester})](\text{ClO}_4)$ (49)



A mixture of  $\text{Cu}(\text{ClO}_4)_2 \cdot 6\text{H}_2\text{O}$  (54 mg; 0.143 mmol) and (*R,S,S*)-trisox (70 mg; 0.150 mmol) in THF (2 mL) was stirred for 1.5 hours. A  $5.8 \cdot 10^{-2} \text{ M}$  solution of diethylmethylmalonate / *t*-BuOK (2.7 mL, 0.157 mmol) was subsequently added and the resulting green mixture was stirred overnight. After removal of the volatiles in vacuo, the crude product was washed with hexane (3 x 5 mL) and the green solid was dried under vacuum. This solid material was extracted with toluene and the resulting suspension

was filtered through a Teflon microfilter (0.2  $\mu\text{m}$ ). Slow vapour diffusion of hexane into the solution at  $-4^{\circ}\text{C}$  gave green crystals of the compound (57 mg; 52%).

elemental analysis calcd (%) C<sub>36</sub>H<sub>40</sub>ClCuN<sub>3</sub>O<sub>11</sub>: C 54.75, H 5.11, N 5.32; found: C 54.39, H 5.09, N 5.36.

## 2. Asymmetric Mannich reaction

*N*-tosyl  $\alpha$ -imino ester was prepared from ethyl glyoxylate and *p*-toluenesulfonyl isocyanate following a literature procedure.<sup>30</sup>

The catalyst solutions for the enantioselective Mannich reaction of the  $\beta$ -ketoester were obtained by taking the appropriate amount of a stock solution and diluting to 1 mL.

### General procedure:

A stock solution of CuClO<sub>4</sub>·6H<sub>2</sub>O (8.3 mg, 22.5  $\mu$ mol) and the desired ligand (33.8  $\mu$ mol) in acetone/Et<sub>2</sub>O (1.5 mL, 1/3 v/v) was prepared under air. The homogeneous solution was stirred for 30 min and successive aliquots were taken to obtain the desired catalyst loading for each run. To each catalyst solution was added ethyl 2-methylacetoacetate (22.5  $\mu$ L, 0.15 mmol) and the solution was cooled down to -28°C. *N*-tosyl- $\alpha$ -imino ester (360  $\mu$ L, 0.18 mmol) in solution in toluene (0.5 mol.L<sup>-1</sup>) was then added. After 36 h at -28°C, the solvent was removed *in vacuo* and the residue was purified by flash chromatography (CH<sub>2</sub>Cl<sub>2</sub>/MeOH 100/1) to yield a colorless oil. Yields and ee-values are the average of at least 2 corroborating runs.

### Determination of enantiomeric excesses

The ee-values of the product was determined by HPLC using a Daicel Chiralpak AD-H column. HPLC method: Hexane/*i*PrOH 95/5, 0.8 mL/min, minor diastereomer: t<sub>R1</sub> = 53.2 min, t<sub>R2</sub> = 55.9 min, major diastereomer: t<sub>R1</sub> = 59.5 min, t<sub>R2</sub> = 66.2 min, detection at 213, 220 and 254 nm.

## 3. Asymmetric $\alpha$ -amination

The catalyst solutions for the enantioselective Mannich reaction of the  $\beta$ -ketoester were obtained by taking the appropriate amount of a stock solution and diluting to 1 mL.

### General procedure:

A stock solution of Cu(OTf)<sub>2</sub> (8.1 mg, 22.5  $\mu$ mol) and the ligand (27  $\mu$ mol) in distilled CH<sub>2</sub>Cl<sub>2</sub> (1.5 mL) was prepared under air. The homogeneous solution was stirred for 30 min and successive aliquots were taken to obtain the desired catalyst loading for each run. To each

---

<sup>30</sup> G. R. Heintzelman, S. M. Weinreb, M. Parvez, *J. Org. Chem.* 1996, **61**, 4594

catalyst solution was added ethyl 2-methylacetoacetate (21.4  $\mu\text{L}$ , 0.15 mmol) and the solution was cooled down to 0°C. Pre-cooled dibenzyl azodicarboxylate (54.8 mg, 0.18 mmol) in solution in  $\text{CH}_2\text{Cl}_2$  (0.5 mL) was then added. After 16 h at 0°C, the product was isolated by flash chromatography (Hexane/EtOAc, 75/25) to yield a colorless oil. Yields and ee-values are the average of at least 2 corroborating runs.

#### Determination of enantiomeric excesses

The ee-values of the product was determined by HPLC using a Daicel Chiralpak AD-H column. HPLC method: Hexane/*i*PrOH 90/10, 1 mL/min,  $t_{\text{R}1}$  = 35 min,  $t_{\text{R}2}$  = 40 min, detection at 213 and 254 nm.

#### Kinetic studies

The comparative studies of the catalytic activities were conducted for each experiment using copper catalysts prepared *in situ* by reacting the respective ligand with the  $\text{Cu}(\text{OTf})_2$  salt at room temperature for 0.5 h in  $\text{CH}_2\text{Cl}_2$ . The catalytic  $\alpha$ -amination reactions were carried out at 0°C. The progress of the reaction was monitored by measuring the disappearance of the ethyl 2-methylacetoacetate by GC, using dodecane as internal standard.

GC method:  $T_{\text{inj}}$  = 200°C,  $T_{\text{det}}$  = 250°C, 20 mL/min He flow, splitless, temperature program: 40°C, 1 min, 25°C/min up to 270°C, 270°C, 2 min;  $t_{\text{R substrate}}$  = 3.5 min,  $t_{\text{R dodecane}}$  = 6.4 min.



## V. X-ray experimental data

X-ray experimental data for palladium complexes **39-44**:

	<b>39</b>	<b>40</b>	<b>43</b>	<b>44</b>
Empirical formula	C <sub>20</sub> H <sub>33</sub> Cl <sub>2</sub> N <sub>3</sub> O <sub>3</sub> Pd	C <sub>29</sub> H <sub>27</sub> Cl <sub>2</sub> N <sub>3</sub> O <sub>3</sub> Pd	C <sub>33</sub> H <sub>34</sub> BCl <sub>2</sub> F <sub>4</sub> N <sub>3</sub> O <sub>3</sub> Pd	C <sub>24</sub> H <sub>35</sub> N <sub>3</sub> O <sub>6</sub> Pd
Formula weight	540.81	642.84	784.74	567.96
Temperature /K	173	100(2)	100(2)	173
Crystal system	Orthorhombic	Monoclinic	Monoclinic	Monoclinic
Space group	<i>P</i> 2 <sub>1</sub> 2 <sub>1</sub> 2 <sub>1</sub>	<i>P</i> 2 <sub>1</sub>	<i>P</i> 2 <sub>1</sub>	<i>P</i> 2 <sub>1</sub>
Unit cell dimensions				
<i>a</i> / Å	8.7083(1)	10.2954(10)	9.1344(4)	10.4450(2)
<i>b</i> / Å	10.8395(1)	10.0926(10)	20.6281(10)	10.0975(2)
<i>c</i> / Å	24.8911(4)	13.0348(13)	9.3599(4)	14.0887(3)
$\beta$		101.537(2)	111.4780(10)	90.161(5)
Volume / Å <sup>3</sup>	2349.56(5)	1327.0(2)	1641.17(13)	1485.91(5)
<i>Z</i>	4	2	2	2
Density (calcd.) / Mgm <sup>-3</sup>	1.53	1.609	1.588	1.27
Absorpt. Coeff. / mm <sup>-1</sup>	1.042	0.938	0.790	0.661
<i>F</i> <sub>000</sub>	1112	652	796	588
Crystal size / mm <sup>3</sup>	0.10 × 0.06 × 0.06	0.20 × 0.05 × 0.05	0.30 × 0.30 × 0.30	0.20 × 0.16 × 0.10
$\theta$ range for data collect. / °	2.5 to 30.02	2.02 to 32.08	1.97 to 32.01	2.5 to 30.05
Index ranges	-12 ≤ <i>h</i> ≤ 12, -15 ≤ <i>k</i> ≤ 15, -34 ≤ <i>l</i> ≤ 35	-15 ≤ <i>h</i> ≤ 14, -14 ≤ <i>k</i> ≤ 15, 0 ≤ <i>l</i> ≤ 19	-13 ≤ <i>h</i> ≤ 12, -30 ≤ <i>k</i> ≤ 25, 0 ≤ <i>l</i> ≤ 13	-14 ≤ <i>h</i> ≤ 14, -14 ≤ <i>k</i> ≤ 14, -19 ≤ <i>l</i> ≤ 19
Reflections collected		32759	15547	8556
Independent refl. [ <i>R</i> <sub>ini</sub> ]	6871 [0.040]	8646 [0.0583]	8670 [0.0224]	4588 [0.040]
Completeness to $\theta = 30.02^\circ$ / %	99.9	95.6	100	99.8
Absorption correction	Empirical (SHELXA)	Semi-empirical from equivalents	Semi-empirical from equivalents	Empirical (SHELXA)
Max. and min. transm. data / restraints / param.	0.928 and 0.901 4997 / 0 / 262	0.7458 and 0.6070 8646 / 1 / 344	0.7974 and 0.7974 8670 / 8 / 43	1.0000 and 0.9401 3495 / 1 / 306
Goodness-of-fit on <i>F</i> <sup>2</sup>	1.323	1.084	1.072	1.966
Final <i>R</i> indices [ <i>I</i> > 2σ( <i>I</i> )]	<i>R</i> 1 = 0.033, w <i>R</i> 2 = 0.037	<i>R</i> 1 = 0.0372, w <i>R</i> 2 = 0.0688	<i>R</i> 1 = 0.0290, w <i>R</i> 2 = 0.0748	<i>R</i> 1 = 0.038, w <i>R</i> 2 = 0.061
<i>R</i> indices (all data)	<i>R</i> 1 = 0.058, w <i>R</i> 2 = 0.108	<i>R</i> 1 = 0.0560, w <i>R</i> 2 = 0.0750	<i>R</i> 1 = 0.0303, w <i>R</i> 2 = 0.0760	<i>R</i> 1 = 0.051, w <i>R</i> 2 = 0.120
Abs. struct. parameter	-0.02(3)	0.000(19)	-0.021(15)	-0.04(3)
Res. density, max diff. peak & hole / e·Å <sup>-3</sup>	1.115 and -0.304	1.430 and -0.609	1.218 and -0.603	0.895 and -0.317

X-ray experimental data for compound **31a** and copper complex **49**:

	<b>31a</b>		<b>49</b>
Empirical formula	C <sub>14</sub> H <sub>20</sub> N <sub>2</sub> O	Empirical formula	C <sub>50</sub> H <sub>56</sub> ClCuN <sub>3</sub> O <sub>11</sub>
Formula weight	232.32	Formula weight	973.97
Temperature /K	100	Crystal size /mm	0.2-0.2-0.1
Crystal system	Orthorhombic	Crystal system	tetragonal
Space group	<i>P</i> 2 <sub>1</sub> 2 <sub>1</sub> 2 <sub>1</sub>	Space group	<i>P</i> 4 <sub>1</sub> 2 <sub>1</sub> 2
Unit cell dimensions		<i>a</i> /Å	15.9231(8)
<i>a</i> /Å	5.1912(7)	<i>b</i> /Å	
<i>b</i> /Å	11.6401(15)	<i>c</i> /Å	36.637(3)
<i>c</i> /Å	21.277(3)	<i>V</i> /Å <sup>3</sup>	9289.2(9)
$\beta$	90	<i>Z</i>	8
Volume / Å <sup>3</sup>	1285.7(3)	<i>D<sub>c</sub></i> /M·gm <sup>-3</sup>	1.393
<i>Z</i>	4	$\mu$ /mm <sup>-1</sup>	0.593
Density (calcd.) / Mgm <sup>-3</sup>	1.200	Max., min. transmission factors	0.926, 0.890
Absorpt. Coeff. / mm <sup>-1</sup>	0.076	Index ranges, <i>h,k,l</i>	-13...13, 0...19, 0...44
<i>F</i> <sub>000</sub>	504	$\vartheta$ range /°	1.4...25.7
Crystal size / mm <sup>3</sup>	0.15 x 0.15 x 0.10	<i>F</i> <sub>000</sub>	4088
$\theta$ range for data collect. /°	1.91 to 28.70	Refl. collected	117733 [0.0729]
Index ranges	0 ≤ <i>h</i> ≤ 7, 0 ≤ <i>k</i> ≤ 15, 0 ≤ <i>l</i> ≤ 28	Refl. indep. [ <i>R</i> <sub>int</sub> ]	8663
Reflections collected	10195	Data / rest. / par.	8663 / 94 / 615
Independent refl. [ <i>R</i> <sub>int</sub> ]	1931 [0.0669]	Goodness-of-fit on <i>F</i> <sup>2</sup>	1.064
Completeness to $\theta$ = 30.02° /%	100.0	<i>R</i> indices [ <i>I</i> > 2 $\sigma$ ( <i>I</i> )]	<i>R</i> 1 = 0.0529, w <i>R</i> 2 = 0.1395
Absorption correction	Semi-empirical from equivalents	<i>R</i> indices (all data)	<i>R</i> 1 = 0.0657, w <i>R</i> 2 = 0.1485
Max. and min. transm.	0.8624 and 0.7746	Absolute structure parameter	0.002(17)
data / restraints / param.	1931 / 0 / 201	Largest residual peaks /e·Å <sup>-3</sup>	0.522 and -0.754
Goodness-of-fit on <i>F</i> <sup>2</sup>	1.088		
Final <i>R</i> indices [ <i>I</i> > 2 $\sigma$ ( <i>I</i> )]	<i>R</i> 1 = 0.0429, w <i>R</i> 2 = 0.0961		
<i>R</i> indices (all data)	<i>R</i> 1 = 0.0615, w <i>R</i> 2 = 0.1048		
Abs. struct. parameter	4(2)		
Res. density, max diff. peak & hole / e·Å <sup>-3</sup>	0.052, 0.215 and -0.212		





# Résumé

## I. Introduction

Depuis près de vingt ans, le cycle oxazoline occupe une place prépondérante dans la conception de nouveaux ligands chiraux azotés. En raison de leur accessibilité, de leur nature modulaire et de leurs larges applications dans des réactions métallo-catalysées, les molécules contenant un cycle oxazoline chiral sont devenues une des classes de ligands les plus communément utilisés en catalyse énantiosélective. Depuis la première publication en 1986 de l'utilisation en catalyse asymétrique d'un ligand chiral contenant un cycle oxazoline, une grande variété de ligands contenant un ou plusieurs cycles oxazolines incorporants différents hétéroatomes, centres chiraux supplémentaires et caractéristiques structurales spécifiques, ont été utilisés avec succès dans de nombreuses réactions énantiosélectives.<sup>1</sup>

Il existe déjà plusieurs publications dans la littérature portant sur la synthèse et l'utilisation de ligands trisoxazolines<sup>2</sup> mais aucun de ceux-ci ne sont du type 1,1,1-tris(oxazolinyl)éthane qui devrait donner la géométrie la plus adaptée pour coordiner un métal de façon tripodale (Figure 1).

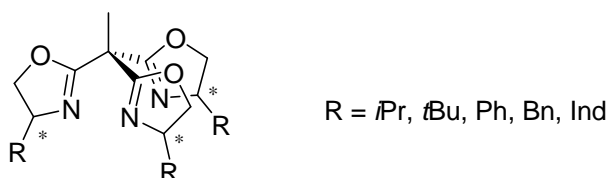


**Figure 1:** Trisoxazolines du type 1,1,1-tris(oxazolinyl)éthane

Le but de ce travail a été de concevoir de nouveaux ligands trisoxazolines de haute symétrie, basé sur une méthode de synthèse développée au sein du groupe. Nous avons ensuite comme objectif d'étudier leur comportement en catalyse énantiosélective et plus particulièrement de déterminer leur intérêt par rapport aux ligands de symétrie  $C_2$  bien établis dans la littérature.

Une étude de l'influence de la symétrie  $C_3$  en catalyse asymétrique par comparaison directe entre des systèmes trisoxazoline-métal et bisoxazoline-métal a donc été effectuée.

<sup>1</sup> H. A. McManus, P. J. Guiry, *Chem. Rev.* **2004**, *104*, 4151.

<sup>2</sup> J. Zhou, Y. Tang, *Chem. Soc. Rev.* **2005**, *34*, 664.

## II. Synthèse des ligands

L'originalité du ligand trisoxazoline développé au sein du laboratoire et employé pour nos études provient du fait que les trois entités oxazolines sont toutes reliées au même atome de carbone. Les tentatives de synthèse d'une telle molécule par formation séquentielle des trois cycles oxazolines ont échoué en raison de la décarboxylation et décomposition des précurseurs durant la formation de la trisoxazoline. Une nouvelle méthode récemment mise au point permet de réaliser la synthèse de dérivés du type 1,1,1-tris(oxazolinyl)éthane par couplage entre une bisoxazoline lithiée et une 2-bromooxazoline (Figure 2).

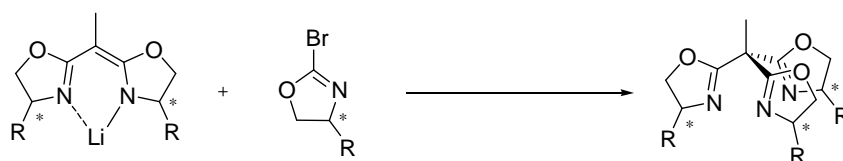


Figure 2: Synthèse du ligand trisoxazoline

Trois nouvelles trisoxazolines de symétrie  $C_3$  ont été développées durant ce travail avec les substituants suivant sur le cycle oxazoline: (4*R*)-phenyl, (4*S*)-benzyl et (4*R*,5*S*)-indanyl. La modularité de cette voie de synthèse permet aussi d'obtenir des trisoxazolines à groupement mixtes en effectuant le couplage entre une bromooxazoline avec un groupement R et une bisoxazoline contenant de groupements R'. Des trisoxazolines de symétrie  $C_1$  ont également été synthétisées pour être utilisées dans les réactions catalytiques étudiées.

Il a également été démontré que les 2-bromooxazolines, intermédiaires clé de la synthèse des trisoxazolines, se réarrangent thermiquement pour donner les dérivés  $\alpha$ -bromo-isocyanate correspondants. Ces derniers, après réaction avec la phenylethylamine, génèrent sélectivement des aziridines, produits de *N*-cyclisation, ou des aminooxazolines, produits de *O*-cyclisation, selon les conditions réactionnelles employées.

## III. Application en chimie du palladium

L'utilisation de ligands tridentates de symétrie  $C_3$  dans des réactions où ceux-ci interviennent en tant que ligands bidentates dans les étapes stéréosélectivement déterminantes devrait simplifier la stéréochimie des intermédiaires catalytiques clés. Ceci s'appliquerait aux systèmes pour lesquels il y a échange entre les différentes espèces  $\kappa^2$ -coordinées et pour lesquels le troisième bras non-coordiné joue un rôle direct ou indirect dans des étapes clés du cycle

catalytique. La réaction de substitution allylique catalysée au palladium est une réaction appropriée pour tester cette hypothèse.

Des complexes de palladium(II) ont été synthétisés par réaction entre les trisoxazolines respectives et le précurseur  $[\text{Pd}(\text{PhCN})_2\text{Cl}_2]$ . A température ambiante, la perte de la symétrie  $C_3$  du ligand est observée en RMN du  $^1\text{H}$  et indique un mode de coordination bidentate de la trisoxazoline. Des études RMN à température variable ainsi qu'une série d'expériences de transfert de magnétisation montrent un échange entre les cycles oxazoline coordonnés et non-coordinés. Pour les complexes  $[(i\text{Pr-trisox})\text{PdCl}_2](\mathbf{1})$  et  $[(\text{Ind-trisox})\text{PdCl}_2](\mathbf{2})$ , les valeurs des paramètres d'activation du processus fluxionnel ont pu être déterminées ( $\mathbf{1}$ :  $\Delta H^\ddagger = 75.6 \pm 0.5 \text{ kJ}\cdot\text{mol}^{-1}$ ,  $\Delta S^\ddagger = 14.0 \pm 1.5 \text{ J}\cdot\text{mol}^{-1}$ ;  $\mathbf{2}$ :  $\Delta H^\ddagger = 79.4 \pm 2.0 \text{ kJ}\cdot\text{mol}^{-1}$ ,  $\Delta S^\ddagger = 9.3 \pm 6.0 \text{ J}\cdot\text{mol}^{-1}$ ). Les faibles entropies d'activation n'indiquent la présence ni d'un mécanisme de substitution associatif, ni d'un mécanisme de substitution dissociatif dominant pour ce processus fluxionnel. Tenant compte des études mécanistiques effectuées concernant les substitutions sur les complexes de  $\text{Pd}^{\text{II}}$  plan carré, nous présumons que l'échange entre cycles oxazoline coordonnés et libres a un caractère légèrement associatif impliquant ainsi la formation d'une espèce intermédiaire pentacoordinée de palladium(II).

Des complexes de palladium(0) ont également été isolés par réaction entre le ligand désiré et le précurseur  $[\text{Pd}(\text{nbd})(\text{alcène})]$  (alcène = anhydride maléique (ma) ou tetracyanoéthylène (tcne)) en substituant le norbornadiène par le ligand. Pour les complexes  $[(\text{Ph-trisox})\text{Pd}(\text{ma})]$  et  $[(i\text{Pr-trisox})\text{Pd}(\text{ma})]$  une analyse par diffraction des rayons X indique une géométrie trigonale plane avec le ligand trisoxazoline coordonné de façon bidentate et le dernier site de coordination occupé par l'alcène qui adopte l'une des deux orientations diastéréotopiques différentes possibles. En RMN du  $^1\text{H}$ , la symétrie des signaux du ligands indique un échange dynamique des cycles oxazolines pour ces complexes ainsi qu'un équilibre entre les diastéréomères présents en raison des différentes orientations possibles de l'alcène par rapport à l'hétérocycle libre. Des études RMN à basse température ont permis de figer les processus fluxionnels et dans certains cas d'obtenir la barrière d'activation  $\Delta G^\ddagger$  des échanges observés.

Le but de notre étude est de déterminer si la présence d'un troisième bras sur le ligand chiral modifie l'activité et la sélectivité en catalyse asymétrique ayant dans l'espèce active un ligand bidentate. Comme citée précédemment, la réaction test utilisée est la réaction d'alkylation allylique (Figure 3).

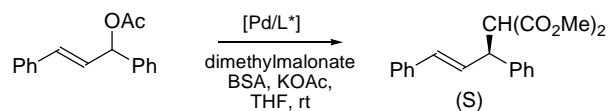


**Figure 3:** Réaction d'alkylation allylique étudiée

Dans cette optique, nous nous sommes penchés sur l'utilisation de ligands diazotés purement bidentates qui nous permettraient d'effectuer une comparaison logique. Nous avons donc réalisé une comparaison directe entre quatre couples différents trisoxazoline/bisoxazoline qui se distinguent par le substituant présent sur l'hétérocycle (Figure 4).

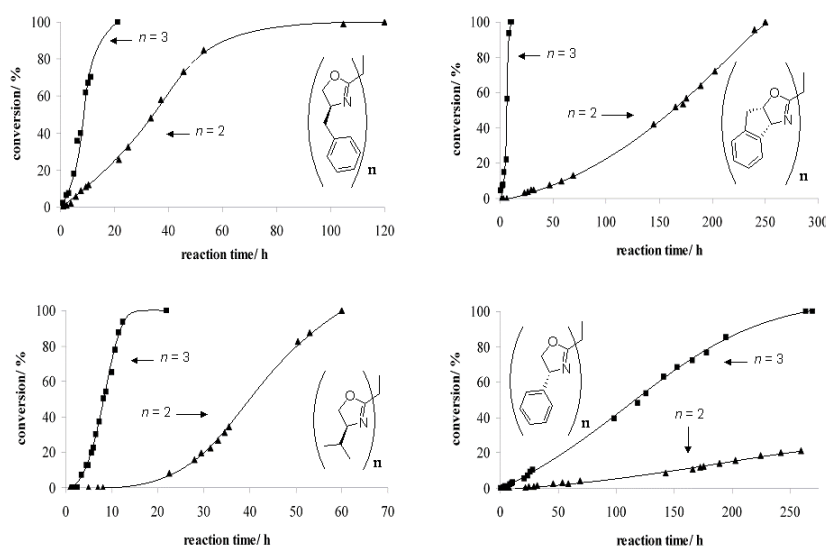


**Figure 4:** Comparaison des courbes de conversion entre les systèmes avec ligands bisoxazoline ou trisoxazoline

Les systèmes trisoxazoline/palladium induisent en général une meilleure énantiosélectivité comparés à leurs analogues bisoxazoline/palladium. Une réduction significative de la période d'induction ainsi qu'une augmentation de la vitesse de réaction ont également été observés avec les ligands tridentates. Ces dernières observations ont été confirmées avec l'étude de systèmes comportant des bisoxazolines fonctionnalisées avec un bras coordinant.

#### IV. Application en chimie du cuivre

Les ligands bisoxazolines sont intensivement utilisés en catalyse asymétrique d'acide de Lewis avec le Cu(II) avec en général de bonnes activités et sélectivités. Cependant, l'utilisation d'une charge catalytique importante est nécessaire en raison de la labilité des ligands coordonnés au cuivre. Un ligand tridentate favorisant une coordination faciale est censé limiter cette



décoordination en stabilisant l'état stationnaire du complexe. En effet, la coordination du troisième cycle oxazoline devrait inhiber les propriétés d'acide de Lewis du complexe, comme montré récemment dans des études théoriques sur des catalyseurs de type  $\text{Cu}^{\text{II}}$ -bisoxazoline. Le passage de l'espèce au repos à l'espèce active à 17 électrons nécessite la décoordination d'une unité oxazoline et l'ouverture du système (Figure 5). Le ligand présentant une symétrie  $C_3$ , cette décoordination permet l'obtention de la même espèce active, quelle que soit le cycle oxazoline concerné.

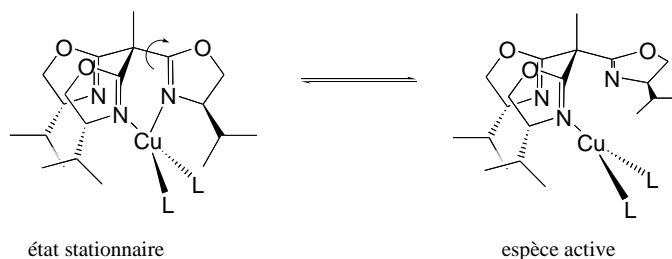


**Figure 5:** Equilibre entre l'espèce active et l'état stationnaire

Pour tester ce concept d'hémilabilité du cuivre(II) des complexes du type  $[\text{Cu}^{\text{II}}(\text{triso})]$  ont été utilisés dans la réaction asymétrique de Mannich entre un  $\beta$ -cétoester et une imine activée et dans la réaction catalytique d' $\alpha$ -amination d'un  $\beta$ -cétoester (Figure 6).

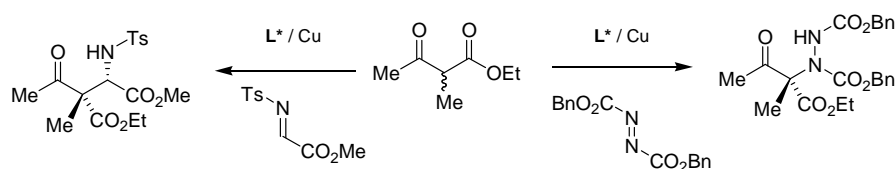


**Figure 6:** Réactions de Mannich et d' $\alpha$ -amination étudiées

Pour les deux réactions, il a été montré que les ligands trisoxazolines sont actifs et sélectifs dans les catalyses énantiosélectives de type acide de Lewis avec le cuivre(II). En comparaison directe avec leurs analogues bisoxazolines, les trisoxazolines se sont avérés être plus efficaces pour des charges catalytiques faibles (réaction de Mannich avec 10 et 0.01 mol% de catalyseur: 90% et 90% ee respectivement pour la triso; 84% et 66% ee respectivement pour la BOX). Un ligand tridentate, limitant la labilité, combiné à la symétrie  $C_3$ , limitant le nombre d'espèces actives possibles, aboutit donc à un système catalytique supérieur aux systèmes contenant les bisoxazolines correspondantes.



## Kurzfassung

Diese Arbeit beschreibt die Koordinationschemie und die katalytische Anwendung der Familie der 1,1,1-Tris(oxazalinyl)-ethanliganden („Trisox“). Die hier beschriebenen Untersuchungen behandeln in erster Linie den Einfluß der dreizähligen Rotationssymmetrie der Liganden sowie die Rolle des dritten Oxazolinarms in katalytischen Reaktionen, deren Intermediate einen bidentaten Koordinationsmodus des Trisoxliganden beinhalten.

Zu Beginn wird die Synthese hochsymmetrischer chiraler 1,1,1-Tris(oxazalinyl)ethanliganden, die Phenyl-, Benzyl- oder Indanylsubstituenten tragen, sowie nichtsymmetrischer Bis- und Trisoxazoline beschrieben, die gemischte Substituenten an der 4-Position des Oxazolins tragen. Bei den bromierten Monooxazolin-Zwischenstufen wurde eine Isomerisierung beobachtet, bei der durch thermisch induzierte Umlagerung aus den 2-Bromoxazolinen die korrespondierenden  $\alpha$ -Bromo-isocyanat-Derivate entstehen. Diese reagieren mit Phenylethylamin in Abhängigkeit von den Reaktionsbedingungen selektiv entweder zu den *N*-zyklisierten Aziridinen oder den *O*-zyklisierten 2-Aminooxazolinen.

Anschließend wird die Koordinationschemie der Trisoxazolinliganden mit Palladium beschrieben. Es konnten erfolgreich Palladium(II)chlorid- und -allyl-Komplexe und Palladium(0)-Komplexe synthetisiert werden. Im Zuge der Untersuchung des dynamischen Verhaltens dieser Komplexe in Lösung wurden die Aktivierungsparameter des Austauschs der Oxazolinreste bestimmt. Ein systematischer Vergleich der katalytischen Effizienz von Trisox- und Bisox-Palladium-Systemen zeigte, daß die Trisox-basierten Komplexe den jeweils korrespondierenden Bisox-Systemen überlegen sind. Die zusätzliche Donorfunktion des dritten Oxazolinarms scheint eine wichtige Rolle beim Produkt-Substrat-Austausch und der Bildung der aktiven Katalysatorspezies zu spielen.

Abschließend werden zwei kupferkatalysierte Katalysen beschrieben, bei denen die dynamische Koordination der Trisoxazoline an Kupfer(II) ausgenutzt wird. Es konnte gezeigt werden, daß  $C_3$ -symmetrische Trisoxazoline hocheffiziente Kupfer(II)-Komplexe für die enantioselektive Lewisäurekatalyse bilden, deren Aktivität auf der Hemilabilität des divalenten Kupfers basiert. Im direkten Vergleich mit den analogen Bisoxazolinensystemen erwiesen sich die Trisox/Kupfer-Katalysatoren insbesondere bei niedrigen Katalysatorbeladungen als effizienter in der enantioselektiven Mannich-Reaktion und der enantioselektiven  $\alpha$ -Aminierung prochiraler  $\beta$ -Ketoester. Zusätzlich wurden die Auswirkungen der Nutzung chiraler tridentater Podanden im Vergleich zu den besser etablierten bidentaten Bisox-Chelatliganden untersucht.



## Abstract

This thesis describes the coordination chemistry and catalytic applications of the 1,1,1-tris(oxazolinyl)ethane (“trisoX”) family of ligands. The studies described herein are primarily concerned with the effect of the threefold rotational symmetry of the ligands, as well as the role of the third oxazoline arm in catalytic reactions in which there are intermediates that possess a bidentate coordination of the trisoX ligand.

The syntheses of highly symmetrical chiral 1,1,1-tris(oxazolinyl)ethane ligands bearing phenyl, benzyl or indanyl substituents, and of mixed bis- and trisoXazolines is described. The isomerisation of the 2-bromooxazolines was observed, in which the thermally induced rearrangement generates the corresponding  $\alpha$ -bromo-isocyanate derivatives. Reaction of the latter with phenylethylamine led selectively to the *N*-cyclised aziridines or to the *O*-cyclised 2-aminooxazolines, depending on the reaction conditions.

The coordination chemistry of the trisoXazoline ligands with palladium is then described. Palladium(II) chloride and allyl complexes and a number of palladium(0) complexes were successfully synthesised. The dynamic behaviour of these complexes in solution was studied and activation parameters were determined for the exchange of the oxazoline moieties. The systematic comparison of the catalytic efficiency of trisoX- and bisoX-palladium systems in allylic substitution is described. It was demonstrated that the trisoXazoline-based complexes are superior catalysts in direct comparison to the corresponding bisoXazoline-based catalysts. The study showed that the additional donor function appears to play a role in the product/substrate exchange step as well as in the initial generation of the active catalyst.

Finally, the exploitation of the dynamic coordination of the trisoXazolines to copper(II) in two copper-catalysed asymmetric reactions is described. It has been shown that  $C_3$ -symmetric trisoXazolines form highly efficient enantioselective copper(II) Lewis acid catalysts, in which their success is based on the concept of a stereoelectronic hemilability of the divalent copper. In a direct comparison with the analogous bisoXazoline systems, the trisoX/copper catalysts have proven to be more efficient in an enantioselective Mannich reaction as well as an enantioselective  $\alpha$ -amination of prochiral  $\beta$ -ketoesters in presence of low catalyst loadings. To conclude the implications of the use of chiral tridentate podands in stereoselective catalysis compared to the more established bidentate chelates have been highlighted.



*Carole Foltz-César a été membre de la promotion Perikles du Collège Doctoral Européen des universités de Strasbourg pendant la préparation de sa thèse de 2004 à 2007. Elle a bénéficié des aides spécifiques du CDE et a suivi un enseignement hebdomadaire sur les affaires européennes dispensé par des spécialistes internationaux.*

*Ses travaux de recherche ont été effectués dans le cadre d'une convention de cotutelle avec la Ruprecht-Karls-Universität de Heidelberg, Allemagne et l'Université Louis Pasteur de Strasbourg, France.*

*Carole Foltz-César was a member of the European Doctoral College of the Universities of Strasbourg during the preparation of her PhD, from 2004 to 2007, class name Perikles. She has benefited from specific financial supports offered by the College and, along with her mainstream research, has followed a special course on topics of general European interests presented by international experts.*

*This PhD research project has been led with the collaboration of two universities: the Ruprecht-Karls-Universität in Heidelberg, Germany and the Louis Pasteur University in Strasbourg, France.*

